Aus dem Institut für Immunologie
Geschäftsführender Direktor: Prof. Dr. Stefan Bauer
des Fachbereichs Medizin der Philipps-Universität Marburg

in Zusammenarbeit mit dem Paul-Ehrlich-Institut Langen

SAMHD1: HIV-1 restriction, post-translational regulation and function

Inaugural-Dissertation
zur Erlangung des Doktorgrades der Naturwissenschaften

dem Fachbereich Medizin der Philipps-Universität Marburg
vorgelegt von

Moritz Schüssler
aus Herrenberg

Marburg, 2022


BY NC ND

Diese Doktorarbeit wurde in der Nachwuchsgruppe 3 „Zelluläre Aspekte von Pathogen-Wirt-Interaktionen“ unter der Leitung von Dr. Renate König am Paul-Ehrlich-Institut in Langen durchgeführt und dem Promotionsausschuss der Universität Marburg vorgelegt.

Angenommen vom Fachbereich Medizin der Philipps-Universität Marburg
am: 10.10.2022

Gedruckt mit Genehmigung des Fachbereichs Medizin

Dekanin:	Prof. Dr. Denise Hilfiker-Kleiner
Referent:	Prof. Dr. Stefan Bauer/ Dr. Renate König
1. Korreferent/in:	Prof. Dr. Magdalena Huber

TABLE OF CONTENTS

I. ABBREVIATIONS

ADAR1	adenosine deaminase RNA-specific binding protein 1
AGS	Aicardi-Goutières syndrome
AIDS	acquired immunodeficiency syndrome
AmpR	ampicillin resistance gene
APC	allophycocyanin
APOBEC	apolipoprotein B mRNA-editing enzyme catalytic polypeptide-like
ART	antiretroviral therapy
bp	base pairs
BSA	bovine serum albumin
CA	capsid protein
CamR	chloramphenicol resistance gene
CCR5	C-C chemokine receptor type 5
C/EBPα	CCAAT-enhancer binding protein α
cGAMP	cyclic GMP-AMP
cGAS	cGAMP synthase
CD	cluster of differentiation
CNOT1	CR4-NOT transcription complex subunit 1
CDK	cyclin-dependent kinase
CMV	cytomegalovirus
CPSF6	cleavage and polyadenylation specific factor 6
CRISPR	clustered regularly interspaced short palindromic repeats
crRNA	CRISPR RNA
CXCR4	C-X-C motif chemokine receptor 4
CypA	cyclophilin A
D	aspartate
dA	deoxyadenosine
dATP	deoxyadenosine triphosphate
dCTP	deoxycytidine triphosphate
dG	deoxyguanosine
dGTP	deoxyadenosine triphosphate
DDX41	DEAD box helicase 41
dNTP	deoxyribonucleoside triphosphate
dNTPase	deoxyribonucleoside triphosphate triphosphohydrolase
dT	deoxythymidine
dTTP	deoxythymidine triphosphat
DMEM	Dulbecco's Modified Eagle's Medium
DMSO	dimethyl sulphoxide
DPBS	Dulbecco's phosphate-buffered saline
DSB	double-strand break
dsDNA	double-stranded DNA
E. Coli	*Escherichia coli*
EBV	Epstein-Barr virus
ER	estradiol receptor
FACS	fluorescence-activated cell sorting
FCS	fetal calf serum

FVD780	Fixable Viability Dye eFluor 780
FW/ for	forward (primer)
GBP	guanylate-binding protein
gRNA	guide RNA
HAART	highly active ART
H	histidine
HBV	hepatitis B virus
HCMV	human cytomegalovirus
HDR	homology directed repair
HIV	human immunodeficiency virus
HIV-1	HIV type 1
HIV-2	HIV type 2
Hpi	hours post infection
HR	homologous recombination
HRP	horseradish peroxidase
HSV-1	herpes-simplex virus 1
HU	hydroxyurea
HUSH	human silencing hub
IFITM	IFN-induced transmembrane proteins
IFN	interferon
IFI16	interferon gamma inducible protein 16
IL	interleukin
InDel	insertion and deletions
IRF	interferon response factor
iPSC	induced pluripotent stem cell
ISG	interferon stimulated gene
KanaR	kanamycin resistance gene
KO	knock-out
KI	knock-in
Km	Michaelis-Menten constant
LB	lysogeny broth
LC-MS/MS	liquid chromatography with tandem mass spectrometry
LTR	long terminal repeat
MA	matrix protein
mAB	monoclonal antibody
MCMV	murine cytomegalovirus
M-CSF	macrophage colony-stimulating factor
MDA5	melanoma differentiation associated protein 5
MDM	monocyte-derived macrophage
MDDC	monocyte-derived DC
MOI	multiplicity of infection
MOPS	3-(N-morpholino) propanesulfonic acid
MPP8	Meta-Phase phosphoprotein 8
MxB	Myxovirus resistance B
NC	nucleocapsid protein
NF-κB	nuclear factor 'kappa-light-chain-enhancer' of activated B cells
NHEJ	non-homologous end-joining

NLS	nuclear localization signal
NONO	non-POU domain-containing octamer-binding protein
pAB	polyclonal antibody
PacBlue	Pacific Blue
PAMP	pathogen associated molecular pattern
pbs	primer-binding site
PBMC	peripheral blood mononuclear cell
PIC	pre-integration complex
PE	phycoerythrin
PLL	poly-L-lysine
PEI	polyethylenimine
PFA	paraformaldehyde
PMA	phorbol 12-myristate 13-acetate
PP2A	protein phosphatase 2A
ppt	polypurine tract
PR	HIV-1 protease
PRR	pattern recognition receptor
PTM	post-translational modification
PQBP1	polyglutamine binding protein 1
qgPCR	quantitative genomic PCR
RIG-I	retinoic acid inducible gene I
RIPA	radioimmunoprecipitation buffer
RLU	relative light unit
RNP	ribonucleoprotein
RT	reverse transcriptase
RT-qPCR	real time quantitative PCR
RV/ rev	reverse (primer)
SAMHD1	sterile alpha motif and HD domain containing protein
SERINC3/5	serine incorporator 3/5
SIV	simian immunodeficiency virus
SOC	super optimal broth with catabolite repression
ssRNA	single-stranded RNA
ssDNA	single-stranded DNA
STAT1/2	signal transducer and activator of transcription 1/2
TAE	tris-acetate-EDTA
TASOR	transcription activations
TBS	tris-buffered saline
TBST	tris-buffered saline with Tween
TLR	toll-like receptor
TNPO1	transportin-1
tracrRNA	trans-activating crRNA
Trim5α	tripartite-containing motif 5α
VLP	virus-like particle
WT	wild type

II. LIST OF FIGURES

III. LIST OF TABLES

1. INTRODUCTION

1.1 Understanding host-pathogen interactions of HIV-1 is key to develop effective treatments

1.1.1 HIV-1 is a constant threat to world health

Human immunodeficiency virus type 1 (HIV-1) is the causative agent of the acquired immunodeficiency syndrome (AIDS) (Barré-Sinoussi et al. 1983; Gallo et al. 1984; Popovic et al. 1984). The pandemic HIV-1 strain likely was introduced into the human population in the late 19th or early 20th century in western Africa (Worobey et al. 2008; Sharp and Hahn 2011). Multiple zoonotic transmission events of simian immunodeficiency viruses (SIV) not only lead to the introduction of a second type of lentivirus with different phylogeny, HIV-2, into the human population, but also to multiple HIV-1 lineages, the groups M, N, O and P, each resulting from an independent cross-species transmission (Sharp and Hahn 2011; Sauter and Kirchhoff 2019). By far the most prevalent HIV-1 group is the group M, which is further divided into different subtypes or clades. HIV-1 M shows phylogenetic similarities to an SIV strain endemic in chimpanzees from the sub-species *Pan troglodytes troglodytes* in southeastern Cameroon (Keele et al. 2006; Taylor and Hammer 2008; Sharp and Hahn 2011). HIV is primarily transmitted by sexual contact, but can also spread by percutaneous or perinatal infection (Hladik and McElrath 2008). Since the start of the pandemic, 79.3 million people have been infected with HIV (Global HIV & AIDS statistics — Fact sheet 2022).

The pathology of HIV-1 infection can mainly be explained by its cellular tropism. The virus predominantly infects activated cluster of differentiation (CD) 4 positive ($CD4^+$) T helper lymphocytes. After an acute phase of viral replication with mild to moderate flu-like symptoms, a live long chronic infection is established (Deeks et al. 2015). In untreated patients, HIV-1 replication in $CD4^+$ T cells subsequently leads to a progressive loss of $CD4^+$ T cells, ultimately resulting in a severe defect of the immune system, which is the hallmark of AIDS (Deeks et al. 2015). At the late stage of AIDS progression, multiple opportunistic infections finally cause a near complete fatality in untreated patients and a total of 36.3 million AIDS-related deaths (Global HIV & AIDS statistics — Fact sheet 2022).

Antiretroviral therapy (ART) or highly active ART (HAART) is a combinatory medical regimen consisting of multiple classes of anti-retroviral agents, such as nucleoside reverse transcriptase inhibitors, integrase strand transfer inhibitors, non-nucleotide reverse transcriptase inhibitors, protease inhibitors and entry inhibitors (Deeks et al. 2015). Modern HAART leads to a drastic suppression of viral replication and to elimination of the vast majority of replication competent virus. Reminiscent virus replication is low to undetectable. As a consequence HIV positive patients under effective HAART are not considered to be infectious anymore (Eisinger et al. 2019). However, HIV-1 is able to integrate into the host genome (for details see section 1.1.2) and to remain latent in long lived cellular compartments, even under constant suppression by ART. This leads to a failure of virus eradication and to rapid rebound of viral replication and AIDS progression after cessation of ART (Chun et al. 1999; Finzi et al. 1999). Therefore, current HAART strategies are considered to be non-curative. 28.2 million patients receive ART at present (Global HIV & AIDS statistics — Fact sheet 2022), which is a high economic, as well as public and individual health burden (Ndung'u et al. 2019). This is especially true in low-income countries and/or rural areas where affordable access to ART is limited. As a consequence, approximately 680 000 people died in 2020 from AIDS-related illnesses. In addition, the COVID-19 pandemic is affecting treatment and prevention programs worldwide, exacerbating the situation for many persons at risk (Global HIV & AIDS statistics — Fact sheet 2022). Hence, curative HIV-1 treatment strategies are urgently needed. Shock and kill strategies, which are aiming to re-activate latent HIV-1 provirus in order to target persistently infected cells for medical or immunological eradication, as well as strategies based on gene editing approaches, are promising candidates for an HIV-1 cure (Ndung'u et al. 2019; Margolis et al. 2020). However, apart from anecdotal success in the context of entry receptor deficient stem cell transplantation, a cure to HIV-1 has not been achieved (Hütter et al. 2009; Gupta et al. 2020).

Alongside suppression of viral loads and AIDS progression by ART, prevention of HIV-1 infection was and is an important measure to limit the AIDS pandemic. Health education is important to prevent sexual and mother-to-child transmission, as well as transmission by needle sharing or idiopathic causes. Especially in high-risk patient groups, medical post and pre-exposure prophylaxis can reduce the number of newly infected individuals

(Deeks et al. 2015; McCormack et al. 2016; Ndung'u et al. 2019). Nevertheless, still 1.5 million new HIV-1 infections occurred in 2020, highlighting the need for an HIV-1 vaccination that would prevent or reduce new infections in an immunized population. A large number of trials employing different vaccination strategies have been undertaken or are currently running. However until present, none of them showed efficacy sufficient for approval (Hargrave et al. 2021). For both successful HIV-1 vaccine development and for the development of curative HIV-1 therapies, understanding anti-viral immunity and the host-pathogen interaction networks on the cellular, as well as on the level of the entire organism is critical (Ndung'u et al. 2019; Margolis et al. 2020). The need for basic research in immunology, cell biology and virology in this area still is enormous.

1.1.2 The HIV-1 life cycle is interwoven with cellular processes

Like other viruses, HIV-1 relies on the host cell machinery in order to infiltrate a target cell, replicate its genetic material and produce new progeny virus. Many host processes are directly involved in viral replication and thus are crucial for the virus. Host proteins, which are necessary for or promote viral replication are termed host or dependency factors. Host factors are interesting targets for anti-viral therapy, because they are less prone to viral escape or resistance mutations. Already available or even approved drugs targeting cellular factors can be repurposed for anti-viral therapy (Kaufmann et al. 2018). Large scale genetic perturbation screens, as well as proteomic approaches, have highlighted many components of the HIV-1 host-pathogen interaction network and have increased our understanding of the complex interplay between virus and host factors (König et al. 2008; Brass et al. 2008; Zhou et al. 2008; Jäger et al. 2011; Park et al. 2017; Hiatt et al. 2022). Especially early events in HIV-1 infection, seem to be tightly interwoven with cellular processes.

HIV-1 is a lentivirus. Like all members of the *Retroviridae* subfamily, its replication cycle includes an obligate revere transcription step. This is necessary to convert the HIV-1 single-stranded RNA (ssRNA) genome into double-stranded DNA, which, upon integration into the host genome, is the template for *de novo* HIV-1 protein and genomic RNA production (Krupovic et al. 2018). The HIV-1 genome is complex, when compared to other non-lenti retroviruses, and has been formed from several SIV precursors by

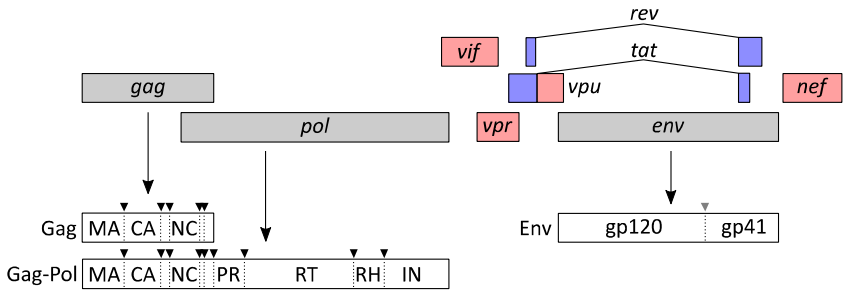

Figure 1: HIV-1 genome organization and polypeptide processing.

The genomic organization of the HIV-1 genome is shown with overlapping reading frames. Common retroviral genes *gag*, *pol* and *env* are highlighted in gray. The non-structural regulatory genes *tat* and *rev* are shown in blue and spliced as indicated. The HIV-1 accessory genes *vif*, *vpr*, *vpu* and *nef* are marked in red. Gag and Gag-Pol polyprotein processing by HIV-1 protease (black arrows) results in mature HIV-1 matrix (MA), capsid (CA), nucleocapsid (NC), protease (PR), reverse transcriptase (RT) with the RNAse H domain (RH), as well as the HIV-1 integrase (IN). For simplification minor cleavage products are not detailed. Proteolytic cleavage of the Env precursor by the host protease furin (gray arrow) gives rise to the envelope glycoproteins gp120 and gp41. The size of open reading frames and proteins as well as the position of cleavage sites is an approximation and not true to scale (Pettit et al. 2005; Kirchhoff 2010; Könnyű et al. 2013; Flint et al. 2015).

multiple recombination events, as well as a chimpanzee and human host adaption process (Sauter and Kirchhoff 2019).

Besides to the three core retroviral genes *gag*, *pol* and *env*, common to all retroviruses, and the two regulatory non-structural genes *tat* and *rev*, the HIV-1 genome contains four accessory genes *vif*, *vpu*, *vpr* and *nef*, in overlapping open reading frames (Fig. 1) (Kirchhoff 2010). Vif, Vpu, Vpr and Nef are HIV-1 effectors that critically influence the HIV-1 infection cycle and are required for HIV-1 infection *in vivo* (Fig. 2) (Harris et al. 2012; Malim and Bieniasz 2012). Vif and Vpr are E3 ubiquitin complex adaptors retargeting cellular factors for ubiquitination and degradation. While Vif is required for the maintenance of HIV-1 genome integrity, Vpr is critical in the manipulation of the host cell cycle and DNA damage response. (He et al. 1995; Mariani et al. 2003; Sheehy et al. 2003; Romani et al. 2015; Rice and Kimata 2015). Vpu is membrane associated and important for HIV-1 budding by down-modulating factors that inhibit HIV-1 release (Dubé et al. 2010). The membranous protein Nef modulates cell surface expression of a number of cellular proteins, *i.e.* the major histocompatibility complex class I, thereby

inhibiting T cell-mediated cytotoxicity (Schwartz et al. 1996; Basmaciogullari and Pizzato 2014). In addition, Nef increases the infectivity of HIV-1 particles (Rosa et al. 2015; Usami et al. 2015). The common retroviral genes each encode a polyprotein, Gag, Gag-Pol and Env, which after processing by the HIV-1 protease (PR) or host protease furin give rise to the structural proteins, necessary for the formation of the infectious viral particle. The Gag polyprotein is the precursor to the matrix protein (MA), the capsid protein (CA) and the nucleocapsid protein (NC, Fig. 1). This processing is dependent on PR in a process called maturation (Fig. 2) (Pettit et al. 2005; Könnyű et al. 2013; Flint et al. 2015). The infectious HIV-1 virion contains two redundant copies of genomic RNA, which are bound by the nucleic acid chaperone NC directly (Levin et al. 2010). The iconic cone shaped HIV-1 Capsid is formed by penta- and hexamers of the CA protein (Campbell and Hope 2015). MA lines the inner surface of the envelope, is required for ordered HIV-1 assembly. It makes contacts to both the envelope and the Capsid (Fig. 2) (Flint et al. 2015). The Gag-Pol fusion peptide is produced by ribosomal frameshifting and results in the reverse transcriptase (RT) with the RNase H domain, the integrase (IN) and the PR (Fig. 1). Gag-Pol is packaged into the infectious viral particle at 50 to 100 copies (Fig. 2) (Pettit et al. 2005; Könnyű et al. 2013; Flint et al. 2015). Also, the accessory HIV-1 proteins Vif, Vpr and Nef are present in the incoming HIV-1 virion (Fig. 2) (Kotov et al. 1999; Khan et al. 2001; Wanaguru and Bishop 2021).

HIV-1 entry is made by two viral glycoproteins, the gp120 or surface and the gp41 or transmembrane components, which are formed from the Env precursor by cleavage mediated through the host protease furin in the Golgi apparatus and decorate the HIV-1 envelope in trimers (Fig. 2) (Flint et al. 2015). HIV-1 gp120 trimers make contact to the surface receptor CD4, which is expressed mainly on T helper lymphocytes, but also on myeloid cells, such as macrophages or dendritic cells (DCs). CD4 binding to gp120 induces a conformational change, ultimately leading to membrane fusion (Fig. 2) (Chen 2019). However, co-receptors are needed to accomplish entry. The C-X-C motif chemokine receptor 4 (CXCR4) or the C-C chemokine receptor type 5 (CCR5) can serve as entry co-receptors (Fig. 2). This explains the tropism of HIV-1 for $CXCR4^+$ or $CCR5^+$ T cells and $CCR5^+$ myeloid cells, such as DCs or macrophages (Gorry et al. 2014; Chen 2019; Hiatt et al. 2021a; Albanese et al. 2022; Claireaux et al. 2022). HIV-1 viruses can be

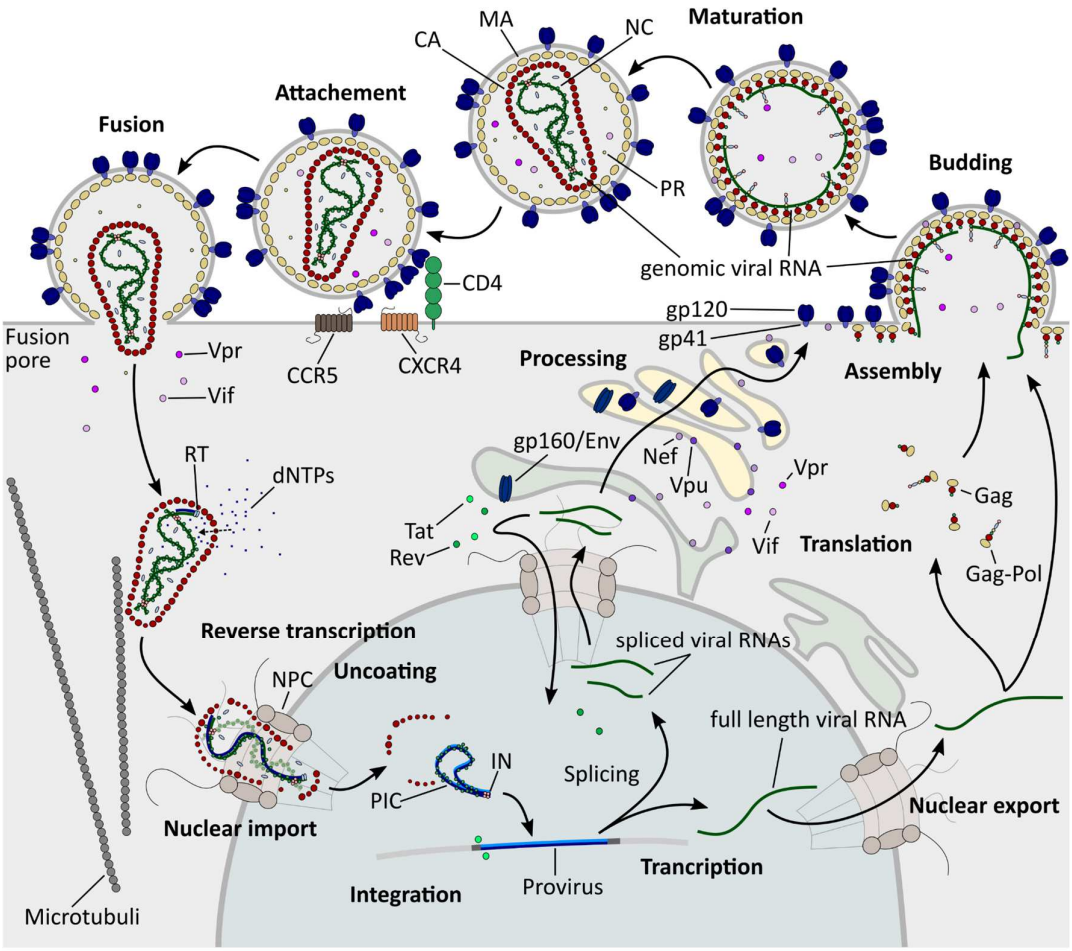

Figure 2: HIV-1 life cycle.

HIV-1 enters the host cell via CD4 and CXCR4 or CCR5 (co-) receptor binding to gp120 trimers, which leads to attachment and fusion. The HIV-1 capsid contains two copies of nucleocapsid (NC) packaged genomic viral RNA and makes access to the host cell through a fusion pore, together with the HIV-1 effector proteins Vpr and Vif. The cone shaped capsid is transported to the nucleus via microtubuli. Reverse transcription is initiated by the HIV-1 reverse transcriptase (RT), as soon as dNTPs access the capsid shell through a pore formed by capsid protein (CA) hexamers. To enter the nucleus, the HIV-1 capsid makes contact to components of the nuclear pore complex (NPC). The entire capsid is able to pass through the NPC. However, at, or soon after, nuclear import, the capsid shell disassembles, deliberating the pre-integration complex (PIC), which consists of the HIV-1 dsDNA genome bound to integrase (IN) tetramer. IN mediates integration into the host genome. The provirus serves as a template for transcription of spliced and unspliced HIV-1 RNAs, which are then exported from the nucleus. Spliced viral RNAs are needed for the translation of the HIV-1 accessory proteins Vif, Vpu, Vpr and Nef, the regulatory proteins Tat and Rev and the envelope protein Env. Env/gp160 is modified by glycosylation and cleavage by host protease furin in the Golgi complex, resulting in trimers of gp41 and gp120, which decorate the HIV-1 envelope. The non-spliced or full-length viral RNA gives rise to the polyproteins Gag and Gag-Pol, as well

as the genomic RNAs. Assembly is driven by Gag and Gag-Pol at the plasma membrane, together with the recruitment of viral RNA and viral effector proteins. After budding, Gag and Gag-Pol proteins are processed by HIV-1 protease (PR) into matrix (MA), CA, NC, RT and IN proteins. Maturation results in the infectious HIV-1 particle (Campbell und Hope 2015; Flint et al. 2015; Jacques et al. 2016; Chen et al. 2019; Bedwell und Engelman 2021; Naghavi 2021, Zila et al. 2021).

characterized as being CXCR4 or CCR5 tropic. Whereas the latter are predominantly found among transmitted virus clones early in infection, CXCR4 tropic viruses are more likely to occur late in infection. (Keele et al. 2008; Wilen et al. 2012). The importance of CCR5 as a co-receptor in early HIV-1 infection is highlighted by the relative resistance of individuals harboring CCR5 deletions or low CCR5 expression to HIV-1 infection and/or pathology (Liu et al. 1996; Samson et al. 1996; Claireaux et al. 2022).

After fusion with the plasma membrane, the viral capsid cone is released into the cytosol and relies on the actin cytoskeleton for short range movement. For long-range transport to the nuclear periphery, HIV-1 depends on, controls and exploits the microtubule network (Fig. 2) (Da Santos Silva et al. 2020; Naghavi 2021). Lentiviruses, in contrast to other non-lenti retroviruses, can infect non-cycling cells. As a consequence, lentiviruses need to access the nucleoplasm via the nuclear pore. To achieve this, HIV-1 CA makes contact with several nucleoporins (König et al. 2008; Di Nunzio et al. 2012; Buffone et al. 2018). In order for infection to proceed and to allow completion of reverse transcription and/or integration into the host genome, the HIV-1 capsid at one point has to at least partially disassemble (Xu et al. 2013; Campbell and Hope 2015; Francis and Melikyan 2018). However, whether HIV-1 gains access the nucleus before or after disassembly of the capsid shell and if reverse transcription is initiated and accomplished in the cytoplasm or after nuclear entry, was long, and partially remains, a matter of open debate (Campbell and Hope 2015; Bejarano et al. 2018; Bedwell and Engelman 2021). New high resolution and cryo-electron microscopy data, as well as experiments with capsid destabilizing mutants and agents, suggest that the entire intact HIV-1 core can penetrate the nuclear pore and that core disassembly is initiated at or after the passage through the nuclear pore complex (Fig. 2) (Burdick et al. 2020; Selyutina et al. 2020a; Müller et al. 2021; Zila et al. 2021). Earlier evidence suggested HIV-1 reverse transcription to happen mainly in the cytoplasm and to be required for nuclear entry and uncoating (Arhel et al. 2007; Hulme et al. 2011; Yang et al. 2013). In contrast, recent

studies proof that at least in some circumstances nuclear entry does precede reverse transcription (Dharan et al. 2020; Selyutina et al. 2020a). Again, host factors, such as cleavage and polyadenylation specific factor 6 (CPSF6), cyclophilin A (CypA) and transportin-1 (TRN-1), might modulate the kinetics of uncoating, as well as the initiation and completion of reverse transcription, in a cell type-dependent manner (Bejarano et al. 2019; Fernandez et al. 2019; Zhong et al. 2021).

HIV-1 reverse transcription and DNA synthesis requires deoxynucleotide triphosphate (dNTP) substrates and HIV-1 replication efficiency correlates with cellular dNTP levels (Gao et al. 1993; Korin and Zack 1999; Plesa et al. 2007). As a logical consequence, initiation of HIV-1 reverse transcription does require at least partial accessibility of the inner capsid core for cellular dNTPs. This is achieved by dNTP permeable dynamic pores in the CA hexamers (Fig. 2) (Jacques et al. 2016; Xu et al. 2020). Reverse transcription of HIV-1 is performed by co-packaged HIV-1 RT and initiated via binding of a host derived cellular tRNA, which is complementary to the primer-binding site (pbs, Fig. 3) (Flint et al. 2015; Hughes 2015). This leads to initiation of the synthesis of the (-) strand DNA and the reverse transcription of the R U5 sequence at the 5’ end of the viral RNA genome, while the RNA template strand is degraded by RNase H. This replication intermediate is called (-) strong-stop DNA. The R sequence is complementary to a respective r sequence at the 3’ end of the poly-adenylated HIV-1 RNA, which allows a template exchange and the continuation of DNA synthesis in 3’ to 5’ direction (Fig. 3) (Flint et al. 2015). Meanwhile, RNase H generates RNA fragments from the genomic RNA template, among them the polypurine tract (ppt). Ppt can serve as a primer for (+) strand DNA synthesis (Fig. 3), which terminates at the encounter of the tRNA primer due to a modified base in the tRNA. This replication intermediate is called (+) strong stop DNA. The (-) strand DNA synthesis continues until reverse transcription of the PBS (Flint et al. 2015). Complementarity between PBS of the (-) and the (+) DNA strand allows pairing and completion of the double-stranded DNA (dsDNA), which is then linearized by strand displacement (Fig. 3) (Flint et al. 2015). The final dsDNA contains two long terminal repeats (LTRs), each consistent of a sequence of U3, R and U5. LTRs are important for the subsequent integration process and contain transcription, polyadenylation and packaging signals. Stochastically, also rare circular dead-end by-products are formed if strand displacement fails or the ends of linear dsDNA self-ligate. According to the

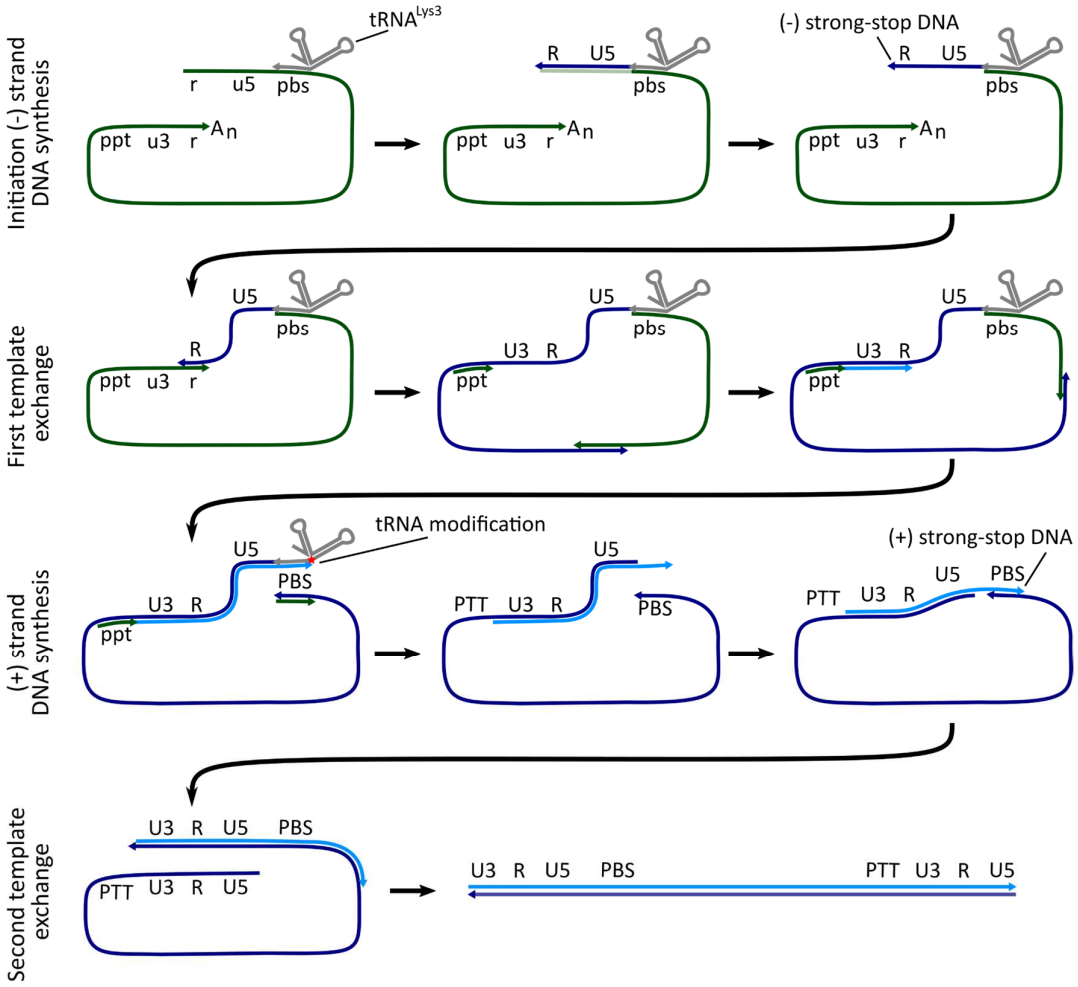

Figure 3: HIV-1 reverse transcription.

HIV-1 reverse transcription is initiated from a host-derived tRNA primer (gray) complementary to the primer-binding site (pbs). This allows priming of the (-) strand DNA synthesis (dark blue). The (-) strong-stop DNA fragment, compromises the R and U5 sequence of the HIV-1 genome. The polyadenylated (A_n) RNA template (green) is degraded by the viral RNase H. Complementarity between the R/r regions allows annealing, template exchange and continuation of reverse transcription. While the (-) strand DNA is synthesized, the (+) strand DNA synthesis (light blue) is initiated from a polypurine tract (ppt) RNA primer, generated by RNAse H digest of the genomic RNA template. (+) strand DNA synthesis stops upon encounter of a modified tRNA base. (-) strand DNA is synthesized until it reaches the 5' end of the pbs region. RNAse H-mediated cleavage of tRNA and ppt primer allows the pairing of complementary PBS DNA on both DNA strands. The resulting intermediate is called (+) strong-stop DNA. Displacement of the (-) DNA strand allows the second template exchange and subsequent termination of (-) strand and (+) strand DNA synthesis. The final linear reverse transcribed dsDNA HIV-1 genome contains long terminal repeats (LTRs) consisting of the U3, R and U5 region. The 3' end of RNA and DNA is indicated with an error (Flint et al. 2015; Hughes 2015).

presence of one or two LTRs, they are called one-LTR or two-LTR- (2-LTR) circles (Flint et al. 2015). Even though the HIV-1 capsid contains two copies of the viral RNA genome, only one dsDNA genome is generated. However, recombination and template switching between the two ssRNA templates occurs frequently (Hu and Temin 1990; Levy et al. 2004; Rawson et al. 2018).

HIV-1 integration is catalyzed by an IN tetramer bound to the LTRs, bringing together the extremities of the newly synthesized viral dsDNA and forming the pre-integration complex (Fig. 2). The 3' ends are processed and a concerted cleavage and ligation reaction is initiated, leading to a HIV-1 genome-host DNA-hybrid, the gapped intermediate (Flint et al. 2015). For gap repair, host proteins belonging to the non-homologous end-joining (NHEJ) DNA double-strand break (DSB) repair pathway, such as DNA-dependent protein kinase (DNA-PK), Ku70 and Ligase IV are required (Daniel et al. 1999; Li et al. 2001; Daniel et al. 2004; Skalka and Katz 2005; Knyazhanskaya et al. 2019). The integrated viral DNA, or provirus, now serves as a template for HIV-1 protein expression and transcription of the unspliced RNA genome (Fig. 2). Splicing is necessary to give rise to templates for translation of non-structural HIV-1 proteins and Env. Assembly of structural viral proteins and recruitment of genomic HIV-1 RNA finally leads to the release of viral particles and, after proteolytic maturation, to infectious viral progeny (Fig. 2) (Flint et al. 2015).

1.1.3 Innate immune sensing of HIV-1

Innate immune sensing of viral infections is essential to mount an effective anti-viral immune response. Sensing of viral pathogens or pathogen infection is necessary to activate, recruit and coordinate innate immune cells and effectors, to prime and sustain adaptive immune responses, as well as to coordinate the innate and adaptive immune response on the level of an organism. Sensing of pathogens is achieved through the recognition of pathogen associated molecular patterns (PAMPs) by so called pattern recognition receptors (PRR) (Murphy et al. 2012). Viral sensing through PAMPs leads to activation of downstream signaling pathways and transcription of anti-viral genes. Interferons (IFNs) and other cytokines are induced by innate immune recognition.

IFNs act in a paracrine and autocrine manner to induce and amplify the expression of anti-viral genes, so called interferon stimulated genes (ISGs), and to induce an anti-viral state (Murphy et al. 2012). IFN signaling and seems to be of particular importance early in HIV-1 infection. Transmitted or founder viruses display low IFN sensitivity (Parrish et al. 2013; Iyer et al. 2017). However, sensing of HIV-1 and the resulting IFN response is inefficient, leading to a non-optimal initiation and coordination of the innate and adaptive anti-viral immunity. Understanding HIV-1 sensing will be vital to develop novel therapeutic approaches and vaccination strategies (Yin et al. 2020).

Several HIV-1 PAMPs can be recognized by cellular PRRs early after HIV-1 entry. Incoming viral RNA was shown to be a ligand for cellular RNA sensors residing in the endolysosomal compartment, such as toll-like receptor (TLR) 7 and 8, or the cytosolic RIG-I-like receptors retinoic acid inducible gene I (RIG-I) and melanoma differentiation associated protein 5 (MDA5) (Gringhuis et al. 2010; Lepelley et al. 2011; Solis et al. 2011; Berg et al. 2012; Ringeard et al. 2019; Meås et al. 2020). TLRs signal through nuclear factor kappa-light-chain-enhancer of activated B cells (NF-κB), which is a central transcriptional regulator of innate immune genes (Murphy et al. 2012). RIG-I and MDA5 activation promotes aggregation of mitochondrion associated mitochondrial antiviral-signaling protein (MAVS), leading to the interferon response factor (IRF) mediated enhanced expression of IFNs and ISGs. Following secretion IFNs can enhance ISG expression in an paracrine and autocrine manner through signal transducer and activator of transcription 1 and 2 (STAT1/2)-dependent pathways (Ablasser and Hur 2020). In addition to sensing of incoming viral genomic RNA, *de novo* expression of intron containing HIV-1 RNA and abortive HIV-1 RNA transcripts were shown to trigger immune activation through the MAVS adaptor protein, independently of RIG-1 and MDA5 (Gringhuis et al. 2017; Akiyama et al. 2018; McCauley et al. 2018).

The HIV-1 capsid determines the breath of HIV sensing by protecting the HIV genome and thereby limiting the amount of HIV-1 nucleic acids available for sensing (Lahaye et al. 2013; Campbell and Hope 2015; Sumner et al. 2020). However, the capsid shell itself can serve as a PAMP (Yoh et al. 2015; Yoh et al. 2022). The HIV-1 capsid lattice can trigger tripartite-containing motif 5α (TRIM5α)-dependent immune signaling through the NF-κB axis, while non-POU domain-containing octamer-binding protein (NONO) can sense

HIV capsid in the nucleus through cyclic GMP-AMP synthase (cGAS) (see below) (Pertel et al. 2011; Lahaye et al. 2018).

Reverse transcription generates viral dsDNA, as well as different replication intermediates such as ssDNA and RNA:DNA hybrids, which can trigger the activation of several cytosolic PRRs. cGAS, interferon gamma inducible protein 16 (IFI16) and DEAD box helicase 41 (DDX41) were shown to be activated in response to HIV-1 reverse transcribed DNA in different cellular contexts and to induce differential downstream signaling. DDX41 can bind retroviral DNA:RNA hybrids, in mouse macrophages and DCs, resulting in stimulator of interferon genes (STING) activation (Stavrou et al. 2018). IFI16 is a DNA sensor detecting complete and abortive HIV-1 reverse transcribed DNA in macrophages and $CD4^+$ T cells isolated from tonsils (Jakobsen et al. 2013; Monroe et al. 2014). While IFI16 can stimulate the STING pathway similar to DDX41 and cGAS, it seems also able to trigger inflammasome activation and pyroptosis, a specialized form of inflammatory programmed cell death (Jakobsen et al. 2013; Monroe et al. 2014).

Whereas IFI16 and DDX41 likely contribute to HIV-1 sensing in a cell type-dependent manner, cGAS is commonly accepted as the major sensor of HIV-1 infection in immune cells (Gao et al. 2013a; Yin et al. 2020). cGAS binds DNA from cellular, bacterial and viral origin, leading to activation and aggregation of cGAS in the cytoplasm (Gao et al. 2013b; Ablasser and Hur 2020). Upon stimulation, cGAS produces the cyclic GMP-AMP dinucleotide (cGAMP), which serves as a second messenger for downstream activation of STING (Ablasser and Hur 2020). Endoplasmic reticulum resident STING binds cGAMP and upon translocation to the Golgi-apparatus serves as a platform for TANK-binding kinase 1 (TBK1) recruitment and IRF3 phosphorylation (Ablasser and Hur 2020; Zhang et al. 2020). Once phosphorylated, IRF3 translocates to the nucleus and acts as a transcription factor to induce IFN expression. Moreover, TBK1 can signal downstream via the NF-κB axis (Ablasser and Hur 2020). For HIV-1 sensing reverse transcription is required and cGAS seems to preferentially bind Y-form DNA, partially double-stranded secondary structures in the HIV-1 ssDNA (Gao et al. 2013a; Yoh et al. 2015; Herzner et al. 2015). Due to low abundancy of HIV-1 reverse transcription products in an infected cell - one copy is sufficient for productive infection - it is believed that co-sensors are required for cGAS-mediated HIV-1 sensing. In this line, the polyglutamine binding protein 1 (PQBP1) binds to HIV-1 capsid and recruits cytosolic cGAS to the HIV-1 capsid

lattice and thus to sites of HIV-1 reverse transcription (Yoh et al. 2015; Yoh et al. 2022). NONO might have a similar role in sensing HIV-1 reverse transcription products that gained access to the nucleus (Lahaye et al. 2018; Yin et al. 2020).

Concomitantly, the availability and accessibility of HIV-1 reverse transcription products critically determines the magnitude of HIV-1 sensing. By restricting the accessibility of HIV-1 PAMPs, the HIV-1 capsid is a major determinant of HIV-1 sensing (Yin et al. 2020; Zuliani Alvarez et al. 2022). Also, TREX1, a cellular DNA exonuclease, critically influences the amount of HIV-1 DNA available for cGAS activation (Yan et al. 2010; Wheeler et al. 2016; Kumar et al. 2018). In conclusion, cellular factors influencing HIV-1 entry, reverse transcription and uncoating might have dramatic effects on cell type specific sensing, as well as on the initiation, the breath and concertation of innate and adaptive responses, making them attractive targets to improve HIV-1 (immune-) therapy and vaccination (Schott et al. 2017; Yin et al. 2020).

1.1.4 Restriction factors interfere with HIV replication at multiple levels

Host proteins can not only be beneficial for virus replication. Some cellular factors have the capability to strongly inhibit viral replication and are therefore termed anti-viral restriction factors (Harris et al. 2012). Restriction factors typically promote a reduction in viral infectivity or production of progeny virus over several orders of magnitude. Some of them are able to completely block viral replication or transmission. This has important implications in zoonotic infections. Species barriers can only be overcome, when viruses are able to coopt with new, host specific restriction factors (Sauter and Kirchhoff 2019). Viruses do so by implementing counteracting measures (Harris et al. 2012; Malim and Bieniasz 2012). This can be achieved by avoidance of the anti-viral restriction, *i.e.*, through changes in the viral target structure, the viral life cycle, the cellular tropism or alternative infection routes. In addition, viruses have evolved direct counteraction mechanism, so called counteracting factors, actively preventing the action of a given restriction factor. Often these counteracting factors are accessory proteins or viral effector proteins. In the case of HIV-1 Vif, Vpu, Vpr and Nef, but also the structural protein Env counteract cellular restriction factors (Fig. 4) (Harris et al. 2012; Malim and Bieniasz 2012). Prevention of expression, proteolytic cleavage or targeting for

degradation, post-translational modification, blocking of interaction sites, as well as retargeting to different cellular compartments or complexes can be modes of actions.

Restriction factors are broad acting. They target shared viral structures or characteristic requirements of the viral life cycle rather than specific viral protein epitopes or nucleic acid sequences. The evolution of an effective restriction factor is shaped by a history of diverse viral infections. Since restriction factors also impose a strong selective pressure towards the pathogen, this leads to an arms race between host and pathogen and to traits of rapid positive selection such as a high ratio of synonymous to non-synonymous mutations (Duggal and Emerman 2012).

Restriction factors are commonly understood as part of the intrinsic or innate immune system and as such are heavily connected to innate sensing and signaling pathways. *I.e.* most restriction factors are induced by IFN treatment and belong to the class of ISGs (Harris et al. 2012; Schott et al. 2017).

Similar to host dependency factors, a number of HIV-1 restriction factors were identified by genetic perturbation screens, in presence or absence of IFN stimulation (Liu et al. 2011; OhAinle et al. 2018; Jimenez-Guardeño et al. 2019; OhAinle et al. 2020). Also, overexpression of ISGs was used to screen for candidate anti-viral factors (Schoggins et al. 2011; Schoggins et al. 2014). However, another strategy proved to be successful in the context of HIV-1 restriction. Lentiviruses heavily rely on rewiring the host proteasome and lysosome degradation pathways for depletion of cellular restriction factors. Proteomic profiling approaches, as well as the analysis of the HIV effector protein interactome, were extremely productive in identifying factors that block lentiviral replication (Berger et al. 2011; Hrecka et al. 2011; Jäger et al. 2011; Laguette et al. 2011; Chougui et al. 2018; Yurkovetskiy et al. 2018; Greenwood et al. 2019; Liu et al. 2019; Naamati et al. 2019). Several selected anti-lentiviral restriction factors are highlighted in Figure 4. In HIV-1 infection, restriction factors limit the production, shedding and infectivity of HIV-1 particles.

A famous and potent example is tetherin, which is able to block the release of HIV-1 particles from infected cells, in a manner enhanced by IFN signaling (Neil et al. 2007; Neil et al. 2008; Perez-Caballero et al. 2009; van Damme et al. 2008; Liberatore and Bieniasz 2011). Tetherin does so by physically tethering budding HIV-1 particles on the

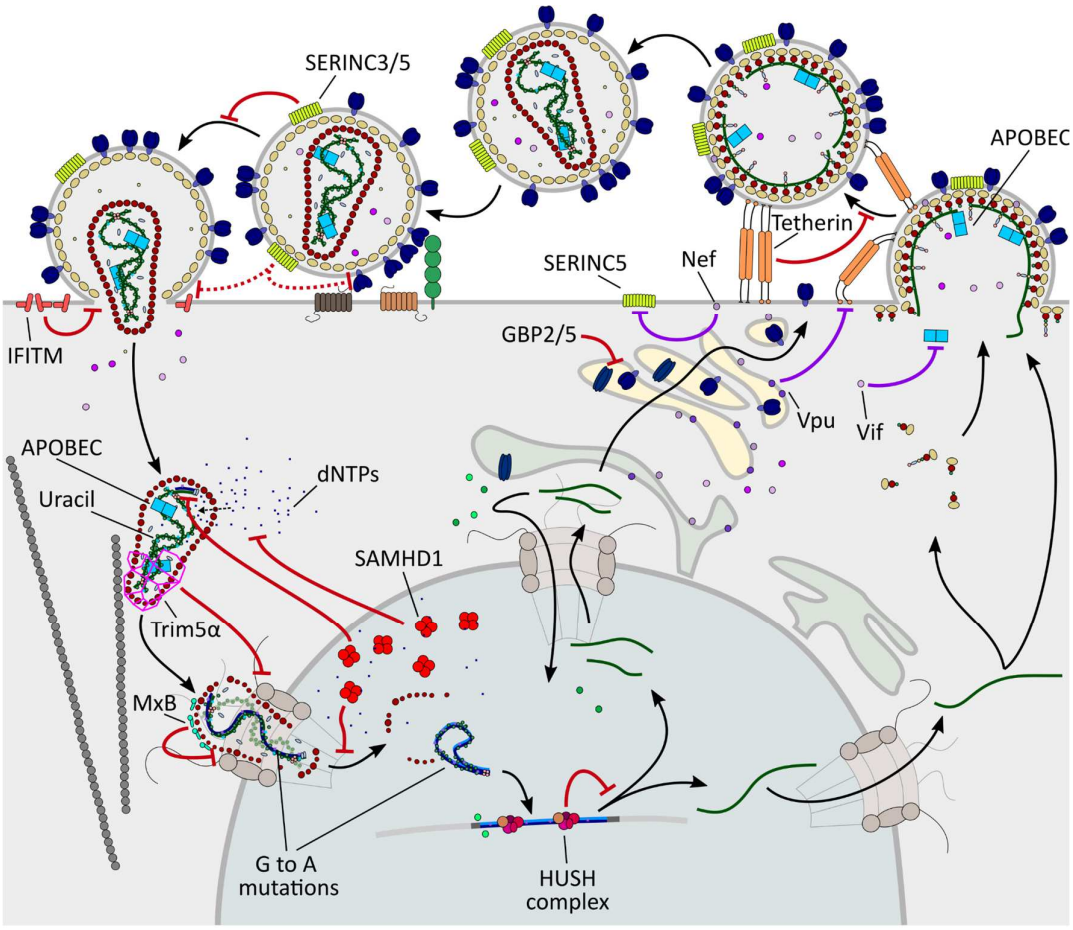

Figure 4: Restriction factors active against HIV-1.

Overview of relevant restriction factors active against specific steps of HIV-1 replication (red blunt arrows) and counteracting mechanisms (purple blunt arrows) employed by viral effector proteins. HIV-1 translation is suppressed by the human silencing hub (HUSH) complex, through epigenetic silencing and RNA degradation (Chougui et al. 2018; Yurkovetskiy et al. 2018; Seczynska et al. 2022; Matkovic et al. 2022). Guanylate-binding protein 2 and 5 (GBP2/5) inhibit processing of HIV-1 Env by interfering with furin cleavage (Krapp et al. 2016; Braun et al. 2019). Tetherin physically retains budding HIV-1 particles by sequestering them at the plasma membrane (Neil et al. 2008; Perez-Caballero et al. 2009; Hinz et al. 2010). Tetherin surface expression is reduced by HIV-1 effector Vpu-mediated E3 ubiquitin ligase recruitment and proteasomal degradation, as well as endolysosomal translocation and interference with tetherin trafficking (Neil et al. 2008; van Damme et al. 2008; Goffinet et al. 2009; Iwabu et al. 2009; Mitchell et al. 2009; Dubé et al. 2011). Serine incorporator 5 and 3 (SERINC3/5) become part of the viral envelope at budding and inhibit viral entry by interfering with fusion pore formation or Env protein rearrangement after binding to CD4. The HIV-1 effector Nef prevents SERINC5 incorporation through endocytosis and lysosomal degradation of SERINC5 in the producing cell (Cano-Ortiz et al. 2022). HIV-1 fusion is also inhibited by IFN-induced transmembrane proteins (IFITMs) localized at the target cell membrane (Marziali

and Cimarelli 2021). Myxovirus resistance B (MxB) and tripartite-containing motif 5α (Trim5α) bind to the capsid and inhibit HIV-1 nuclear entry. Trim5α forms cage like structures on the capsid lattice in absence of CypA, while MxB seems to interfere with the interaction of CA with host factors, such as nucleoporins (Stremlau et al. 2004; Goujon et al. 2013; Kane et al. 2013; Liu et al. 2013; Dicks et al. 2018; Kane et al. 2018; Staeheli und Haller 2018; Kim et al. 2019b; Selyutina et al. 2020b; Yu et al. 2020). Apolipoprotein B mRNA-editing enzyme catalytic polypeptide-like proteins (APOBECs) are co-packaged into budding HIV-1 particles and associate to HIV-1 RNA. Through cytosine deamination they generate uracil residues, which upon reverse transcription leads to G to A hypermutation in the HIV-1 genome. HIV-1 Vif recruits an E3 ubiquitin ligase complex to efficiently deplete APOBEC3G in the producing cell (Harris und Dudley 2015). Sterile alpha motif and HD domain containing protein (SAMHD1) is a dNTPase mainly localizing in the nucleus, which blocks HIV-1 reverse transcription. SAMHD1 may act through depletion of cellular dNTPs, which are required for HIV-1 reverse transcription (Majer et al. 2019).

surface of cells, which is achieved by its unusual architecture, *i.e.* a transmembrane region and a glycosylphosphatidylinositol anchor separated by a long coiled-coil domain (Fig. 4) (Perez-Caballero et al. 2009; Hammonds et al. 2010; Hinz et al. 2010). To overcome tetherin-mediated restriction, HIV-1 Vpu reduces tetherin surface levels by recruitment of an E3 ligase and proteasomal degradation, via endo-lysosomal sequestration and by interference with tetherin trafficking (Neil et al. 2008; van Damme et al. 2008; Goffinet et al. 2009; Iwabu et al. 2009; Mitchell et al. 2009; Dubé et al. 2011). Guanylate-binding protein 2 and 5 (GBP2/5) reduce the infectivity of HIV-1 particles produced from interferon simulated macrophages and $CD4^+$ T cells. GBP5 and GBP2 act by interfering with host protease furin-mediated cleavage of the HIV-1 Env precursor, which is required for CD4 receptor-mediated entry (Fig. 4) (Krapp et al. 2016; Braun et al. 2019).

Serine incorporator 5 (SERINC5) and to a lesser extent SERINC3 inhibit HIV-1, when incorporated into the membrane of budding viruses (Fig. 4) (Rosa et al. 2015; Usami et al. 2015; Cano-Ortiz et al. 2022). Even though the exact mechanism is not yet clear, SERINC5 seems to affect the fusion process by altering the fusion pore, or by interfering with HIV-1 Env protein conformation (Cano-Ortiz et al. 2022). SERINC5 is only incorporated in the absence of the HIV-1 accessory protein Nef. Nef reduces SERINC5 surface expression by recruitment of the cyclin-dependent kinase 13 (CDK13)-cyclin K complex, followed by adaptor protein complex 2-dependent endocytosis and lysosomal

degradation (Fig. 4) (Rosa et al. 2015; Usami et al. 2015; Shi et al. 2018; Passos et al. 2019; Staudt and Smithgall 2020; Chai et al. 2021; Cano-Ortiz et al. 2022).

IFN-induced transmembrane proteins (IFITMs) expressed on the plasma membrane and in the endocytic compartment inhibit HIV-1 entry, likely by altering the membrane dynamics in the target cells (Fig. 4) (Lu et al. 2011; Li et al. 2013; Marziali and Cimarelli 2021). Also, IFITMs have been shown to reduce particle infectivity and production by incorporation into the HIV-1 envelope and by interfering with HIV-1 protein expression (Compton et al. 2014; Tartour et al. 2014; Yu et al. 2015; Lee et al. 2018b; Marziali and Cimarelli 2021). The latter might be partially counteracted by Nef (Ahmad et al. 2019). Interestingly, transmitted founder viruses exhibit reduced sensitivity towards IFITMs, indicating that HIV-1 can at least partially circumvent IFITM-mediated restriction (Foster et al. 2016).

Apolipoprotein B mRNA-editing enzyme catalytic polypeptide-like (APOBEC) is a family of cellular cytosine deaminases, which are able to confer cytosine to uracil on ssDNA templates (Harris et al. 2002; Nabel et al. 2013; Harris and Dudley 2015). Although, APOBEC3G is the most extensively studied APOBEC in the context of HIV-1 restriction, APOBEC3D, F and H also show anti-lentiviral activity in human T cells (Harris et al. 2003; Hultquist et al. 2011; Harris and Dudley 2015). APOBECs are co-packaged into budding HIV-1 particles upon viral assembly, a process which involves RNA and HIV-1 Gag binding (Fig. 4) (Schäfer et al. 2004; Bogerd and Cullen 2008; Apolonia et al. 2015; Harris and Dudley 2015). With the infection of a new host cell and initiation of reverse transcription, the ssDNA template in form of the partially reverse transcribed HIV-1 genome becomes available for APOBEC cytosine to uracil editing. The HIV-1 RT reads uracil as thymine or deoxythymidine (dT) in ssDNA, ultimately leading to deoxyguanosine (dG) to deoxyadenosine (dA), or G to A, hypermutation, which can be lethal or sub-lethal and eventually cause to degradation of the viral genome (Fig. 4) (Harris et al. 2003; Mangeat et al. 2003; Zhang et al. 2003; Harris and Dudley 2015). The HIV-1 accessory protein Vif is a potent counteraction mechanism against APOBEC3G. Vif recruits the cullin-5-RING E3 ubiquitin ligase complex to APOBEC3G in productively infected cells, thereby causing proteasomal degradation of APOBEC3G (Fig. 4) (Mariani et al. 2003; Sheehy et al. 2003; Yu et al. 2003). Retroviral and APOBEC co-evolution has led to positive selection and diversity in APOBEC genes, as well as to an adapted HIV-1

Vif being able to target human APOBEC3D, F, G and H for degradation (Compton et al. 2012; Sauter and Kirchhoff 2019; Ito et al. 2020).

TRIM5α was originally described as a species specific restriction factor, which forms cage-like structures on the lentiviral capsid lattice (Fig. 4) (Stremlau et al. 2004; Yu et al. 2020). Subsequent studies showed however that also human TRIM5α is capable to efficiently restrict HIV-1 in human macrophages and $CD4^+$ T cells, but only in the absence of CypA. Interestingly, CypA prevents Trim5α through concurrence for the CA binding site (Kim et al. 2019b; Selyutina et al. 2020b).

Myxovirus resistance B (MxB) is a potent interferon induced restriction factor inhibiting an HIV-1 post-entry step (Goujon et al. 2013; Kane et al. 2013; Liu et al. 2013). MxB binds to the HIV-1 capsid lattice in the cytoplasm, and inhibits nuclear uptake of HIV-1 capsid or PIC, possibly via interference with binding of one or several host factors such as CypA, nucleoporins or transportin-1 (TNPO1) (Liu et al. 2013; Kane et al. 2018; Dicks et al. 2018; Staeheli and Haller 2018). HIV-1 CA mutants were observed that escape MxB binding and restriction. Nevertheless, MxB escape mutants rarely occur, indicating a significant fitness cost of MxB counteraction (Goujon et al. 2013; Kane et al. 2013; Liu et al. 2013).

An example for restriction factors which inhibit HIV-1 expression post-integration is the human silencing hub (HUSH) complex consisting of transcription activation suppressor (TASOR), meta-phase phosphoprotein 8 (MPP8) and periphilin. HUSH limits HIV-1 expression in $CD4^+$ T cells and T cell lines (Fig. 4) (Chougui et al. 2018; Yurkovetskiy et al. 2018). It was shown that the HUSH complex mediates epigenetic silencing of intron-less mobile elements (Tchasovnikarova et al. 2015; Tunbak et al. 2020; Seczynska et al. 2022). Also, the HUSH component TASOR seems to recruit the CR4-NOT transcription complex subunit 1 (CNOT1) RNA degradation pathway to repress LTR driven HIV-1 expression (Matkovic et al. 2022). HIV-2 and SIV Vpx and several Vpr accessory proteins from different HIV-2 strains and SIV lineages are able to mark TASOR for proteasomal degradation by enhancing the interaction of TASOR with the DCAF ubiquitin ligase adaptor (Chougui et al. 2018; Yurkovetskiy et al. 2018). However somewhat surprising, HIV-1 and SIVcpz Vpr is not able to degrade TASOR, implying that the HIV-1 ancestors have lost their HUSH counteraction activity (Chougui et al. 2018; Yurkovetskiy et al. 2018; Sauter and Kirchhoff 2019).

Taken together, the HIV-1 life cycle is inhibited at multiple steps by diverse restriction mechanisms, which led to the evolution of effective counteracting mechanisms executed by HIV-1 effectors. Again, the recent identification of novel confirmed and potential restriction factors (Chougui et al. 2018; Yurkovetskiy et al. 2018; Hiatt et al. 2021a), illustrates that the cell intrinsic anti-viral networks are not yet completely uncovered.

1.2 SAMHD1 is a major anti-lentiviral restriction factor

1.2.1 SAMHD1 is a dNTPase with multiple cellular functions

Sterile alpha motif and HD domain containing protein (SAMHD1) is a potent anti-viral restriction factor active against a broad range of human pathogens (Fig. 5). Importantly, SAMHD1 is also a central regulator of cellular nucleic acid homeostasis and involved in multiple steps of DNA replication and repair processes (Fig. 5) (Majer et al. 2019). Likely, the anti-viral activity of SAMHD1 and its homeostatic functions are interconnected. Therefore, it is essential to understand the cellular functions of SAMHD1 in absence of viral infection, in order to understand how it acts as a restriction factor active against HIV-1 and other viruses. SAMHD1 is expressed in most human tissues and cells, but shows a higher expression in immune cells, namely in different T cell, monocyte, macrophage and DC subsets. In concordance with this, SAMHD1 expression clusters with genes associated with monocytes, macrophages and DCs (Uhlén et al. 2015; Uhlen et al. 2019; Karlsson et al. 2021). Only some immortalized cell lines show moderate to high SAMHD1 expression (Uhlén et al. 2015). Most cell lines show very low levels of SAMHD1 and expression is generally downregulated in cancer cells (Schott et al. 2022). SAMHD1 expression is regulated by transcription factors, promotor methylation and micro RNAs (Silva et al. 2013; Jin et al. 2016; Yang et al. 2016; Riess et al. 2017). Even though in a cell type-dependent manner, IFN seems to modestly upregulate SAMHD1 expression by IRF3 binding to the SAMHD1 promotor and microRNA downregulation. SAMHD1 is therefore considered an ISG (Yang et al. 2016; Riess et al. 2017).

SAMHD1 contains a SAM and an HD domain (Fig. 6A and C). SAM domains are known to mediate protein-protein interactions with SAM-containing and non-containing proteins,

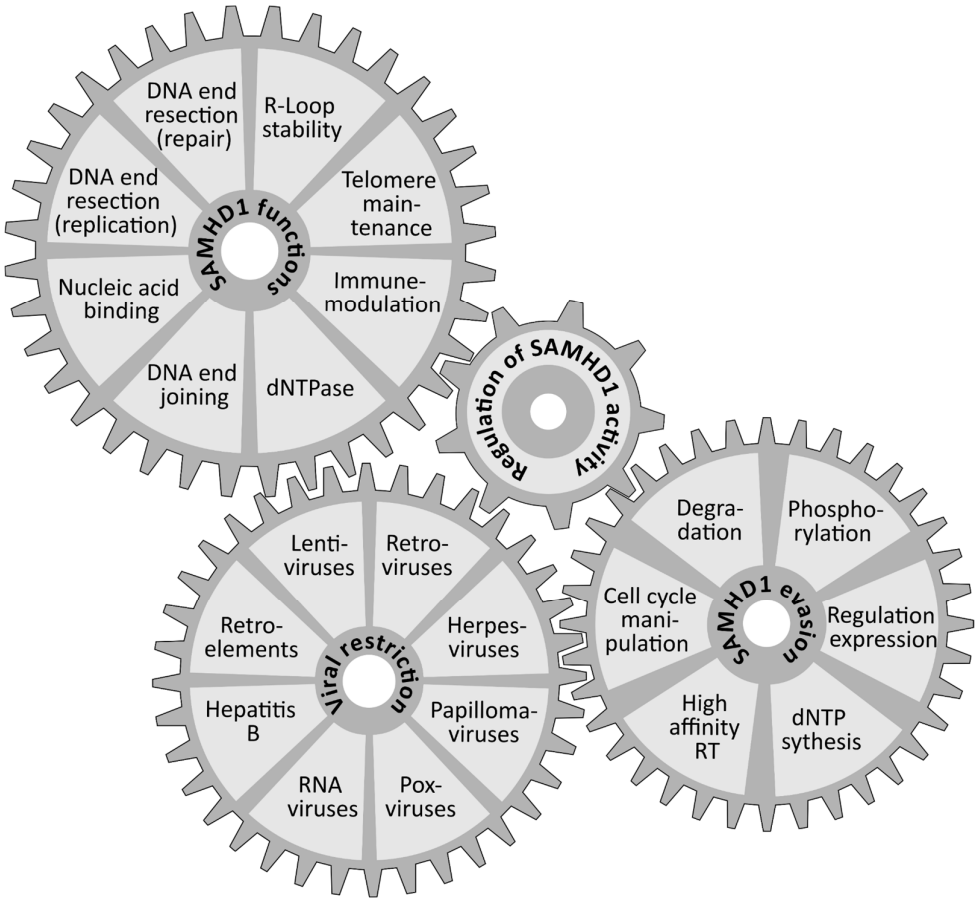

Figure 5: Cellular and anti-viral functions of SAMHD1.

SAMHD1 is a multifunctional protein. Its role in the maintenance of cellular homeostasis is strongly intertwined with anti-viral restriction and viral evasion mechanisms, as well as the regulation of SAMHD1 (Majer et al. 2019). SAMHD1 is the major cellular dNTPase but was also shown to function in DNA repair and replication, by enhancing DNA end resection. SAMHD1 modifies DNA end joining, telomere maintenance and R-loop stability and seems to directly interfere with innate immune signaling pathways (Majer et al. 2019; Akimova et al. 2021; Park et al. 2021). It is currently unclear which cellular function(s) of SAMHD1 mediate its capability to restrict diverse human viruses. SAMHD1 was shown to inhibit reverse transcribing viruses, such as lenti- and non-lenti retroviruses, as well as Hepatitis B virus and retroelements, but also herpesviruses and poxviruses, which are large DNA viruses (Businger et al. 2019; Kim et al. 2019a; Majer et al. 2019). More recently, SAMHD1 was proposed to affect small DNA papillomavirus replication and, surprisingly, to be able to inhibit RNA viruses (James et al. 2019; Li et al. 2020; Silva et al. 2021). A block to viral replication imposed by SAMHD1 exerts substantial pressure towards a virus and favors the evolution of efficient counteracting mechanisms. Degradation of SAMHD1 is achieved by different lentiviral Vpx and Vpr proteins, but also by HCMV and enterovirus 71 (Sauter et al. 2019; Hyeon et al. 2020; Li et al. 2020). Also, SAMHD1 transcription might be regulated by viral factors.

Other evasion strategies are the use of high affinity reverse transcriptases (RTs) to overcome low dNTP levels, or increasing dNTP *de novo* syntheis (Majer et al. 2019). Moreover, the anti-viral function of SAMHD1 is influenced by different regulatory mechanisms. Post-translational modification, namely phosphorylation at residue T592, leads to loss of restriction against HIV-1, but also herpesviruses (Majer et al. 2019; Businger et al. 2019; Kim et al. 2019a). Herpesviruses can induce SAMHD1 phosphorylation by virus encoded kinases (Businger et al. 2019; Kim et al. 2019a). In addition, since SAMHD1 T592 phosphorylation is cell cycle-dependent, perturbation of the cell cycle, *i.e.* by lentiviral effector proteins affects SAMHD1 pT592 status and therefore its anti-viral restriction capacity (Majer et al. 2019). Illustration adapted from Majer et al. 2019.

but also to mediate interactions with nucleic acids in some cases (Qiao and Bowie 2005). However, to date no physiological SAM-dependent interaction has been identified for human SAMHD1 (Majer et al. 2019).

When active, SAMHD1 forms tetramers. To present, only the HD domain could be crystallized, both as monomer and tetramer (Fig. 6B) (Ji et al. 2014). However, artificial intelligence-mediated structural modelling, such as AlphaFold allows the prediction of SAM domain structure and the position of the C- and N-terminus (Fig. 6C to E) (Pettersen et al. 2021; Jumper et al. 2021) While modelling of the structured HD domain shows a high degree of confidence and large overlaps with the results from crystallography, especially the prediction of the N- and C terminus is less confident, suggesting flexibility (Fig. 6 D and E) (Ji et al. 2014).

SAMHD1 harbors an N-terminal nuclear localization signal formed by the residues ^{11}KRPR^{14} and is predominantly localized nuclear (Fig. 6A and C) (Brandariz-Nuñez et al. 2012). The HD domain of is situated between residue 110 and 599 and is named after the central catalytic histidine (H206) and aspartate (D207) residues (Fig. 6A and C). The structure of its catalytic core is shared among a superfamily of metal-dependent phosphohydrolases (Fig. 6F and G) (Aravind and Koonin 1998). Consistently, SAMHD1 was found to have phosphohydrolases activity and to convert all four deoxyribonucleoside triphosphates (dNTPs), deoxyadenosine triphosphate (dATP), deoxyadenosine triphosphate (dGTP), deoxycytidine triphosphate (dCTP) and deoxythymidine triphosphat (dTTP) into triphosphate and the respective nucleotide.

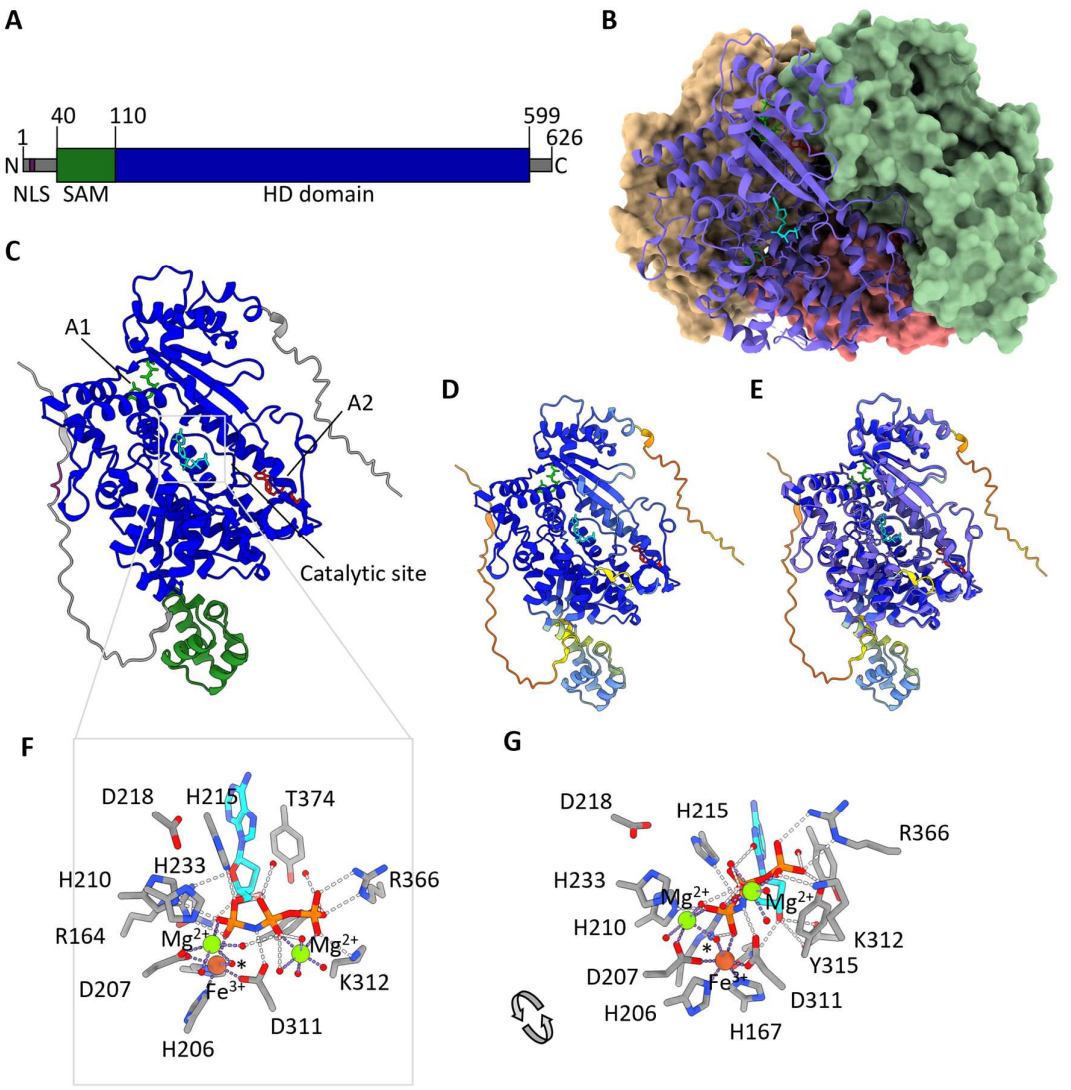

Figure 6: SAMHD1 domains and structure.

(A) The SAM (40-109) and a HD domain (110-599), as well as the N-terminal nuclear localization signal (NLS; 11-14) are shown for SAMHD1 (Ahn et al. 2016). **(B)** Crystal structure of the SAMHD1 tetramer is illustrated as determined by Ji et al. 2014 (4TO0) for the SAMHD1 113-626 H206R_D207N mutant activated with allosteric activators GTP (green) and dATP (red). The substrate dCTP is shown in light blue. Secondary structure of one SAMHD1 monomer is highlighted. Large parts of the SAMHD1 structure cannot be crystallized due to the high degree of flexibility in the N- and C-terminus, as well as internal loops. **(C)** For visualization SAMHD1 was modeled using AlphaFold protein structure prediction (Q9Y3Z3) (Jumper et al. 2022). SAMHD1 domains are colored as in **(A)**. The allosteric binding sites A1 and A2 are occupied by GTP and dATP, respectively. In the catalytic center dCTP was placed. The position of the nucleotides was modeled by structural comparison between the AlphaFold prediction and the SAMHD1 structure by Ji et al. 2014, using the Matchmaker tool of ChimeraX (Petterson et al. 2021). **(D, E)** As anticipated the

fidelity of the predicted structure of the flexible N- and C-terminus is low (red to yellow). However, the structure of the SAMHD1 HD domain was modeled with high confidence (blue) and strongly overlaps with the crystallographic data (purple). The model of the SAM domain was obtained with medium fidelity (yellow to blue), although the position with respect to the HD domain might be variable. **(F, G)** The composition of the catalytic site as determined by Morris et al. 2020 (6TX0) for the residues 109-626 of the SAMHD1 D137N mutant in complex with a non-cleavable dATP homolog (dAMPNPP) is shown. The position and identity of the amino acids forming the catalytic pocket, as well as iron and magnesium ions are highlighted. The water molecule coordinated by Mg^{2+} and Fe^{3+}, which is used for nucleophilic attack is marked by an asterisk.

Thereby, SAMHD1 is able to deplete cellular dNTPs and to reduce the dNTP pool size (Goldstone et al. 2011; Powell et al. 2011; Lahouassa et al. 2012; Franzolin et al. 2013). The deoxyribonucleoside triphosphate triphosphohydrolase (dNTPase) activity of SAMHD1 is uncommon and apart from SAMHD1 only found in few enzymes isolated from bacteria (Kondo et al. 2007; Langton et al. 2020). Recently, the enzymatic activity of SAMHD1 has been characterized in more detail and was shown to depend on two central metal ions that coordinate a hydroxide molecule for nucleophilic attack and resolution of the phosphoester bond (Fig. 6 F and G) (Morris et al. 2020).

The dNTPase activity of SAMHD1 is regulated by allosteric binding of GTP or dGTP and any dNTP at the allosteric sites A1 and A2, respectively (Fig. 6C) (Goldstone et al. 2011; Powell et al. 2011; Ji et al. 2013; Hansen et al. 2014). Allosteric occupancy of A1 results in SAMHD1 dimerization, while dNTP binding to A2 leads to a SAMHD1 tetramer with full enzymatic activity (Fig. 6B) (Ji et al. 2013; Yan et al. 2013; Hansen et al. 2014). GTP is thought to be a main activator of SAMHD1 due to its high abundancy and to its ability to maintain the active SAMHD1 tetramer even after dNTP depletion (Amie et al. 2013; Hansen et al. 2014).

SAMHD1 is a major regulator of cellular dNTP levels (Rampazzo et al. 2010; Franzolin et al. 2013). However, cellular dNTP levels are also regulated by the ribonucleoside-diphosphate reductase (RNR), which catalyzes dNTP *de novo* synthesis. RNR activity is partially regulated in a cell cycle-dependent manner by R2 subunit degradation at mitotic exit (Chabes and Thelander 2000). Dysregulated dNTP levels can have dramatic consequences for cellular homeostasis (Mathews 2015). While sufficiently high dNTP levels are critical for DNA replication in S-Phase, constitutively high levels of dNTPs can lead to cell cycle arrest (Chabes and Stillman 2007). Excessive dNTP levels can cause the

mutator phenotype, which is marked by an increased rate of spontaneous mutations due to replication infidelity (Weinberg et al. 1981; Buckland et al. 2014; Williams et al. 2015). This is more significant when dNTP levels are imbalanced (Kumar et al. 2011; Buckland et al. 2014; Watt et al. 2016; Schmidt et al. 2019b). In addition, by altering dNTP levels, SAMHD1 affects DNA damage repair. The NHEJ pathway is used to repair DNA DSBs in non-cycling cells, by re-joining processed DNA ends. Processing leads to random insertions and deletions (InDels) at the repair site. In absence of SAMHD1, increased dNTP levels lead to longer insertions due to enforced polymerase processivity (Akimova et al. 2021). In conclusion, the dNTP metabolism and therefore SAMHD1 is of importance for both, the emergence of cancer and the maintenance cancer cell replication, and is thus an attractive target for medical therapies (Schott et al. 2022). This is even more true since SAMHD1 was shown to degrade important nucleoside based anti-cancer metabolites (Herold et al. 2017a; Herold et al. 2017b; Schneider et al. 2017). Not surprisingly a number of SAMHD1 mutations are associated with different types of cancer (Schott et al. 2022).

Early after its discovery and the description of its dNTPase activity, SAMHD1 was proposed to have single stranded nucleic acid binding activity with a preference for ssRNA (Goncalves et al. 2012; Beloglazova et al. 2013; Tüngler et al. 2013; Seamon et al. 2015). Binding of ssRNA or ssDNA to SAMHD1, *i.e.* to the dimer-dimer interface, might regulate SAMHD1 complexation and thus influence other functions of SAMHD1, such as the dNTPase activity (Seamon et al. 2016). The initially observed ssRNA and ssDNA directed nuclease activity of SAMHD1 was later revealed to result from co-purification impurities (Seamon et al. 2015).

More recently, SAMHD1 was implemented in DNA replication and DNA repair (Daddacha et al. 2017; Coquel et al. 2018). DNA replication, especially under stress, can lead to stalled replication forks. In order to allow progression and completion of DNA replication, stalled forks need to be resolved, which requires processing by exonucleases, so called end resection (Quinet et al. 2017). SAMHD1 was proposed to participate in this process, by an interaction with MRE11 and the stimulation of MRE11 exonuclease activity (Coquel et al. 2018). Similarly, SAMHD1 was proposed to recruit CtIP, another exonuclease, to sites of DNA damage (Daddacha et al. 2017). Homologous recombination (HR) is a DNA DSB repair pathway, which requires a homologue DNA

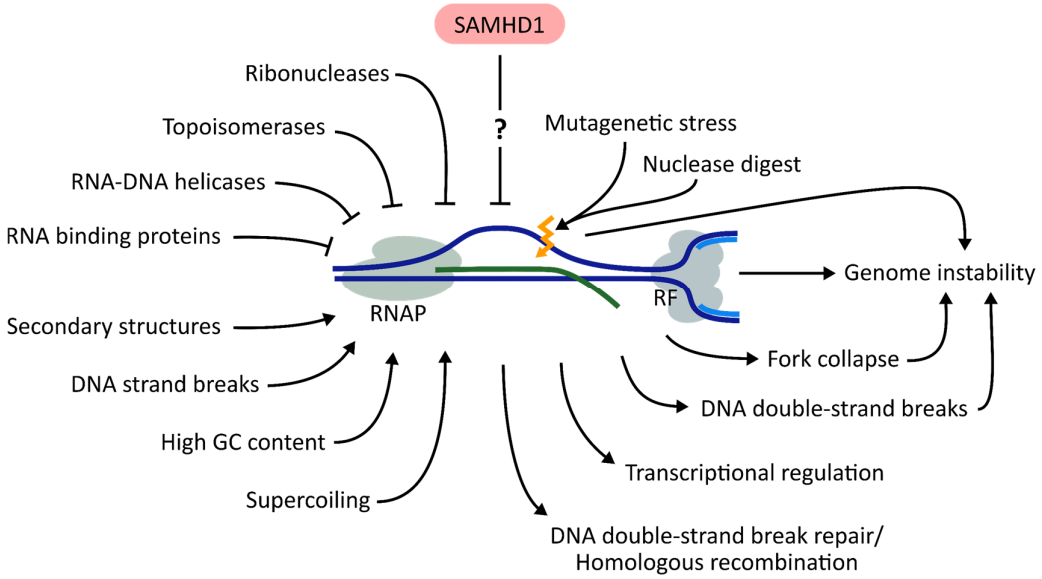

Figure 7: R-Loops.

R-loops are RNA:DNA hybrid structures physiologically occurring at sites of transcription replication conflicts. Both co- and anti-directional processing of RNA polymerase (RNAP) and replication forks (RFs) can stabilize R-loops. R-loops are regulated by RNA binding proteins, RNA-DNA helicases, topoisomerases and ribonucleases. Recently, SAMHD1 was suggested to inhibit R-loops through a not further defined mechanism. R-loops loops occurring at transcription replication conflicts are favored by secondary structures in the ssDNA, a high GC content in actively transcribed genes and DNA supercoiling. Also, R-loops can be induced by DNA double- or single-strand breaks. Conversely, R-loops are involved in DNA double-strand break repair by homologous recombination. In addition, they seem to play a role in transcriptional regulation. In R-loops, the ssDNA loop is accessible to mutagenic stress and nuclease digest, which is one mechanism leading to R-loop induced genome instability. In addition, non-resolved R-loops can lead to DNA double-strand breaks or RF collapse, again increasing the cellular burden of genome instability (García-Muse and Aguilera 2019; Hegazi et al. 2020; Park et al. 2021).

region, *i.e.* a sister chromatid, to serve as a template for DNA repair. Processing of DNA DSB ends is required for HR, which can be achieved by CtIP (Ranjha et al. 2018). Thus, recruitment of exonucleases for dsDNA processing seems a shared mechanism of SAMHD1 in DNA repair and the resolution of stalled replication forks (Majer et al. 2019). In addition to this, SAMHD1 was proposed to be involved in the prevention of R-loops. R-loops are DNA-RNA hybrid structures (Fig. 7). Using RNA:DNA hybrid sequencing, Park et al. could detect an accumulation of R-loops in SAMHD1 deficient fibroblasts (Lim et al. 2015; Park et al. 2021). R-Loops physiologically occur at sites of transcription-

replication conflicts and are thought to be involved in transcriptional regulation, but also to cause DNA instability (Fig. 7) (García-Muse and Aguilera 2019). Exposed ssDNA in R-loops is prone to mutagenic stress or nucleases. Stabilized R-loops can lead to replication fork collapse and DNA DSBs (Fig. 7) (García-Muse and Aguilera 2019). Accordingly, cells actively avoid R-loops by a battery of cellular factors, such as RNA binding proteins, topoisomerases, RNA-DNA helicases and ribonucleases such as RNase H1/2 (Fig. 7) (García-Muse and Aguilera 2019). In contrast, R-loop formation is enhanced by negative supercoiling, nicks or secondary structures in the DNA, as well as GC-rich transcriptionally active regions. Also, defects in RNase H and RNA-DNA helicases can favor R-loop formation (Fig. 7) (Hegazy et al. 2020; Cristini et al. 2022). Moreover, R-loops have been shown to be facilitated by single-strand and double-strand DNA breaks, but also to enhance DNA DSB repair by HR (Fig. 7) (García-Muse and Aguilera 2019; Hegazy et al. 2020; Ouyang et al. 2021). The notion that SAMHD1 is involved in R-loop biology underlines its role as an important regulator of the nucleic acid metabolism.

Besides, SAMHD1 seems to modulate several additional cellular processes, such as telomerase maintenance, immunoglobulin hypermutation and class switch recombination, the post-transcriptional control of regulatory T cell transcription factors, as well as leukemic cell line proliferation and apoptosis (Bonifati et al. 2016; Kodigepalli et al. 2018; Kim et al. 2018; Majerska et al. 2018; Thientosapol et al. 2018; Husain et al. 2020). Even though, the detailed functional connections are not yet resolved, this makes clear that SAMHD1 is a critical factor in multiple processes ranging from maintenance of cellular homeostasis and carcinogenesis, to shaping adaptive immune responses.

Mutations in SAMHD1 have not only been associated with cancer, but also with inflammatory syndromes. Namely, mutations in *SAMHD1* can be causative for the Aicardi-Goutières syndrome (AGS) (Rice et al. 2009; Crow et al. 2015; Schott et al. 2022). AGS is an auto-inflammatory disease, which is marked among others by severe neuro-inflammation and developmental disorders. Besides SAMHD1, mutations in other proteins involved in the cellular nucleic acid metabolism such as the major DNA exonuclease TREX1, ribonuclease RNase H2 subunits RNase H2A, B and C, the adenosine deaminase RNA-specific binding protein 1 (ADAR1), as well as in the RIG-I-like receptor MDA5 can cause AGS (Crow et al. 2015). In all cases, the common mechanism of auto-inflammation seems to be dysregulation of the nucleic acid metabolism and, as a

consequence, aberrant DNA damage and/or nucleic acid sensing, leading to elevated IFN levels and systemic inflammation (Rice et al. 2009; Crow et al. 2015). With regards to impaired SAMHD1 function, several pathways to innate immune stimulation via nucleic acid sensing are plausible (Majer et al. 2019; Schott et al. 2022). As described above, SAMHD1 mutation leads to aberrant cellular dNTP levels, which is likely to mediate genomic instability and DNA damage signaling (Kretschmer et al. 2015). Additionally, in the absence of SAMHD1, resolution of stalled replication forks or DNA damage-response might be inhibited, because SAMHD1-mediated recruitment of endonucleases and dsDNA trimming is impaired. This again could lead to aberrant translocation of nascent ssDNA into the cytoplasm. ssDNA might self-hybridize and activate the cGAS-STING DNA sensing pathway, ultimately leading to the induction of IFN and ISGs (Härtlova et al. 2015; Coquel et al. 2018; Schott et al. 2022). Similarly, R-loops have recently been identified as a source of immunostimulatory ssDNA in DNA damage response, as well as TREX1 and RNAse H2 deficiency (Chatzidoukaki et al. 2021; Cristini et al. 2022; Giordano et al. 2022). Finally, SAMHD1 was also proposed to actively suppresses innate immune signaling, by interfering with the NF-κB signaling pathway at multiple levels (Chen et al. 2018; Espada et al. 2021). By inhibiting this pathway, SAMHD1 might modulate baseline inflammatory signaling and/or sensing of endogenous nucleic acids. In summary, SAMHD1 is a central regulator of the cellular nucleic acid metabolism, mainly through its role as the major cellular dNTPase, but also as a key component in the DNA replication and DNA damage responses.

1.2.2 SAMHD1 is an anti-viral restriction factor limiting HIV-1 replication

The accessory protein Vpx is expressed by several primate lentiviruses, namely, HIV-2, as well as SIV from sooty mangabey, rhesus macaque, red capped mangabey and mandrill. In contrast, HIV-1 and it's direct ancestor, the chimpanzee SIV, do not encode *vpx* (Laguette et al. 2012; Sauter and Kirchhoff 2019). Vpx is co-packaged into budding HIV-2 and SIV through interaction with the Gag P6 motif and released into the cytosol after fusion (Accola et al. 1999; Sunseri et al. 2011). Macrophages and DCs are restrictive towards HIV-1 infection. The accessory protein Vpx was shown to overcome this block to HIV-1 infection by proteasomal degradation of an unknown cellular restriction factor

(Goujon et al. 2007; Kaushik et al. 2009; Srivastava et al. 2008). Mass spectrometry analysis of proteins bound to recombinant Vpx identified SAMHD1 as a potential target of Vpx (Berger et al. 2011; Hrecka et al. 2011; Laguette et al. 2011).

Subsequently, biochemical analysis revealed that Vpx targets SAMHD1 for proteasomal degradation by recruiting the CRL4 E3 ubiquitin ligase through interaction with SAMHD1 and the substrate recognition adaptor DCAF1 (Laguette et al. 2011; Hrecka et al. 2011; Ahn et al. 2012; Schwefel et al. 2014). Two modes of interaction were discovered. HIV-2 and SIVmac Vpx target a C-terminal recognition motif, while Vpx from other SIV lineages targets the n-terminus of SAMHD1 (Laguette et al. 2012; Fregoso et al. 2013; Ahn et al. 2012; Schwefel et al. 2015). Lentiviral Vpx proteins and SAMHD1 both show signs of co-evolution and experienced strong positive selection, emphasizing that SAMHD1 is a relevant restriction factor for lentiviruses (Laguette et al. 2012; Zhang et al. 2012; Fregoso et al. 2013).

SAMHD1 blocks HIV-1 replication in myeloid cell lines, monocyte-derived macrophages (MDMs) and monocyte-derived DCs (MDDCs), as well as $CD14^+$ peripheral blood mononuclear cells (PBMCs) (Laguette et al. 2011; Berger et al. 2011; Hrecka et al. 2011; Hiatt et al. 2021a). Importantly, SAMHD1 is also active in resting $CD4^+$ T cells, but not activated T cells (Baldauf et al. 2012; Descours et al. 2012; Albanese et al. 2022). SAMHD1 inhibits HIV-1 infection early in the replication cycle. Depletion of SAMHD1 does not affect HIV-1 entry, but leads to an increase of late and early reverse transcription products in infected cells, indicating that SAMHD1 specifically targets reverse transcription (Fig. 5) (Goujon et al. 2007; Srivastava et al. 2008; Hrecka et al. 2011; Baldauf et al. 2012; Descours et al. 2012).

SAMHD1 is a cellular dNTPase and HIV-1 replication was shown early to be sensitive to cellular dNTP levels (Gao et al. 1993; Korin and Zack 1999; Plesa et al. 2007; Goldstone et al. 2011). Therefore, SAMHD1 was proposed to inhibit HIV-1 reverse transcription by limiting cellular dNTPs (Goldstone et al. 2011; Baldauf et al. 2012; Kim et al. 2012; Lahouassa et al. 2012). Interestingly, in MDMs and resting $CD4^+$ T cells, in which SAMHD1 is restrictive, dNTP levels are below the Michaelis-Menten constant (K_m) of HIV-1 RT, while SAMHD1 depletion in increases cellular dNTP concentrations sufficiently to allow optimal reverse transcription (Kennedy et al. 2010; Lahouassa et al. 2012; Schott et al. 2018). Also, mutants of HIV-1 RT with reduced dNTP affinity show increased sensitivity

towards SAMHD1 (Lahouassa et al. 2012; Arnold et al. 2015). These correlative data linking SAMHD1 dNTPase and anti-viral restriction, is sustained by experimental evidence. An increase of cellular dNTPs by exogenous addition of dNs overcomes SAMHD1-mediated restriction, while blocking RNR-mediated dNTP *de novo* synthesis by hydroxyurea (HU) treatment mediates a block to HIV-1 infection in non-restrictive cells (Lahouassa et al. 2012; Baldauf et al. 2012; Welbourn and Strebel 2016). Also, mutants of the SAMHD1 lacking normal dNTPase activity have been used to sustain this hypothesis (Tab. 17). Mutants of the catalytic core residues H206 and D207 or mutants partially or entirely lacking the HD domain, as well as mutants of residues critical for allosteric regulation were not able to rescue HIV-1 replication after overexpression in a SAMHD1-negative myeloid background (Tab. 17) (Laguette et al. 2011; Lahouassa et al. 2012; White et al. 2013b; Ryoo et al. 2014; Arnold et al. 2015).

Nevertheless, several lines of evidence challenge the idea that the dNTPase alone is responsible for HIV-1 restriction (Majer et al. 2019). Experiments combining HU treatment and dNTPase-negative mutants, showed that SAMHD1 might be able to restrict Vpx deficient SIV replication independent of a reduction in dNTP levels (Welbourn et al. 2013). Most importantly however, the post-translational regulation of SAMHD1 anti-viral activity seems to be disconnected from its enzymatic function (for details see section 1.3.2).

1.2.3 SAMHD1 is a broad acting anti-viral restriction factor

SAMHD1 is not only active against HIV-1, but also against other primate lentiviruses deficient for Vpx (Baldauf et al. 2012; Lahouassa et al. 2012; White et al. 2013a). Not surprisingly, it is also active against non-primate lentiviruses such as bovine, feline and equine immunodeficiency viruses, which share a common viral replication cycle (Fig. 5) (Gramberg et al. 2013; White et al. 2013a; Mereby et al. 2018). SAMHD1 sequence and anti-retroviral activity is highly conserved in cats, cattle and horses. Equine and bovine SAMHD1 show dNTPase activity (Mereby et al. 2018). Non-lenti retroviruses are also affected by SAMHD1 (Fig. 5). Murine leukemia virus, a *Gammaretrovirus* and Mason Pfizer monkey virus, a *Betaretrovirus* are restricted by SAMHD1 in macrophage-like cells and SAMHD1 depletion enables infection (Gramberg et al. 2013). Also, reverse

transcription of the *Alpharetrovirus* Rous sarcoma virus and the *Deltaretrovirus* human T-cell lymphotropic virus type 1 is blocked by SAMHD1, even though SAMHD1 depletion is not sufficient to enhance productive infection or transmission (Kaushik et al. 2009; Gramberg et al. 2013; Sze et al. 2013).

Retrotransposons are endogenous reverse transcribing elements distributed throughout the genome. Whereas most of them are heavily truncated or mutated and not functional anymore, some retroelements, such as the LINE-1 element, are able to express RNA and proteins, leading to reverse transcription and re-integration of the LINE-1 sequence into the human genome (Eickbush and Jamburuthugoda 2008). Although the biological mechanisms differs in detail, retrotransposons, and even more LTR retrotransposons, share similarities to primitive retroviruses, such as their genomic architecture, as well as the obligate reverse transcription and integration steps in the respective life cycles (Eickbush and Jamburuthugoda 2008). Therefore, it is not surprising that SAMHD1 inhibits LINE-1 retrotransposition (Fig. 5) (Zhao et al. 2013). Although dNTPs are required in for LINE-1 reverse transcription, SAMHD1 restriction seems to be independent of its dNTPase activity. Regulation of LINE-1 protein expression, as well as LINE-1 sequestration into stress granules have been discussed (Zhao et al. 2013; Hu et al. 2015; Gao et al. 2019).

Hepatitis B virus (HBV), which belongs to the same order as retroviruses, *Ortervirales*, is also inhibited by SAMHD1 (Fig.5) (Jeong et al. 2016; Sommer et al. 2016; Krupovic et al. 2018). HBV requires reverse transcription of its RNA genome to produce infectious particles. However in contrast to retroviruses, reverse transcription is mostly completed before budding (Beck 2007). Accordingly, SAMHD1 depletion in HBV infected cells or cells transfected with HBV containing plasmids increased extra- and intracellular reverse transcribed HBV DNA (Jeong et al. 2016; Sommer et al. 2016). Reverse transcription of the large HBV genome requires important amounts of dNTPs. In line with this, SAMHD1 dNTPase activity seems to be required for HBV restriction (Jeong et al. 2016; Sommer et al. 2016; Hu et al. 2018a). Conversely, SAMHD1 might favor HBV infection in target cells, due to its role in the DNA damage response, which is necessary for HBV DNA circularization (Majer et al. 2019; Wing et al. 2019).

Several large DNA viruses, such as the alphaherpesvirus herpes-simplex virus 1 (HSV-1), the betaherpesviruses human and murine cytomegalovirus (HCMV and MCMV), the

gammaherpesvirus Epstein-Barr virus (EBV), as well as attenuated poxviruses are targets of SAMHD1-mediated restriction (Fig. 5) (Kim et al. 2013; Hollenbaugh et al. 2013; Businger et al. 2019; Deutschmann et al. 2019; Kim et al. 2019a; Sliva et al. 2019; Zhang et al. 2019). With regards to herpesviruses, most studies point towards a DNA replication-dependent phenotype of SAMHD1-mediated inhibition. Late gene expression, which is replication-dependent, as well as the amount of amplified viral DNA in the cytosol or supernatant and the produced infectious viral particles, but not early gene expression, seem to be increased upon SAMHD1 depletion (Hollenbaugh et al. 2013; Kim et al. 2013; Businger et al. 2019; Deutschmann et al. 2019). Importantly, SAMHD1 also restricts MCMV replication *in vivo* in a mouse model (Deutschmann et al. 2019). With regards to HSV-1, SAMHD1 restriction seems to be overcome by exogenous dNs and to be dependent on catalytic residues (Kim et al. 2013). However, also an effect on HCMV early gene expression was suggested. This effect proposedly relies on the SAMHD1-mediated interference with NF-κB signaling (Kim et al. 2019a). NF-κB is a driver of HCMV early gene expression. This example indicates that SAMHD1 may act at several steps of the herpesvirus life cycle (Kim et al. 2019a).

More recently, SAMHD1 was shown to restrict replication of viruses with a short DNA genome such as human papillomavirus 16 and could affect papillomavirus induced carcinogenesis (Fig. 5) (James et al. 2019). Curiously, SAMHD1 was also proposed to inhibit RNA virus replication, such as the porcine reproductive and respiratory syndrome virus and the enterovirus 71, (+)-ssRNA viruses of the *Nidovirales* and the *Picornavirales* order, as well as the influenza A virus, a segmented (-)-ssRNA virus of the *Orthomyxoviridae* family (Fig. 5) (Yang et al. 2014; Li et al. 2020; Silva et al. 2021). These viruses do not require dNTPs. As a consequence SAMHD1 dNTPase activity cannot be causative for RNA virus restriction. In conclusion, SAMHD1 is a broad acting anti-viral factor, targeting viruses from distinct clades, with diverse evolutionary origins and modes of replication.

1.2.4 Viral counteraction mechanisms allow evasion of SAMHD1-mediated restriction

Several of the aforementioned viruses have developed counteracting mechanisms that block or circumvent SAMHD1-mediated restriction (Fig. 5). Most primate lentiviruses express Vpx or Vpr proteins able to degrade SAMHD1 via the proteasome pathway. The non-Vpx encoding equine lentivirus however is was proposed to degrade SAMHD1 in a Rev and lysosome-dependent manner (Ren et al. 2021). Similar to primate lentiviruses, HCMV and enterovirus 71 might be able to mark SAMHD1 for proteasomal degradation by retargeting of the cullin-RING and TRIM21 E3 ubiquitin ligases, respectively (Hyeon et al. 2020; Li et al. 2020).

A possibility to circumvent SAMHD1 dNTPase-mediated restriction is used by HIV-1 and HBV. Both, HIV-1 and HBV encode RT enzymes with low K_m values. *I.e.* the K_m values of HIV-1 RTs are lower than those of the RTs from HIV-2 or SIVs encoding Vpx (Lenzi et al. 2014). K_m values of the HBV and HIV-1 RT are comparable, suggesting that both viruses have evolved RT enzymes with high affinity for dNTPs, to partially overcome SAMHD1-mediated restriction, probably in a cell type-dependent manner (Fig. 5) (Gaillard et al. 2002; Lenzi et al. 2014). A related viral strategy to counteract SAMHD1 is the induction of *de novo* dNTP synthesis (Fig. 5). HBV and MCMV increase RNR subunit expression (Lembo et al. 2000; Lembo et al. 2004; Cohen et al. 2010; Ricardo-Lax et al. 2015). HSV-1, EBV and vaccinia virus encode functional homologues of RNR subunits, while several herpesviruses encode thymidine kinases, thereby increasing cellular dNTP and dTTP levels upon infection (Field and Wildy 1978; Cameron et al. 1988; Goldstein and Weller 1988; Jacobson et al. 1989; Lembo et al. 2000; Gammon et al. 2010).

SAMHD1 is regulated in a cell cycle-dependent manner by phosphorylation at residue T592 (for details see 1.3.1). Several viruses manipulate the post-translational regulation of SAMHD1 by either controlling the cell cycle or directly phosphorylating SAMHD1 (Fig. 5). Recently, herpesviruses such as HCMV, MCMV and EBV have been shown to phosphorylate SAMHD1 at residue T592 through virus encoded homologues of cellular CDKs, thereby inactivating SAMHD1 (Businger et al. 2019; Deutschmann et al. 2019; Zhang et al. 2019). On the other hand, HIV-1 manipulates the cell cycle through the combined action of the accessory proteins Vpr and Vif, leading to and G_2/M arrest and enhanced G_1 to S-phase transition in infected target cells (Jowett et al. 1995; He et al.

1995; Sakai et al. 2006; Berger et al. 2015; Rice and Kimata 2015; Romani et al. 2015). SAMHD1 in S and G_2/M-phase is inactive against HIV-1, indicating that cell cycle manipulation could be an evasion strategy employed by HIV-1 to partially avoid SAMHD1 restriction (Schott et al. 2018).

Taken together, SAMHD1 seems to exert substantial evolutionary pressure upon large groups of viruses, forcing them to counteract SAMHD1 restriction by developing efficient counteracting mechanisms. This makes it even more surprising that HIV-1 and its direct chimpanzee SIV ancestors, with the adaptation to the chimpanzee host, have lost Vpx, and thereby the ability to efficiently degrade SAMHD1 (Lim et al. 2012; Etienne et al. 2013; Sauter and Kirchhoff 2019). As a consequence, HIV-1 replication is blocked in important HIV-1 target cells such as macrophages, DCs and resting $CD4^+$ T cells with long reaching consequences for HIV-1 pathophysiology. The question arises whether the loss of Vpx as an efficient counteraction mechanism against SAMHD1 may possibly be beneficial for HIV-1 *in vivo* and could have been a prerequisite for the pandemic spread of HIV-1 (Schott et al. 2017).

1.2.5 SAMHD1 shapes the immune response to HIV-1

SAMHD1 was shown to be a central player in cellular homeostasis and absence of SAMHD1 expression *i.e.* in AGS patients leads to sever autoinflammation due to perturbations in cellular replication and DNA damage response, which again mediates accumulation of nucleic acids and IFN-response (Schott et al. 2022). In addition, SAMHD1 was proposed to inhibit NF-κB signaling by interacting and interfering with multiple elements of the pathway (Chen et al. 2018; Espada et al. 2021). Whether this is dependent or independent of SAMHD1 dNTPase activity is unclear and might be cell type specific (Chen et al. 2018; Qin et al. 2020). Both mechanisms seem to regulate baseline inflammation and immune responses towards divers pathogens and PAMPs, such as RNA viruses, including coronaviruses, or lipopolysaccharides (Barrett et al. 2022; Oo et al. 2022).

However, with regards to HIV-1, SAMHD1 interferes with innate sensing on an additional level. As detailed above, detection of HIV-1 infection by PRRs, namely the cGAS-STING pathway, is critically dependent on the amount of reverse transcribed HIV-1 DNA

available for sensing. Myeloid effector cells, such as macrophages and DCs, are HIV-1 target cells due to the expression of HIV-1 (co-) receptors (Honeycutt et al. 2016). Macrophages and DCs are primary immune sentinels and vital in the coordination of innate and adaptive anti-viral immune response towards HIV-1 (Luban 2012; Rodrigues et al. 2017; Kruize and Kootstra 2019). However, SAMHD1 is active in macrophages and DCs and block HIV-1 reverse transcription, thereby limiting the availability of HIV-1 reverse transcription products for HIV-1 sensing (Hrecka et al. 2011; Laguette et al. 2011). Indeed, only in the absence of SAMHD1, efficient immune activation can occur in conditions resembling physiological infection, *i.e.* at low multiplicity of infection (MOI) (Goujon et al. 2007; Manel et al. 2010; Gao et al. 2013a; Maelfait et al. 2016; Yin et al. 2020). This is not only true for the activation of inflammatory circuits, but also for the cytokine response towards HIV-1 infection in $CD14^+$ myeloid cells, as well as antigen presentation and cytotoxic $CD8^+$ T cell responses primed by infected DCs *in vitro* and myeloid cells in mouse models *in vivo* (Berger et al. 2011; Ayinde et al. 2015; Maelfait et al. 2016). Interestingly, low induction of SAMHD1 expression in HIV-1 infected DCs from elite controllers, a patient group controlling HIV-1 replication in absence of ART, correlates with the efficiency of HIV-1 specific $CD8^+$ T cell response (Martin-Gayo et al. 2015). Thus, SAMHD1 restriction of HIV-1 in myeloid cells might have dramatic consequences on the immune response in patients and is an interesting target for therapeutic manipulation in order to augment the immunogenicity and control of HIV-1 in infected patients (Schott et al. 2017; Ndung'u et al. 2019; Margolis et al. 2020).

1.3 The regulation of SAMHD1 function and anti-viral activity is still not completely understood

1.3.1 The anti-lentiviral activity of SAMHD1 is regulated by phosphorylation at residue T592

Both, cycling and resting $CD4^+$ T cells express SAMHD1 (Baldauf et al. 2012; Descours et al. 2012). However, only in resting, but not in activated $CD4^+$ T cells, SAMHD1 blocks reverse transcription (Baldauf et al. 2012). Also, SAMHD1 blocks HIV-1 infection in macrophage-like THP-1 or in U937 cells, only after phorbol 12-myristate-13-acetate (PMA)-activation induced G_1/G_0 cell cycle arrest. Similarly, SAMHD1 shows no anti-viral

activity in dividing cell lines such as HeLa cells (Goujon et al. 2008; Sharova et al. 2008; Cribier et al. 2013). Because this phenotype seems not dependent on SAMHD1 expression levels, these findings indicated that SAMHD1-mediated anti-lentiviral activity is regulated by post-translation modifications (PTMs).

Using mass spectrometry based approaches, SAMHD1 was shown to be phosphorylated at residue T592 by cellular kinases CDK1 and CDK2 in complex with cyclin A2 (Fig. 8) (Cribier et al. 2013; White et al. 2013b; Welbourn et al. 2013). CDK1 and 2 recognize a conserved ^{592}TPQK^{595} target signal at the C-terminus adjacent to residue, while cyclin A2 binding is dependent on residues L620 and F621 (Fig. 8A) (Cribier et al. 2013; St Gelais et al. 2014; Yan et al. 2015). T592 phosphorylation is low in non-cycling cells, such as primary monocytes or MDMs, macrophage-like PMA-activated THP-1, as well as in quiescent or resting $CD4^+$ T cells (Cribier et al. 2013; White et al. 2013b; Welbourn et al. 2013). However in cycling cells, such as activated $CD4^+$ T cells, cycling THP-1 cells or HeLa cells, SAMHD1 phospho-T592 (pT592) abundancy is high, directly correlating with its restrictive capacity in these cell types (Cribier et al. 2013; Welbourn et al. 2013; White et al. 2013b). SAMHD1 is phosphorylated at position T592 upon entry into S-Phase and phosphorylation is maintained through G_2- and early M-phase.

At mitotic exit SAMHD1 is rapidly dephosphorylated, leading to a near complete non-phosphorylated SAMHD1 pool in G_1 cell cycle phase (Fig. 8B). This is also true when cells are arrested in G_1/G_0 and/or are terminally differentiated (Schott et al. 2018; Tramentozzi et al. 2018). Rapid SAMHD1 dephosphorylation is achieved by the cell cycle-dependent protein phosphatase 2A (PP2A) in complex with the regulatory subunit B55α (Fig. 8B) (Schott et al. 2018). The PP2A-B55α holoenzyme interacts with a basic patch, which serves as recognition motif at the c-terminus of SAMHD1 surrounding the residue T592 (Schott et al. 2018). In non-cycling cells, such as MDMs, PP2A-B55α also seems to be required to maintain low levels of pT592 (Fig. 8B) (Schott et al. 2018). On the other side, different CDK-cyclin complexes, such as CDK4-cyclin D2 and CDK2/6-cyclin D3 seem to modulate SAMHD1 phosphorylation and thus anti-viral activity in macrophages (Fig. 8B) (Ruiz et al. 2015; Badia et al. 2016).

The phospho-status of SAMHD1 can be influenced by cytokines and drugs. Type I and II IFNs can downmodulate SAMHD1 phosphorylation, a mechanism which was proposed

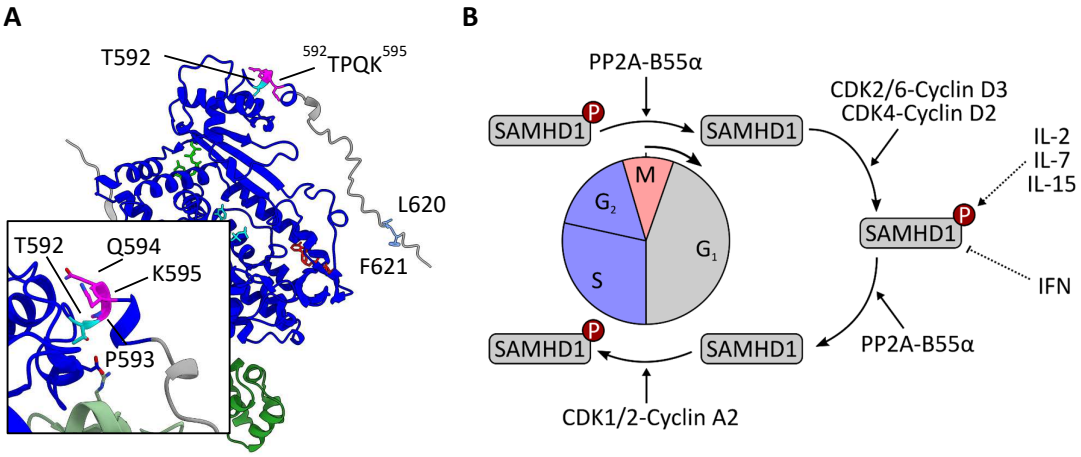

Figure 8 : Cell cycle-dependent regulation of SAMHD1 T592 phosphorylation.

(A) SAMHD1 is phosphorylated at residue T592 (light blue). Phosphorylation by CDK1/2 is dependent on the ^{592}TPQK^{595} CDK interaction motif (magenta) and the residues L620 and F621 (blue), which are required for cyclin A2 recruitment (Cribier et al. 2013; St Gelais et al. 2014; Yan et al. 2015). **(B)** SAMHD1 T592 phosphorylation is cell cycle-dependent. Upon entry into S-phase, SAMHD1 is phosphorylated at residue T592 by the CDK1/2-cyclin A2 complex (Cribier et al. 2013; Welbourn et al. 2013; White et al. 2013b). Phosphorylation is maintained throughout S- and G_2/M-phase. Upon mitotic exit, SAMHD1 is rapidly de-phosphorylated at residue T592 via the PP2A-B55α holoenzyme and PP2A-B55α is required to maintain T592 dephosphorylation in G_1/G_0 (Schott et al. 2018). In contrast, CDK2/6-cyclin D3 and CDK4-cyclin D2 complexes can phosphorylate SAMHD1 in terminally differentiated cells such as macrophages (Ruiz et al. 2015; Badia et al. 2016). Also, interleukins (IL-2, IL-7 and IL-15), as well as type I and II interferons (IFN) can modulate SAMHD1 T592 phospho-status (Pauls et al. 2014a; Coiras et al. 2016; Mlcochova et al. 2017; Kueck et al. 2018; Manganaro et al. 2018; Szaniawski et al. 2018). **(A)** AlphaFold modelling of SAMHD1 structure (Q9Y3Z3) (Jumper et al. 2022) was colored as in Fig. 6.

to enhance the anti-viral activity of SAMHD1 in macrophages (Fig. 8B) (Mlcochova et al. 2017; Kueck et al. 2018; Szaniawski et al. 2018). IL-2, IL-7 and IL-15 stimulate CD4$^+$ T cell proliferation and thus cell cycle dependent SAMHD1 phosphorylation, which correlates with susceptibility to HIV-1 infection and can be counteracted by tyrosine kinase inhibitors (Fig. 8B) (Pauls et al. 2014b; Pauls et al. 2014a; Bermejo et al. 2016; Coiras et al. 2016; Manganaro et al. 2018).

Correlative data to SAMHD1 T592 phosphorylation and loss of SAMHD1-mediated HIV-1 restriction was supported by mutagenic analysis (Tab. 17). To investigate the role of the T592 phospho-site in the regulation of anti-viral restriction in macrophage-like cells, phosphomimetic T592E or T592D mutants, which resemble pT592 according to the

negative charge, as well as non-phosphorylatable or phosphoablative T592A or T592V mutants were tested for their restrictive potential by retroviral transduction and overexpression in SAMHD1-negative PMA-activated U937 cells. As expected from the correlative data, phosphomimetic T592E or T592D mutations lead to loss of restriction, as compared to the otherwise restrictive overexpressed wild type (WT) SAMHD1 protein. In contrast, T592A or T592V mutant overexpression inhibited HIV-1 replication (Welbourn et al. 2013; White et al. 2013b; Ryoo et al. 2014; Arnold et al. 2015). Thus, a large body of evidence supports the role of T592 phosphorylation in the regulation of HIV-1 restriction. However, mutagenic data is limited to artificial overexpression models, which makes it difficult to draw conclusions in more physiological settings (see 1.3.1). In particular, how exactly SAMHD1 T592 phosphorylation governs anti-viral activity against HIV-1 is heavily debated (Majer et al. 2019).

1.3.2 How T592 phosphorylation regulates SAMHD1 function is still unclear

As this is also the case for anti-viral activity (see above), SAMHD1 T592 phosphorylation and dNTPase activity seem to correlate. In cell cycle synchronized HeLa cells, high SAMHD1 pT592 levels in S- and G_2/M-phase of the cell cycle coincides with high dNTP levels and a low HIV-1 restrictive potential. In contrast, HIV-1 restrictive G_1/G_0 cells are marked by low pT592 and low cellular dNTP levels (Schott et al. 2018). Mutagenic data however failed to proof a connection between SAMHD1 T592 phosphorylation and SAMHD1 dNTPase activity (Majer et al. 2019). While some reports, indicate an effect of SAMHD1 T592 phosphorylation on oligomerization or tetramer stability of SAMHD1, this effect seems not sufficient to reduce SAMHD1 dNTPase activity of pT592 SAMHD1 or SAMHD1 phospho-mutants *in vitro* (Welbourn et al. 2013; White et al. 2013b; Arnold et al. 2015; Yan et al. 2015; Bhattacharya et al. 2016). In addition, not only WT or phosphoablative T592A or T592V mutants were able to reduce dNTP levels, when overexpressed in PMA-activated U937 cells, but also phosphomimetic T592E or T592D mutants (Welbourn et al. 2013; White et al. 2013b; Welbourn and Strebel 2016). Thus, there is an obvious discrepancy between the proposed anti-viral dNTPase function and the regulation of SAMHD1 anti-viral activity by T592 phosphorylation (Fig.9).

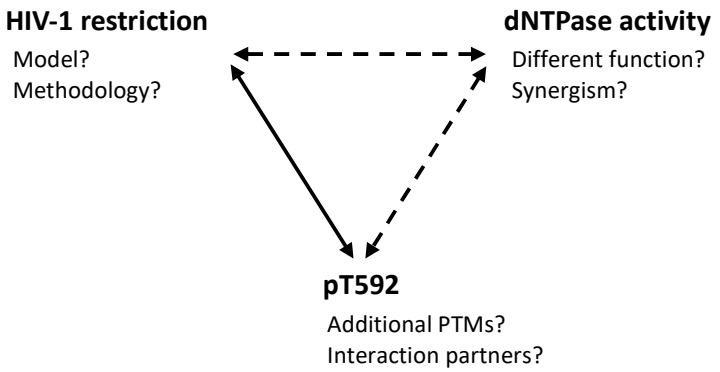

Figure 9: How can SAMHD1 function, anti-viral restriction and T592 phospho-regulation be connected? The connection between anti-lentiviral activity of SAMHD1 and T592 phospho-regulation is well established. However, if SAMHD1 T592 phosphorylation is directly linked to SAMHD1 dNTPase and if the dNTPase activity mediates SAMHD1 anti-viral activity, is currently unclear (Majer et al. 2019). This could be due to limitations in the models and methodologies employed to investigate this relationship. Alternatively, further SAMHD1 functions might mediate or contribute to anti-viral restriction. Also, SAMHD1 regulation might be more complex and additional post-translational modifications (PTMs), or interaction partners could modulate SAMHD1 anti-viral and enzymatic activity (Majer et al. 2019).

This lack of consistency might be due to several reasons. One possibility is that SAMHD1 regulation is still incompletely understood and more complex than previously assumed (Fig. 9, see discussion for more details). In this line, SAMHD1 was shown to be not only modified by phosphorylation at residue T592, but also to be subject to acetylation, SUMOylation, ubiquitination, O-linked-N-acetylglucosaminylation and phosphorylation at multiple additional residues, as well as to harbor redox sensitive cysteines (for more details see discussion) (Welbourn et al. 2013; White et al. 2013b; Lamoliatte et al. 2014; Elia et al. 2015; Hendriks et al. 2017; Lee et al. 2017; Lumpkin et al. 2017; Hu et al. 2021; Martinat et al. 2021). Understanding the connection between SAMHD1 PTMs, its anti-viral activity and enzymatic function is crucial to develop therapies directed against SAMHD1 and HIV-1. As a consequence, this project aims at better understanding the post-translational regulation of SAMHD1 at residue T592, but also to identify new potential regulatory phospho-sites, which might affect SAMHD1 anti-viral function.

In addition to an underestimation of SAMHD1 regulatory complexity, an alternative hypothesis to explain the missing link between pT592, anti-viral restriction and SAMHD1 dNTPase activity, could be that the dNTPase activity is not or not alone mediating the anti-viral restriction activity of SAMHD1 (Fig. 9, see section 1.2.1, Fig. 5 and discussion

for details) (Majer et al. 2019). In this line, we were investigating new aspects of SAMHD1 biology, such as its role in R-loop resolution to better understand the functional repertoire of SAMHD1 (Park et al. 2021).

Finally, the lack of convincing experimental evidence linking T592 phospho-regulation and dNTPase activity might be due to sheer limitations in the experimental systems used to study the complex relationship between HIV-1 restriction, the regulation of SAMHD1 and its enzymatic function (Fig. 9). In this work, we will therefore propose new technical approaches to study these interconnections more systematically.

1.3 Better models are needed to improve our understanding of SAMHD1 regulation

1.3.1 Current models to study SAMHD1-mediated HIV-1 restriction in myeloid cells are limited

As delineated in section 1.1.3, myeloid cells, such as macrophages and DCs are important target cells in HIV-1 infection, because they are primary innate sensors of HIV-1 PAMPs. Also, they have a central role in initiating and coordinating the innate and adaptive anti-viral immune responses. In addition to that, myeloid cells are interesting targets in the context of HIV-1 latency and resistance to ART. Viral replication in patients can efficiently be controlled by ART. However, after cessation of ART, HIV-1 replication quickly rebounds. Because they are long lived, myeloid cells are discussed as important viral reservoir in patients under ART and as an source of replication competent HIV-1 upon rebound (Sattentau and Stevenson 2016; Honeycutt et al. 2017; Bertram et al. 2019; Ganor et al. 2019). SAMHD1 is an active restriction factor in macrophages and DCs (Hrecka et al. 2011; Laguette et al. 2011). Understanding the macrophage reservoir and the contribution of SAMHD1-mediated restriction in these cells, will be crucial to develop curative therapies, which aim to deplete latently infected cells. More knowledge will also be vital in order to better understand and manipulate HIV-1 sensing and anti-viral immunity.

However, models to genetically study SAMHD1-mediated HIV-1 restriction in myeloid cells are scarce. While primary human mature dendritic cells or macrophages are very difficult to obtain, MDMs or MDDCs can be more accessible models to study SAMHD1-

mediated anti-viral restriction in primary cells (Laguette et al. 2011; Hrecka et al. 2011). However, MDMs and MDDCs are hard to manipulate genetically, due to a limited life span and SAMHD1-mediated resistance to lentiviral transduction, which prohibits the study of SAMHD1 mutants by overexpression in this context (Lee et al. 2018a). While the first methods to genetically deplete genes in MDMs and MDDCs using CRISPR/Cas9 systems are emerging, targeted gene editing to modify single residues in these cell types are still not available (Freund et al. 2020; Hiatt et al. 2021b; Jost et al. 2021). Induced pluripotent stem cell (iPSC) derived macrophages might be an option and first iPSC clones harboring SAMHD1 mutations, which are either patient derived or introduced by gene editing, have been published (Fuchs et al. 2020; Sürün et al. 2020). Also, iPSCs are amenable to lentiviral transduction and overexpression of modified transgenes (Ackermann et al. 2017). However, their culture and differentiation into macrophages or dendritic cells is extremely labor and cost intensive and would not allow to study large sets of SAMHD1 mutants (Lee et al. 2018a; Vaughan-Jackson et al. 2021).

Therefore, most if not all genetic studies in myeloid cell types, namely also those investigating the role of SAMHD1 PTMs for SAMHD1-mediated anti-viral restriction, so far relied on PMA-activated promonocytic THP-1 or U937 cell lines (Majer et al. 2019). PMA is a protein kinase C activator (Castagna et al. 1982; Boneh et al. 1989). Apart from the induction of a macrophage-like phenotype, treatment with PMA activates non-physiological intracellular pathways, which might alter the outcome of viral restriction experiments and be especially problematic in the context of SAMHD1 post-translational regulation (Chanput et al. 2010; Zeng et al. 2015; Majer et al. 2019). Consequently, alternative and innovative myeloid cell models, which are genetically accessible, cost effective, but maintain a high degree of physiology and rely on physiological myeloid differentiation pathways are urgently needed.

So far, lenti- or retroviral transduction mutant constructs of SAMHD1 were used to test SAMHD1 variants for anti-viral restriction. In this case, SAMHD1-negative U937 or SAMHD1 KO THP-1 cells were transduced with SAMHD1 mutants, selected and then tested for viral restriction after PMA-activation (Majer et al. 2019). The excessive use of retroviral overexpression to test mutants has several disadvantages. In this context, an exogenous promotor mediates overexpression of SAMHD1. The regulation, timing and levels of exogenous SAMHD1 expression very likely do not resemble those of the

endogenous SAMHD1 protein, driven by its natural promoters and enhancers (Majer et al. 2019). Also, PMA-activation is known to drive a strong activation of viral promotors, such as the commonly used CMV promotor and thereby again enhances artificial expression levels in this system. This could lead to dysregulation of overexpressed SAMHD1 protein (Löser et al. 1998; Shifera and Hardin 2009; Majer et al. 2019). In addition, transduction in most cases is followed by subsequent purifying selection using fluorescence or antibiotic resistance markers. The selection process might influence activation or the phenotype of the transduced cell population (Majer et al. 2019). Also, the selected population is polyclonal and likely is not stable over time, which impacts the outcome of serial experiments (Felipe Diaz-Griffero personal communication).

Finally, PMA-treated U937 cells which are used with few exceptions for these experiments and are commonly assumed to not show endogenous expression of SAMHD1, do in fact produce low amounts of SAMHD1 protein, which is further enhanced in the context of IFN signaling (Riess et al. 2017). Even low levels of endogenous WT protein might affect the outcome of experiments analyzing the restrictive effect of overexpressed SAMHD1 mutants.

In conclusion, genetic approaches to study the regulation and function of SAMHD1 are limited to overexpression systems, which are prone to an artificial bias due to high expression levels, translational and post-translational dysregulation, as well as ill-defined genetic backgrounds. To draw final conclusions on SAMHD1 function and regulation, genetic tools, which are not based on overexpression, are urgently needed to confirm the current paradigms and to resolve open questions in SAMHD1 biology. Therefore, we aim at implementing and refining new genetic tools, such as gene editing to modify endogenous SAMHD1 protein and to study mutants of SAMHD1 in a physiological context and regulation. We want to combine these genetic approaches with novel myeloid model systems of SAMHD1 biology and HIV-1 restriction, to obtain a better understanding of SAMHD1 regulation and function in myeloid cells.

1.3.2 Transdifferentiated BlaER1 cells are a novel myeloid model

Recently, transdifferentiated BlaER1 cells, a novel myeloid cell model resembling macrophages, was successfully used to study innate immune signaling (Rapino et al.

2013; Gaidt et al. 2016; Gaidt et al. 2017; Vierbuchen et al. 2017). The concept of transdifferentiation was originally developed, as a treatment approach for hemorrhagic malignancies. By overexpression of transcription factors, a terminal differentiation block in leukemia or lymphoma cells can be induced, overcoming the unlimited replication potential of malignant cells. Ideally this is combined with a general sensitization for senescence and cell death (Nowak et al. 2009).

The leucine zipper CCAAT-enhancer binding protein α (C/EBPα) is a myeloid transcription factor, which plays essential roles in early hematopoietic development, as well as granulo- and monopoiesis (Friedman 2015; Avellino and Delwel 2017). In addition to its role in myelopoiesis, C/EBPα seems to limit the self-renewal potential of hematopoietic cells and is frequently mutated in hemorrhagic malignancies such as acute myeloid leukemia (Pabst et al. 2001; Zhang et al. 2004; Friedman 2015; Avellino and Delwel 2017). By overexpression of C/EBPα fused to the regulatory domain of the estradiol receptor (ER) and subsequent estradiol treatment, the group around Thomas Graf was able reprogram a pre-B cell line into macrophage-like cells (Bussmann et al. 2009). Estradiol treatment leads to nuclear translocation of the C/EBPα-ER fusion protein and induction of a myeloid transcription program (Bussmann et al. 2009).

The BlaER1 cell line resulted from the transduction of the lymphoblastic B cell line RCH-ACV with a retroviral vector encoding the C/EBPα-ER fusion construct and GFP, followed by subsequent enrichment for GFP positive cells and subcloning (Jack et al. 1986; Bussmann et al. 2009; Rapino et al. 2013). Estradiol treatment of BlaER1 cells results in near complete transdifferentiation into macrophage-like cells, which is marked by strong morphologic changes, as well as a gradual loss of B cell marker CD19 and acquisition of macrophage marker CD11b (Rapino et al. 2013). Consequently, Rapino et al. could show that estradiol treated BlaER1 cells are terminally arrested in G_1/G_0 and gain phagocytic activity. Most importantly, transdifferentiation induces a myeloid transcriptional profile in BlaER1 cells, which closely resembles the one found in MDMs (Rapino et al. 2013).

Subsequently, Moritz Gaidt and the group around Veith Hornung further developed the BlaER1 cell model to study innate immune pathways. Importantly, they showed that cycling BlaER1 cells are prone to genetic manipulation by gene knock-out (KO) or lentiviral transduction and overexpression of mutant protein (Gaidt et al. 2016).

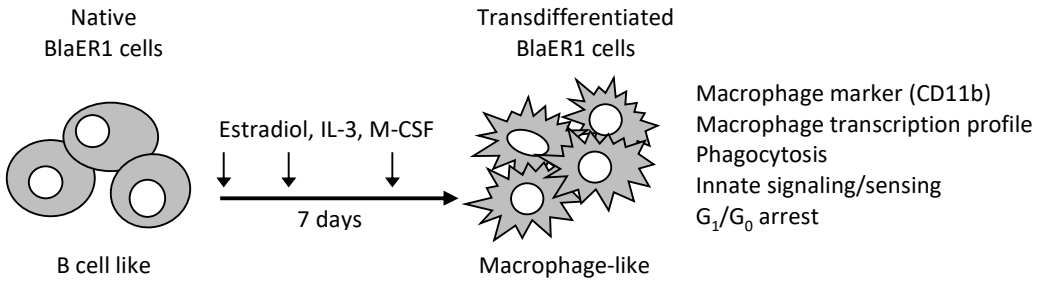

Figure 10 BlaER1 transdifferentiation.

BlaER1 cells are B cell derived. However, upon treatment with estradiol, IL-3 and M-CSF for 7 days they acquire a macrophage-like phenotype. This process of transdifferentiation is dependent on the induction of the myeloid transcription factor CEBP/α fused to the estradiol receptor and marked by loss of B cell marker CD19, as well as acquisition of the macrophage marker CD11b. Transdifferentiated BlaER1 cells show an expression profile resembling MDMs, high phagocytic activity and are responsive to various innate stimuli. Importantly, transdifferentiation also leads to a G1/G0 arrest (Rapino et al. 2013).

To sustain the induction of a macrophage-like phenotype, they treated BlaER1 cells with IL-3 and macrophage colony-stimulating factor (M-CSF) in addition to estradiol for 7 days (Fig. 10) (Gaidt et al. 2018). Due to their high degree of physiology and genetic accessibility, BlaER1 cells have been successfully used to study different innate immune signaling pathways, notably toll-like and NOD-like receptor signaling (Rapino et al. 2013; Gaidt et al. 2016; Gaidt et al. 2017; Vierbuchen et al. 2017).

The novel approach of cellular transdifferentiation allows the generation of macrophage-like cells from an unlimited pool of genetically accessible cells. We hypothesized that transdifferentiated BlaER1 cells might be a promising model to study SAMHD1-mediated restriction of HIV-1 in myeloid cells. So far, BlaER1 cells have not been used to study HIV-1 infection, sensing or anti-viral restriction. Also, no data is available on SAMHD1 expression or anti-viral activity in transdifferentiated BlaER1 cells. Therefore, we wanted to establish BlaER1 cells as a novel model for HIV-1 infection and SAMHD1-mediated anti-viral restriction, as well as regulation in macrophage-like cells.

1.3.3 CRISPR/Cas9 allows targeted mutagenesis of endogenous protein

Clustered regularly interspaced short palindromic repeats (CRISPR) are repetitive DNA sequences present in bacterial genomes and belong to an ancient bacterial anti-phage

defense system. They encode for CRISPR RNAs (crRNAs) complementary to phage DNA, which after annealing with a trans-activating CRISPR RNA (tracrRNA) and subsequent processing can recruit CRISPR-associated endonucleases, such as Cas9, to digest and deplete foreign DNA (Lander 2016).

Today, the CRISPR/Cas9 system has very successfully been adapted and optimized as a genetic tool to manipulate eukaryotic genes, namely also in human cells, and is now a standard tool for genetic manipulation both *in vitro* and *in vivo* (Ran et al. 2013; Mali et al. 2013; Lander 2016). The functional CRISPR/Cas9 system for gene modification consists of the Cas9 protein, a tracrRNA and the crRNA complementary to the target region (Fig. 11A). Once introduced into the cell, the crRNA leads to the recruitment of the Cas9-crRNA-tracrRNA ribonucleoprotein (RNP) complex to the complementary target region and the Cas9 endonuclease executes a blunt dsDNA cleavage (Fig. 11A) (Sander and Joung 2014). For Cas9, the DSB is introduced specifically 3 base pairs (bps) 3' of the protospacer adjacent motif (PAM). The PAM sequence is a short Cas specific recognition sequence that is absolutely required for editing, but not present on the complementary crRNA (Sander and Joung 2014). In non-cycling cells, in absence of a homologous sister chromatid, double-strand DNA breaks are commonly repaired through NHEJ, leading to random InDels at the repair site. If an appropriate target site early in a given gene is chosen, frameshift and premature stop-codons introduced by InDels will lead to heavy truncation, altered peptide sequence and non-sense-mediated decay in the modified protein (Fig. 11A) (Mali et al. 2013; Nambiar et al. 2022). Commonly this is referred to as CRISPR/Cas9 knock-out (KO).

Effective CRISPR/Cas9 complex recruitment is critical to achieve high editing efficiencies and depends on the target site sequence. Also, off-target efficiency of crRNA is strongly determined by the sequence composition. Numerous prediction tools are able to identify crRNAs with a high on-target, but low off-target efficiency (Doench et al. 2014; Doench et al. 2016). In order to deliver the specific CRISPR/Cas9 system into a cell, methods relying on plasmid transfection, (retro-) viral transduction, as well as mRNA transfection have successfully been used (Ran et al. 2013; Sander and Joung 2014; OhAinle et al. 2018). However, due to immunogenicity of nucleic acids, *in vitro* complexation and delivery of RNPs consisting of Cas9 protein, as well as

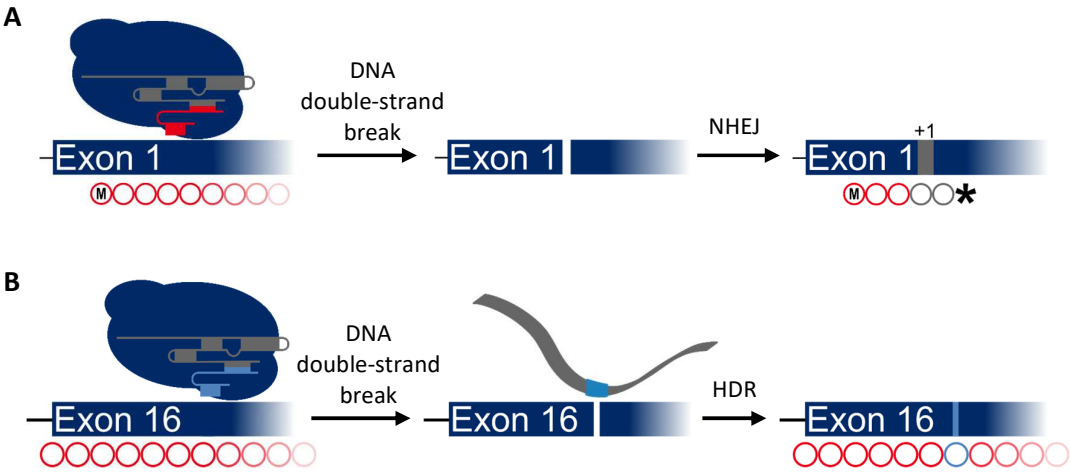

Figure 11: CRISPR/Cas9-mediated knock-out and knock-in.

(A, B) CRISPR/Cas9 ribonucleoproteins (RNPs) consist of Cas9 protein (dark blue), tracrRNA (grey) and the target specific crRNA (red or light blue). The crRNA recruits the CRISPR/Cas9 RNP to the intended target site, at which the endonuclease activity of the Cas9 protein generates a DNA double-strand break. **(A)** Under normal conditions, the DNA double-strand break is repaired by non-homologous end joining (NHEJ), which is the repair pathway predominantly active in G_1/G_0 cells. NHEJ leads to random insertions and deletions at the repaired DNA gap. This eventually leads to a frameshift and premature stop-codons. If expression of the protein is prevented by premature stop codons and nonsense-mediated decay, this is commonly referred to as CRISPR/Cas9 knock-out. **(B)** By providing a correction template, in this case an ssDNA oligo, with homologies surrounding the CRISPR/Cas9 target site, the DNA double-strand break can be repaired by homology directed repair (HDR). Thereby, intended mutations or whole protein domains present on the correction template will be introduced upon repair. The process of gene correction is called CRISPR/Cas9 knock-in (Sander and Joung 2014).

synthetically generated tracRNA and crRNA gained importance, especially in immunocompetent cell lines or primary cells (Hultquist et al. 2016; Seki and Rutz 2018). In addition to KO, CRISPR/Cas9 can also be used to precisely manipulate genes in order to achieve single nucleotide exchange and individual amino acid substitution, while preserving the integrity of the surrounding genetic environment. Gene editing or CRISPR/Cas9 knock-in (KI) relies on the same principles as CRISPR/Cas9 KO (Fig. 11B). However, for CRISPR/Cas9 KI, a DNA correction template is provided to repair the DSB introduced by the Cas9 endonuclease via homology directed repair (HDR) (Sander and Joung 2014). The HDR repair template consists of a central mismatch region containing the desired sequence, which flanked by two homology arms. The central mismatch region can compromise a single nucleotide exchange, short protein tags or even whole

protein domains. Repair templates can be provided as plasmids, as well as linear double- or single strand DNA templates (Sander and Joung 2014). Generally, ssDNA oligonucleotides have the advantage of easy synthesis and delivery and are less prone to trigger inflammatory responses upon introduction into target cells (Chen et al. 2011; Paquet et al. 2016).

HDR efficiency usually is low, but can be increased using chemically modified ssDNA, with optimized homology arms (Renaud et al. 2016; Richardson et al. 2016; Paquet et al. 2016). Also, short distance between cutting and intended mutation site, as well as silent mutations preventing recurrent cutting of the CRISPR/Cas9 complex and compounds favoring HDR over NHEJ, can dramatically increase editing efficiencies (Paquet et al. 2016; Skarnes et al. 2019). Thus, CRISPR/Cas9 KI allows the introduction of selected point mutations into the human genome.

There are several advantages of gene editing using CRISPR/Cas9 KI over mutant protein overexpression, to study the effect of mutations on protein function. First, while the exogenous protein is usually expressed at high levels and under the control of viral or other artificial promotors, the modified protein expressed from the endogenous locus, maintains the physiological regulation of the WT allele. In this line, both promotors and enhancers remain intact. Also, the gene of interest maintains its normal splicing pattern, including alternative isoforms. In contrast, exogenous intronless constructs, such as retro- or lentiviral vectors are silenced and modified epigenetically (Tchasovnikarova et al. 2015; Seczynska et al. 2022). Thus, we concluded that CRISPR/Cas9 KI is an interesting tool to study mutants of SAMHD1, especially in the context of post-translational regulation, and would overcome most if not all technical concerns and limitations of traditional mutagenic approaches using overexpression. Therefore, we decided to use CRISPR/Cas9 KI to study SAMHD1 phospho-regulation by mutagenesis in combination with BlaER1 cells as a myeloid cell model.

2. MATERIAL AND METHODS

2.1 Material

2.1.1 Bacterial strains

Table 1: List of bacterial strains

Strain	Genotype	Source
DH5α	F- ϕ80*lac*ZΔM15 Δ(*lac*ZYA-*arg*F) U169 *rec*A1 *end*A1 *hsd*R17 (rk-, mk+) *pho*A *sup*E44 λ- *thi*-1 *gyr*A96 *rel*A1	Thermo Fischer
Stbl3	F-*mcr*B *mrrhsd*S20(rB-, mB-) *rec*A13 *sup*E44 *ara*-14 *gal*K2 *lac*Y1 *pro*A2 *rps*L20(StrR) *xyl*-5 λ-*leumtl*-1	Thermo Fischer

2.1.2 Cell lines

Table 2: List of cell lines

Cell Line	Description	Source/ reference
HEK 293T/17	Human embryonic kidney derived; SV40 large T antigen; ATCC No. CRL-11268	Lab stock (Pear et al. 1993)
HEK 293T/17 SAMHD1 KO	CRISPR/Cas9-mediated KO of SAMHD1 Plasmid: pSpCas9(BB)-2A-GFP_SAMHD1 (ex1)	Kerstin Schott [a]
HeLa	Human cervical adenocarcinoma derived	Shuh Narumiya, Kyoto University, Japan (Schmitz et al. 2010)
HeLa SAMHD1 KO	CRISPR/Cas9-mediated KO of SAMHD1 Plasmid: pSpCas9(BB)-2A-GFP_SAMHD1 (ex1)	Nina Hein-Fuchs [a]
HeLa TZM-bl	Expression of CD4 and CCR5; HIV-1 promotor-dependent luciferase and β-galactosidase expression	NIH AIDS reagent program (Wei et al. 2002)
THP-1	Human acute monocytic leukemia derived; ATCC No. TIB-202	Sumit Chanda, Sanford Burnham Prebys, La Jolla, USA
BlaER1	Human RCH-ACV B-cell leukemia derived; expression of β-Estradiol receptor-C/EBPα fusion protein and GFP	Thomas Graf, Centre for Genomic Regulation, Spain (Rapino et al. 2013)
BlaER1 SAMHD1 KO	CRISPR/Cas9-mediated KO of SAMHD1 Ribonucleoprotein: crSAMHD1_ex1	This work
BlaER1 SAMHD1 KI T592A	CRISPR/Cas9-mediated KI of SAMHD1 T592A Ribonucleoprotein and ssDNA oligo: crSAMHD1_ex16, ssDNA_BlaER1_crRNA-SAMHD1_ex16_IX_T592A	This work
BlaER1 SAMHD1 KI T592E	CRISPR/Cas9-mediated KI of SAMHD1 T592A Ribonucleoprotein and ssDNA oligo: crSAMHD1_ex16, ssDNA_BlaER1_crRNA-SAMHD1_ex16_IX_T592E	This work

[a] Present member of NG3 Host-Pathogen Interactions group

2.1.3 Plasmids

Table 3: List of Plasmids

Plasmid	Description	Source/ reference
pcDNA3.1(+)	mammalian expression plasmid; CMV promoter; *AmpR*	Thermo Fischer
pcDNA3.1(+)-nFlag-SAMHD1	expression of N-terminally Flag tagged codon optimized SAMHD1	André Berger, Paul-Ehrlich-Institut, Germany (Berger et al. 2011)
pcDNA3.1(+)-nFlag-SAMHD1 mutants	expression of N-terminally Flag tagged codon optimized SAMHD1 mutants	
	S33A, S33D, T21A_T25A_S33D, T21E_T25E_S33A, D207A,	This work
	T21A, T21E, T25A, T25E, T21A_T25A, T21E_T25E, D137N, H167A, D311A, Y315A, Q548A, T579A, T579E, T592A, T592E, T579A_T592A, T597A, T592E, T579E_T592A, T597E_T592E	Kerstin Schott [a] (Sommer et al. 2016)
	R145Q	Catharina Majer [a]
pCMV-VSV-G	expression of VSV-G; Addgene plasmid #8454; *AmpR*	Addgene (Stewart et al. 2003)
pEGFP-C1	expression of EGFP; CMV promotor; *KanaR*	Takara
pEGFP-C1-SAMHD1	expression of N-terminally EGFP tagged codon optimized SAMHD1	Kerstin Schott [a]
pENTR1A	Gateway entry vector; *KanaR*	Thermo Fischer
pENTR1A-empty	Gateway entry clone depleted for *CamR* and *ccdB*	This work
pENTR1A-nEGFP-SAMHD1	Gateway entry clone encoding N-terminally EGFP tagged codon optimized WT SAMHD1	This work
pENTR1A-nFlag-SAMHD1 WT or mutants	Gateway entry clone encoding N-terminally Flag tagged codon optimized WT SAMHD1 or T21A, T21E, T25A, T25E, S33A, S33D, T21A_T25A_S33D, T21E_T25E_S33A, D137N, R145Q, D207A H167A, D311A, Y315A, Q548A, T579A, T579E, T592A, T592E, T579A_T592A, T597A, T592E, T579E_T592A, T597E_T592E mutants	This work
pLX304	3rd generation lentiviral gateway destination vector; *BlastR*; Addgene plasmid #25890; *AmpR, CamR*	Addgene (Yang et al. 2011)
pLX304-empty	3rd generation lentiviral gateway destination clone depleted for *CamR* and *ccdB*; *AmpR*	This work
pLX304-nFlag-SAMHD1 WT or mutants	3rd generation lentiviral gateway destination clone encoding N-terminally Flag tagged codon optimized WT SAMHD1 or T21A, T21E, T25A, T25E, S33A, S33D, T21A_T25A_S33D, T21E_T25E_S33A, D137N, R145Q, D207A H167A, D311A, Y315A, Q548A, T579A, T579E, T592A, T592E, T579A_T592A, T597A, T592E, T579E_T592A, T597E_T592E mutants; *AmpR*	This work
pNL4.3 E^- R^- luc	Expression vector based on HIV-1 proviral clone pNL4.3; firefly luciferase inserted into *nef; env* and *vpr* deficient	Nathaniel Landau, New York University School of Medicine, USA (Connor et al. 1995)

pNL4.3 IRES mCherry E^- R^+	Expression vector based on HIV-1 proviral clone pNL4.3; mCherry inserted after *nef; env* deficient	Frank Kirchhoff, University of Ulm, Germany
pMDL-gp-RRE	3rd generation lentiviral packaging plasmid; expression of HIV-1 Gag/Pol; *AmpR*; Addgene #12251	Lab stock (Dull et al. 1998)
pRSV-rev	3rd generation lentiviral packaging plasmid; expression of HIV-1 Rev; *AmpR*; Addgene #12253	Lab stock (Dull et al. 1998)
pSIV3$^+$	Expression vector based on SIV_{mac251}; expression of SIV_{mac251} proteins namely Vpx; *env* and *nef* deficient; packaging signal (Ψ) deficient; *AmpR*	Nicolas Manel, Institut Curie, Paris (Nègre et al. 2000)
pU6-(SAMHD1_ex1)_CBh-Cas9-T2A-mCherry	Expression of mCherry, S. pyogenes Cas9_2A_GFP and a sgRNA directed against SAMHD1 exon 1 (ATC GCA ACG GGG ACG CTT GG); *AmpR*	Nina Fuchs [a] (van Chu et al. 2015)

[a] Present member of NG3 Host-Pathogen Interactions group
Ampicillin resistance gene (AmpR), cytomegalovirus (CMV), chloramphenicol resistance gene (CamR), kanamycin resistance gene (KanaR)

2.1.4 Oligonucleotides

Table 4: List of primers used for mutagenesis

Target mutation	Primer [a]	Primer sequence (5' to 3')	Annealing temperature
S33A	SAM_S33A_7x_for	CCGAGGCCGATTGGGACCCTGGCCTGGAACTG	72°C [b]
	SAM_S33A_7x_rev	CAGTTCCAGGCCAGGGTCCCAATCGGCCTCGG	
S33D	SAM_S33D_7x_for	CCGAGGCCGATTGGGCACCTGGCCTGGAACTG	72°C [b]
	SAM_S33D_7x_rev	CAGTTCCAGGCCAGGTGCCCAATCGGCCTCGG	
D207A	SAM_D207A_for	CGGCCTGTGTCACGCTCTGGGACACGGCC	72°C [b]
	SAM_D207A_rev	GGCCGTGTCCCAGAGCGTGACACAGGCCG	

[a] Primer in forward (for) or reverse (rev) orientation
[b] PCR protocol using KAPA HiFi HotStart ReadyMix (Roche)

Table 5: List of primers for sequencing of plasmids

Primer	Orientation [a]	Primer sequence (5' to 3')	Plasmids
T7	FW	TAATACGACTCACTATAGGG	pcDNA3.1(+) and derivates
BGH Reverse	RV	TAGAAGGCACAGTCGAGG	pcDNA3.1(+) and derivates
CMV Forward	FW	CGCAAATGGGCGGTAGGCGTG	pLX304 and derivates
WPRE-R	RV	CATAGCGTAAAAGGAGCAACA	pLX304 and derivates
pEGFP_for	FW	TTTAGTGAACCGTCAGATC	pEGFP-C1 and derivates
pEGFP_rev	RV	TTTAAAGCAAGTAAAACCTC	pEGFP-C1 and derivates

[a] Primer in forward (FW) or reverse (RV) orientation

Table 6: List of primers for detection of SMRV contamination

Primer[a]	Primer sequence (5' to 3')	Annealing temperature	Reference
F-SMRV-env	GGCGGACCCCAAGATGCTGTG	65°C[b]	(Uphoff et al. 2010)
R-SMRV-env	TGGGCTAGGCTGGGGTTGGAGATA	65°C[b]	(Uphoff et al. 2010)
F-SMRV-gag	TCAGAGCCCACCGAGCCTACCTAC	65°C[b]	(Uphoff et al. 2010)
R-SMRV-gag	CAGCGCAGCACGAGACAAGAAAA	65°C[b]	(Uphoff et al. 2010)

[a] Primer in forward (F) or reverse (R) orientation
[b] PCR protocol using GoTaq polymerase (Promega)

Table 7: List of primers for TIDE or ICE assays and sequencing

Assay	Primer [a]	Primer sequence (5' to 3')	Annealing temperature
TIDE assay SAMHD1 KO	SAM_Seq_Gen-23_FW	GATTTGAGGACGACTGGACTGC	64°C [b]
	SAM_Seq_Gen1116_RV	GTCAACTGAACAACCCCAAGGT	
Sequencing SAMHD1 KO	SAMHD1_Exon 1_III-EX1_FW	TTCTAGCCACGCCCTTTCGC	60°C [c]
	SAMHD1_Exon 1_III-EX1_RV	GAGCCTGCTCCCATCCTACGAA	
ICE assay and sequencing SAMHD1 KI T592	SAM_Seq_Gen58570_FW	CATGAAGGCTCTTCCTGCGTAA	61°C [d] 62°C [c]
	SAM_Seq_Gen59708_RV	ACAAGAGGCGGCTTTATGTTCC	
mRNA sequencing SAMHD1 KI T592	SAMHD1_mRNA_Seq_1630_FW	GTAAGACTGCCCCCAACAGA	58°C [b,c] 59°C [d]
	SAMHD1_mRNA_Seq_2624_RV	TCTTTACCCCAACCTGGCAC	

[a] Primer in forward (FW) or reverse (RV) orientation
[b] PCR protocol using KAPA HiFi HotStart ReadyMix (Roche)
[c] PCR protocol using GoTaq polymerase (Promega)
[d] PCR protocol using KOD Hot Start DNA Polymerase (Merck)

Table 8: List of primers for RT-qPCR

Primer [a]	Primer sequence (5' to 3')	Target gene	Annealing temperature	Reference
hISG54 fwd	CAGCTGAGAATTGCACTGCAA	*ISG54*	56°C	(Yoh et al. 2015)
hISG54 rev	GTAGGCTGCTCTCCAAGGAA			
hRPL13A fwd	CCTGGAGGAGAAGAGGAAAGAGA	*RPL13A*	56°C	(Yoh et al. 2015)
hRPL13A rev	TTGAGGACCTCTGTGTATTTGTCAA			

[a] Primer in forward (for) or reverse (rev) orientation

Table 9: List of primers and probes for qgPCR

Target site	Oligonucleotide	Oligonucleotide sequence (5' to 3')
SAMHD1 exon 16 (T592)	forward primer	CTGGATTGAGGACAGCTAGAAG
	reverse primer	CAGCATGCGTGTACATTCAAA
	probe	/56-FAM/AAATCCAAC/Zen/TCGCCTCCGAGAAGC/3IABkFQ/

Table 10: List of crRNAs

crRNA	Target DNA sequence (5' to 3')	Catalogue number	Source/ reference
crRNA-CD19-1	CTCCCTCCCAGATCTCAGGG	CM-017576-01	Horizon Discovery
crRNA-CD19-2	TCCCTCGGTGGGAGACACGG	CM-017576-02	Horizon Discovery
crRNA-NTC		U-007501-01	Horizon Discovery
crRNA-SAMHD1_ex1_NF	ATCGCAACGGGGACGCTTGG		Horizon Discovery
crRNA-SAMHD1_ex16_IX	TTTTTTTGAGGTGTTATGAG		Horizon Discovery
crRNA-GFP	TAAAAGAAATGGCATTGATG		Horizon Discovery (Glaser et al. 2016)

Non-targeting control (NTC)

Table 11: List of ssDNA homologous recombination templates

Oligonucleotide	DNA sequence (5' to 3')	Source/ reference
ssDNA_BlaER1_crRNA-SAMHD1_ex16_IX_T592A	T*A*G GAT GGC GAT GTT ATA GCC CCA CTC ATA GCA CCT CAA AAA AAG GAA TGG AAC GAC AG*T*A	Horizon Discovery
ssDNA_BlaER1_crRNA-SAMHD1_ex16_IX_T592E	T*A*G GAT GGC GAT GTT ATA GCC CCA CTC ATA GAA CCT CAA AAA AAG GAA TGG AAC GAC AGT*A*C	Horizon Discovery
ssDNA_GFPtoBFP	/AlT-R-HDR1/A*C*CCT GAA GTT CAT CTG CAC CGG CAA GCT GCC CGT GCC CTG GCC CAC CCT CGT GAC CAC CCT GAG CCA CGG GGT GCA GTG CTT CAG CCG CTA CCC CGA CCA CAT GAA GCA CGA CTT CAA GTC CGC CAT G*C*C/AlT-R-HDR2/	IDT (Glaser et al. 2016)

*Phosphothioate

2.1.5 Antibodies

Table 12: List of primary antibodies for immunoblot

Antibody	Species/ clonality	Dilution	Clone	Catalogue number	Source
anti-CDK1	mouse (mAB)	1:2000 in BSA	POH1	9116	CST
anti-Cyclin A2	rabbit (pAB)	1:1000 in BSA		18202-1-AP	Proteintech
anti-Cyclin B1	rabbit (pAB)	1:1000 in BSA		4138	CST
anti-GAPDH	rabbit (mAB)	1:1000 in BSA	14C10	2118	CST
anti-SAMHD1	rabbit (pAB)	1:2000 in milk		A303-691A	Bethyl
anti-SAMHD1	rabbit (pAB)	1:2000 in milk		12586-1-AP	Proteintech
anti-SAMHD1-pT592	rabbit (mAB)	1:1000 in BSA	D702M	89930	CST

Monoclonal antibody (mAB), polyclonal antibody (pAB)

Table 13: List of secondary antibodies for immunoblot

Antibody	Linked to	Species/ clonality	Catalogue number	Source
anti-mouse IgG	HRP	horse (pAB)	7076	CST
anti-rabbit IgG	HRP	goat (pAB)	7074	CST

Horseradish peroxidase (HRP), polyclonal antibody (pAB)

Table 14: List of antibodies for flow cytometry

Antigen/ fluorochrome	Isotype	Dilution	Clone	Source
CCR5-PE	mouse IgG1, κ	1:25	T21/8	BioLegend
CD1a-PE	mouse IgG2b, κ	1:12.5	SK 9	BioLegend
CD4-APC	mouse IgG1, κ	1:5	RPA-T4	BioLegend
CD11b-APC	mouse IgG1, κ	1:50	ICRF44	BioLegend
CD11c-VioBlue	mouse IgG2b	1:12.5	MJ4-27G12	Miltenyi
CD14-PacBlue	mouse IgG2a, κ	1:25	M5E2	BioLegend
CD19-PE	mouse IgG1, κ	1:50	SJ25C1	BioLegend
CD163-PE	mouse IgG1, κ	1:25	GHI/61	BD
CD206-APC	mouse IgG1, κ	1:25	19.2	BD
CXCR4-PE-Cy5	mouse IgG2a, κ	1:5	12G5	BD
$Iso_{(IgG1, \kappa)}$-PE	mouse IgG1, κ		MOPC-21	BioLegend
$Iso_{(IgG1, \kappa)}$-APC	mouse IgG1, κ		MOPC-21	BioLegend
$Iso_{(IgG2a, \kappa)}$-PacBlue	mouse IgG2a, κ		MOPC-173	BioLegend
$Iso_{(IgG2b)}$-PE	mouse IgG2b, κ		MG 2b-57	BioLegend
$Iso_{(IgG2b)}$-VioBlue	mouse IgG2b		IS6-11E5.11	Miltenyi
SAMHD1	rabbit pAB	1:500		Proteintech
$Iso_{(IgG (H+L))}$	rabbit pAB			CST
anti-rabbit IgG-DyLight 405	goat pAB	1:500		Thermo Fisher

Allophycocyanin (APC), pacific Blue (PacBlue), phycoerythrin (PE), polyclonal antibody (pAB)

2.1.6 Buffer and solutions

Table 15: List of buffers and solutions

Buffer	Formulation
Fluorescence-activated cell sorting (FACS) Buffer	10% FCS, 0.1% Sodium acetate in DPBS
Lysis Buffer	0.2 mg/ml Proteinase K, 1 mM CaCl2, 3 mM $MgCl_2$, 1 mM EDTA, 1% Triton X-100, 10 mM Tris (pH 7.5)
3-(N-morpholino)propanesulfonic acid (MOPS) running buffer	1 M MOPS, 1 M Tris, 69.3 mM SDS, 20.5 mM EDTA
NET lysis buffer	50 mM Tris-HCl (pH 7.4), 150 mM NaCl, 15 mM EDTA (pH 7.4), 1% NP-40
Dulbecco's hosphate-buffered saline (DPBS) without Ca^{2+}/ Mg^{2+}	137 mM NaCl, 2.7 mM KCl, 1.47 mM KH_2PO_4, 8.1 mM Na_2HPO_4
Radioimmunoprecipitation buffer (RIPA) buffer	2 mM EDTA, 1% glycerol, 137 mM NaCl, 1% NP40, 0.1% SDS, 0.5% sodium deoxycholate, 25 mM Tris-HCl (pH 8.0)
Super optimal broth with catabolite repression (SOC) medium	2.66% SOB medium (Roth), 0.36% D-Glucose
Stripping buffer	2% SDS, 62.5 mM Tris-HCl (pH 6.8), 100 mM 2-mercaptoethanol
Tris-acetate-EDTA (TAE) buffer	40 mM Tris-HCl (pH 7.4), 20 mM acetate, 1 mM EDTA
Tris-buffered saline (TBS)	50 mM Tris-HCl (pH 7.4), 150 mM NaCl
Tris-buffered saline with Tween (TBST)	TBS, 0.1% Tween 20
X-Gal staining solution	2 mM $K_3[Fe(CN)_6]$, 2 mM $K_4[Fe(CN)_6]$, 0.8 µM $MgCl_2$, 0.4 mg/ml X-Gal

2.2 Methods

2.2.1 Molecular cloning and mutagenesis

Transformation and plasmid preparation

For clonal purification of plasmids in bacteria, chemically competent *Escherichia coli (E. coli)* (Tab. 1) were transformed by heat shock (20 min on ice; 45 s at 42°C; 2 min on ice), resuspended in super optimal broth with catabolite repression (SOC) medium (1 h at 37°C) and plated out on 3.7% lysogeny broth (LB) agar (Merck) supplemented with the respective (Tab. 3) selection antibiotics ampicillin (1 mg/ml) or kanamycin (1 mg/ml) over night at 37°C. Plasmids containing recombinatory sequences, *i.e.* lentiviral untranslated regions, were propagated in the Stbl3 strain. Amplification of plasmids was performed by inoculation into liquid LB medium (Miller) supplemented with the respective selection antibiotics (37°C, overnight). Plasmid preparation was performed using GeneJet Plasmid Miniprep Kit (Thermo Fisher) or NucleoBond Xtra Midi Kit (Macherey-Nagel). DNA concentrations were measured using Nanodrop2000 (Thermo Fisher).

Site directed mutagenesis

Site directed mutagenesis using pcDNA3.1(+)-nFlag-SAMHD1 (0.4 ng/µl) and mismatch primer (Eurofins, 0.6 µM, Tab. 4) was performed together with KAPA HiFi HotStart ReadyMix (Roche) supplemented with 0.08 µM dNTPs (NEB). Following PCR amplification (3 min, 95°C; 35x (20 s, 98°C; 15 s, 72°C; 7.5 min, 72°C); 7.5 min, 70°C) the PCR product was digested with 20 U DpnI (NEB, 1 h, 37°C) mixed with Gel loading dye (NEB) and purified by gel electrophoresis on a 0.75% Agarose (Biozym) gel in TAE buffer supplemented with GelRed (Biotium) for DNA visualization. Subsequently, the isolated DNA fragment was extracted using NucleoSpin Gel and PCR Clean-up Kit (Macherey-Nagel) and transformed into chemically competent bacteria. Resulting plasmid preparations were verified using restriction enzyme digest and Sanger sequencing (LGC). To avoid off-target mutations resulting from PCR errors on the pcDNA3.1(+) backbone, the modified nFlag-SAMHD1 insert was cloned back into the original backbone (see below).

Molecular cloning of plasmids

For conventional cloning, plasmid inserts and backbones were digested using the respective NEB high fidelity enzymes according to manufacturer's recommendations. BamHI and XhoI were used for backcloning of nFlag-SAMHD1 into pcDNA3.1(+) backbone after site directed mutagenesis as well as to transfer nFlag-SAMHD1 into the pENTR1A backbone. NotI was used to deplete Chloramphenicol resistance gene and *ccdB* gene from pENTR1A backbone to create an empty control plasmid. After restriction digest (1-2 h, 37°C) and gel purification, 50 ng backbone was ligated with the appropriate amount of insert (250 ng x ratio length insert to backbone) using 400 U T4 DNA ligase (NEB) at 16°C overnight. The ligated plasmids were then transformed into chemically competent bacteria. For Gateway cloning to generate expression clones, 150 ng Entry clone and 150 ng Destination vector (Tab. 3) were incubated with 2 µl LR Clonase II (Thermo Fisher) at 21°C overnight. The reaction was stopped by incubation with 2 µg Proteinase K (Thermo Fisher; 10 min, 37°C), before transformation into chemically competent Stbl3 bacteria. All generated plasmids were verified by analytic test digest and Sanger sequencing.

2.2.2 Cultivation of mammalian cell lines

Cell lines were free of mycoplasma contamination, as tested by PCR Mycoplasma Test Kit II (PanReac AppliChem). Adherent cells were centrifuged 5 min at 300g and non-adherent cells 10 min at 200g.

Cultivation of 293T and HeLa cells

Adherent HEK 293T/17 and HeLa cells (Tab. 2) were cultured in Dulbecco's Modified Eagle's Medium (DMEM; Merck) supplemented with 10% fetal calf serum (FCS; Sigma-Aldrich) and 2 mM L-glutamine (Merck) at 37°C and 5% CO_2. Upon confluency or for cell seeding, cells were washed with DPBS, detached using Trypsin-EDTA (0.25% Trypsin, 0.1% EDTA in DPBS) and resuspended in fresh cell culture medium.

Cultivation and PMA-activation of THP-1 cells

Non-adherent THP-1 or U937 cells were grown in RPMI-1640 (Merck) supplemented with 10% FCS and 2 mM L-glutamine at 37°C and 5% CO_2. For PMA-activation and induction of an adherent macrophage-like phenotype 4 x 10^4 or 2 x 10^6 cells per well of a 96- or 6-well tissue culture treated plate respectively, were treated with 60 ng/ml or 100 ng/µl PMA (Merck) for 24 or 48 h, as indicated.

Cultivation and transdifferentiation of BlaER1 cells

BlaER1 cells were passaged in RPMI supplemented with 10% FCS and 2 mM L-glutamine at 37°C and 5% CO_2. For transdifferentiation, the original transdifferentiation protocol (Gaidt et al. 2018) was adapted to 6-well format. Therefore, 1 x 10^6 BlaER1 cells per well of a 6-well tissue culture plate were treated with 10 ng/ml human recombinant M-CSF, IL-3 (PeproTech) and 100 nM β-estradiol (Merck) for 7 days. Half of the cell culture supernatant was replaced with fresh medium containing cytokines and β-estradiol at days 2 and 6. At day 7 cells were harvested by pipetting, counted, and used for downstream assays. To prevent excessive cell death after transdifferentiation, cells were centrifuged at 100g only and care was taken to avoid stress due to low temperature.

SMRV detection PCR and quantification of reverse transcriptase activity

For detection of integrated SMRV *gag* and *env* DNA sequences, genomic DNA was extracted from cells using DNeasy Blood & Tissue Kit (Qiagen). PCR amplification was performed using GoTaq polymerase (Promega; 2 min, 94°C; 35x (20 s, 94°C; 30 s, 65°C; 15 s, 72°C); 5 min, 72°C) together with 0.6 µM F-SMRV-env and R-SMRV-env or F-SMRV-gag and R-SMRV-gag primer (Tab. 6) (Uphoff et al. 2010). SAM_Seq_Gen58570_FW and SAM_Seq_Gen59708_RV primer were used as loading controls (2 min, 94°C; 35x (20 s, 94°C; 30 s, 62°C; 45 s, 72°C); 5 min, 72°C). Amplificates were separated and visualized on a 1.0% agarose gel. For quantification of SMRV reverse transcriptase activity, supernatant of native or transdifferentiated BlaER1 or cycling THP-1 cells was collected by centrifugation (200g, 10 min) and passed through a 0.45 µm filter. Reverse transcriptase activity was quantified using C-type RT Activity Kit (CAVIDI) following the instructions of the manufacturer.

2.2.3 CRISPR/Cas9-mediated knock-out and knock-in

Complexation and nucleofection of CRISPR/Cas9 ribonucleoproteins or plasmids

For CRISPR/Cas9 mediate KO and KI, CRISPR/Cas9 RNPs were assembled *in vitro*, as previously described (Hultquist et al. 2016; Seki and Rutz 2018). Therefore, 200 pmol Edit-R Modified Synthetic crRNA (Tab. 10) was incubated with 200 pmol Edit-R CRISPR-Cas9 Synthetic tracrRNA (Horizon Discovery) for 30 min at 37°C. Then, 40 pmol Edit-R Cas9 Nuclease protein NLS (Horizon Discovery) or 40 pmol Cas9-NLS (QB3 Macrolab) were added and again incubated for 15 min at 37°C. For nucleofection, 1 x 10^6 sub-confluent BlaER1 cells were mixed with complexed RNPs or 1 µg plasmid DNA and nucleofected using the 4D-Nucleofector X Unit and SF Cell line Kit (Lonza). Program DN-100 was applied. For CRISPR/Cas9 KI, RNPs were introduced together with 100 pmol of the respective ssDNA HR template. After nucleofection, cells were split into two wells of a 96-well tissue culture plate and allowed to rest for 24 h (KO) or 48 h (KI) in RPMI supplemented with 20% FCS and 2 mM L-glutamine at 37°C and 5% CO_2. If indicated for the specific experiment, 30 µM HDR enhancer V1 (IDT) were added after nucleofection for 24 h, to increase KI efficiency.

Assays to estimate efficiency of CRISPR/Cas9 treatment

Sanger sequencing based computational deconvolution assays, *i.e.* the TIDE and the ICE assay, were used to estimate the efficiency of CRISPR/Cas9-mediated KO and KI (Brinkman et al. 2018; Hsiau et al. 2018). Therefore, CRISPR/Cas9 KO or KI cell pools were collected 24 h or 5 days after nucleofection, respectively. DNA was isolated using DNeasy Blood & Tissue Kit (Qiagen). Subsequently, PCR amplification using appropriate primer pairs (Tab. 7) was performed. To estimate the efficiency of CRISPR/Cas9-mediated SAMHD1 KO, the surrounding region was amplified using KAPA HiFi HotStart ReadyMix and 0.3 µM of SAM_Seq_Gen-23_FW and SAM_Seq_Gen1116_RV primers (3 min, 95°C; 35x (20 s, 98°C; 15 s, 64°C; 45 s, 72°C); 1.5 min, 72°C), isolated from gel and subjected to Sanger sequencing using the SAM_Seq_Gen-23_FW primer. For quantification of HDR events at nucleotides encoding residue T592, 0.3 µM SAM_Seq_Gen58570_FW and SAM_Seq_Gen59708_RV were used together with KOD

Hot Start DNA Polymerase (Merck; 2 min, 95°C; 35x (20 s, 95°C; 15 s, 61°C; 15 s, 70°C)) to amplify the region of interest. SAM_Seq_Gen58570_FW was used for sequencing. The non-baseline corrected Sanger sequencing reads were subjected to TIDE (https://tide.nki.nl/) or ICE (https://www.synthego.com/products/bioinformatics/crispr-analysis) algorithm (Brinkman et al. 2018; Hsiau et al. 2018).

Single cell dilution and cultivation of CRISPR/Cas9 treated cells

To generate single cell clones, CRISPR/Cas9 RNP treated cell pools were subjected to limited dilution. Therefore, 0.1 to 0.2 cells per well of a 96-well tissue culture plate were seeded in RPMI supplemented with 20% FCS, 2 mM L-glutamine, 250 mg/L penicillin and 152 mg/L streptavidin at 37°C and 5% CO_2. Fresh medium was added once. After 3-4 weeks, plates were checked for confluent clones. In case of CRISPR/Cas9 KI, one part of the resuspended confluent clones was frozen in 90% FCS and 10% dimethyl sulphoxide (DMSO; Carl Roth) in 96-well V-bottom plates at -80°C, while the other part was used for DNA extraction and KASP assay screening.

Genetic and molecular characterization of CRISPR/Cas9 knock-out clones

KO single cell clones were grown until they reached confluency in a 24-well tissue culture plate and then tested for absence of SAMHD1 expression by immunoblot (see 2.28.). Frameshift and premature stop-codons on both *SAMHD1* alleles were confirmed by TA cloning and allele specific sequencing. Therefore, the region surrounding the crRNA target site was amplified using 0.6 µM of SAM_Seq_Gen-23_FW and SAM_Seq_Gen1116_RV primers (Tab. 7) together with the GoTaq polymerase (Promega; 3 min, 95°C; 35x (20 s, 98°C; 30 s, 60°C; 45 s, 72°C); 1.5 min, 72°C). After gel cleanup amplicons were ligated into pGEM T-Easy Vector II (Promega) according to manufacturer's protocol, followed by transformation into DH5α cells. Transformed bacteria were grown on 9‰ X-Gal containing LB agar supplemented with ampicillin for blue/ white selection. White colonies were expanded. The purified plasmids were then tested for single insertion using EcoRI (NEB) digest and sequenced with the SAM_Seq_Gen-23_FW primer.

Screening of clones using KASP assay for knock-in

Single cell clone suspensions were pelleted by centrifugation (300g, 10 min) and resuspended in Lysis buffer (Tab. 15) for crude lysate preparation (10 min, 65°C, 15 min, 95°C) (Schmid-Burgk et al. 2014). Lysates were diluted 1:10 and analyzed by custom design end point PCR assay (KASP assay, LGC), according to manufacturer's protocol on a CFX384 Touch Real-Time PCR Detection System (BioRad). DNA obtained from WT and pooled KI cells originally prepared for the ICE assay was used as a control. Single cell clones scoring positive for the mutant allele in a bi-allelic discrimination plot were considered as candidates, unfrozen, expanded and analyzed further.

Genetic and molecular characterization of CRISPR/Cas9 knock-in cells

Homozygous or heterozygous CRISPR/Cas9 KI was confirmed by Sanger sequencing of candidate clones using the same amplification strategy as detailed for the ICE assay. For heterozygous T592E KI, allele specific sequencing was performed, as indicated for CRISPR/Cas9 KO, using SAM_Seq_Gen-23_FW and SAM_Seq_Gen1116_RV primers and a slightly different PCR protocol (2 min, 94°C; 35x (20 s, 94°C; 30 s, 62°C; 45 s, 72°C); 1.5 min, 72°C). To exclude large genomic deletions, quantitative genomic PCR (qgPCR) assay was performed (Weisheit et al. 2020). Therefore, 60 ng of fresh prepared DNA from homozygous KI clones was used in a PrimeTime Gene Expression assay (IDT), together with an appropriate set of primers and a probe (IDT; Tab. 9) on a CFX384 Touch Real-Time PCR Detection System. Human TERT TaqMan Copy Number Reference Assay was used as a copy number reference (Thermo Fischer). For detection of T592 KI variants in expressed mRNA, RNA from transdifferentiated BlaER1 clones was isolated using Nucleospin RNA extraction Kit (Macherey Nagel). 1.5 µg of isolated RNA was treated with 1 U of DNase I in DNase I Reaction Buffer (Thermo Fischer; 15 min, 21°C). The reaction was stopped by addition of 1 µl STOP solution (Thermo Fischer; 10 min, 70°C). Reverse transcription was performed with SuperScript III First-Strand Synthesis System for RT-PCR (Thermo Fischer), using the provided Oligo(dT)20 primer and according to manufacturer's protocol, followed by RNAse H digest. For amplification, KOD Hot Start DNA Polymerase (2 min, 95°C; 35x (20 s, 95°C; 10 s, 59°C; 15 s, 70°C)) or KAPA HiFi HotStart ReadyMix (3 min, 95°C; 35x (20 s, 98°C; 15 s, 58°C; 60 s, 72°C); 60 s, 70°C) were used, together with 3 µl of 1:40 or 1:10 diluted cDNA respectively, as well as 0.3 µM

SAMHD1_mRNA_Seq_1630_fw and SAMHD1_mRNA_Seq_2624_rv primers (Tab. 7). Following gel cleanup, the PCR product was sequenced with the SAMHD1_mRNA_Seq_1630_fw primer. Also, TA cloning and allele specific sequencing of cDNA was performed as described in the previous sections, after amplification with GoTaq polymerase (3 min, 95°C; 35x (20 s, 98°C; 30 s, 58°C; 45 s, 72°C); 1.5 min, 72°C) using 0.5 µM of the same primer and 3 µl of 1:10 diluted cDNA.

2.2.4 Transient cDNA overexpression

Transient cDNA overexpression was achieved by transfection using polyethylenimine (PEI) reagent (Sigma-Aldrich) or Lipofectamine 2000 (Thermo Fischer). In order to test the expression of plasmids, 7.5 x 10^5 293T/17 cells were seeded per well of a 6-well tissue culture plate. The next day, 8 µl of 18 µM PEI reagent were diluted in 125 µl OptiMEM (Thermo Fischer) and again mixed 1:1 with 2 µg plasmid DNA pre-diluted in the same volume of OptiMEM. After incubating 20 min at room temperature (RT), the transfection mixture was added to the cells. Cell culture medium was changed directly before and one day after transfection. Cell lysates were obtained two days post transfection (see section 2.2.8). PEI transfection protocol was also used for production of HIV-1 reporter virus and virus-like particles containing Vpx (VLP-Vpx; see section 2.2.6). Lipofectamine 2000 was used according to manufacturer's protocol for lentiviral particle production and immunofluorescence (for details see sections 2.2.5).

2.2.5 Lentiviral transduction of cDNA

Production of lentiviral particles

3rd generation lentiviral particles were produced by Lipofectamine 2000 based transfection of HEK 293T/17 cells in 6 cm tissue culture dishes. Therefore, 1.2 x 10^6 cells were seeded on a 6 cm dish pre-coated with 0.01 mg/mL poly-L-lysine (PLL; Sigma-Aldrich; 30min, 37°C) and co-transfected one day after seeding with 2.6 µg pMDL-gp-RRE, 2 µg pCMV-VSV-G, 1 µg pRSV-rev and 4 µg of the respective pLX304 based lentiviral transfer plasmid. At day one after transfection, medium was replaced. Cell culture supernatant was harvested at day two and three after transfection, passed through a 0.45 µm syringe filter and stored in three aliquots at -80°C. For particle production in 10

cm dish format, the same strategy was used, but multiplying the variable inputs by factor 2.5 to obtain 5 aliquots of viral particles at both days of harvest.

Transduction and selection of mammalian cells

BlaER1 cells were transduced 3 times with particle containing supernatant. Therefore, one aliquot of lentiviral particles was added to 1 x 10^5 cells per well of a 6-well plate. Transduction was enhanced by spinoculation (200g, 1.5 h, 32°C) and treatment with 8 µg/ml Polybrene Transfection Reagent (Merck) for 3 h together with the addition of viral particles. The next day, cells were centrifuged at 200g for 10 min and resuspended in 1 ml fresh medium, before the next aliquot of lentiviral particles was added. If stated for the specific experiment, transduced cells were selected for 7 days with 10 µg/ml blasticidin (Invivogen). The blasticidin containing medium was changed once and cells were split in a way to avoid confluency. After selection, cells were passaged at least for one week before using them in experiments.

2.2.6 HIV-1 infection experiments

Production of HIV-1 reporter virus particles and VLP-Vpx

For production of VSV-G pseudotyped HIV-1 luciferase and HIV-1-mCherry single cycle reporter viruses, 2 x 10^7 HEK 293T/17 cells were seeded in 175 cm^2 tissue culture flasks and transfected with 5.8 µg pCMV-VSV-G, together with 11.6 µg of the respective pNL4.3 E^- R^- luc or pNL4.3 IRES mCherry E^- R^+ vector (Tab. 3) and 70 µl of 18 µM PEI. Vpx containing VLPs were produced using 2.3 µg pCMV-VSV-G and 15.2 µg $pSIV3^+$ in an analogue manner. Particle containing supernatant was harvested at day 2 and 3 after transfection, centrifuged to pellet cell debris (1500rpm, 10 min, 4°C), filtered through a 0.45 µm filter and digested with 1 U/ml DNAase I (NEB; 1 h, RT). Viral particles then were chilled on ice for 2 h, purified through a 20% sucrose gradient (2h, 106750g, 4°C), resuspended in DPBS, pooled and stored in aliquots at -80°C. HIV-1 particles were titrated on HeLa TZM-bl β-galactosidase reporter cells. Therefore, 1.5 x 10^6 cells were seeded on a 96-well tissue culture plate for 24 h. Viral particles were then added in serial dilutions in 8 technical replicates. Infection was allowed to proceed for 2 days, before washing twice with DPBS and paraformaldehyde (PFA) fixation (15 min, RT). After two

additional washing steps, X-Gal staining solution (Tab. 15) was applied overnight at 37°C and TCID50 was calculated.

Infection of mammalian cells

For HIV-1 infection, 3 x 10^4 transdifferentiated BlaER1 cells per well of a 96-well F-bottom tissue culture plate were seeded in 100 µl cell culture medium. BlaER1 cells were allowed to settle for 2 h. For luciferase readout, cells were seeded in white 96-well F-bottom tissue culture treated plates in technical triplicates. For mCherry readout, 6-12 wells were seeded per condition in order to obtain sufficient cells for flow cytometry. HIV-1 single cycle reporter virus pNL4.3 E^- R^- luc (HIV-1-luc) or pNL4.3 IRES mCherry E^- R^+ (HIV-1-mCherry) particles were added according to the indicated MOI diluted in 50 µl cell culture medium, followed by spinoculation (1.5 h, 200g, 32°C) and incubation at 37°C and 5% CO_2 for 24 h. For luciferase readout, 50 µl of Britelite plus reagent (PerkinElmer) was added per well and incubated for 5 min at RT. Luciferase signal was measured on a Pherastar FS (BMG). For flow cytometry readout of HIV-1-mCherry infection, cells were re-suspended and transferred into V-bottom plates, centrifuged (200g, 10 min, 4°C), pooled and proceeded as detailed in section 2.2.10. VLP-Vpx particles were applied together with HIV-1, as indicated. The amount of VLP-Vpx used in all experiments was optimized for complete SAMHD1 degradation. To show VLP-Vpx-mediated SAMHD1 degradation, 4.4 x 10^5 transdifferentiated BlaER1 cells were treated in a 12-well tissue culture plate in the same conditions and concentrations as stated above.

2.2.7 RT-qPCR

For real time quantitative PCR (RT-qPCR), RNA was isolated using Nucleospin RNA extraction Kit (Macherey-Nagel) and analyzed for mRNA expression in technical triplicates, using QuantiTect SYBR Green RT-PCR Kit (QIAGEN) in 384-well format on a CFX384 (30 min, 50°C; 15 min, 95°C; 44x (15 s, 95°C; 1 min, 56 °C, 1 min, 72°C). Melting curve analysis was performed (15 s, 95°C; 1°C /s, 60-95°C). Primers for RT-qPCR are detailed in Tab. 8.

2.2.8 Immunoblot

For immunoblot, cells were washed in DPBS, lysed in RIPA buffer (Tab. 15) supplemented with proteinase and phosphatase inhibitor (Roche) for 30 min on ice. Lysate was cleared (30 min, 15000g, 4°C) and protein content was measured by Bradford assay using Protein Assay Dye Reagent Concentrate (BioRad). 20 µg total protein were denatured (10 min, 70°C) in NuPAGE LDS Sample Buffer and Reducing Reagent (Thermo Fischer) and separated on a NuPAGE 4-12% Bis-Tris gradient gel (Thermo Fischer) in MOPS running buffer (Tab. 15) supplemented with NuPAGE antioxidant (Thermo Fischer) at 180 V in an XCell SureLock Mini-Cell (Thermo Fischer) for 1.5 h. Transfer was performed in NuPAGE Transfer buffer (Thermo Fischer) supplemented with 9.4% methanol and NuPAGE antioxidant, using an XCell II Blot Module in NuPAGE Transfer Buffer (Thermo Fischer) onto a Hybond P 0.45 PVDF membrane (GE Healthcare) at 30 V for 1 h and 50 min. The membrane was blocked in 5% bovine serum albumin (BSA; Carl Roth) or 5% milk powder (Carl Roth) in TBST (Tab. 15; 2 h, 4°C) and cut horizontally according to target antigens. Primary antibodies listed in Tab. 12 were diluted in 5% BSA or milk powder in TBST and were applied overnight at 4°C under constant agitation. After washing three times in TBST (10 min, RT), anti-rabbit or -mouse IgG, horseradish peroxidase (HRP)-linked antibodies were applied (Tab. 13; 2 h, 4°C) and the membrane was again washed three times with TBST (10 min, RT), before detection on a FUSION FX7 (Vilber Lourmat) using ECL Prime reagent (GE). If required, membranes were stripped of bound antibody in stripping buffer (Tab 15; 1 h, 65°C). Band densities were determined with FUSION software (Vilber Lourmat).

2.2.9 Immunoprecipitation and phosphoproteomics

For mass spectrometric analysis of SAMHD1 residue phosphorylation, endogenous SAMHD1 was purified by immunoprecipitation and separated by gel electrophoresis. Therefore, 2-5 x 10^7 transdifferentiated BlaER1, native THP-1 or THP-1 cells activated with PMA for 48 h were washed in DPBS and lysed in NET lysis buffer (Tab. 15) supplemented with protease and phosphatase inhibitors for 30 min on ice. The lysate was cleared by centrifugation (15000g, 15 min, 4°C) and protein concentration was determined by Bradford assay. 300 µg protein were diluted in 0.1% NP-40 in TBS

supplemented with protease and phosphatase inhibitors and incubated under constant rotation with 7 µg of anti-SAMHD1 (Proteintech; 2 h, 4°C). Protein G Sepharose 4 Fast Flow (GE Healthcare) beads were washed twice in 0.01% NP-40 in TBS (5 min, 4°C; 2000 rpm, 2 min), re-suspended in protein lysate pre-incubated with antibody and incubated for 1 h at 4°C. Subsequently, the beads were washed twice in 0.1% NP-40 in TBS and three time in TBS in the presence of protease and phosphatase inhibitors. After three additional washing steps in H_2O, the beads were boiled in NuPAGE LDS Sample Buffer (5 min, 95°C) and separated on a NuPAGE 4-12% Bis-Tris gradient gel (1.5 h, 180 V). Then, the gel was stained with Coomassie Brilliant Blue R-250 (BioRad; 3 h, RT) and washed overnight in H_2O. The appropriate size band was cut out, subjected to in-gel digest with 18 µl of 20 ng/µl MS grade trypsin (Pierce) in the presence of 0.01% ProteaseMax (Promega) in 200 mM ammonium bicarbonate and 10 mM Tris (pH 8.5). After absorption of the latter solution, 25 µl of 0.01% ProteaseMax in 50 mM ammonium bicarbonate and 10 mM Tris (pH 8.5) were added and incubated at 37°C overnight. The resulting peptide mixture was subjected to C18 Zip Tip clean-up (Merck) before being analyzed by targeted mass spectrometry in tSIM/ddMS2 mode with high-resolution LC-MS/MS, using an Ultimate 3000 Nano Ultra High Pressure Chromatography (UPLC) system interfaced with a Q Exactive Hybrid Quadrupole-Orbitrap mass spectrometer via an EASY-spray (C-18, 15 cm) column (Thermo Fisher).

Table 16: Target peptides and phosphopeptides for tSIM/ddMS2 analysis

Phosphorylation sites covered	Peptide sequence + # phosphates	I	II
T21, S23, T25, S27, S33	TPSNTPSAEADWSPGLELHPDYK + 0-5 PHOS	1-5	0-2
S18, T21, S23, T25, S27, S33	CDDSPRTPSNTPSAEADWSPGLELHPDYK + 0-3 PHOS	1-3	0-3
T74, S84	ENEITGALLPCLDESR + PHOS	1	0-1
S102	LLSYIQR + PHOS	1	-
S278, S283	EQIVGPLESPVEDSLWPYK + PHOS	1	1
T411, T420	ISTAIDDMEAYTK + PHOS	1	1
T463, T460	NLFKYVGETQPTGQIK + PHOS	1	-
T463, T460	YVGETQPTGQIK + PHOS	1	-
T579, T592	NFTKPQDGDVIAPLI(T/A/E)PQK + 0-2 PHOS	1-2	0-1
T579, T592	NFTKPQDGDVIAPLI(T/A/E)TPQKK + 0-2 PHOS	1-2	0-1
T579, T592	NFTKPQDGDVIAPLITPQKK* + 0-2 PHOS	1-2	1-2
T592	PQDGDVIAPLITPQK + 0-1 PHOS	1	0-1
T592	PQDGDVIAPLITPQKK + 0-1 PHOS	1	0-1
	GGFEEPVLLK		
	VGNIIDTMITDAFLK		

Data analysis was executed using Skyline software. Phosphopeptide precursor peak areas in the different conditions were normalized according to the peak area of a non-phosphorylated SAMHD1 peptide (GGFEEPVLLK) in each condition. Relative phosphopeptide abundances were derived from MS1 or (sum of) fragment peak areas. Distinction between different phospho-forms of the same peptide was made by only considering distinguishing fragment peak areas.

2.2.10 Flow cytometry

Cell cycle synchronization and analysis by flow cytometry

Cell cycle synchronization and analysis in HeLa cells was performed by double thymidine block, as described earlier (Schott et al. 2018). 5 x 10^5 HeLa cells were seeded in a 10 cm dish. The following day, the cell culture supernatant was changed to medium containing 2 mM thymidine. After 16 h at 37°C, cells were washed three times in DPBS and medium supplemented with 25 µM 2'-deoxycytidine was added for 8 h at 37°C. Then thymidine treatment was repeated, followed by a 2nd release with 25 µM 2'-deoxycytidine containing medium. Time points post 2nd release were harvested as indicated. Therefore, cells were harvested using trypsin and washed twice in DPBS before downstream immunoblot and flow cytometry analysis. While harvesting and washing, cells were kept on ice or at 4°C. Subsequently, HeLa cells were fixed by dropwise addition of ice cold 70% ethanol (2h, 4°C) and washed twice in DPBS before staining. Then, cells were passed through a 60 µM cell strainer, stained with FxCycle PI/RNase Staining Solution (Thermo Fisher; 30 min, RT) and analyzed on an LSRFortessa Cell Analyzer (BD). FCS Express V6 (De Novo Software) was used for gating and cell cycle quantification in living GFP$^+$ single HeLa cells as described previously (Schott et al. 2018).

Analysis of cell surface expression and reporter virus infection

For flow cytometry analysis of BlaER1 transdifferentiation and expression of cell surface markers, 1 x 10^6 native or transdifferentiated BlaER1 cells were collected, washed once in FACS buffer (Tab. 15; 10 min, 300g, 4°C) and stained with the respective antibodies or isotype controls (Tab. 12), together with Fixable Viability Dye eFluor 780 (FVD780;

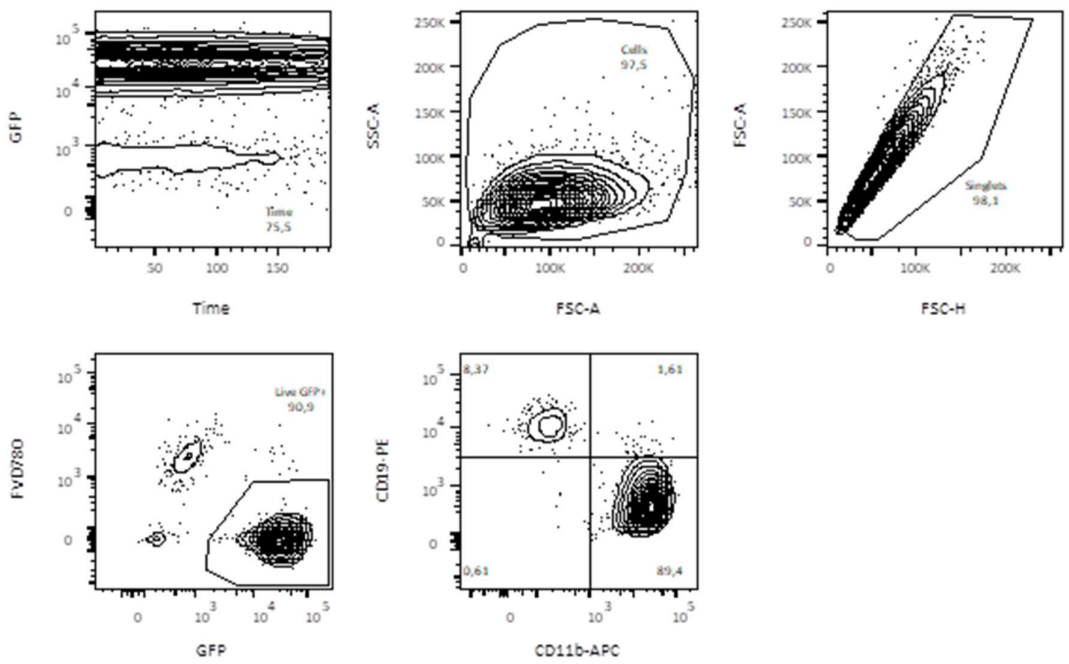

Figure 12: Gating strategy for analysis of BlaER1 transdifferentiation and cell surface marker expression. Flow cytometry gating strategy for quantification of $CD19^-$ $CD11b^+$ transdifferentiated BlaER1 cell population in bulk transdifferentiated cells, with parent to daughter gates shown from the upper left to the lower right. For analysis of transdifferentiation, cells were measured on an LSRFortessa Cell Analyzer (BD). FlowJo (BD) was used for gating, quantification and visualization.

Thermo Fischer; 20 min, 4°C). For analysis of BlaER1 transdifferentiation and surface marker expression, FC Block (BD) was added to the staining cocktail. Stained cells were washed in FACS buffer twice and fixed in 2% paraformaldehyde (30 min, RT), before analyzing on a LSR II instrument (BD). The gating for FACS analysis of BlaER1 transdifferentiation and expression of cell surface markers with FlowJo V10 (BD) is detailed in Fig. 12. For readout of HIV-1-mCherry infection, cells were washed and stained with CD11b-APC and FVD780, as detailed above. Infected cells were fixed, analyzed on a BD LSRFortessa and quantified with FlowJo, as illustrated in Fig. 13.

Intracellular staining for SAMHD1 expression

For intracellular SAMHD1 staining in HIV-1-mCherry infection experiments, BlaER1 cells pooled form 12 infected wells of a 96 well plate (see 2.2.6) were stained with CD11b-APC and FVD780 in 96-well V-bottom plates, as detailed above. Subsequent to cell

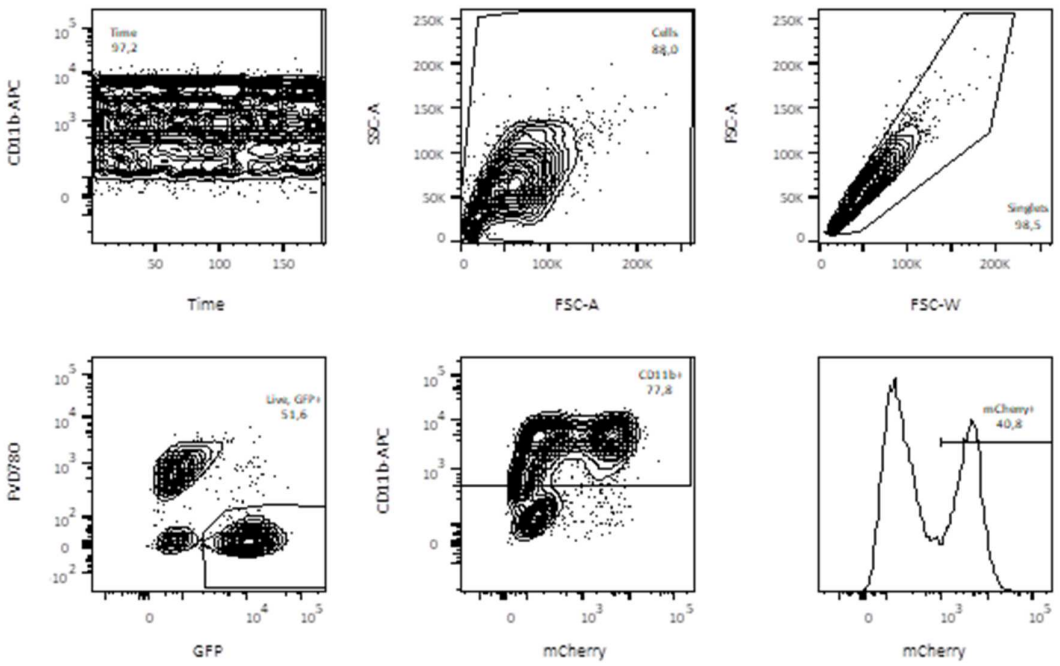

Figure 13: Gating strategy for quantification of HIV-1-mCherry reporter virus infection in transdifferentiated BlaER1 cells.

Flow cytometry gating strategy for quantification of HIV-1-mCherry reporter virus infection in the $CD11b^+$ transdifferentiated BlaER1 cell population, with parent to daughter gates shown from the upper left to the lower right. For analysis of infection, cells were measured on an LSRFortessa Cell Analyzer (BD). FlowJo (BD) was used for gating, quantification and visualization.

surface staining and washing, cells were fixed in pre-warmed Cytofix Buffer (BD; 37°C, 10 min). After centrifugation (300g, 10 min, 4°C), Cytofix Buffer was discarded and cells were permeabilized with chilled Perm Buffer III (BD; 2min on ice). Permeabilization was stopped by addition of FACS buffer and cells were washed twice before staining with anti-SAMHD1 or an isotype control (Tab. 12; 60 min, RT). Then, cells were again washed twice and stained with secondary anti-rabbit antibody coupled to DyLight 405 (Tab. 14; 60 min RT). After two additional washing steps, stained cells were analyzed on a BD LSRFortessa, employing the gating strategy detailed in Fig. 14.

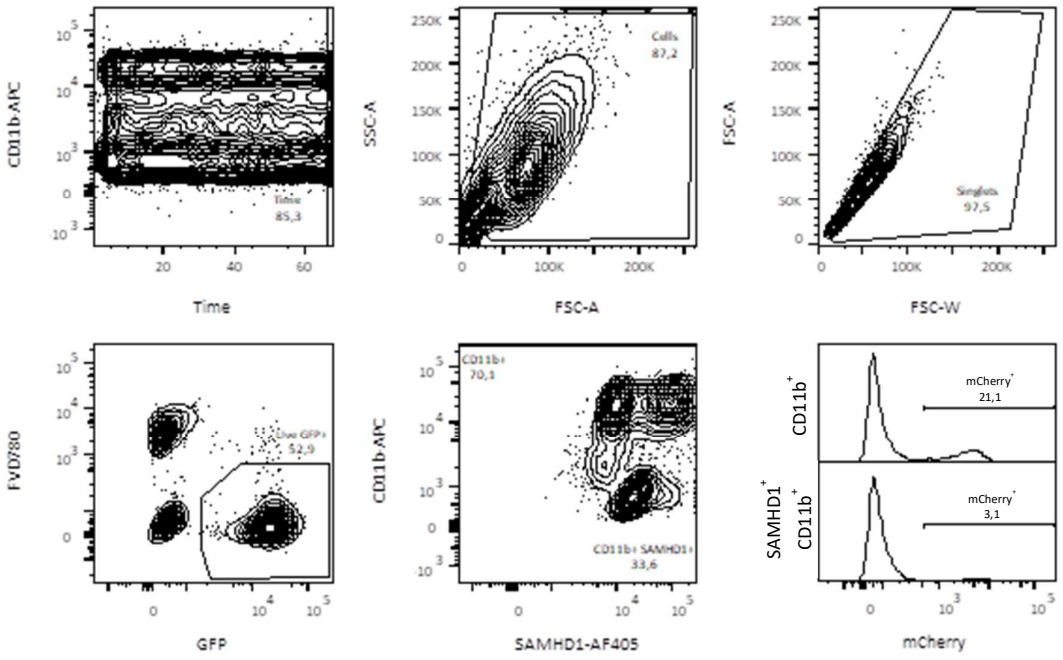

Figure 14: Gating strategy for quantification of HIV-1-mCherry reporter virus infection in SAMHD1 overexpressing transdifferentiated BlaER1 cells.

Flow cytometry gating strategy for quantification of HIV-1-mCherry reporter virus infection in SAMHD1$^+$ CD11b$^+$ transdifferentiated BlaER1 cells after bulk transduction for SAMHD1 overexpression. Parent to daughter gates are shown from the upper left to the lower right. For a nalysis of infection, cells were measured on an LSRFortessa Cell Analyzer (BD). FlowJo (BD) was used for gating, quantification and visualization.

2.2.11 Quantification of cellular dNTP content and concentration

For measurement of cellular dNTP levels, 2 x 10^6 transdifferentiated BlaER1 cells or 293T cells transfected with 8 µg of pcDNA3.1(+)-nFlag-SAMHD1 using Lipofectamin 2000 in a six well format for 48 h, were washed in DPBS and incubated with 65% ice cold methanol (95°C, 3 min) in order to extract dNTPs. After centrifugation (14 000 rpm, 3min, 4°C), cell free supernatant was vacuum dried at 45°C and quantification of all four dNTPs by single nucleotide incorporation assay was performed, as described previously (Diamond et al. 2004). CD19 depletion was accomplished using CD19 microbeads and MS columns (Miltenyi), following manufacturer's recommendations. Cell volumes were determined by seeding respective cell types on a Cell Carrier-96 well plate (Perkin Elmer) coated with 10% Poly-D-Lysine (Sigma; 1.5h, RT). After centrifugation (5 min, 300g), cells were fixed in 4% PFA (15 min, 37°C), permeabilized with 0.1% Triton X-100 in DPBS (5 min, 37°C)

and stained using HCS CellMask Deep Red Stain (Thermo Fischer; 30 min, RT). Z-Stack of stained cells was acquired using confocal imaging platform Operetta (Perkin Elmer) and volume was calculated as a sum of cell areas in all relevant Z-stacks using Harmony software (Perkin Elmer).

2.2.12 Protein structure prediction

For protein structure prediction, AlphaFold implemented in the UCSF ChimeraX software was used (Jumper et al. 2021; Pettersen et al. 2021; Varadi et al. 2022). SAMHD1 protein prediction structure as predicted by AlphaFold (AF-Q9Y3Z3-F1-model_v2) was used. For comparative analysis of SAMHD1 mutants *de novo* predictions were generated for full length human SAMHD1 amino acid sequence (UniProtKB Q9Z3Y3) or manually annotated mutants using the ChimeraX AlphaFold (host: https://colab.research.google.com/github/sokrypton/ColabFold/blob/main/AlphaFold2.ipynb) or the RoseTTAFold (host: http://robetta.bakerlab.org/) prediction tools (Baek et al. 2021; Jumper et al. 2021; Pettersen et al. 2021; Varadi et al. 2022; Mirdita et al. 2022). To estimate the effect of SAMHD1 mutants on protein stability, DynaMut analysis was applied (Rodrigues et al. 2018).

2.2.13 Statistics

Statistical analysis was performed using GraphPad Prism (V9). If not otherwise stated, mean and standard deviation of biological replicates are indicated. Linear regression was used to analyze infections over a wide range of MOIs. Statistical significance was assessed using unpaired two-tailed t-test, as well as non-parametric Kruskal-Wallis test or parametric One-Way ANOVA, corrected against multiple testing using Dunn's or Dunnet correction, respectively. The level of statistical significance is indicated in figures with asterisks (* $p < 0.05$; ** $p < 0.01$; *** $p < 0.001$; **** $p < 0.0001$; ns, not significant).

3. RESULTS

3.1 Transdifferentiated BlaER1 cells are a novel macrophage model to study SAMHD1-mediated restriction

3.1.1 BlaER1 transdifferentiation is reliable and robust

Myeloid models to study HIV-1 restriction by mutagenesis are largely limited to PMA-activated macrophage-like cells. In order to expand our toolkit and to study SAMHD1 restriction and regulation in a more physiological macrophage model, we decided to establish transdifferentiated BlaER1 cells, as a novel model for HIV-1 infection in myeloid cells. Native B cell derived BlaER1 cells are transdifferentiated into macrophage-like cells via induction of the macrophage transcription factor CEBPα, which was fused to the estradiol receptor. Transdifferentiation is sustained by IL-3 and M-CSF treatment (Rapino et al. 2013). We used a transdifferentiation protocol adapted to the 6-well format (Stefan Bauer, unpublished), which enabled us to generate transdifferentiated BlaER1 macrophage-like cells in larger cell culture volumes, as compared to the original protocol described for the 96-well format (Gaidt et al. 2016; Gaidt et al. 2018). To control for successful and reliable transdifferentiation using this adapted protocol, we analyzed B cell marker CD19 and macrophage marker CD11b expression on native and transdifferentiated BlaER1 cells by flow cytometry. As demonstrated earlier (Rapino et al. 2013), transdifferentiation of BlaER1 cells resulted in loss of CD19 and acquisition of CD11b in the vast majority of cells (Fig. 15A). Using the adapted protocol, transdifferentiation was highly reproducible and yielded 89.3 ± 8.8% (n = 33) of $CD19^-$ $CD11b^+$ cells in living GFP^+ BlaER1 cells (Fig. 15B). Only in two out of 33 transdifferentiation attempts, we detected less than 75% of $CD19^-$ $CD11b^+$ (open circles Fig. 15B), which we considered outliners and for which the cells were not used for downstream experiments. Thus, BlaER1 transdifferentiation using the adapted protocol (Stefan Bauer, unpublished) is highly reproducible and yields a high proportion of $CD19^-$ $CD11b^+$ macrophage-like BlaER1 cells.

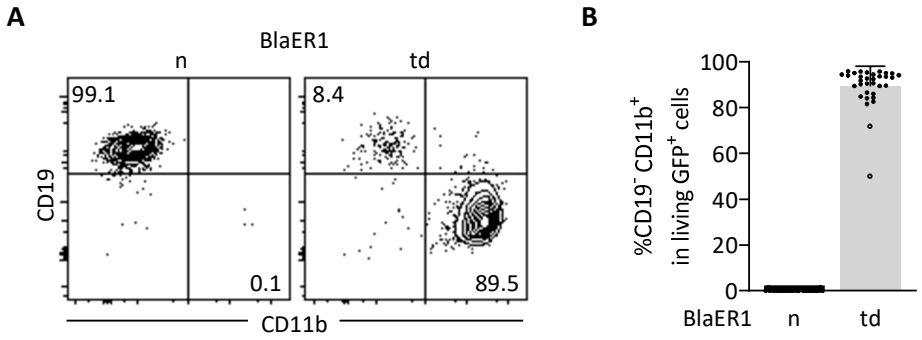

Figure 15 : BlaER1 transdifferentiation is reliable and robust.

(A) Representative flow cytometry analysis of CD19 and CD11b surface expression in native (n) and transdifferentiated (td) BlaER1 cells. Relative frequencies of $CD19^+$ $CD11b^-$ and $CD19^-$ $CD11b^+$ cell populations are indicated as % of living GFP^+ cells (n = 33). **(B)** Relative quantification of macrophage-like $CD19^-$ $CD11b^+$ cells in living GFP^+ native (n) or transdifferentiated (td) BlaER1 cells. Every dot represents an individual transdifferentiation approach. Experiments in which transdifferentiated BlaER1 cells show < 75% $CD19^-$ $CD11b^+$ cells in living GFP^+ cells were excluded from downstream analysis (open circles). Error bars correspond to standard deviation (n_n = 30, n_{td} = 33).

3.1.2 Transdifferentiated BlaER1 cells express macrophage markers and HIV-1 (co-) receptors

With transdifferentiation, the transcriptome of BlaER1 cells changes drastically and they adopt a gene expression profile closely resembling human monocyte-derived macrophages (Rapino et al. 2013). In order to validate these findings on a protein level, we analyzed surface expression of monocyte, macrophage and DC markers CD14, CD163, CD206, CD11c and CD1a by flow cytometry (Fig. 16). In concordance with their B cell ontogeny, native BlaER1 cells did not express CD14, CD163, CD206, CD11c or CD1a. After transdifferentiation however, the vast majority of BlaER1 cells showed CD163 and CD11c expression (Fig. 16), which, together with the expression of CD11b (Fig. 15), is in line with a myeloid phenotype. CD14 expression, a marker mainly found in monocytes and tissue resident macrophages, was differentially distributed in the transdifferentiated BlaER1 cell population (Fig. 16) (Uhlen et al. 2019; Karlsson et al. 2021). Few cells remained $CD14^-$, while most cells showed intermediate or high CD14 expression, indicating that two subpopulations of transdifferentiated BlaER1 cells might exist. Also, a subset of BlaER1 cells acquired macrophage and myeloid DC marker CD206

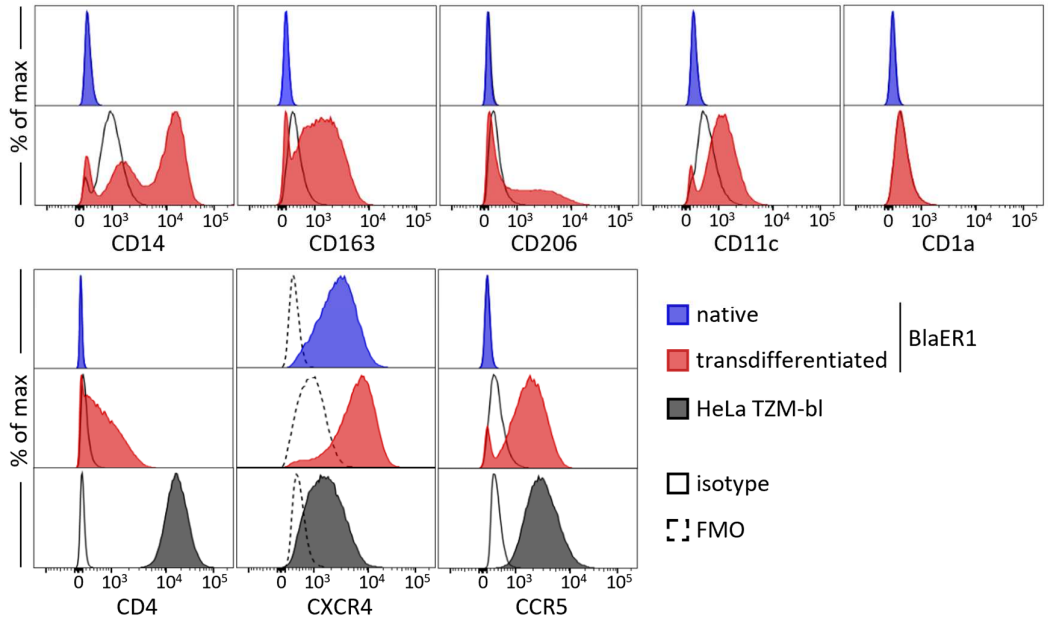

Figure 16: Transdifferentiated BlaER1 cells express macrophage markers and HIV-1 (co-) receptors.
Cell surface expression of indicated monocyte-derived macrophage or dendritic cell associated markers CD14, CD163, CD206 or CD11c and CD1a respectively, as well as HIV-1 (co-) receptors CD4, CXCR4 (CD184) and CCR5 (CD195), as analyzed by flow cytometry in living GFP$^+$ cells of native (blue) and transdifferentiated (red) BlaER1 cells. HeLa TZM-bl cells were used as positive controls for HIV-1 (co-) receptors. Solid or dashed black lines indicate respective isotype or fluorescence minus one (FMO) control (n = 3).

expression, after transdifferentiation (Uhlen et al. 2019; Karlsson et al. 2021). We did not detect CD1a expression in transdifferentiated BlaER1 cells. CD1a is a marker of Langerhans cells, as well as for some myeloid DC and monocyte subsets (Uhlen et al. 2019; Karlsson et al. 2021). Taken together, transdifferentiated BlaER1 cells express surface markers associated with a monocyte or macrophage-like phenotype.

In vivo, macrophages are a relevant HIV-1 target cells due to HIV-1 receptor CD4 and CXCR4 or CCR5 co-receptor surface expression and their role in HIV-1 transmission, persistence and pathogenesis (Verani et al. 1998; Sattentau and Stevenson 2016). By flow cytometry analysis, we could detect CD4 and CCR5 surface expression on the majority of transdifferentiated, but not native BlaER1 cells (Fig. 16). CCR5 expression in transdifferentiated BlaER1 cells was comparable to HeLa TZM-bl cells, which were previously modified for overexpression of CCR5 and CD4 (Platt et al. 1998). CD4

expression in transdifferentiated BlaER1 cells was low, as compared to HeLa TZM-bl cells, but clearly higher than the isotype control in the main macrophage-like population. CXCR4 is expressed on both native and transdifferentiated BlaER1 cells at levels slightly higher than in HeLa TZM-bl cells (Fig. 16). In conclusion, expression of HIV-1 (co-) receptors indicates that macrophage-like transdifferentiated BlaER1 cells might be amenable to infection with non-pseudotyped CCR5- and CXCR4- tropic HIV-1.

3.1.3 BlaER1 cells carry a productive endogenous retrovirus and show elevated baseline ISG levels

BlaER1 cells have successfully been used to study innate immune signaling (Gaidt et al. 2016; Gaidt et al. 2017; Greulich et al. 2019). However, several groups (Oliver Keppler, Veith Hornung, Stefan Bauer, personal communication) reported a possible contamination of the BlaER1 cell line with the squirrel monkey retrovirus (SMVR), an endogenous retrovirus present in a number of cell lines (Uphoff et al. 2010; Uphoff et al. 2019). In order to test, whether our batch was also affected, we used SMRV *env* and *gag* specific PCR (Uphoff et al. 2010). SMRV *env* and *gag* were detected in early passage BlaER1 cells, as well as in SAMHD1 KO single cell clones derived from the original BlaER1 cell batch (for details see section 3.2.3), but not in other cell lines used in this work (Fig. 17A).

BlaER1 cells have been generated based on the RCH-ACV cell line, which previously has not been reported to be infected with SMRV and for which the original stocks are SMRV-negative (Thomas Graf, unpublished). Likely, SMRV was accidentally transmitted from a SMRV-positive cell line by co-culture (Thomas Graf, personal communication) with SMRV-positive Namalwa cells (Uphoff et al. 2010). To test if the SMRV clone present in BlaER1 cells is able to produce viral particles, we measured C-type retrovirus reverse transcription (RT) activity in the cell free supernatant obtained from native and transdifferentiated BlaER1 cells (Fig. 17B). RT activity was clearly detectable in native WT BlaER1 cells. In transdifferentiated WT and SAMHD1 KO BlaER1 cells, we detected lower levels of C-type retrovirus RT activity, which however was consistently above the background activity found in non-contaminated cells (Fig. 17B). Therefore, we conclude

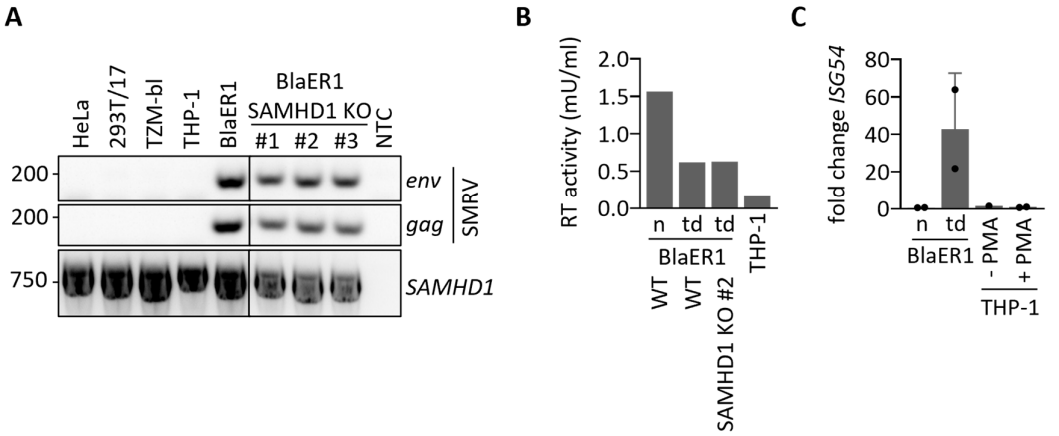

Figure 17: BlaER1 cells carry productive endogenous retrovirus and show elevated baseline ISG levels.
(A) Detection of SMRV *gag* and *env* in genomic DNA isolated from indicated cell types or no template control (NTC) by PCR amplification. Primers specific for SAMHD1 exon 16 were used as controls (n = 1). **(B)** Measurement of C-type retrovirus reverse transcriptase (RT) activity in cell free supernatant obtained from native (n) and transdifferentiated (td) BlaER1, as well as cycling THP-1 cells (n = 1). **(C)** RT-qPCR analysis of *ISG54* mRNA expression in native (n) and transdifferentiated (td) BlaER1 cells, as well as cycling (- PMA) THP-1 or THP-1 cells activated for 24 h with 60 ng/ml PMA (+ PMA). *ISG54* mRNA expression was normalized to *RPL13a* and again to PMA-activated THP-1 cells according to $2^{-\Delta\Delta Ct}$ method. Error bars indicate standard deviation of biological triplicates (n = 2).

that native BlaER1 cells are in principle able to produce infectious SMRV particles and should be handled and quarantined accordingly.

Endogenous retroviruses can modify innate sensing and might serve as a source of PAMPs to trigger immune activation and ISG response (Schmidt et al. 2019a; Srinivasachar Badarinarayan and Sauter 2021). To evaluate if transdifferentiated BlaER1 cells could be used as a model for HIV-1 sensing in macrophages, we analyzed baseline ISG expression in native and transdifferentiated BlaER1 cells. While we could not observe elevated *ISG54* expression in native BlaER1 cells, when compared to cycling and PMA-activated THP-1 cells, we observed high baseline *ISG54* expression in transdifferentiated BlaER1 cells (Fig. 17C). Therefore, due to SMRV contamination and elevated baseline ISG levels, BlaER1 cells might not be an ideal model to study HIV-1 sensing and induction of ISG response in macrophage-like cells. However, this caveat can very likely be overcome using adequate control conditions.

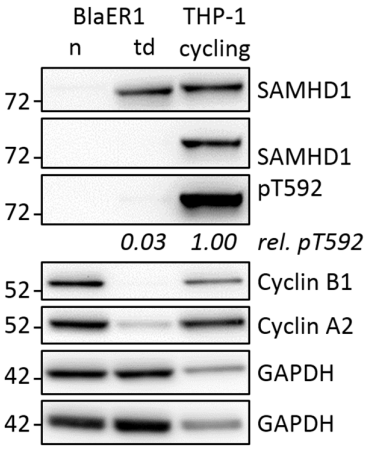

Figure 18 : Transdifferentiated BlaER1 cells express SAMHD1 which is dephosphorylated at residue T592.
Representative immunoblot analysis of SAMHD1, Cyclin B1 and Cyclin A2 expression in native (n) and transdifferentiated (td) BlaER1 cells, as well as cycling THP-1 cells. GAPDH was used as a loading control. Mean of SAMHD1 T592 phosphorylation (pT592) relative to total SAMHD1 expression in transdifferentiated BlaER1 cells was normalized to cycling THP-1 cells (n = 6).

3.1.4 Transdifferentiated BlaER1 cells express SAMHD1 dephosphorylated at residue T592

SAMHD1 is a major anti-lentiviral restriction factor in myeloid cells (Hrecka et al. 2011; Berger et al. 2011; Laguette et al. 2011). To test if transdifferentiated BlaER1 cells could serve as a model to study SAMHD1-mediated HIV-1 restriction in macrophages, we analyzed SAMHD1 expression by immunoblot. Transdifferentiated, but not native BlaER1 cells showed a high level of SAMHD1 expression, which was comparable to cycling THP-1 cells (Fig. 18). Also, SAMHD1 in transdifferentiated BlaER1 cells was completely dephosphorylated at residue T592. Relative SAMHD1 T592 phosphorylation was 31-fold lower in transdifferentiated BlaER1 compared to cycling THP-1 cells (0.032 ± 0.013 relative SAMHD1 pT592 normalized to cycling THP-1, n = 6, Fig. 18). SAMHD1 T592 de-phosphorylation is an important pre-requisite for SAMHD1-mediated HIV-1 restriction. SAMHD1 T592 phosphorylation is mediated by cyclin A2 in complex with CDK1 in cycling cells (Cribier et al. 2013; Welbourn et al. 2013; White et al. 2013b). In line with this, cyclin A2 and cyclin B1 expression was drastically reduced in transdifferentiated BlaER1 cells (Fig. 18). Low cyclin expression also confirms the reported G_1/G_0 arrest in transdifferentiated BlaER1 cells (Rapino et al. 2013). Taken together, high expression of SAMHD1 completely dephosphorylated at residue T592 suggests that SAMHD1 could serve as an active restriction factor in transdifferentiated BlaER1 cells.

3.2 SAMHD1 is a major HIV-1 restriction factor in transdifferentiated BlaER1 cells

3.2.1 VLP-Vpx-mediated SAMHD1 depletion increases HIV-1 infection in transdifferentiated BlaER1 cells

HIV-2 and SIV_{mac} effector protein Vpx targets SAMHD1 for proteasomal degradation leading to fast and efficient depletion of SAMHD1 (Berger et al. 2011; Hrecka et al. 2011; Laguette et al. 2011). To define the restrictive capacity of SAMHD1 in the context of transdifferentiated BlaER1 cells, we infected the cells with a single-cycle HIV-1 luciferase reporter virus (HIV-1-luc), in presence or absence of VLPs containing SIV_{mac251} Vpx (VLP-Vpx). VLP-Vpx treatment led to efficient degradation of SAMHD1 (0.013 ± 0.007 relative SAMHD1 expression normalized to no VLP-Vpx, n = 3) (Fig. 19A) and strongly increased HIV-1-luc infection (Fig. 19B). Comparison of linear regression of untreated or VLP-Vpx treated cells, revealed a significant increase over a wide range of MOIs. Thus, SAMHD1 seems to efficiently block HIV-1 infection of transdifferentiated BlaER1 cells. This block can be overcome by VLP-Vpx treatment in *trans*.

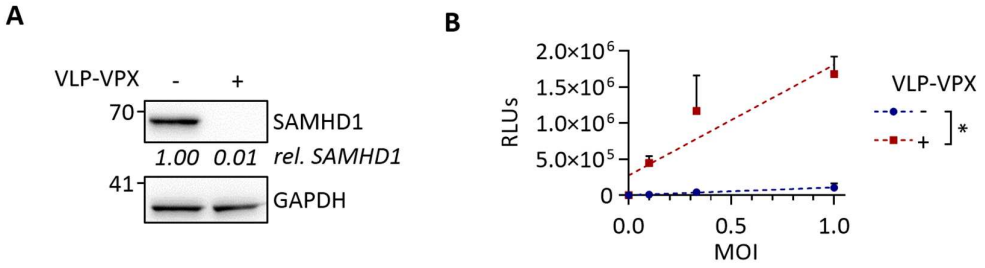

Figure 19: VLP-VPX-mediated SAMHD1 depletion increases HIV-1 infection in transdifferentiated BlaER1 cells.

(A) Transdifferentiated BlaER1 cells were treated with VLP-Vpx or medium for 24 h. SAMHD1 degradation was measured by immunoblot and quantified relative to GAPDH expression, followed by normalization to medium treated control (mean of n = 3). **(B)** VLP-Vpx or medium treated transdifferentiated BlaER1 cells were infected at the time point of treatment with VSV-G pseudotyped HIV-1 single-cycle luciferase reporter virus pNL4.3 E^- R^- luc at an MOI of 0.1, 0.33 and 1. Relative light units (RLUs) were quantified by luciferase measurement in cells at 24 hours post infection (hpi). Linear regressions (dashed lines) were calculated and differences of slopes tested for significance ($p = 0.0125$, n = 3, unpaired t-test). Error bars correspond to standard deviation (* $p < 0.05$).

3.2.2 CRISPR/Cas9 ribonucleoprotein-mediated knock-out is efficient in BlaER1 cells

In order to genetically study SAMHD1 and to validate its anti-viral restriction by forward genetics, we decided to use the CRISPR/Cas9 KO technology. So far, CRISPR/Cas9 KO in BlaER1 cells was achieved using plasmid-based guide RNA (gRNA) and Cas9 co-expression systems (Ran et al. 2013; Schmid-Burgk et al. 2014; Gaidt et al. 2016). Even though this methodology can be highly efficient, recent evidence indicates that RNP based CRISPR/Cas9 KO can reach a higher efficiency especially in primary cells, but also in delicate or hard to transfect cell lines (Hultquist et al. 2016; Seki and Rutz 2018). Therefore, we adopted the published methodology and developed a KO pipeline, in which Cas9 RNP is assembled with tracrRNA and gene specific crRNA *in vitro* and subsequently introduced into native BlaER1 cells via nucleofection (Fig. 20A). By optimizing the standard nucleofection protocol, we were able to reach high nucleofection efficiencies (up to 42%) in BlaER1 cells (data not shown). To assess KO efficiency in BlaER1 cells, we designed crRNAs directed against *CD19* and monitored CD19 surface expression 120 h after RNP nucleofection by flow cytometry. Depending on the specific crRNA target sequence, RNP treatment resulted in 35 to 60% $CD19^-$ KO cells, indicating our CRISPR/Cas9 RNP protocol to be highly efficient in BlaER1 cells (Fig. 20B). The TIDE assay allows an estimation of CRISPR/Cas9 InDel efficiencies in bulk preparation of cells (Brinkman et al. 2018) (Fig. 20A). When generating SAMHD1 KO cells, we directly compared CRISPR/Cas9 InDel efficiencies in BlaER1 cells treated with a RNP directed against SAMHD1 exon 1 (crRNA-SAMHD1-ex1_NF) or a plasmid based system (pU6-(SAMHD1_ex1)_CBh-Cas9-T2A-mCherry), targeting the same sequence (Fig. 20C). InDel efficiency in RNP treated cells was high (60.3%) and 4-fold higher than in cells in which the plasmid based CRISPR system was introduced by nucleofection. Low efficiency of the CRISPR plasmid system might be explained by a higher proportion of cell death in the plasmid treated condition and a non-optimal expression of promotors in native BlaER1 cells (data not shown). In conclusion, we show that RNP based CRISPR/Cas9 strategy in BlaER1 cells is highly efficient and might be superior to plasmid-based CRISPR/Cas9 KO approaches.

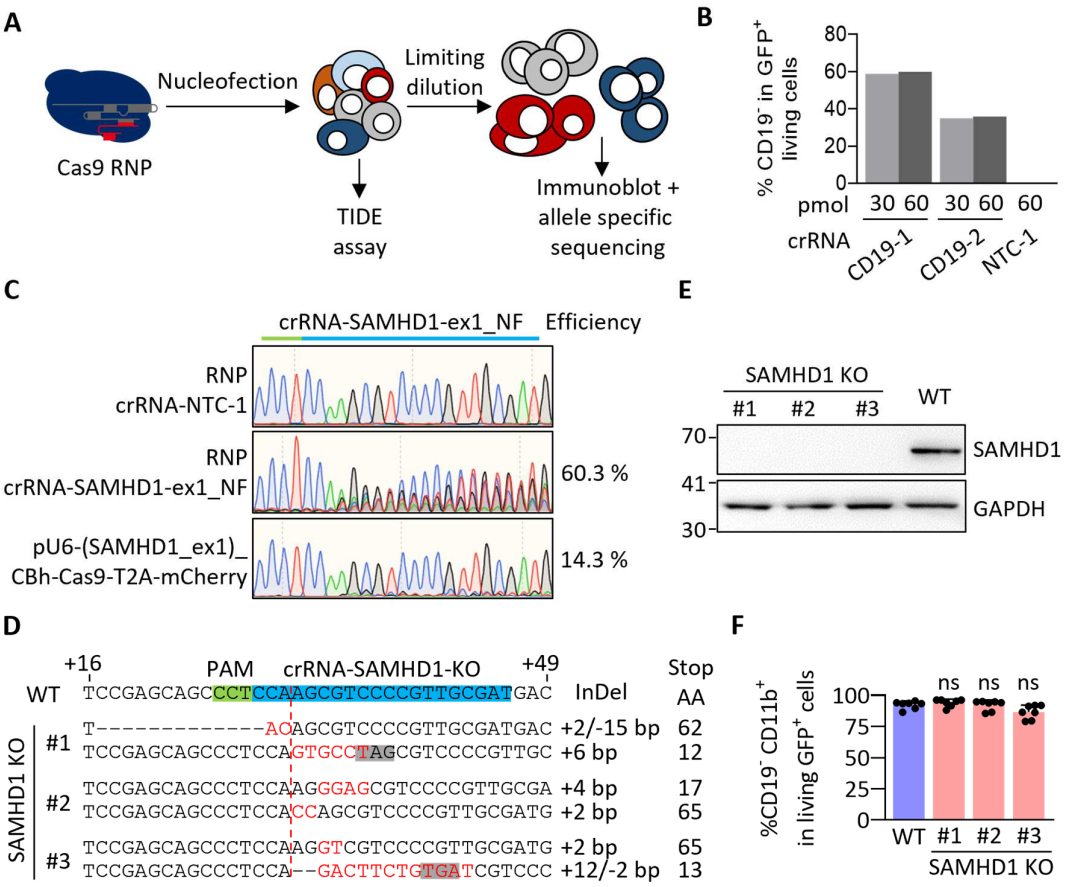

Figure 20: Strategy based on CRISPR/Cas9 ribonucleoprotein allows efficient generation of SAMHD1 knock-out BlaER1 cells.

(A) Our CRISPR/Cas9 knock-out (KO) strategy was based on *in vitro* assembled ribonucleoprotein (RNP) consistent of Cas9 protein tracrRNA and a target specific crRNA. RNPs were introduced into cells via nucleofection and the efficiency of InDel formation was analyzed using TIDE assay in bulk preparations (Brinkman et al. 2018). Bi-allelic KO in single cell clone generated by limited dilution was analyzed by allele specific sequencing and confirmed by immunoblot on the protein level. **(B)** Native BlaER1 cells were nucleofected with CRISPR/Cas9 protein after *in vitro* complexation with one of two crRNA targeting the *CD19* gene (crRNA-CD19-1 and crRNA-CD19-2) or a non-targeting control (crNTC-1). CD19 expression in living GFP⁺ BlaER1 cells was analyzed 120 h after nucleofection, by flow cytometry (n = 1). **(C)** Sanger sequencing reads of bulk preparations obtained from BlaER1 cells nucleofected with non-targeting control RNPs (crNTC-1), RNPs targeting SAMHD1 exon 1 (crRNA-SAMHD1-ex1_NF), or a plasmid encoding Cas9 and a CRISPR guide RNA targeting the same sequence. Efficiencies of InDel formation as determined by TIDE assay are indicated (n = 1). **(D)** Single cell clones generated from crRNA-SAMHD1-ex1_NF treated BlaER1 cells were Sanger sequenced after TA-cloning to separate alleles and aligned to WT. The extent of insertions (red) and/or deletions (InDels) are indicated, as well as the position of the premature stop codon (gray) introduced by the respective genetic modification. **(E)** Genetically confirmed SAMHD1 knock-out clones were analyzed via immunoblot for SAMHD1 expression in transdifferentiated BlaER1 cells.

GAPDH was used as loading control (n = 7). **(E)** Percentage of $CD19^-$ $CD11b^+$ cells in living GFP^+ transdifferentiated WT and SAMHD1 KO cells were quantified by flow cytometry (#1 *p = 0.6679*, #2 *p > 0.9999*, #3 *p = 0.1913*, n = 7, Kruskal–Wallis test). Error bars correspond to standard deviation (ns, not significant).

3.2.3 CRISPR/Cas9-mediated knock-out of SAMHD1 in BlaER1 cells

Since generation of InDels using RNPs directed against SAMHD1 exon 1 seemed highly efficient, we also anticipated a high frequency of phenotypic SAMHD1 KO. Indeed, after generation of single cell clones by limited dilution (Fig. 20A), we screened for absence of SAMHD1 expression in transdifferentiated BlaER1 cells by immunoblot and could identify several clones that showed no detectable SAMHD1 protein expression. In order to validate potential KO clones on a genetic level, we performed allele specific Sanger sequencing. Three clones showed bi-allelic InDels resulting in a frameshift and a premature stop codon after not more than 65 amino acids (Fig. 20D). The parental RCH-ACV cell line of BlaER1 cells does not harbor a duplication in chromosome 20, suggesting that all available SAMHD1 loci were detected and are modified in the SAMHD1 KO clones (Jack et al. 1986). Importantly, the exact sequence of all six InDels was non-identical (Fig. 20D), indicating that we could identify three completely independent single cell SAMHD1 KO clones. Genetically validated SAMHD1 KO clones were again confirmed for absence of detectable SAMHD1 expression in transdifferentiated BlaER1 cells (Fig. 20E). Importantly, transdifferentiation of BlaER1 SAMHD1 KO single cell clones still was highly efficient and not affected by SAMHD1 KO (Fig. 20F).

3.2.4 SAMHD1 knock-out relieves block to HIV-1 reporter virus infection in BlaER1 macrophages

To test the restrictive potential of transdifferentiated SAMHD1 KO BlaER1 cells clones, we performed an infection experiment using HIV-1-luc at MOI 0.1, 0.33 and 1. As expected, genetic depletion of SAMHD1 led to a strong increase of HIV-1-luc infection over a wide range of MOIs (Fig. 21A). Comparing linear regressions calculated based on different MOIs, we saw a highly significant increase of HIV-1-luc infection in all three validated SAMHD1 KO clones. Even though BlaER1 transdifferentiation is highly efficient, a minor $CD11b^-$ $CD19^+$ cell population persists (Fig. 21B) and might contribute to the

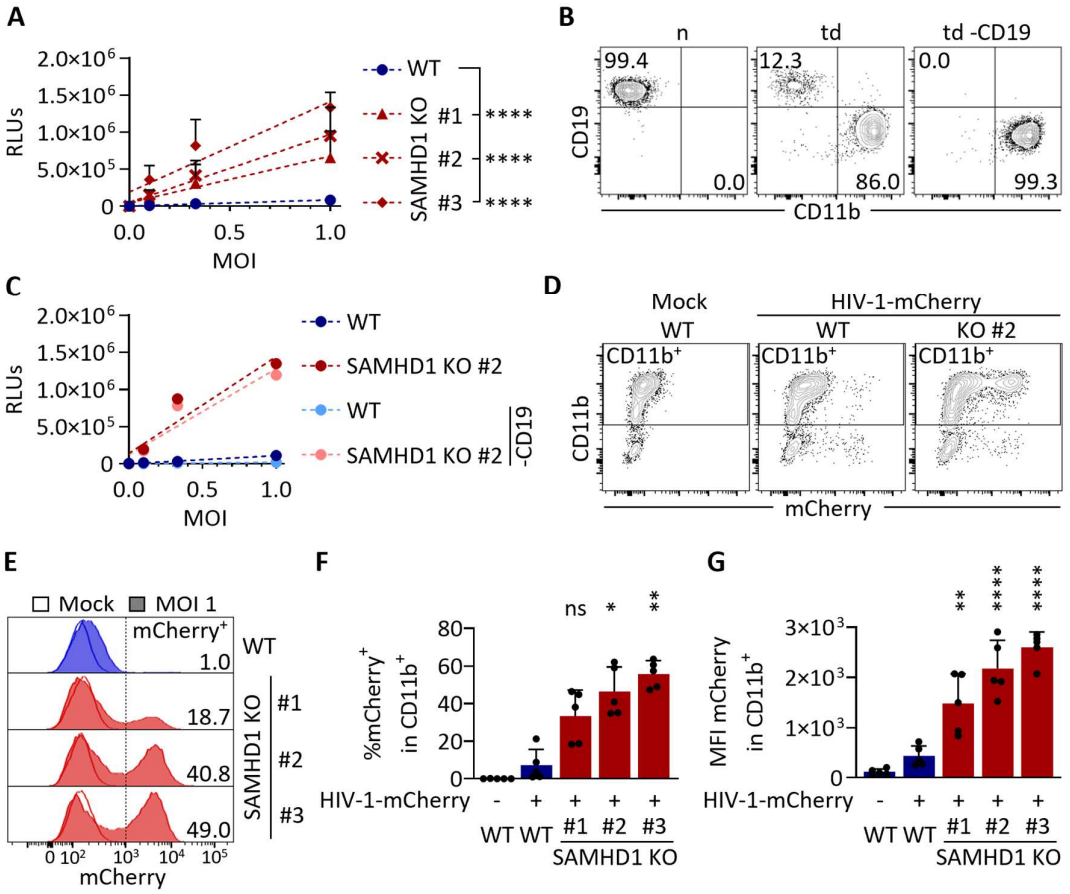

Figure 21 SAMHD1 knock-out relieves block to HIV-1 reporter virus infection in BlaER1 macrophages.

(A) Transdifferentiated BlaER1 WT and SAMHD1 KO cell clones were infected with pNL4.3 E^- R^- luc (VSV-G) and RLUs quantified 24 hpi. Statistical significance of differences between linear regressions (dashed lines) in SAMHD1 KO clones compared to WT are indicated ($p < 0.0001$ for Clone #1, 2 and 3, n = 7, One-way ANOVA). (B) Residual $CD19^+$ cells in transdifferentiated BlaER1 cell preparations, were depleted using magnetic bead separation and infected with pNL4.3 E^- R^- luc (VSV-G) (C). RLUs were quantified 24 hpi and linear regressions are shown (n = 1). Error bars indicate standard deviation of technical triplicates. (D, E, F, G) Transdifferentiated WT and SAMHD1 KO cell clones were infected with VSV-G pseudotyped HIV-1 single cycle mCherry reporter virus pBR HIV1 M NL4.3 IRES mcherry E^- R^+ at MOI 1. Living GFP^+ were analyzed for CD11b expression (D) and percentage of $mCherry^+$ cells was quantified by flow cytometry in living GFP^+ $CD11b^+$ BlaER1 cells at 24 hpi. (E) Representative histograms are shown for mock and HIV-1 mCherry reporter virus infected transdifferentiated WT and SAMHD1 KO BlaER1 cell clones. Percentage of $mCherry^+$ in living GFP^+ $CD11b^+$ BlaER1 cells (F) or mean fluorescence intensity is shown (G). Bar graphs indicate mean of experiments, dots individual biological replicates for $\%mCherry^+$ cells (Clone #1 $p = 0.3633$, #2 $p = 0.0360$, #3 $p = 0.0013$, n = 5, Kruskal–Wallis test) and MFI (Clone #1 $p = 0.0053$, #2 $p < 0.0001$, #3 $p < 0.0001$, n = 5, One-way ANOVA). (A, F, G) Error bars correspond to standard deviation of biological replicates (* $p < 0.05$; ** $p < 0.01$; **** $p < 0.0001$; ns, not significant).

luciferase signal measured after infection with HIV-1-luc or bias the number of $CD11b^+$ infected cells and thus might affect the outcome of infection experiments.

To investigate the impact of this minor native-like cell population on HIV-1-luc infection, we performed CD19 depletion on transdifferentiated WT and SAMHD1 KO BlaER1 cells using magnetic bead separation (Fig. 21B). CD19 depletion drastically reduced the proportion of residual native-like $CD19^+$ $CD11b^-$ cells in transdifferentiated BlaER1 cells below 0.05%, leading to highly pure (> 99%) $CD19^-$ $CD11b^+$ macrophage-like cell population. We infected the purified cells with HIV-1-luc (Fig. 21C). CD19 depletion slightly decreased the level of infection in SAMHD1 KO, but importantly reduced the level of residual infection in WT BlaER1 cells to a minimum, consistent with the hypothesis that residual native-like cells support HIV-1 infection independent of SAMHD1-mediated restriction.

To rule out a potential confounding effect of a minor $CD11b^-$ native-like population, we developed a flow cytometry workflow combining the use of a single-cycle HIV-1-mCherry reporter virus (HIV-1-mCherry) together with staining for living $CD11b^+$ cells. Using this strategy, we could specifically analyze and quantify the infection in transdifferentiated $CD11b^+$ macrophage-like BlaER1 cells, even though a substantial proportion of $CD11b^-$ cells was infected at 24 hours post infection (hpi) (Fig. 21D and E). HIV-1-mCherry infection, as measured by the percentage of $mCherry^+$ cells and by mean fluorescence (MFI) in $CD11b^+$ living GFP^+ transdifferentiated BlaER1 cells, was strongly and significantly increased upon SAMHD1 KO at 24 hpi (Fig. 21F and G). This confirms that SAMHD1 is a major anti-lentiviral restriction factor in macrophage-like transdifferentiated BlaER1 cells. We conclude that transdifferentiated BlaER1 cells are a good model to study SAMHD1-mediated HIV-1 restriction.

3.3 CRISPR/Cas9 knock-in strategy validates regulation of SAMHD1 by phosphorylation at T592

3.3.1 Overexpressed SAMHD1 is hyperphosphorylated

Previous analysis of the restrictive potential of SAMHD1 mutants has so far been limited to assays employing SAMHD1 overexpression and rescue of restriction in a SAMHD1-

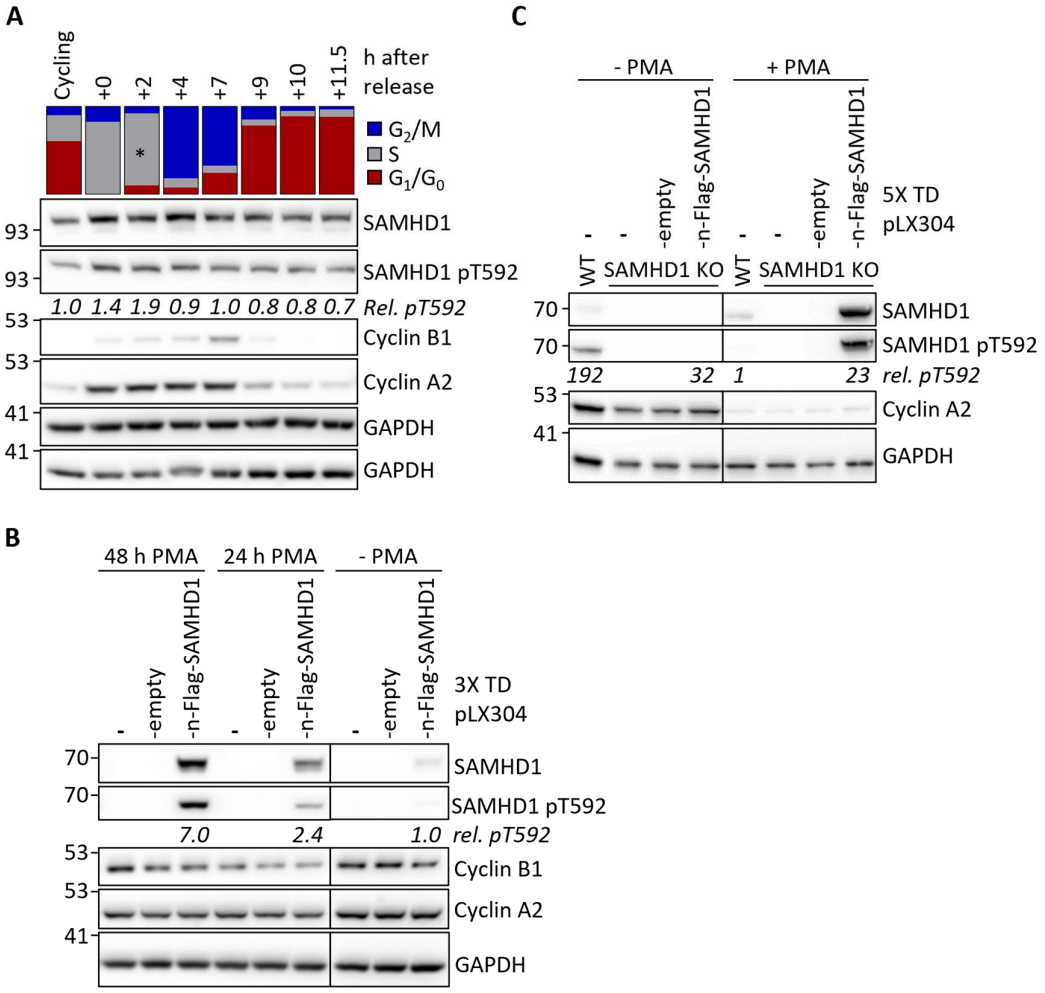

Figure 22: Overexpressed SAMHD1 is hyperphosphorylated.

(A) Hela cells 3X transduced with pLX304-nEGFP-SAMHD1 and selected for blasticidin resistance were synchronized using double thymidine block and analyzed for SAMHD1 expression and T592 phosphorylation at several time points post release by immunoblot. Ratio of SAMHD1 T592 phosphorylation (pT592) relative to SAMHD1 expression was normalized to cycling HeLa cells. Cell cycle distribution was analyzed by flow cytometry using automated cell cycle determination (* manual cell cycle gating) (n = 1). **(B)** Immunoblot analysis of U937 cells transduced 3X with empty or nFlag-SAMHD1 encoding pLX304 lentiviral particles and selected for blasticidin resistance. Cells were differentiated with 100 ng/ml PMA for indicated time span. Relative SAMHD1 T592 phosphorylation was normalized to non-PMA treated cells overexpressing SAMHD1. Data generated by Paula Rauch under supervision (n = 1). **(C)** Immunoblot analysis of SAMHD1 KO THP-1 cells transduced 5X with respective pLX304 particles and selected for blasticidin resistance. THP-1 cells were activated as indicated with 60 ng/ml PMA for 24 or 48 h. Relative SAMHD1 T592 phosphorylation was normalized to endogenous SAMHD1 of PMA-treated WT THP-1 cells (n = 1).

negative background *i.e.* PMA-activated U937 cells (Cribier et al. 2013; Welbourn et al. 2013; White et al. 2013b). However, we and others repeatedly failed to reliably reproduce even the well-established phenotype of phospho-mimetic T592E and phosphoablative T592A mutant overexpression in U937 and SAMHD1 KO THP-1 cells (not shown, Michael Schindler personal communication). This was found independent of the specific lenti- or retroviral vector system used, as well as of the level of SAMHD1 expression achieved in bulk cell preparations (not shown). Additionally, rescue of SAMHD1-mediated restriction in PMA-activated SAMHD1-negative U937 and SAMHD1 KO THP-1 cells lacked consistency and seemed to be unstable over time even though the cell population was selected for successful transgene integration (not shown, Felipe Diaz-Griffero personal communication). We thus hypothesized that overexpressed SAMHD1 might be dysregulated with regards to residue T592 phosphorylation, as compared to endogenous SAMHD1 expressed at physiological levels. This again might affect anti-viral activity.

In order to better understand the effect of SAMHD1 overexpression on SAMHD1 T592 phosphorylation, we analyzed cell cycle-dependent (de-) phosphorylation of overexpressed nEGFP-SAMHD1 in HeLa cells after release from double thymidine block. Cyclin expression and cell cycle analysis by flow cytometry indicated successful cell cycle synchronization of nEGFP-SAMHD1 overexpressing HeLa cells (Fig. 22A). However, overexpressed nEGFP-SAMHD1 showed only a minor increase in T592 phosphorylation in cells blocked in S-phase (+0 and +2 h) and upon progression through G_2 (+4 and +7 h), when compared to cycling or G_1/G_0 HeLa cells. Also, no drastic decrease of T592 phosphorylation was observed upon transition through mitosis (Fig. 22A, +9 to +11.5h). This was in stark contrast to cell cycle-dependent pT592 levels of endogenous SAMHD1 in synchronized HeLa cells (Schott et al. 2018) and indicates that overexpressed SAMHD1 is inadequately regulated by cell cycle-dependent mechanisms.

To validate these findings for PMA-activated myeloid cells, we analyzed SAMHD1 phosphorylation upon overexpression in U937 and SAMHD1 KO THP-1 cells (Fig. 22B and C). PMA treatment strongly induced expression of pLX304-nFlag-SAMHD1 construct in U937 and THP-1 cells. Indeed, also T592 phosphorylation reached high levels in PMA-activated U937 and THP-1 cells overexpressing SAMHD1. Surprisingly, PMA treatment of U937 cells overexpressing SAMHD1 did increase T592 phosphorylation 2.4- to 7.0-

fold relative to cycling U937 cells (Fig. 22B). In concordance, even though low cyclin A2 expression in PMA-treated THP-1 cells suggested a near complete cell cycle arrest in G_1/G_0, T592 phosphorylation of overexpressed SAMHD1 was 23-fold higher in PMA-activated THP-1 cells compared to the phosphorylation ratio of the endogenous SAMHD1 protein (Fig. 22C).

In summary, overexpression of SAMHD1 leads to dysregulation of cell cycle-dependent T592 phosphorylation. Importantly, SAMHD1 in common myeloid models, such as PMA-activated U937 and THP-1 cells, is hyperphosphorylated when overexpressed. This might impact anti-retroviral activity of SAMHD1 and affect stability and reliability of these model systems. Alternative methods to validate the restrictive activity of SAMHD1 mutants in the myeloid models are urgently needed.

3.3.2 CRISPR/Cas9 ribonucleoprotein-mediated knock-in can be achieved in BlaER1 cells

One possibility to overcome problems with SAMHD1 mutant overexpression would be the introduction of specific mutations into the endogenous *SAMHD1* locus. Recent developments in the field of gene editing using CRISPR/Cas9-mediated KI allow the introduction of single nucleotide changes at the genomic level via HR (Paquet et al. 2016; Renaud et al. 2016). However, efficiency of CRISPR/Cas9 KI is highly cell type-dependent. Efficient delivery of Cas9, gRNA and HDR template are key determinants of KI efficiency (Renaud et al. 2016). In addition, other cell intrinsic features *i.e.* the activity and choice of the different DNA DSB repair pathways clearly have a strong impact on KI efficiency (Liu et al. 2018b; van Chu et al. 2015; Maruyama et al. 2015). In order to avoid cell death induced by nucleofection of plasmid DNA (not shown), we decided to combine efficient delivery of Cas9 RNPs together with correction templates in form of ssDNA oligonucleotides, which can, especially when chemically modified, serve as good HDR template (Chen et al. 2011; Paquet et al. 2016; Renaud et al. 2016) and might be less immunogenic (Gaidt et al. 2017; Bartok and Hartmann 2020).

BlaER1 cells express GFP. In order to easily quantify CRISPR/Cas9 KI efficiency in cycling BlaER1 cells, we made use of a GFP to BFP conversion assay (Glaser et al. 2016). Here, introduction of a GFP-specific Cas9 RNP together with a ssDNA correction template

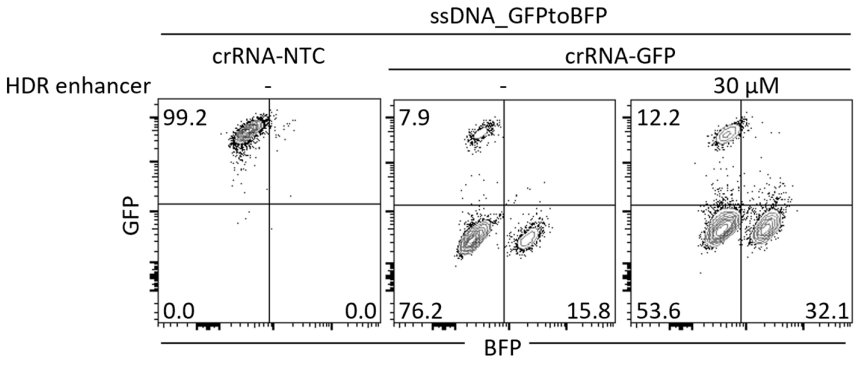

Figure 23: CRISPR/Cas9 ribonucleoprotein mediated knock-in in BlaER1 cells.

Cas9 RNP containing non-targeting crRNA-NTC or crRNA-GFP, directed against GFP, together with an ssDNA correction template introducing a mutation that confers GFP to BFP mutation (ssDNA_GFPtoBFP), were introduced into BlaER1 cells by nucleofection. As indicated, HDR enhancer was applied at 30 µM for 24 h after nucleofection. GFP to BFP conversion was measured by flow cytometry after 9 days. The percentage the parental living cell gate is shown (n = 1).

confers single nucleotide exchange leading to a GFP Y167H mutation and to GFP to BFP conversion. This can easily be measured by flow cytometry. Nucleofection of BlaER1 cells with RNPs containing crRNA-GFP-1 and ssDNA_GFPtoBFP led to the conversion of a substantial fraction (15.8%) of GFP^+ BlaER1 cells into BFP^+ cells 9 days after nucleofection, indicating that CRISPR/Cas9 KI can achieve high frequencies in BlaER1 cells (Fig. 23). Only a minor fraction of BlaER1 cells remained GFP^+, suggesting that overall efficacy of delivery and CRISPR editing was high. However, a large fraction of BlaER1 cells (76.2%) lost GFP expression without acquiring BFP expression. This indicates that non-homologous repair pathways are highly active in cycling BlaER1 cells, introducing random InDels in a large fraction of cells and outcompeting ssDNA correction template-dependent HDR.

Small molecule-mediated inhibition of the NHEJ pathway or promotion of HDR pathways has been shown to favor HDR-dependent KI over insertions of InDels in various settings (Liu et al. 2018b; van Chu et al. 2015; Maruyama et al. 2015). Indeed, the commercially available Alt-R HDR Enhancer, led to a 2-fold increase in the efficiency of GFP to BFP conversion in cycling BlaER1 cells (Fig. 23). In conclusion, CRISPR/Cas9 RNP nucleofection together with the use of ssDNA correction templates allows CRISPR KI in cycling BlaER1 cells.

3.3.3 Generation and validation of SAMHD1 mutants introduced via CRISPR/Cas9-mediated knock-in into BlaER1 cells

To generate endogenous SAMHD1 mutants of the residue T592 via CRISPR/Cas9-mediated KI, we developed a pipeline based on the introduction of RNPs and ssDNA correction templates using nucleofection into cycling BlaER1 cells (Fig. 24A). Nucleofected cells were separated by limited dilution. Based on bulk sequencing, as well as TIDER and ICE assay (Brinkman et al. 2018; Hsiau et al. 2018), we expected low frequency of HDR events and a high proportion of alleles harboring non-specific InDels (Fig. 24E). To overcome this hurdle, we screened for KI candidate clones using the allele-specific KASP-genotyping PCR screening assay (Fig. 24B). CRISPR/Cas9 KI in $KASP^+$ candidate clones was validated by Sanger sequencing (Fig. 24C). Quantitative genomic PCR (qgPCR) was used to exclude large genomic deletions (Fig. 24D) (Weisheit et al. 2020).

Indeed, using Sanger sequencing, we were able to identify several homozygous KI clones harboring the SAMHD1 T592A or T592E mutation (Fig. 24C). Initially we were also able to identify heterozygous SAMHD1 T592E and T592A mutants (Fig. 24C). However, when analyzing the expression of both *SAMHD1* allele variants in heterozygous SAMHD1 mutants by reverse transcription and bulk, as well as allele specific Sanger sequencing of mRNA obtained from transdifferentiated BlaER1 cell clones, we were only able to identify the mutant allele (not shown). This indicated the absence of expression for the WT *SAMHD1* allele. Therefore, heterozygous SAMHD1 mutants were not included in downstream analysis. CRISPR/Cas9 KI can lead to loss of single alleles and to pseudo-homozygosity (Weisheit et al. 2020). Quantification of allele numbers of *SAMHD1* exon 16 revealed that the majority of homozygous single cell T592A and T592E KI clones still contained two alleles of *SAMHD1* exon 16 (Fig. 24D). However, we could identify one out of 8 clones (Clone X), showing loss of one allele in qgPCR, indicative of pseudo-homozygosity (Weisheit et al. 2020). In total, we were able to generate and validate two homozygous T592A, as well as three homozygous T592E BlaER1 KI mutants, corresponding to a homozygous KI frequency of ~1% and highlighting the necessity of KASP pre-screening to reduce the number of KI candidates (Fig. 24E). In our hands, prediction of KI efficiency using ICE and TIDER assays was not reliable and the outcome rather dependent on the specific mutation introduced (Fig. 24E).

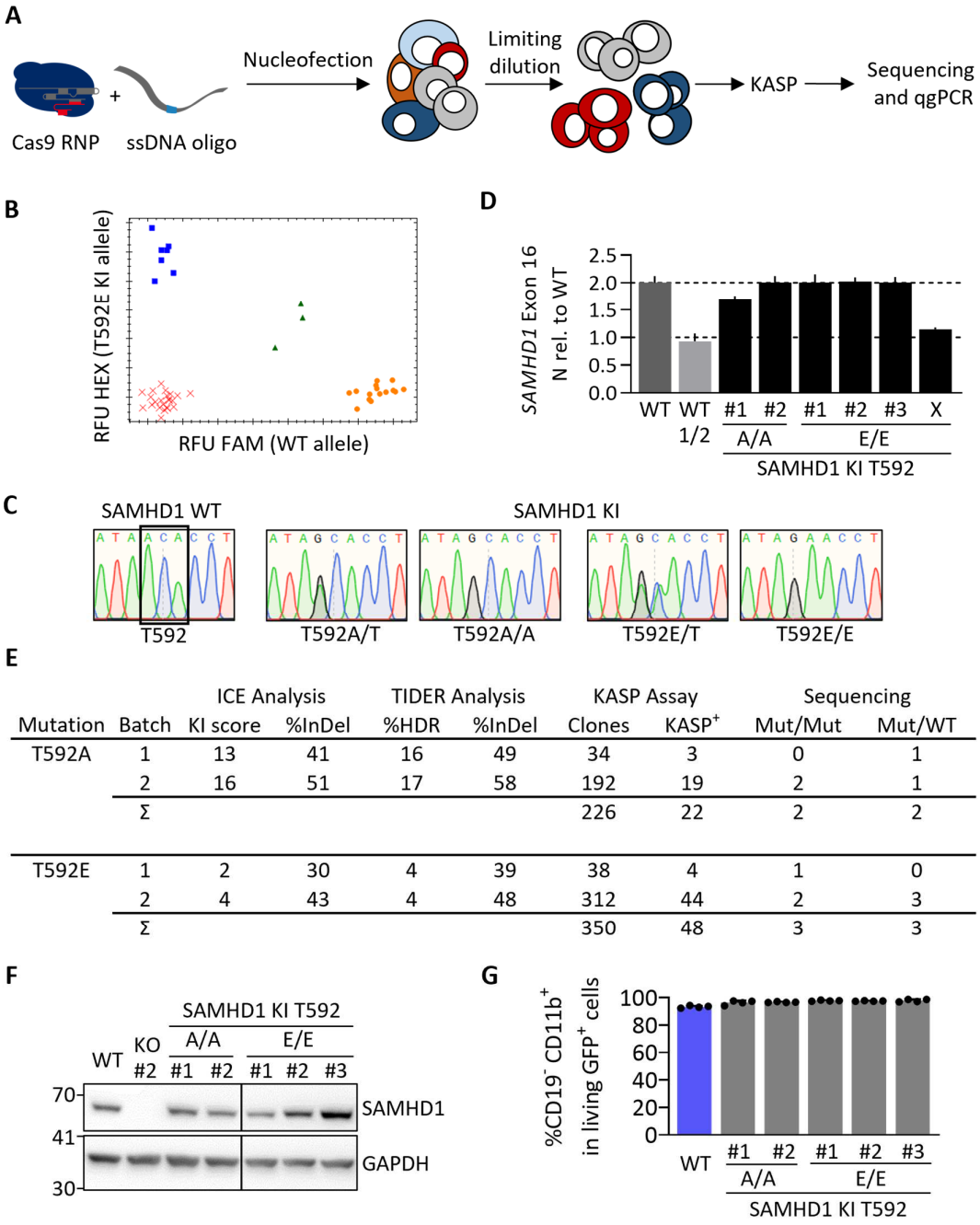

Mutation	Batch	ICE Analysis KI score	ICE Analysis %InDel	TIDER Analysis %HDR	TIDER Analysis %InDel	KASP Assay Clones	KASP Assay KASP+	Sequencing Mut/Mut	Sequencing Mut/WT
T592A	1	13	41	16	49	34	3	0	1
	2	16	51	17	58	192	19	2	1
	Σ					226	22	2	2
T592E	1	2	30	4	39	38	4	1	0
	2	4	43	4	48	312	44	2	3
	Σ					350	48	3	3

Figure 24: A pipeline to generate mutants of SAMHD1 by CRISPR/Cas9 mediated knock-in.

(A) Schematic representation of CRISPR/Cas9 meditated knock-in (KI) to generate mutants of SAMHD1 in BlaER1 cells. Cas9 ribonucleoprotein (RNP) together with ssDNA correction template was introduced into BlaER1 cells via nucleofection. Single cell clones generated by limiting dilution were screened using KASP assay and validated by Sanger sequencing and quantitative genomic PCR (qgPCR) (Weisheit et al. 2021). **(B)** Exemplary, allelic discrimination plot generated by KASP analysis of CRISPR/Cas9 SAMHD1 T592E KI single cell clones. Relative fluorescence units (RFUs) are given for WT (FAM) and mutant (HEX) specific PCR probes. Individual clones have been assigned into WT (yellow dots), heterozygous (green triangles)

and homozygous KI (blue squares) populations. Homo- and heterozygous candidate clones were assigned to be $KASP^+$ and were analyzed further. **(C)** Representative sections of Sanger sequencing traces obtained from genomic *SAMHD1* exon 16, highlighting successful mono- or bi-allelic single base exchange at the base triplet corresponding to amino acid position T592 in BlaER1 SAMHD1 KI T592A and T592E mutant single cell clones. No further mismatches were found up- or downstream of the section shown. Two independent sequencing runs were performed per clone. Homozygous T592E mutants were additionally confirmed by allele specific sequencing after TA-cloning. **(D)** Quantitative genomic PCR for *SAMHD1* exon 16 against reference gene *TERT* was performed and $2^{-\Delta ct}$ value obtained from SAMHD1 KI clones normalized to WT, to obtain the allele number. As a control half of the WT (WT 1/2) DNA was inoculated and Δct of *SAMHD1* calculated against ct of *TERT* which was obtained in the WT with normal DNA amount. Error bars indicate standard deviation of technical triplicates in a representative experiment (n = 2). **(E)** Table comparing KI efficiencies as estimated from ICE or TIDER assays (Brinkman et al. 2018; Hsiau et al. 2018) to experimental efficiency of KI for our KI approaches (two batches per mutation). Number of single cell clones obtained from CRISPR/Cas9 RNP and ssDNA correction oligo treated BlaER1 cells and number of clones scoring positive in KASP assay, as well as homo- (Mut/Mut) and heterozygous (Mut/WT) mutants identified by Sanger sequencing and confirmed by qgPCR, are shown. **(F)** Transdifferentiated SAMHD1 KI BlaER1 cells were analyzed by immunoblot for SAMHD1 expression and compared to WT cells. GAPDH was used as a loading control (representative for n = 3). **(G)** Percentage of $CD19^-$ $CD11b^+$ cells in living GFP^+ transdifferentiated WT and SAMHD1 KI cells were quantified by flow cytometry. Error bars indicated standard deviation of biological replicates (n = 4).

In order to confirm the functionality of SAMHD1 T592E and T592A KI clones, we analyzed expression of SAMHD1 and BlaER1 transdifferentiation. SAMHD1 mutant protein in transdifferentiated homozygous T592A and T592E KI BlaER1 single cell clones was similar to WT protein in the respective parental cell line (Fig. 24F). Also, SAMHD1 KI had no negative impact on BlaER1 transdifferentiation (Fig. 24G). In summary, using our pipeline we were able to introduce homozygous T592A and T592E mutations into the endogenous *SAMHD1* locus of BlaER1 cells.

3.3.4 Homozygous SAMHD1 T592E, but not T592A mutation leads to loss of HIV-1 restriction in transdifferentiated BLaER1 cells

In order to test endogenous SAMHD1 mutants for their HIV-1 restriction potential, we infected several clones of transdifferentiated homozygous SAMHD1 phosphoablative T592A and phosphomimetic T592E KI BlaER1 cell mutants with HIV-1-luc reporter virus at a variety of MOIs and measured relative light units (RLUs) after 24 hpi (Fig. 25A).

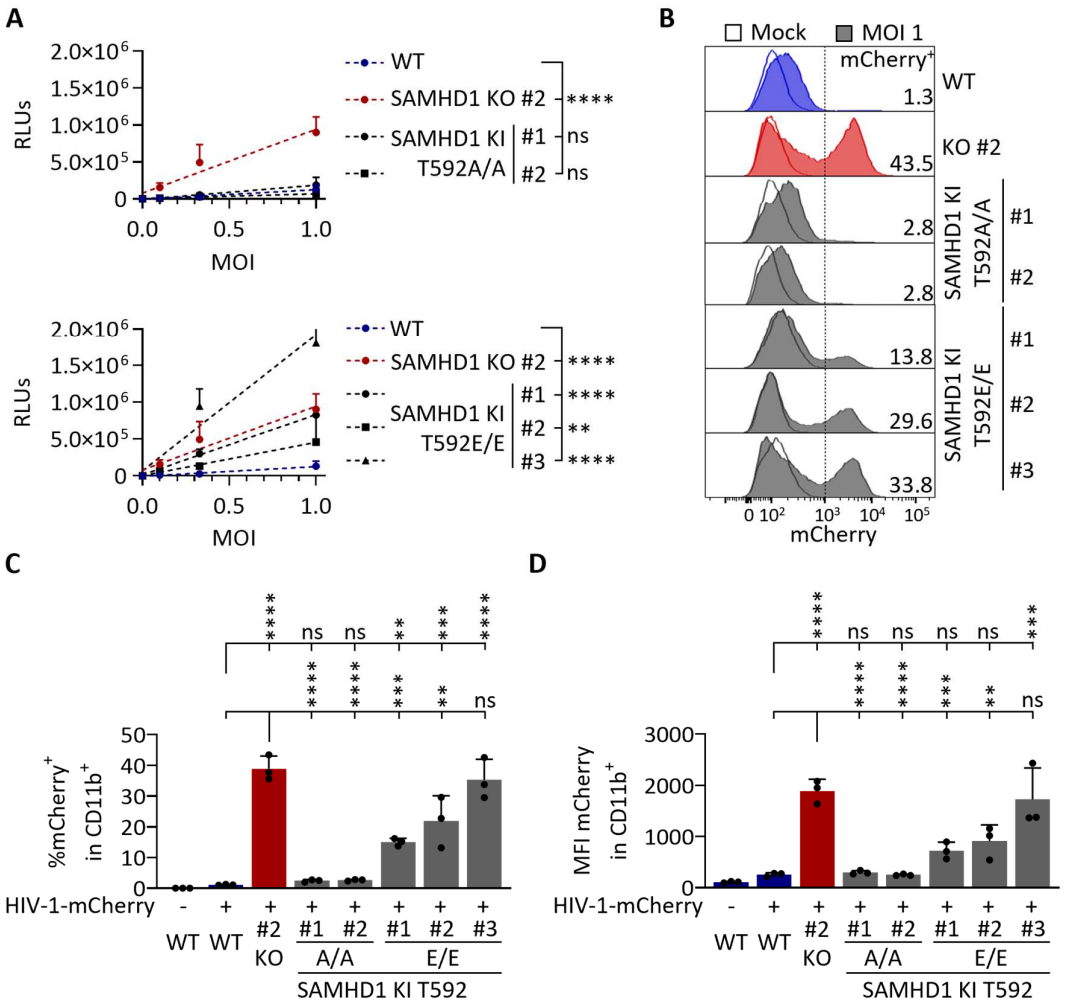

Figure 25: Homozygous SAMHD1 T592E, but not T592A mutation leads to loss of HIV-1 restriction in transdifferentiated BLaER1 cells.

(A) Transdifferentiated BlaER1 WT and SAMHD1 KO cell clones were infected with pNL4.3 E^- R^- luc (VSV-G) and RLUs were quantified 24 hpi. Statistical significance of differences between linear regressions (dashed lines) in SAMHD1 KI clones compared to WT are indicated (KO *p < 0.0001,* T592A/A Clone #1 *p = 0.9375*, #2 *p = 0.9065,* T592E/E Clone #1 *p < 0.0001*, #2 *p = 0.0053*, #3 *p < 0.0001*, n = 7, One-way ANOVA). **(B, C)** Transdifferentiated homozygous SAMHD1 T592E and T592A BlaER1 KI clones were infected with VSV-G pseudotyped HIV-1 single cycle mCherry reporter virus pBR HIV1 M NL4.3 IRES mcherry E^- R^+ at MOI 1. Percentage of $mCherry^+$ cells was quantified by flow cytometry in living GFP^+ $CD11b^+$ BlaER1 cells at 24 hpi. **(B)** Representative histograms are shown for mock and HIV-1 mCherry reporter virus infected cells. Percentage of $mCherry^+$ cells in living GFP^+ $CD11b^+$ BlaER1 cells is indicated (n = 3). Percentage of $mCherry^+$ cells in infected SAMHD1 KI clones **(C)** or mean fluorescence intensity were quantified **(D)**. Bar graphs indicate mean of experiments for %$mCherry^+$ cells, dots individual biological replicates (against WT: KO *p < 0.0001,* T592A/A Clone #1 *p = 0.9977*, #2 *p = 0.9949,* T592E/E Clone #1 *p = 0.0070*, #2 *p = 0.0002*, #3 *p < 0.0001;* against KO: T592A/A Clone #1 *p < 0.0001*, #2 *p < 0.0001,* T592E/E Clone #1 *p <*

0.0001, #2 *p = 0.0013*, #3 *p = 0.7947,* n = 3, Kruskal–Wallis test) or MFI mCherry (against WT: KO *p < 0.0001,* T592A/A Clone #1 *p = 0.9997*, #2 *p > 0.9999,* T592E/E Clone #1 *p = 0.2414*, #2 *p = 0.0615*, #3 *p = 0.0001;* against KO: T592A/A Clone #1 *p < 0.0001*, #2 *p < 0.0001,* T592E/E Clone #1 *p = 0.0009*, #2 *p = 0.0039*, #3 *p = 0.9477,* n = 3, One-way ANOVA). Error bars correspond to standard deviation of biological replicates (** *p < 0.01*; *** *p < 0.001*; **** *p < 0.0001*; ns, not significant).

SAMHD1 T592E mutation led to a strong and significant increase in HIV-1-luc infection in all three homozygous SAMHD1 T592E mutant clones, which was consistent over a broad range of MOIs. In contrast, both homozygous SAMHD1 T592A mutant clones were resistant to HIV-1-luc infection, similar to WT BlaER1 cells (Fig. 25A).

To confirm this, we infected transdifferentiated homozygous SAMHD1 T592A and T592E mutant BlaER1 KI clones with HIV-1-mCherry. We measured the increase of the percentage of mCherry$^+$ cells and the MFI of mCherry in CD19$^+$ macrophage-like living GFP$^+$ cells, comparing them to the infection in WT and SAMHD1 KO cells. In all three clones, homozygous SAMHD1 T592E mutation significantly increased HIV-1-mCherry infection up to 31-fold in terms of percentage of mCherry$^+$ cells (Fig. 25B and 25C). In contrast, transdifferentiated SAMHD1 T592A KI mutant clones completely preserved their restrictive potential and behaved like WT BlaER1 cells upon challenge with HIV-1-mCherry reporter virus (Fig. 25B and 25C). Similar, analysis of MFI of mCherry in CD11b$^+$ cells revealed a loss of HIV-1-mCherry restriction in all three homozygous SAMHD1 T592E KI clones, indicating that the observed phenotype is independent of artificial thresholds introduced by manual gating (Fig. 25D).

Thus, using CRISPR/Cas9 KI, we were able to validate the loss of HIV-1 restriction in SAMHD1 phosphomimetic T592E mutants in macrophage-like cells. In this model, mutants of SAMHD1 are analyzed in the native genomic context and show physiological expression levels, confirming the role of T592 phosphorylation in the regulation of the anti-viral activity of SAMHD1.

3.3.5 SAMHD1 T592E or T592A knock-in does not affect dNTP levels in transdifferentiated BlaER1 cells

Previous reports on the effect of SAMHD1 T592 phosphorylation on SAMHD1 dNTPase activity were in-conclusive (Majer et al. 2019). This might be at least partially due to the extensive use of overexpression models, when studying SAMHD1 phospho-site mutants

for their effect on dNTPase activity. Therefore, we wanted to correlate the effect of endogenous SAMHD1 T592 mutations on the HIV-1 restrictive potential with the cellular dNTPase activity in transdifferentiated BlaER1 cells.

To do so, we measured intracellular dNTP levels of transdifferentiated BlaER1 WT, SAMHD1 KO and SAMHD1 T592A or T592E KI cells by primer extension assay (Tab. 17). Transdifferentiated WT BlaER1 cells contained low amounts of dATP (846 ± 63 fmol/10^6 cells, n = 5), dCTP (788 ± 117 fmol/10^6 cells, n = 5), dGTP (724 ± 94 fmol/10^6 cells, n = 5) and dTTP (933 ± 342 fmol/10^6 cells, n = 5). Native WT BlaER1 cells showed substantially higher dATP amounts than transdifferentiated BlaER1 cells (7407 fmol/10^6 cells). Accordingly, depletion of the minor fraction of $CD19^+$ cells after transdifferentiation further reduced the levels of dATP (578 fmol/10^6 cells), dCTP (661 fmol/10^6 cells), dGTP (295 fmol/10^6 cells) and dTTP (448 fmol/10^6 cells).

Table 17: dNTP concentrations in BlaER1 cells with reference to literature values

Cell type (reference)	Genotype	dATP [µM]	dCTP [µM]	dGTP [µM]	dTTP [µM]
native BlaER1	WT	9,25			
transdifferentiated BlaER1	WT	1,51	1,22	1,40	1,83
	SAMHD1 KO #2	4,39	1,89	5,92	5,88
	T592A/T592A #1	1,51	1,28	1,34	1,72
	T592A/T592A #2	0,99	1,20	0,63	0,92
	T592E/T592E #1	0,99	1,19	0,92	1,41
	T592E/T592E #2	1,32	1,59	1,34	1,48
transdifferentiated BlaER1 -CD19	WT	1,02	1,16	0,52	0,79
resting T cells (Diamond et al. 2004)		1,72	1,88	1,51	1,67
activated T cells (Diamond et al. 2004)		5,09	5,91	4,53	7,91
MDMs (Schott et al. 2018)		0,02	0,05	0,07	0,02

Since the activity of HIV-1 RT is likely to be dependent on cellular dNTP concentrations rather than total dNTP pools, we determined cellular dNTP concentrations as a function of transdifferentiated BlaER1 cell volume (569 ± 138 µm^3, n_{cells} = 15) (Tab. 17). We found transdifferentiated WT BlaER1 cells to harbor dNTP concentrations, similar or lower to those found in resting T cells (Diamond et al. 2004). Depletion of incompletely transdifferentiated ($CD19^+$) cells from bulk preparations of transdifferentiated BlaER1 cells further reduced dNTP concentrations (Tab. 17). As expected, SAMHD1 KO led to a significant increase in cellular dATP (2.3-fold), dGTP (3.2-fold) and dTTP (2.2-fold) levels

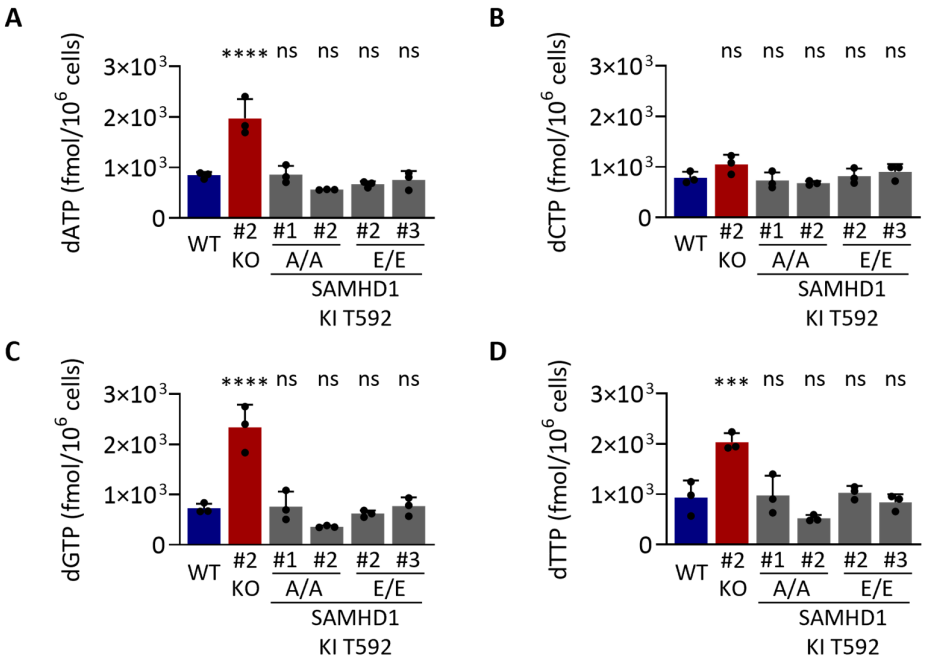

Figure 26 : SAMHD1 T592E or T592A knock-in does not affect dNTP levels in transdifferentiated BlaER1 cells.

(A, B, C, D) Cellular dNTP levels were measured in transdifferentiated homozygous SAMHD1 T592E and T592A BlaER1 KI mutants. dNTP amounts were compared to transdifferentiated WT and SAMHD1 KO BlaER1 cells. Amount of dATP **(A)**, dCTP **(B)**, dGTP **(C)** or dTTP **(D)** is depicted per 1 x 10^6 cells. Bar graphs indicate mean of experiments, dots individual biological replicates (**(A)** KO *p < 0.0001,* T592A/A Clone #1 *p = 0.9999*, #2 *p = 0.2879,* T592E/E Clone #2 *p = 0,6838*, #3 *p = 0.9532;* **(B)** KO *p = 0,1567,* T592A/A Clone #1 *p = 0.9775*, #2 *p = 0.8370,* T592E/E Clone #2 *p = 0,9996*, #3 *p = 0.7927;* **(C)** KO *p > 0,0001,* T592A/A Clone #1 *p = 0.9997*, #2 *p = 0.2837,* T592E/E Clone #2 *p = 0,9724*, #3 *p = 0.9997;* **(D)** KO *p = 0,0005,* T592A/A Clone #1 *p = 0.9989*, #2 *p = 0.1957,* T592E/E Clone #2 *p = 0,9757*, #3 *p = 0.9849*, n = 3, One-way ANOVA). Error bars correspond to standard deviation (*** p < 0.01; **** p < 0.0001; ns, not significant).

in transdifferentiated BlaER1 cells, as compared to WT cells while dCTP levels were not affected (Fig. 26). Importantly however, neither homozygous SAMHD1 T592E, nor T592A mutations in any clone led to an increase of cellular dNTP levels (Fig. 26). This suggests that SAMHD1 T592 phosphorylation does not regulate the levels or concentrations of cellular dNTPs in transdifferentiated BlaER1 cells.

3.3.6 SAMHD1 T592E or T592A knock-in does not affect dNTP pool composition in transdifferentiated BlaER1 cells

SAMHD1 T592 phosphorylation has been proposed to alter SAMHD1 substrate specificity (Jang et al. 2016). To test if SAMHD1 T592 mutation and thus SAMHD1 T592 phosphorylation alter cellular dNTP composition, we compared relative dNTP levels in transdifferentiated BlaER1 WT, SAMHD1 KO and SAMHD1 T592A and T592E KI mutants (Fig. 27). Since SAMHD1 KO only slightly affected cellular dCTP levels, dNTP composition in transdifferentiated BlaER1 SAMHD1 KO cells was shifted towards dATP, dGTP and dTTP. In contrast, neither SAMHD1 T592E nor SAMHD1 T592A KI mutants showed consistent differences in cellular dNTP composition (Fig. 27). In summary, dNTP measurements in transdifferentiated BlaER1 cells, harboring homozygous phosphomimetic T592E or phosphoablative T592A mutations in the endogenous *SAMHD1* locus indicate that phosphorylation at SAMHD1 residue T592 has no major impact on cellular dNTP pools and is therefore unlikely to regulate SAMHD1 dNTPase activity in cells.

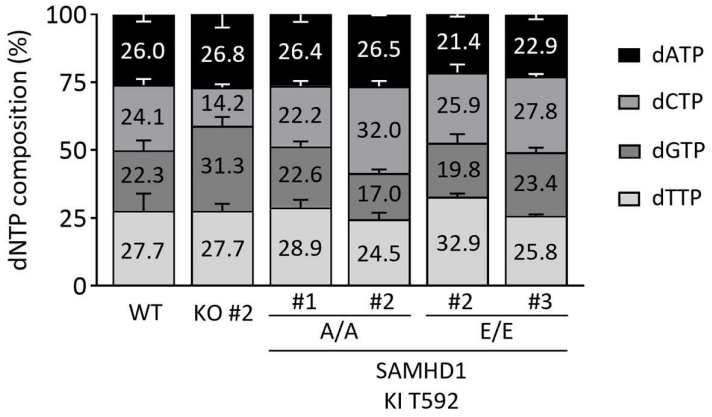

Figure 27 : SAMHD1 T592E or T592A knock-in does not affect dNTP pool composition in transdifferentiated BlaER1 cells.

Cellular dNTP levels were measured in transdifferentiated homozygous SAMHD1 T592E and T592A BlaER1 KI mutants and compared to transdifferentiated WT BlaER1 and SAMHD1 KO cells. dNTP composition in individual BlaER1 SAMHD1 KI clones is shown, with total dNTP content set as 100%. Error bars indicate standard deviation of biological replicates (n = 3).

3.3.7 Vpx-mediated degradation of SAMHD1 T592E increases HIV-1 infection similar to Vpx-treated SAMHD1 knock-out cells

SAMHD1 might harbor several anti-viral functions which synergize to restrict HIV-1 replication (Welbourn and Strebel 2016; Majer et al. 2019). These functions might cooperate in co-dependent or additive manner. Even though SAMHD1 dNTPase function seems not connected with the loss of restriction introduced by the T592E KI mutation, it still might contribute to restriction.

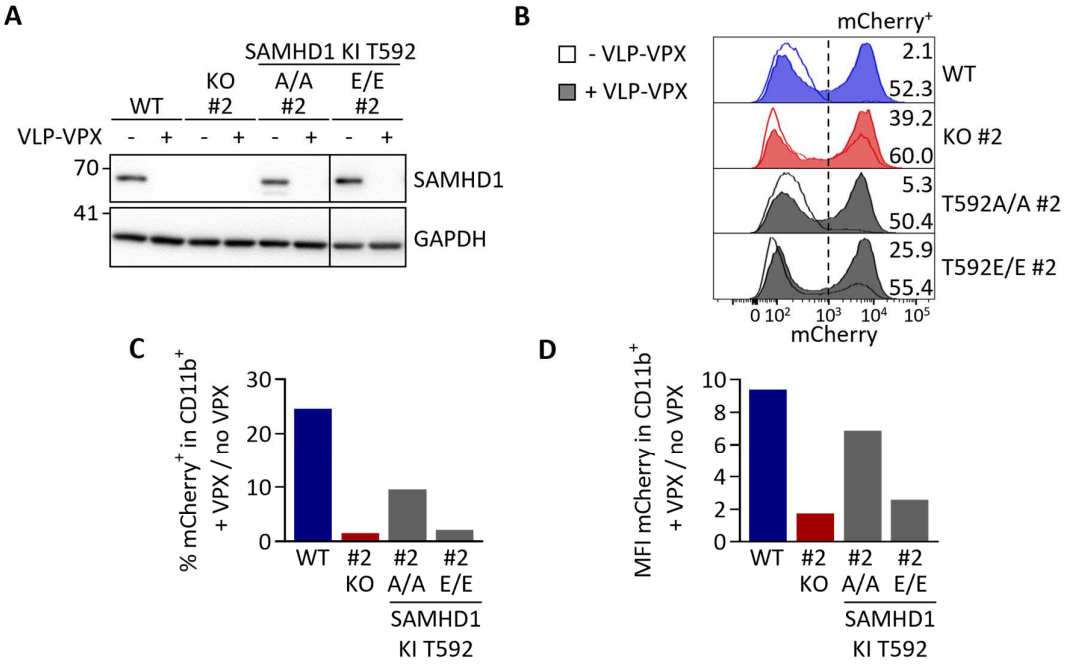

Figure 28 : VPX mediated degradation of SAMHD1 T592E mutant does not further increase infection with HIV-1 reporter viruses.

Transdifferentiated WT BlaER1, SAMHD1 KO, as well as SAMHD1 T592A or T592E KI clones were treated with VLP-Vpx or medium for 24 h. **(A)** Immunoblot of lysates obtained from transdifferentiated BlaER1 WT or KI cells treated with VLP-Vpx or medium. **(B, C, D)** Transdifferentiated BlaER1 cells were infected with VSV-G pseudotyped HIV-1 single cycle mCherry reporter virus pBR HIV1 M NL4.3 IRES mcherry E^- R^+ (HIV-1-mCherry) at MOI 1 in presence or absence of VLP-Vpx. Infection was quantified by flow cytometry at 24 hpi. **(B)** Histograms show mCherry signal distribution in infected cells with or without VLP-Vpx treatment. %$mCherry^+$ cells in living GFP^+ $CD11b^+$ BlaER1 cells is indicated for infection with (lower number) and without (upper number) treatment. Fold increase in infection in cells treated with VLP-VPX relative to untreated cells was calculated for %$mCherry^+$ **(C)** or MFI of mCherry **(D)** in living GFP^+ $CD11b^+$ BlaER1 cells (n = 1).

Interestingly, two homozygous T592E KI clones showed lower levels of HIV-1-mCherry infection compared to the SAMHD1 KO clone #2 (Fig 25C and D). To understand if this was due to clonal effects, which were also observed for SAMHD1 KO (Fig. 21F and G), or to a residual anti-viral activity of the SAMHD1 T592E mutant, we depleted SAMHD1 via VLP-Vpx treatment in transdifferentiated BlaER1 WT, SAMHD1 KO as well as homozygous T592A KI clone #2 and T592E KI clone #2 and tested for restriction of HIV-1-mCherry reporter virus (Fig. 28). As expected, VLP-Vpx led to the complete depletion of WT, T592A and T592E mutant SAMHD1 (Fig. 28A). While VLP-Vpx co-treatment in WT cells resulted in a 25.6- and 9.4-fold increase in the percentage of $mCherry^+$ cells and mCherry MFI, respectively, VLP-Vpx treatment had no such effect on BlaER1 SAMHD1 KO cells (Fig. 28B, C and D). Infection in homozygous T592A mutant was increased by 9.6- and 6.9-fold. In contrast, VLP-Vpx treatment had only a minimal effect on infection rate and mCherry MFI in T592E KI clone #2 (2.1- and 2.6-fold). The increase of infection rate and MFI in SAMHD1 T592E KI cells was comparable to the one observed in SAMHD1 KO control cells (1.7- and 1.5-fold) and thus likely due to non SAMHD1 related effects of Vpx. Even if preliminary, this data could indicate that SAMHD1 T592E mutant has no or only a very minor residual restrictive activity towards HIV-1, again, arguing against the dNTPase activity to be an independent anti-viral functional entity of SAMHD1.

3.4 An adapted overexpression strategy allows screening of SAMHD1 mutants for anti-viral restriction in transdifferentiated BlaER1 cells

3.4.1 SAMHD1 mutant overexpression in transdifferentiated SAMHD1 knock-out BlaER1 cells only partially recapitulates published results

We could demonstrate that genetic manipulation of endogenous SAMHD1 using CRISPR/Cas9-mediated KI allows the validation of SAMHD1 phosphorylation sites with a high degree of physiology in transdifferentiated BlaER1 cells. However, in order to screen a large number of SAMHD1 mutants for their effect on SAMHD1 anti-viral restriction activity, CRISPR/Cas9 KI comes with a substantial work burden. Therefore, we decided to implement a reliable model system to prescreen SAMHD1 mutants by overexpression. Rescue of SAMHD1 restrictive activity in myeloid cells has so far been

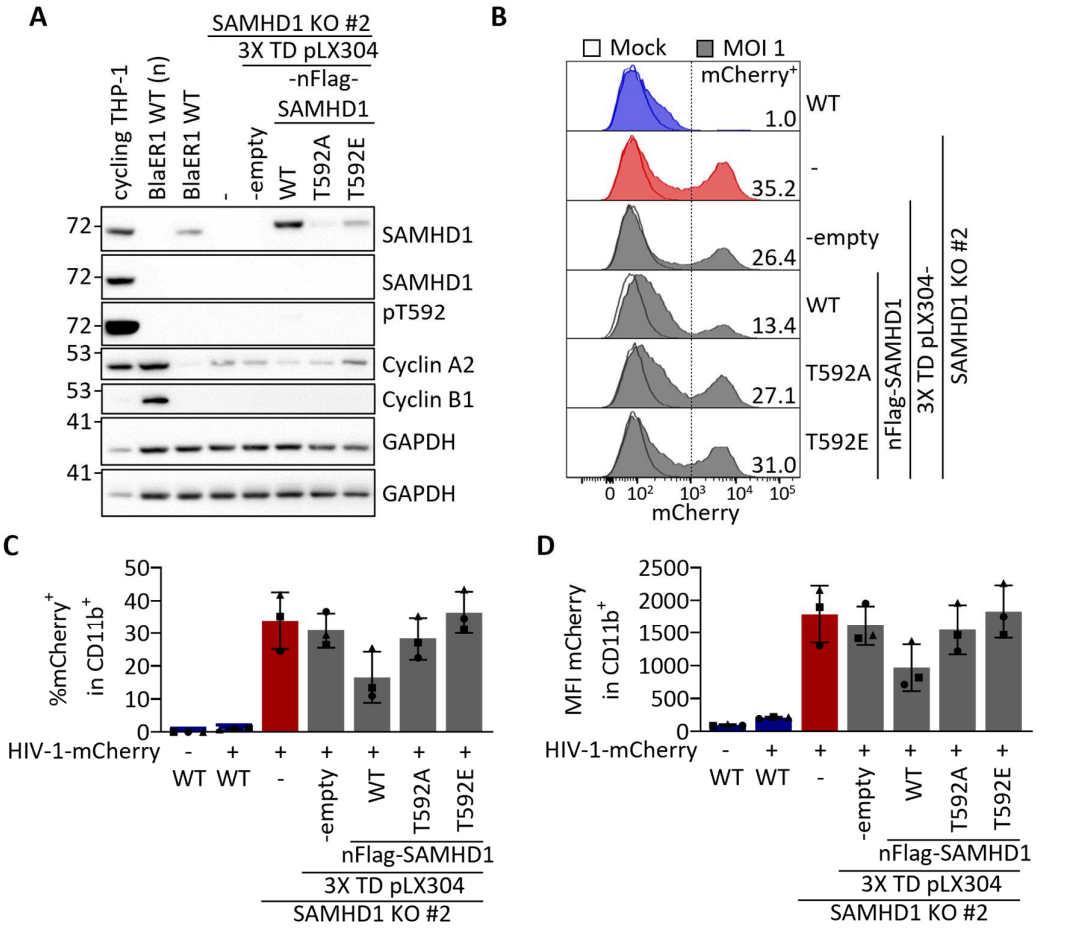

Figure 29: SAMHD1 mutant overexpression in transdifferentiated SAMHD1 knock-out BlaER1 cells only partially recapitulates published results.

BlaER1 SAMHD1 KO #2 cells were transduced three times with lentiviral pLX304 vectors encoding WT nFlag-SAMHD1 or T592A and T592E mutants and subsequently selected for blasticidin resistance. **(A)** Immunoblot analysis of SAMHD1 expression and phosphorylation in transduced transdifferentiated SAMHD1 KO BlaER1 cells. Cycling THP-1, as well as native (n) and transdifferentiated WT BlaER1 cells served as a control. Cyclin A2 and B1 were detected. GAPDH was used as a loading control (representative for n = 3). **(B, C, D)** Transdifferentiated BlaER1 WT or SAMHD1 KO cell clones, as well as SAMHD1 KO cells transduced with lentiviral vectors for SAMHD1 mutant overexpression were infected with VSV-G pseudotyped HIV-1 single cycle mCherry reporter virus pBR HIV1 M NL4.3 IRES mcherry E^- R^+ at MOI 1. Percentage of $mCherry^+$ cells was quantified by flow cytometry in living GFP^+ $CD11b^+$ BlaER1 cells at 24 hpi. **(B)** Representative histograms are shown for mock and HIV-1 mCherry reporter virus infected cells. Percentage of $mCherry^+$ cells in living GFP^+ $CD11b^+$ BlaER1 cells is indicated (representative for n = 3). Percentage of $mCherry^+$ cells in infected SAMHD1 KI clones **(C)** or mean fluorescence intensity is shown **(D)**. Bar graphs indicate mean of experiments for $\%mCherry^+$ cells or MFI mCherry, symbols represent individual biological replicates. Error bars correspond to standard deviation of biological replicates.

performed by transduction of SAMHD1 mutant constructs into SAMHD1-negative U937 or SAMHD1 KO THP-1 cells (Cribier et al. 2013; White et al. 2013b; Welbourn et al. 2013). However, as detailed in section 3.3.1, we failed to implement these model systems. Transdifferentiated BlaER1 cells show low levels of SAMHD1 phosphorylation. Also, transdifferentiation relies on the induction of a myeloid transcription program, which might lead to a more profound dephosphorylation of SAMHD1 in transdifferentiated BlaER1 cells, possibly circumventing problems with hyperphosphorylation of overexpressed protein. Therefore, we wanted to test if SAMHD1 overexpression can be used to rescue HIV-1 restriction in transdifferentiated BlaER1 SAMHD1 KO cells and to test mutants of SAMHD1 for restrictive activity.

To do so, we transduced cycling BlaER1 SAMHD1 KO clone #2 with lentiviral particles encoding WT nFlag-SAMHD1 or T592A and T592E mutants. Also, we used an empty control vector, not encoding any protein. We enriched transduced cells using antibiotic resistance. After transdifferentiation, exogenous nFlag-SAMHD1 was strongly expressed in the transduced and selected cell lines (Fig. 29A). While the nFlag-SAMHD1 T592E mutant showed good expression similar to endogenous SAMHD1, T592A mutation lead to a drastic reduction in nFlag-SAMHD1 expression, consistent with what we and others observed previously (not shown) (Herrmann et al. 2018). To test the restrictive activity of overexpressed SAMHD1 in transdifferentiated BlaER1 cells, we infected them with HIV-1-mCherry reporter virus and analyzed mCherry expression in $CD11b^+$ transdifferentiated cells (Fig. 29B, C and D). Overexpression of WT nFlag-SAMHD1 only slightly reduced infection with HIV-1-mCherry reporter virus both in terms of percentage of $mCherry^+$ cells and MFI of mCherry in transdifferentiated $CD11b^+$ BlaER1 cells (Fig. 29B, C and D). In contrast to our results obtained using CRISPR/Cas9 KI, we could not see a restrictive phenotype upon overexpression of nFlag-SAMHD1 T592A. Likely this was due to a low expression of the nFLag-SAMHD1 T592A mutant after transduction in transdifferentiated BlaER1 cells (Fig. 29A). We thus concluded that the current overexpression strategy is not suitable to analyze the restrictive phenotype of SAMHD1 mutants by overexpression in transdifferentiated BlaER1 cells.

3.4.2 SAMHD1 overexpression yields a heterogenous pool of cells differentially expressing SAMHD1

To better understand the composition of the polyclonal cell pool obtained after transduction with lentiviral particles encoding SAMHD1, we generated single cell clones from the transduced and selected polyclonal BlaER1 cell population. Surprisingly, expression of exogenous SAMHD1 in transdifferentiated BlaER1 cells varied strongly in-between the individual single cell clones (Fig. 30A). While some cell clones showed an expression similar to the polyclonal population, other clones showed strongly increased or reduced nFlag-SAMHD1 expression. Importantly, one clone showed no detectable SAMHD1 expression, even though antibiotic resistance indicated successful transduction and expression of the resistance marker.

To test the effect of differential SAMHD1 expression on HIV-1 restriction, we infected transdifferentiated BlaER1 single cell clones overexpressing nFlag-SAMHD1 with HIV-1-mCherry reporter virus (Fig. 30B). Interestingly, most of the single cell clones showed complete resistance to HIV-1-mCherry infection. The level of restriction in most single cell clones was even higher compared to the parental pool cell population. Importantly, nFlag-SAMHD1 expression did not correlate with the level of residual HIV-1-mCherry infection in transdifferentiated BlaER1 cells (Fig. 30C). In fact, minimal nFlag-SAMHD1 expression in clone 8 was sufficient to convert resistance to HIV-1 infection, similar to clones expressing 60-fold more nFlag-SAMHD1. Single cell clone #9 showed no detectable expression of nFlag-SAMHD1 (Fig. 30A). Accordingly, this clone was completely permissive to HIV-1-mCherry infection at the same extent as empty control transduced transdifferentiated SAMHD1 KO BlaER1 cells (Fig. 30B). These results indicate, that even after stringent selection, the polyclonal transduced cell population contains cells, which do not express exogenous nFlag-SAMHD1 after transdifferentiation. Absence of HIV-1 restriction in a proportion of the polyclonal cell population could explain the incomplete restriction phenotypes overexpressed SAMHD1.

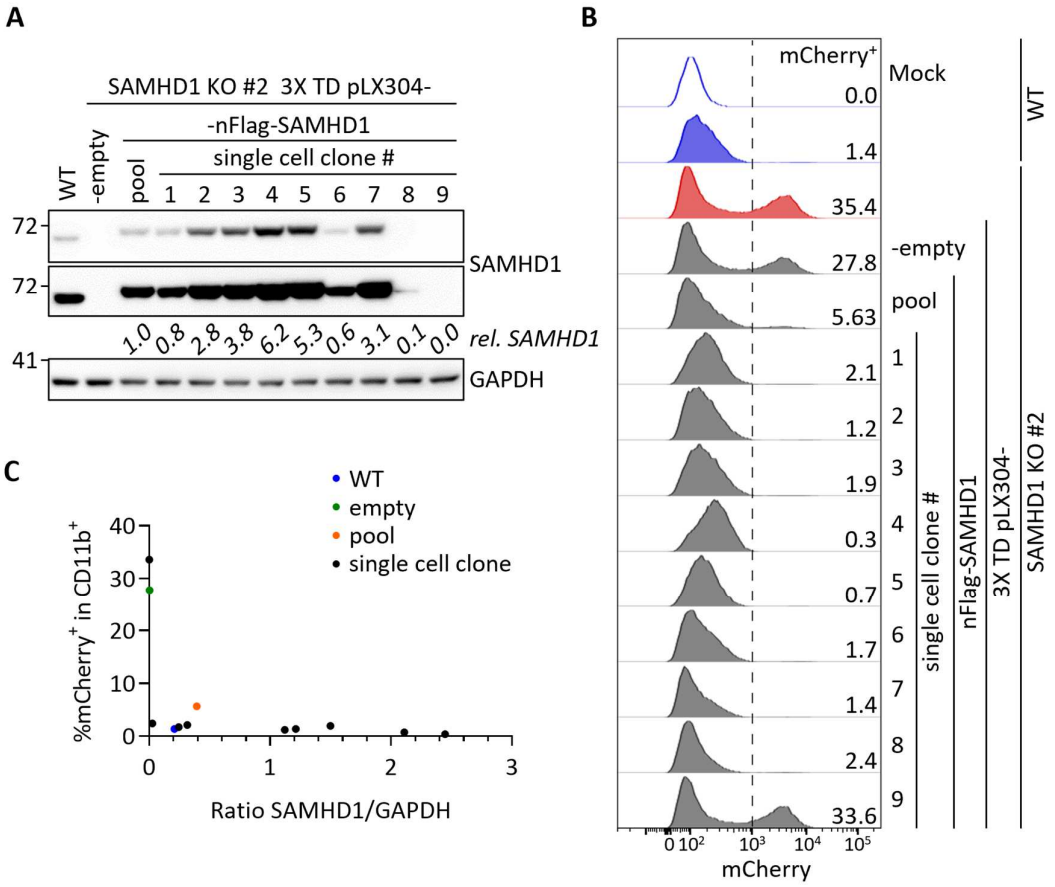

Figure 30: SAMHD1 overexpression yields a heterogenous pool of cells differentially expressing SAMHD1.

Single cell clones originating from BlaER1 SAMHD1 KO #2 cells transduced three times with lentiviral pLX304 vectors encoding nFLag-SAMHD1 and selected for blasticidin resistance were generated by limiting dilution. **(A)** Immunoblot analysis of SAMHD1 expression in transdifferentiated WT BlaER1 or SAMHD1 KO BlaER1 cells overexpressing SAMHD1 or transduced with an empty control vector. Polyclonal parental population (pool) and nine single cell clones were analyzed for SAMHD1 expression. Low and high exposure images are shown for SAMHD1. Relative SAMHD1 expression was calculated relative to loading control GAPDH and normalized to SAMHD1 expression in the parental cell pool (n = 1). **(B)** Transdifferentiated single cell clones derived from SAMHD1 KO cells transduced with lentiviral vectors for SAMHD1 overexpression were infected with VSV-G pseudotyped HIV-1 single cycle mCherry reporter virus pBR HIV1 M NL4.3 IRES mcherry E^- R^+ at MOI 1. The parental polyclonal cell pool, as well as SAMHD1 KO cells and cells transduced with an empty vector were used as controls. Percentage of $mCherry^+$ cells was quantified by flow cytometry in living GFP^+ $CD11b^+$ BlaER1 cells at 24 hpi. Histograms shown mock and HIV-1 mCherry reporter virus infected cells. Percentage of $mCherry^+$ cells in living GFP^+ $CD11b^+$ BlaER1 cells is indicated (n = 1). **(C)** SAMHD1 expression normalized to GAPDH was plotted against percentage of $mCherry^+$ cells of infected single cell clones and controls (n = 1).

3.4.3 Intracellular staining strategy for overexpressed SAMHD1 increases the performance of flow cytometry-based restriction assay

To better understand the consequence of heterogeneous nFlag-SAMHD1 expression in transduced BlaER1 SAMHD1 KO cell pools in HIV-1 restriction rescue assays, we tested a flow cytometry gating strategy, for which we performed intracellular staining of SAMHD1 (Baldauf et al. 2012). Besides heterogeneous overexpression, long selection processes might also alter the outcome of restriction rescue experiments, for example by favoring inactivating modifications of SAMHD1 highly expressed in cycling cells (Majer et al. 2019). To avoid these problems, we decided to forgo on selection to enrich the successfully transduced cell population.

By 3X transduction of SAMHD1 KO BlaER1 cells, we were able to achieve a considerable level of nFlag-SAMHD1 expression in transdifferentiated cells, even in the absence of selection (Fig. 31A). As observed previously, expression of nFlag-SAMHD1 T592A mutant was lower in the transdifferentiated transduced bulk BlaER1 cell population, as compared to WT or T592E mutant transduced cells. Concordantly, flow cytometry staining of SAMHD1 in transdifferentiated BlaER1 cells showed a significant lower frequency of transdifferentiated BlaER1 cells expressing the nFlag-SAMHD1 T592A mutant compared to the WT construct (Fig. 31B and C). However, in cells which express nFlag-SAMHD1 T592A, the MFI of SAMHD1 in SAMHD1$^+$ CD11b$^+$ cells were similar to WT and to T592E mutant transduced cells (Fig. 31D).

We next wanted to assess the effect of differential expression of mutants on the rescue of HIV-1 restriction. Flow cytometry analysis of HIV-1-mCherry infection of transdifferentiated BlaER1 cells overexpressing SAMHD1 revealed predominant infection of SAMHD1$^-$ cells in nFlag-SAMHD1 transduced cell pools of transdifferentiated BlaER1 cells (Fig. 31B). However, only the nFlag-SAMHD1 T592E mutant transduced cells showed a clear SAMHD1$^+$ mCherry$^+$ cell population in line with the anticipated loss of restriction phenotype. Indeed, when specifically analyzing HIV-1-mCherry reporter virus infection in SAMHD1$^+$ cells, both WT and T592A mutant showed very low frequency of infected cells (Fig. 31E). Restriction of HIV-1-mCherry infection, was highly significant for nFlag-SAMHD1 WT and T592A mutant overexpression, both in terms of the percentage of mCherry$^+$ cells in SAMHD1$^+$ CD11b$^+$ transdifferentiated BlaER1 cells, as well as for MFI

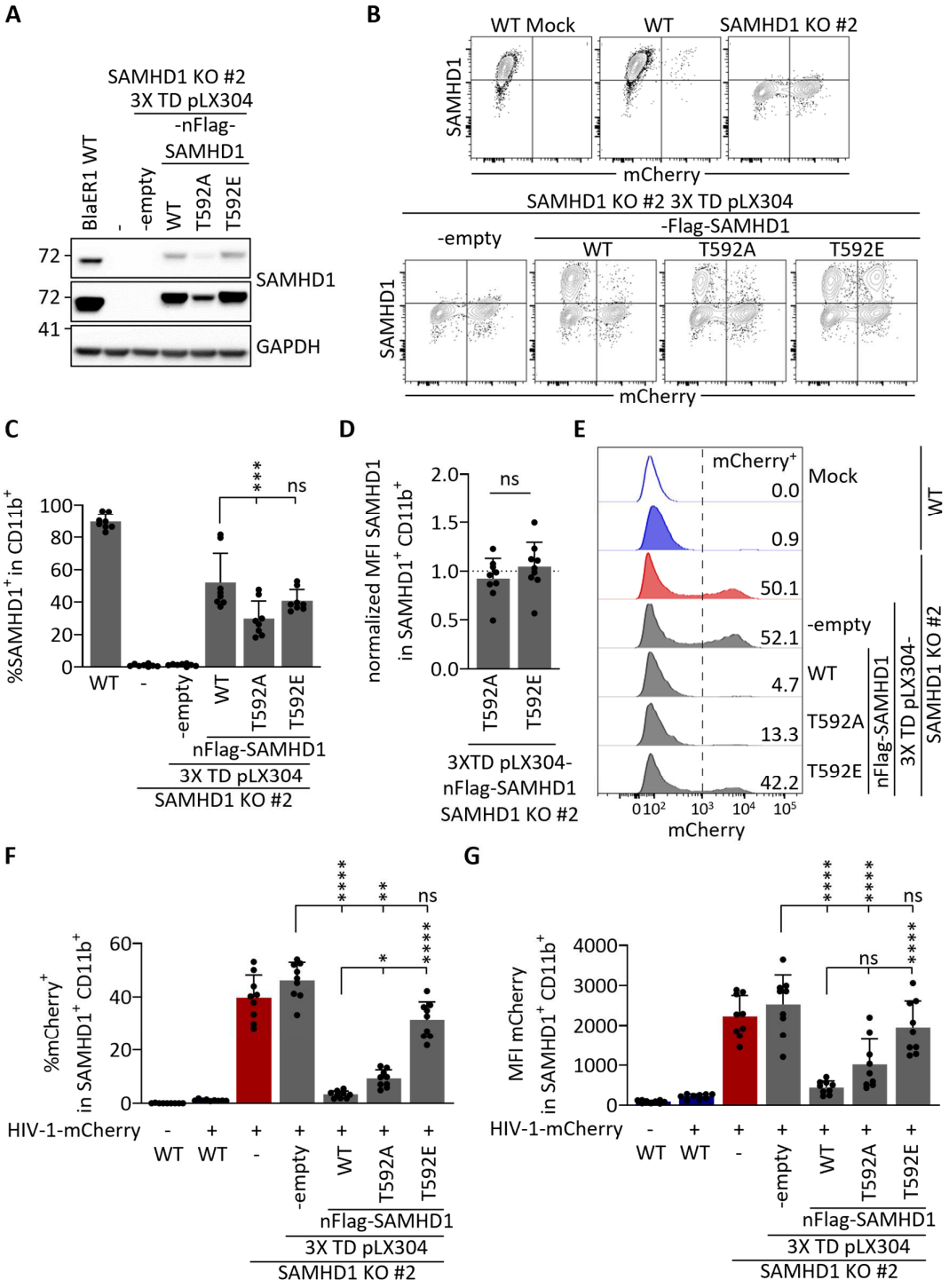

Figure 31: Intracellular staining strategy for overexpressed SAMHD1 increases the performance of flow cytometry-based restriction assay.

BlaER1 SAMHD1 KO clone #2 was transduced three times with lentiviral pLX304 vectors encoding WT nFlag-SAMHD1 or T592A and T592E mutants without subsequent selection. **(A)** Immunoblot analysis of SAMHD1 expression in transduced transdifferentiated SAMHD1 KO BlaER1 cells. Transdifferentiated WT

BlaER1 cells served as a control. Low and high exposure images are shown for SAMHD1. GAPDH was used as a loading control (representative for n = 9). **(B to G)** Transdifferentiated BlaER1 WT or SAMHD1 KO cell clones, as well as SAMHD1 KO cells transduced with lentiviral vectors for SAMHD1 mutant overexpression were infected with VSV-G pseudotyped HIV-1 single cycle mCherry reporter virus pBR HIV1 M NL4.3 IRES mcherry E^- R^+ at MOI 1. **(B)** Density plots show distribution of $mCherry^+$ cells relative to SAMHD1 expression in living GFP^+ $CD11b^+$ BlaER1 cells at 24 hpi as quantified by intracellular staining of SAMHD1 and flow cytometry (representative for n = 9). SAMHD1 expression in $CD11b^+$ transdifferentiated BlaER1 cells was quantified and is shown as $\%SAMHD1^+$ cells (T592A *p = 0.0004,* T592E *p = 0.2672,* n = 8, Friedman test) **(C)** and mean fluorescence intensity (MFI) in $SAMHD1^+$ transdifferentiated BlaER1 cells **(D)**. MFI of SAMHD1 in cells overexpressing mutant SAMHD1 was normalized to WT (*p = 0.2823,* n = 9, unpaired t-test). **(E)** Representative histograms show the distribution of mCherry signal in mock and HIV-1 mCherry reporter virus infected cells. Percentage of $mCherry^+$ cells in living GFP^+ $CD11b^+$ $SAMHD1^+$ BlaER1 cells is indicated (representative for n = 9). Bar graphs indicate mean of experiments for **(F)** $\%mCherry^+$ cells (against WT: T592A *p = 0.0379,* T592E *p < 0.0001;* against -empty: WT *p < 0.0001*, T592A *p = 0.0013,* T592E *p = 0.3679,* n = 9, Kruskal–Wallis test) or **(G)** MFI mCherry (against WT: T592A *p = 0.0604,* T592E *p < 0.0001;* against -empty: WT *p < 0.0001*, T592A *p < 0.0001,* T592E *p = 0.1198,* n = 9, One-way ANOVA) in the $CD11b^+$ $SAMHD1^+$ cell population. Dots represent individual biological replicates. Error bars correspond to standard deviation of biological replicates (* *p < 0.05;* ** *p < 0.01*; *** *p < 0.001*; **** *p < 0.0001*; ns, not significant).

of mCherry in the $SAMHD1^+$ $CD11b^+$ cell population, when compared to empty control vector transduced cells (Fig. 31F and G). As expected, the nFlag-SAMHD1 T592E mutant was not able to restrict HIV-1-mCherry infection and T592E mutation led to a significant increase in the percentage of $mCherry^+$ cells and the MFI of mCherry as compared to the WT SAMHD1 construct (Fig. 31E, F and G). Thus, by using an adapted flow cytometry staining and gating strategy, we were able to specifically assess HIV-1 restriction in SAMHD1 expressing cells and thus to overcome the problematic of differentially expressed SAMHD1 mutants, *i.e.* the T592A mutant, in restriction rescue experiments based on SAMHD1 mutant overexpression.

3.4.4 Several residues of the dNTPase catalytic center seem to be dispensable for HIV-1 restriction

Phosphorylation of SAMHD1 T592 inhibits HIV-1 restriction but seems not to affect SAMHD1 dNTPase activity. However, if SAMHD1 dNTPase activity is required for anti-viral restriction in transdifferentiated BlaER1 cells, still is unclear. We therefore tested

several published functional SAMHD1 mutants by overexpression for rescue of HIV-1 restriction in SAMHD1 KO cells using our novel flow cytometry staining and gating strategy.

As observed in previous experiments in different cell lines (data not shown), overexpression of several SAMHD1 mutants yields drastically lower expression levels in transdifferentiated BlaER1 cells, when lysates from bulk transduced cells were tested by immunoblot (Fig. 32A). Namely, expression of primary allosteric site mutant R145Q (Rentoft et al. 2016), as well as the catalytic dNTPase core residue mutants H167A and D207A (Morris et al. 2020) was not detectable by immunoblot. Accordingly, expression of R145Q, H167A and D207A on the single cell level was also drastically reduced, both in terms of the percentage of SAMHD1$^+$ cells, as well as in signal intensity (Fig. 32C). In fact, no clear SAMHD1$^+$ population was detected and the SAMHD1 signal was rather continuous from SAMHD1-negative to dim, questioning the functionality and proper folding or localization of these SAMHD1 mutants. As a consequence, these mutants were also not able to restrict HIV-1-mCherry infection in SAMHD1$^+$ CD11b$^+$ transdifferentiated BlaER1 cells (Fig. 32D).

The primary allosteric site mutant D137N and the putative RNase-negative mutant Q548A (Ryoo et al. 2014) showed reduced expression in bulk cell preparations (Fig. 32A). However, the percentage of SAMHD1$^+$ cells was only slightly reduced for Q548A. Together with a slightly shifted SAMHD1$^+$ population in the D137N and Q548A mutant, this indicates that expression levels per cell might be reduced (Fig. 32C). When tested for their restrictive activity, both SAMHD1 D137N and Q548A mutants showed an intermediate restrictive phenotype. Whether this is due to lower expression on single cell level or reduced restriction activity will demand further investigation.

Two additional mutants of the catalytic dNTPase core D311A and Y315A (Morris et al. 2020) showed normal expression both on bulk protein, as well as on the single cell level (Fig. 32A and C). The D311A mutation has been shown to abrogate SAMHD1 dNTPase activity *in vitro* (Goldstone et al. 2011). To confirm that the D311A mutation leads to loss of dNTPase activity in cells, we performed a dNTPase activity rescue experiment by transient transfection of nFlag-SAMHD1 WT or mutants into SAMHD1 KO 293T cells. 293T cells showed 1.7-fold higher dATP levels, when SAMHD1 was genetically depleted by CRISPR/Cas9. Upon transfection of nFlag-SAMHD1 WT, as well as T592A or T592E

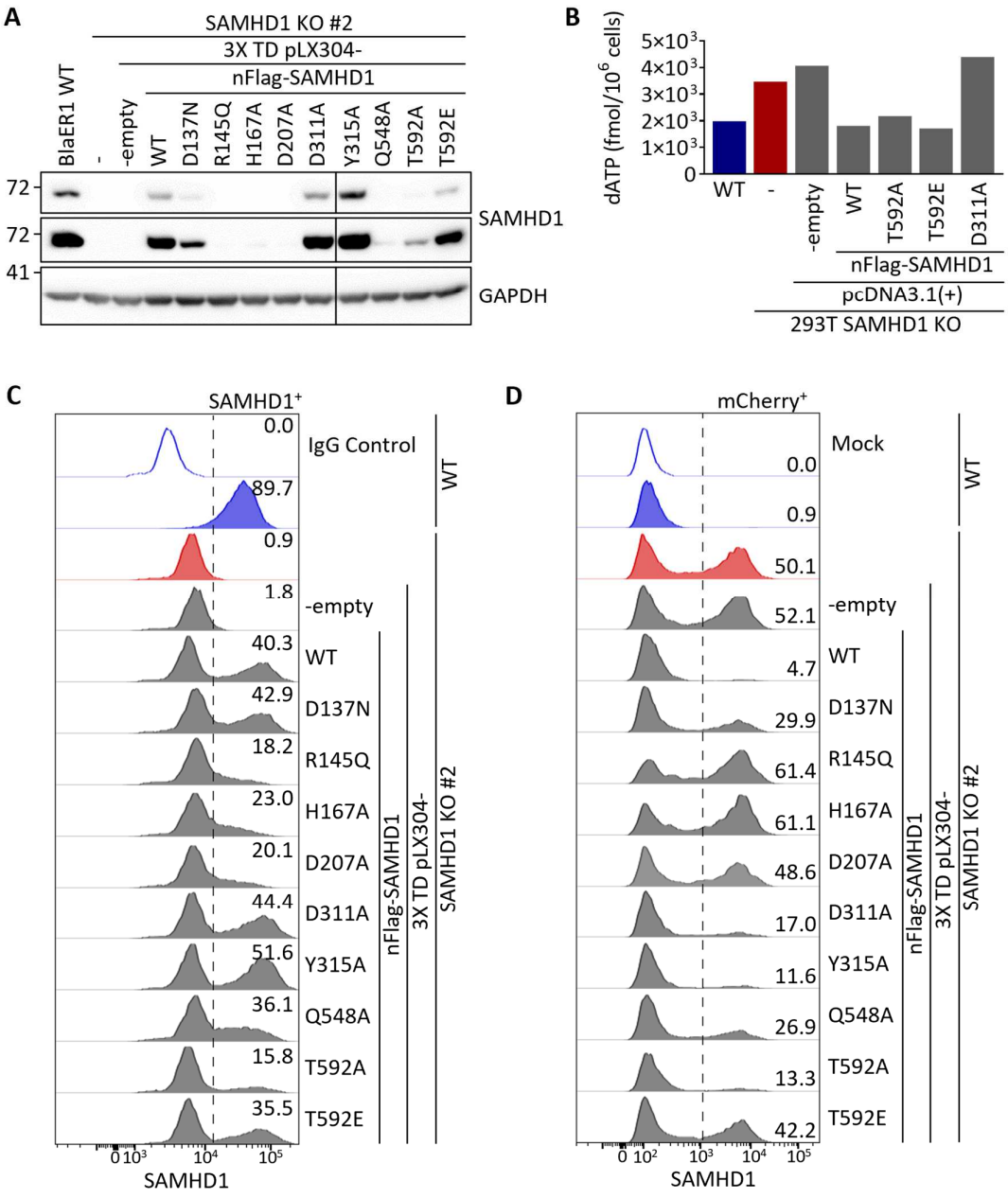

Figure 32: Several residues of the dNTPase catalytic center seem to be dispensable for HIV-1 restriction. BlaER1 SAMHD1 KO clone #2 was transduced three times with lentiviral pLX304 vectors encoding WT nFlag-SAMHD1 or respective SAMHD1 mutants without subsequent selection. Transduction with particles not encoding a transgene (-empty) were used as negative controls. **(A)** Immunoblot analysis of SAMHD1 expression in transduced transdifferentiated SAMHD1 KO BlaER1 cells. Transdifferentiated WT or transduced KO BlaER1 cells served as a control. Low and high exposure images are shown for SAMHD1. GAPDH was used as a loading control (representative for n = 2). **(B)** Measurements of cellular dATP content in 293T WT or SAMHD1 KO cells transfected with nFlag-SAMHD1 WT or SAMHD1 mutant constructs. The amount of dATP is depicted per 1 x 10^6 cells (n = 1). **(C, D)** Transdifferentiated BlaER1 WT

or SAMHD1 KO cell clones, as well as SAMHD1 KO cells transduced with lentiviral vectors for SAMHD1 mutant overexpression were infected with VSV-G pseudotyped HIV-1 single cycle mCherry reporter virus pBR HIV1 M NL4.3 IRES mcherry E^- R^+ at MOI 1. **(C)** Histograms show distribution of SAMHD1 expression in living GFP^+ $CD11b^+$ BlaER1 cells as quantified by intracellular staining of SAMHD1 and flow cytometry (representative for n = 2). Percentage of $SAMHD1^+$ cells in $CD11b^+$ cells is indicated. IgG isotype was used to control for unspecific staining. **(D)** Histograms show the distribution of mCherry signal in mock and HIV-1 mCherry reporter virus infected cells. Percentage of $mCherry^+$ cells in living GFP^+ $CD11b^+$ $SAMHD1^+$ BlaER1 cells is indicated (representative for n = 2).

mutant constructs, we were able to rescue dATP levels to amounts similar to WT cells (Fig. 32B). As expected, transfection of the SAMHD1 D311A mutant did not lower the dATP levels in 293T SAMHD1 KO cells, confirming loss of dNTPase activity of the D311A mutant in cells. Surprisingly, both D311A and Y315A mutant SAMHD1 were able to restrict HIV-1-mCherry infection in transdifferentiated SAMHD1 KO BlaER1 cells to the same level as the T592A mutant (Fig. 32D). This indicates, that at least some SAMHD1 catalytic core residues and thus dNTPase activity might be dispensable for lentiviral restriction in macrophage-like cells.

3.5 Phosphoproteomics of endogenous SAMHD1 allows the identification of novel potential phosphorylation sites

3.5.1 Analysis of phosphorylated residues of endogenous SAMHD1 in myeloid cells

Previously, we performed a non-targeted mass spectrometry analysis of SAMHD1 phosphorylation based on recombinant SAMHD1 protein expressed in Sf9 insect cells. Our results indicated numerous potential SAMHD1 phosphorylation sites. However, if these potential phosphorylation sites are also modified in relevant human HIV-1 target cells and in conditions in which SAMHD1 is expressed from an endogenous locus and at normal expression levels was unclear.

To confirm the presence of phosphorylated residues in a more relevant context, we performed a targeted liquid chromatography with tandem mass spectrometry (LC-MS/MS) analysis of endogenous SAMHD1 (Fig. 33A). In a first attempt we analyzed SAMHD1 phosphorylation in HIV-1 permissive monocytic THP-1 cells in comparison with PMA-activated macrophage-like THP-1 cells, in which SAMHD1 is restrictive towards

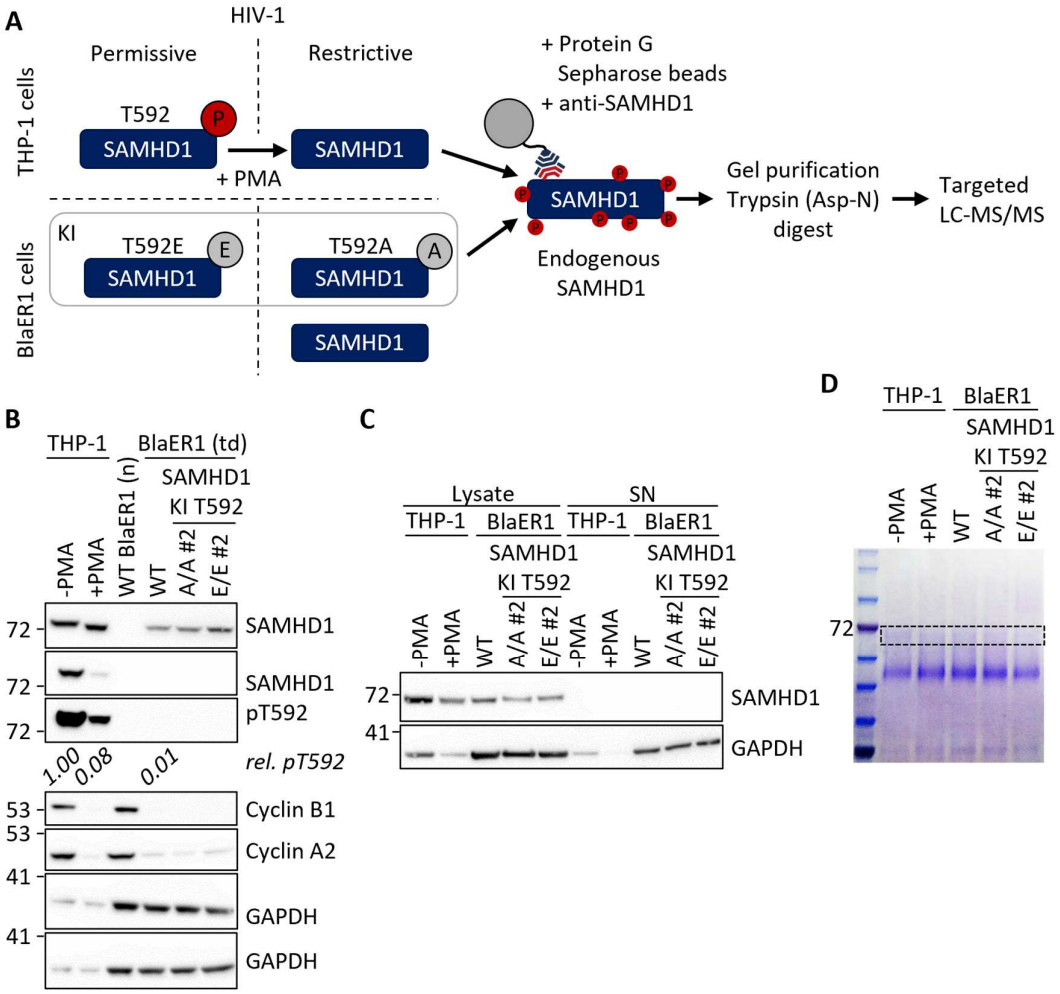

Figure 33: Targeted phospho-mass spectrometry analysis of endogenous SAMHD1 extracted from THP-1 and transdifferentiated BlaER1 cells.

(A) Schematic representation of the workflow used to analyze the phosphorylation of endogenous SAMHD1 in PMA-treated and cycling THP-1 cells, as well as in transdifferentiated WT BlaER1 cells, and SAMHD1 KI T592A and T592E mutant clones by targeted liquid chromatography with tandem mass spectrometry (LC-MS/MS). Phenotype of restriction towards HIV-1, as well as the T592 phosphorylation status is indicated for every cell type. **(B)** Immunoblot analysis of THP-1 cells activated or not with PMA, as well as transdifferentiated WT and SAMHD1 KI BlaER1 cells. Native BlaER1 cells served as a control. SAMHD1 expression and T592 phosphorylation (pT592) together with cyclin B1 and A2 expression was analyzed. Low and high exposure images are shown for SAMHD1 pT592. GAPDH was used as a loading control. Mean of SAMHD1 pT592 relative to total SAMHD1 expression was normalized to cycling THP-1 cells. **(C)** Immunoblot analysis of supernatant (SN) obtained after antibody mediated pulldown of SAMHD1. Lysates before pulldown are shown for comparison. **(D)** Coommasie staining of protein fraction present on Protein G coupled Sepharose beads after SAMHD1 pulldown and separation by SDS-PAGE gel electrophoresis. The isolated SAMHD1 band, which was used for downstream mass spectrometric analysis is highlighted. P-LC-MS/MS measurements were performed by Rita Derua.

HIV-1. Additionally, we validated our findings in a second LC-MS/MS run, in which we included SAMHD1 isolated from macrophage-like BlaER1 cells, which also show SAMHD1-dependent restriction of HIV-1.

As revealed by immunoblot and shown previously, SAMHD1 was phosphorylated at residue T592 in cycling THP-1 cells, whereas PMA-activation led to a strong (12.5-fold) decrease in SAMHD1 T592 phosphorylation in THP-1 cells (Fig. 33B). SAMHD1 T592 phosphorylation was even lower in transdifferentiated BlaER1 cells. Low T592 phosphorylation in PMA-activated THP-1, as well as in BlaER1 cells correlated with low cyclin A2 and B1 expression. In addition to our LC-MS/MS analysis of WT SAMHD1, we also included SAMHD1 T592A and T592E KI mutants in the second targeted mass spectrometry analysis, enabling us to investigate effects of SAMHD1 T592 phosphorylation on further potential phosphorylation sites. Transdifferentiated BlaER1 cells expressed WT SAMHD1 and SAMHD1 T592A and T592E KI mutants at similar levels, while cycling and PMA-activated THP-1 cells harbored slightly higher levels of SAMHD1 (Fig. 33C).

Pulldown of endogenous SAMHD1 using a polyclonal anti-SAMHD1 antibody bound to protein G on Sepharose beads led to loss of SAMHD1 from the supernatant after pulldown (Fig. 33C). A band corresponding to the size of SAMHD1 was visible by gel electrophoresis and Coomassie staining of the protein bound to the Sepharose beads (Fig. 33D).

Targeted LC-MS/MS analysis of trypsin digested SAMHD1 phospho-protein confirmed several potential SAMHD1 phosphopeptides (Fig. 34). The most predominant phosphopeptides were those containing the T579 and T592 residues. Mono-phosphorylated ^{577}NFTKPQDGDVIAPLITPQK^{595} and two isoforms of the mono-phosphorylated ^{577}NFTKPQDGDVIAPLITPQKK^{596} peptides were detected at high abundancies in cycling THP-1 cells, while PMA-activated THP-1 cells and transdifferentiated BlaER1 cells showed strongly reduced abundancies of the mono-phosphorylated forms (Fig. 34). Interestingly, the ^{577}NFTKPQDGDVIAPLITPQKK^{596} di-phosphopeptide was not detected in any of the LC-MS/MS analysis, indicating that T579 and T592 phosphorylation are mutually exclusive. Also, while non-phosphorylated ^{577}NFTKPQDGDVIAPLITPQKK^{596} and ^{581}PQDGDVIAPLITPQK^{595} were detected at very low abundancies, we were able to readily detect the non-phosphorylated

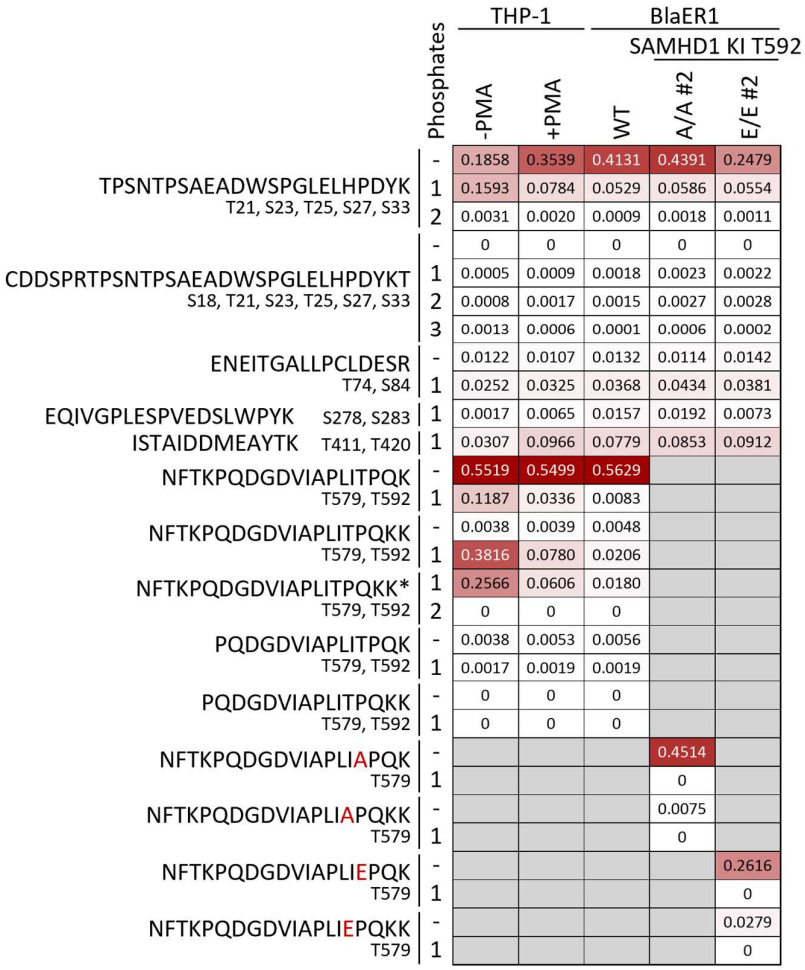

Figure 34: SAMHD1 phospho- and non-phosphopeptide abundancies in THP-1 cells and in transdifferentiated BlaER1 cells.

The heat map shows relative phospho- and non-phosphopeptide abundancies of endogenous SAMHD1 extracted from cycling and PMA-activated, as well as from transdifferentiated BlaER1 WT and homozygous SAMHD1 T592E and T592A KI mutant cells. Abundancies were determined by targeted LC-MS/MS analysis. The peak area of all precursors of the indicated SAMHD1 peptide corresponding to the indicated phosphorylation state were summarized and normalized against the sum of precursor peak areas of the GGFEEPVLLK control peptide, which is not modified by phosphorylation. The gradual increase of the red color intensity in the heat map corresponds to increased abundancy. For each peptide, covered possible phosphorylation sites are indicated. The asterisk indicates a second peptide isoform with identical sequence. The mutations in T592A and T592E introduced by KI are highlighted in red. Peptides which were not retrieved confidentially are weighted with zero abundancy. Peptides that were not retrieved in BlaER1 cells due to T592 mutation are marked in gray. P-LC-MS/MS measurements were performed by Rita Derua (n = 1 for BlaER1 cells, representative for n = 2 for THP-1 cells).

^{577}NFTKPQDGDVIAPLITPQK^{595} form in all conditions, implying that even in cycling THP-1 cells a substantial pool of SAMHD1 not phosphorylated at T579 or T592 might exist (Fig. 34).

Further pinpoint analysis of the C-terminal phosphopeptides revealed high abundancy of T592 and a low abundancy of T579 phosphorylation in cycling THP-1 cells. In fact, pT592 was 14.5-fold (± 2.0, n = 2) and 16.0-fold (± 3.5, n = 2) more abundant in the mono-phosphorylated form of the ^{577}NFTKPQDGDVIAPLITPQK^{595} and ^{577}NFTKPQDGDVIAPLITPQKK^{596} peptide, respectively (data not shown). To better decipher T579 and T592 phosphorylation sites, we performed an alternative AspN-digest followed by LC-MS/MS. Even though the non-phosphorylated ^{585}DVIAPLITPQKKEWN^{599}, as well as the mono-phosphorylated form modified at residue T592 could be readily detected, we were not able to detect mono-phosphorylated ^{585}DVIAPLITPQKKEWN^{599} peptides containing pT579, again emphasizing the low abundancy of pT579 in any condition tested (data not shown). Importantly, both the T579 and the T592 phosphorylation sites on the ^{577}NFTKPQDGDVIAPLITPQKK^{596} phosphopeptide (Fig. 35A and B), but also on the other phosphopeptides covering T579 and T592 (data not shown) were strongly de-phosphorylated upon PMA-activation and showed only residual phosphorylation in transdifferentiated BlaER1 cells. The 8.3-fold T592 dephosphorylation in PMA-treated THP-1 cells for the ^{577}NFTKPQDGDVIAPLITPQKK^{596} phosphopeptide, correlated with our results obtained by immunoblot from the same samples, indirectly validating the phospho-LC-MS/MS approach (Fig. 33B and 35A). Interestingly, even though we specifically targeted mutant T592A and T592E peptides, we were not able to detect a mono-phosphorylated form of any targeted T592A and T592E mutant peptide containing pT579, indicating that phosphorylation at T592 does not favor T579 phosphorylation (Fig. 34).

S278 containing mono-phosphorylated ^{270}EQIVGPLESPVEDSLWPYK^{288} was observed at low abundancy (Fig. 34), but specific peptide fragments were not detected indicating that this phosphopeptide might not be present in any of our conditions (data not shown). Phosphorylated forms of the ^{409}ISTAIDDMEAYTK^{420} peptide covering the residues T411 or T420, was detected at moderate levels and seems to be slightly higher in abundancy in macrophage-like THP-1 and BlaER1 cells compared to cycling THP-1 cells

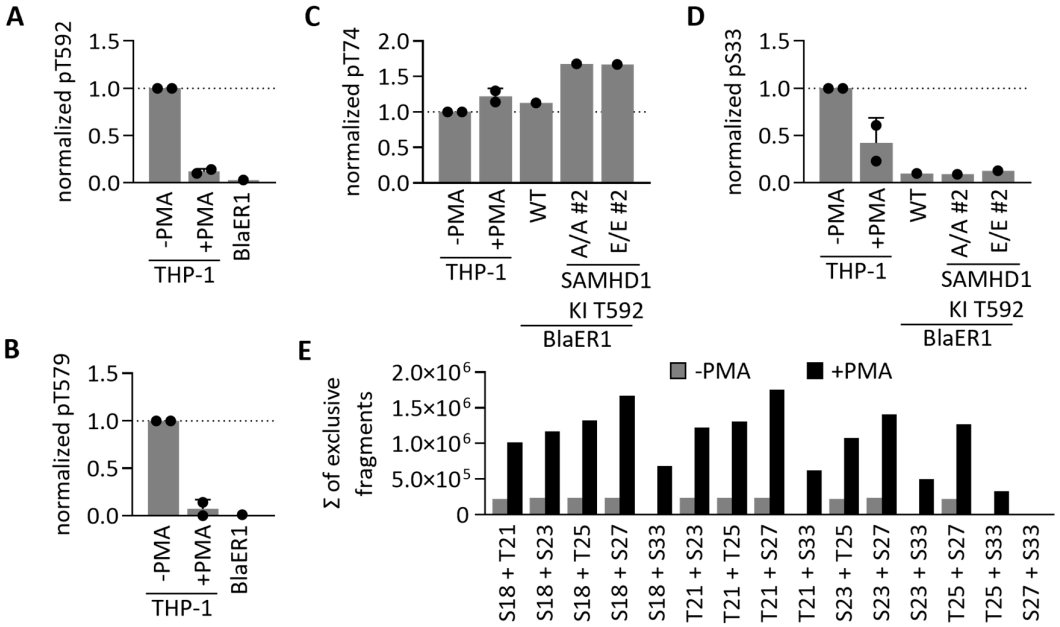

Figure 35: Phosphorylation of SAMHD1 residues in THP-1 cells and in transdifferentiated BlaER1 cells.
(A to D) Pinpoint analysis based on SAMHD1 phosphopeptide fragments. The sum of all relevant fragments, which can distinguish between two or more potential phosphorylation sites present on a phosphopeptide detected by LC-MS/MS, was normalized against the sum of all fragments of the non-phosphorylatabel SAMHD1 peptide GGFEEPVLLK. Subsequently, all conditions were normalized against cycling THP-1 cells. The normalized relative abundancy of **(A)** pT592 and **(B)** pT579 measured for the NFTKPQDGDVIAPLITPQKK, as well as **(C)** pT74 and **(D)** pS33 abundancies are shown. Bar graphs indicate mean of experiments, dots individual biological replicates. Error bars correspond to standard deviation of biological replicates (n = 2 for THP-1, n = 1 for BlaER1) **(E)** The sum of exclusive fragments of all fragments generated from the di-phosphorylated CDDSPRTPSNTPSAEADWSPGLELHPDYKT peptide were calculated for any possible combination of modified residues in cycling and PMA-treated THP-1 cells (n = 1). P-LC-MS/MS measurements and analysis in **(E)** were performed by Rita Derua.

(Fig. 34). A pinpoint analysis suggests that the T411 is not modified, hinting towards a possible T420 phosphorylation (data not shown).

Both in cycling and PMA-activated THP-1 and transdifferentiated BlaER1 cells we were able to detect moderate levels of the mono-phosphorylated ^{70}ENEITGALLPCLDESR^{85} peptide (Fig. 34). A fragment analysis revealed a high abundancy of pT74 in all samples, indicating that T74 phosphorylation is not differentially regulated in the conditions

tested (Fig. 35C). Equal pT74 abundancies in T592A and T592E mutants shows that T74 phosphorylation is not sensitive to T592 phospho-status (Fig. 34 and 35C).

For analysis of potential N-terminal SAMHD1 phospho-residues, we included two peptides, ^{21}TPSNTPSAEADWSPGLELHPDYK^{43} and ^{15}CDDSPRTPSNTPSAEADWSPGLELHPDYK^{43}, in our targeted LC-MS/MS analysis, covering S18, T21, S23, T25, S27 and S33. Mono-phosphorylated ^{21}TPSNTPSAEADWSPGLELHPDYK^{43} was found in high abundancy in cycling THP-1 cells and showed reduced abundancies upon PMA-activation, as well as in transdifferentiated BlaER1 cells, while the abundancy of the non-phosphorylated form of ^{21}TPSNTPSAEADWSPGLELHPDYK^{43} followed an inverse trend (Fig. 34). Fragment analysis revealed that most mono-phosphorylated peptides are modified at residue S33 (data not shown). Interestingly, pS33 levels decreased in THP-1 cells upon PMA treatment 2.4-fold and were even lower in transdifferentiated BlaER1 cells, following pattern of pT592 (Fig. 35D). Importantly, T592A or T592E KI had no influence on relative SAMHD1 pS33 levels (Fig. 35D). While non-modified ^{15}CDDSPRTPSNTPSAEADWSPGLELHPDYK^{43} was not detected, mono-, di- and tri-phosphorylated peptides could be retrieved with relatively low abundancies (Fig. 34). Remarkably, the abundancy of di-phosphorylated ^{15}CDDSPRTPSNTPSAEADWSPGLELHPDYK^{43} seemed slightly higher in macrophage-like cells. An initial fragment analysis of ^{15}CDDSPRTPSNTPSAEADWSPGLELHPDYK^{43} mono-phosphorylated peptide indicated dephosphorylation of T21 and T25 upon PMA-activation of THP-1 cells (data not shown). However, a more sophisticated analysis of potential combinations of N-terminal di-phosphorylation sites in PMA-activated and non-treated THP-1 cells, showed that several combinations of phosphorylated residues might be possible (Fig. 35E). Therefore, our mass spectrometry data points towards a differential regulation of an N-terminal phospho-hub containing the residues S18, T21, S25, S27 and S33 upon PMA-activation in THP-1 cells in which pS33 is downregulated, while phosphorylation of several other residues may be increased (Fig. 35E).

3.5.2 Differential phosphorylation of a possible N-terminal phospho-hub does not alter SAMHD1 expression, localization or T592 phosphorylation and has no effect on anti-viral restriction activity

To test the relevance of the N-terminal phospho-residues T21, T25 and S33, we generated phosphomimetic and phosphoablative mutants of SAMHD1 and tested them for SAMHD1 expression, T592 phosphorylation, SAMHD1 localization and anti-viral restriction activity. In order to account for differential regulation of these residues we included double mutants for T21 and T25, as well as T21A_T25A_S33D and T21E_T25E_S33A triple mutants, modelling an anti-regulatory phospho-status.

The mutants were transduced into cycling SAMHD1 KO BlaER1 cells. All mutants were detected by immunoblot in bulk preparations of transdifferentiated BlaER1 cells (Fig. 36A). None of the mutants showed a consistent effect on SAMHD1 T592 phosphorylation, as measured by immunoblot (Fig. 36A and B). Using flow cytometry analysis of overexpressed SAMHD1 N-terminal phospho-mutants in $CD11b^+$ transdifferentiated BlaER1 cells, we could not detect any differences with regards to the distribution of the $SAMHD1^+$ cell population, percentage of $SAMHD1^+$ cells or the MFI of SAMHD1 in $SAMHD1^+$ cells (Fig. 36C, D and E). This indicates that the phospho-status of T21, T25 or S33, as well as combinations of these potential N-terminal phospho-sites do not affect SAMHD1 expression nor T592 phosphorylation in macrophage-like cells.

SAMHD1 is predominantly localized nuclear due to a nuclear localization signal (NLS) located at the n-terminus between residue K11 and R14 (Fig. 6A and C) (Brandariz-Nuñez et al. 2012; Schaller et al. 2014). Since the investigated potential N-terminal phospho-residues are close to the NLS, we hypothesized that they might influence cellular SAMHD1 distribution. We therefore tested all mutants for localization defects upon transient transfection into 293T cells. By confocal imaging with nuclear DAPI and cytoplasm counterstaining we did not detect an increased nucleus to cytoplasm ratio of the SAMHD1 signal for any of the N-terminal phosphorylation site mutants (Fig. 37A and B). As a control, the ΔNLS mutant showed clear cytoplasmic localization (Fig. 37A and B). Also, no striking differences in nuclear distribution, namely no nuclear aggregates, were observed (Fig. 37B), suggesting that phosphorylation of T21, T25 or S33 does not affect SAMHD1 localization.

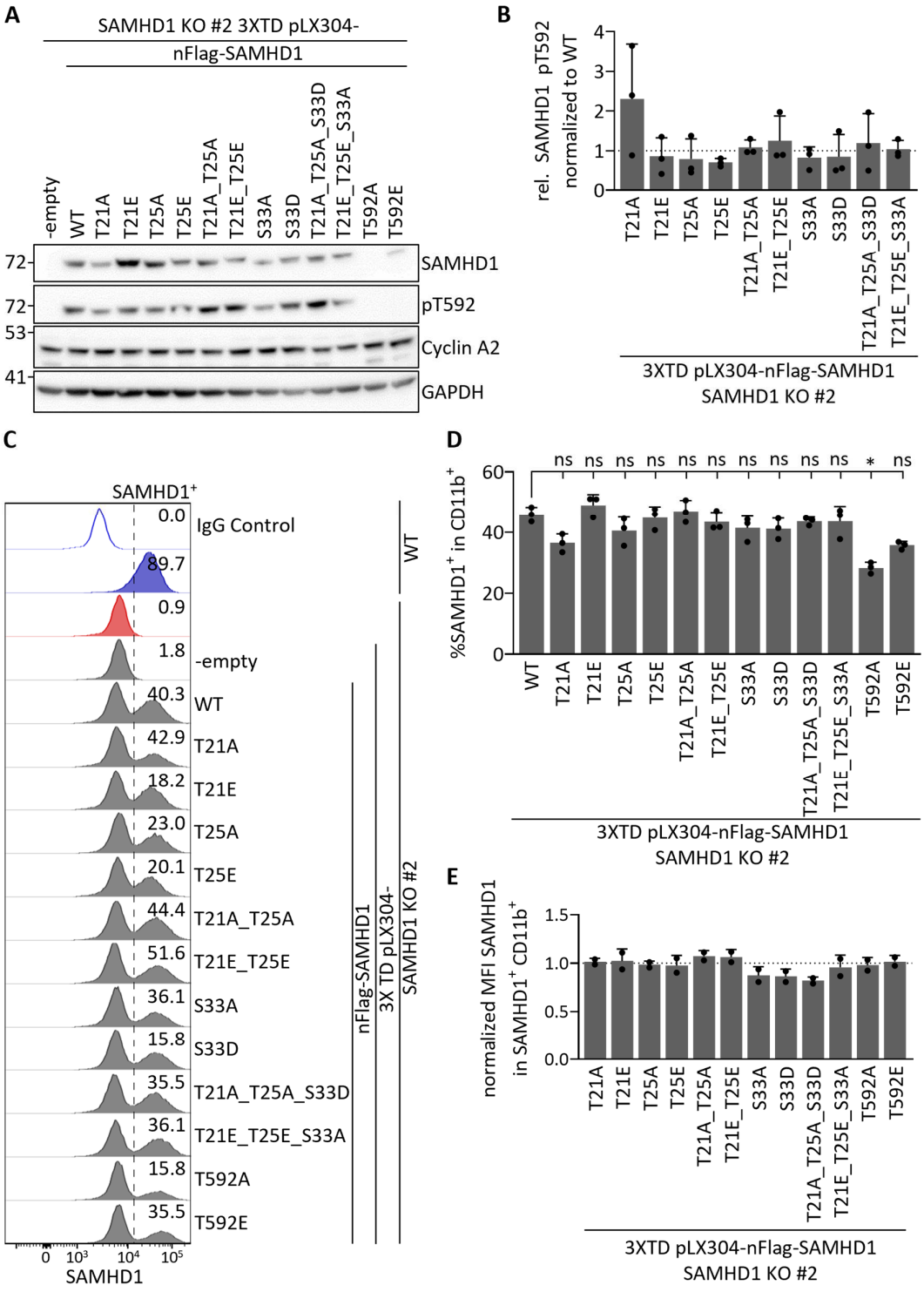

Figure 36: Differential phosphorylation of N-terminal phospho-hub does not alter SAMHD1 expression or T592 phosphorylation.

BlaER1 SAMHD1 KO clone #2 was transduced three times with lentiviral pLX304 vectors encoding WT nFlag-SAMHD1 or n-terminal phospho-site mutants without subsequent selection. Transduction with particles not encoding a transgene (-empty) were used as negative controls. **(A)** Immunoblot analysis of

SAMHD1 and cyclin A2 expression, together with SAMHD1 T592 phosphorylation in transduced transdifferentiated SAMHD1 KO BlaER1 cells. GAPDH was used as a loading control (representative for n = 3). **(B)** SAMHD1 T592 phosphorylation (pT592) in N-terminal phospho-site mutants was normalized to total SAMHD1 expression and again to pT592 level in WT nFlag-SAMHD1 transduced transdifferentiated SAMHD1 KO BlaER1 cells (n = 3). **(C)** Histograms show distribution of SAMHD1 expression in living GFP^+ $CD11b^+$ BlaER1 cells as quantified by intracellular staining of SAMHD1 and flow cytometry (representative for n = 3). The cells analyzed are infected with HIV-1-mCherry reporter virus as detailed below. Percentage of $SAMHD1^+$ cells in $CD11b^+$ cells is indicated. IgG isotype was used to control for unspecific staining. Bar charts show quantification of SAMHD1 expression in $CD11b^+$ transdifferentiated BlaER1 cells as percentage of $SAMHD1^+$ cells **(D)** (T21A $p = 0.2888$, T21E to T21E_T25E_S33A $p > 0.9999$, T592A $p = 0.0398$, T592E $p = 0.2069$, n = 3, Kruskal-Wallis test) and mean fluorescence intensity (MFI) of the signal corresponding to the SAMHD1 staining in $SAMHD1^+$ transdifferentiated BlaER1 cells **(E)**. MFI of SAMHD1 in cells overexpressing mutant SAMHD1 was normalized to WT (n = 3). Bar graphs indicate mean of experiments. Dots represent individual biological replicates. Error bars correspond to standard deviation of biological replicates (* $p < 0.05$; ns, not significant).

Next, we tested the restrictive activity of SAMHD1 T21, T25 and S33 mutants, as well as the indicated combinations, for their capability to restrict HIV-1-mCherry infection upon overexpression in transdifferentiated BlaER1 cells. Using the gating and staining strategy described above, we specifically analyzed HIV-1-mCherry infection in cells expressing nFlag-SAMHD1 WT or mutants (Fig. 38A). All N-terminal phospho-mutants tested, showed a restrictive potential similar to WT protein. More specifically percentage of $mCherry^+$ cells in $SAMHD1^+$ $CD11b^+$ cells was not increased compared to WT nFlag-SAMHD1 overexpression and the MFI of mCherry in $SAMHD1^+$ $CD11b^+$ cells was significantly lower, when compared to the empty vector control and not significantly different from WT nFlag-SAMHD1 transduced cells (Fig. 38B and C). Of note, also none of the combinatory T21A_T25A_S33D and T21E_T25E_S33A mutations affected HIV-1-mCherry reporter virus restriction upon overexpression in transdifferentiated SAMHD1 KO BlaER1 cells. Accordingly, we conclude that phosphorylation of T21, T25 and S33, as well as combinations of differential phosphorylation between these residues, do not regulate the anti-viral restriction activity of SAMHD1 in macrophage-like cells.

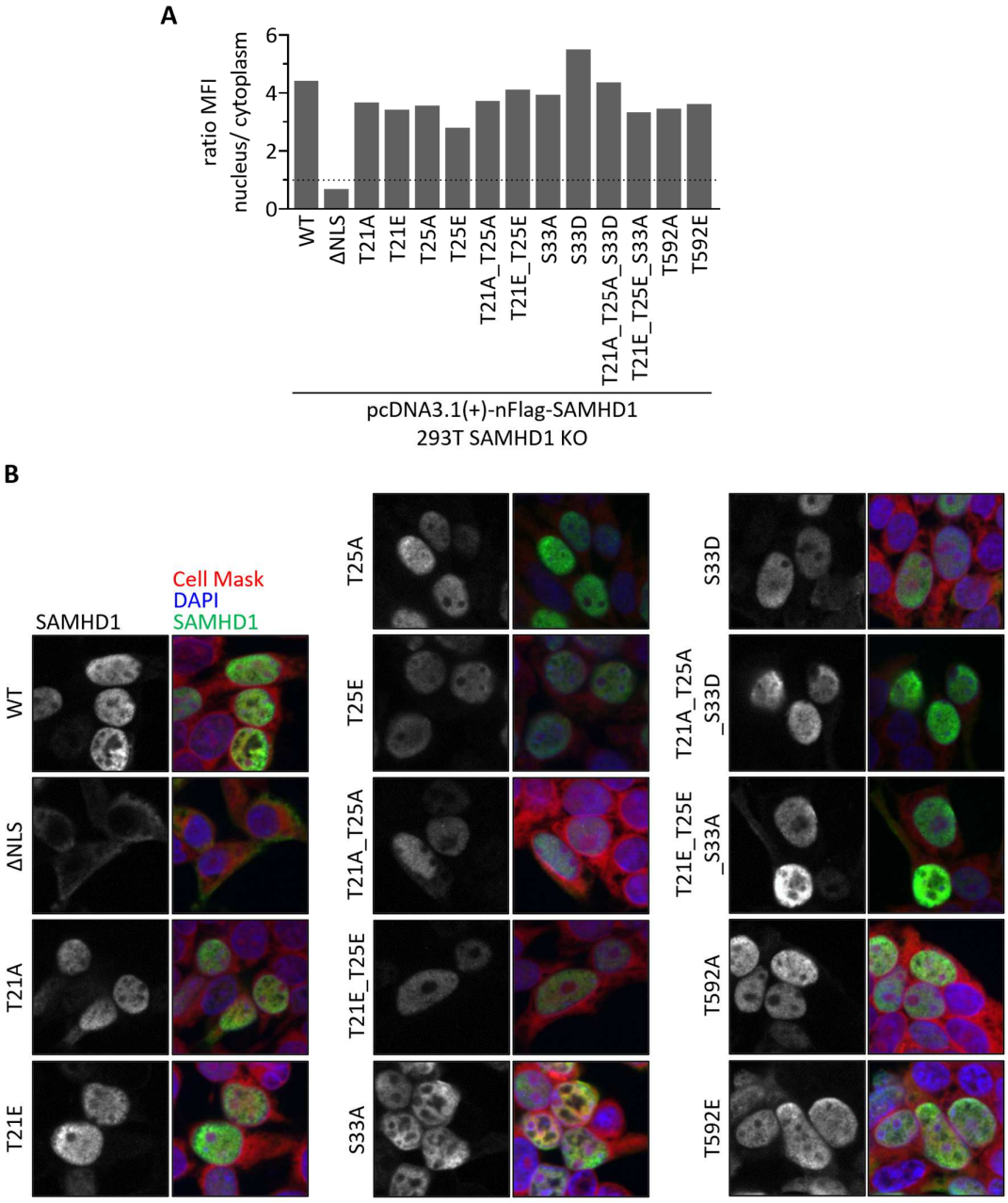

Figure 37: Differential phosphorylation of N-terminal phospho-hub does not alter SAMHD1 localization. 293T SAMHD1 KO cells were transfected with nFlag-SAMHD1 WT and n-terminal phosphorylation site mutants, as well as a with ΔNLS control. Immunofluorescence staining of SAMHD1, together with DAPI and Cell Mask counterstaining allowed quantification of SAMHD1 localization after transient transfection and was analyzed by automated confocal imaging. **(A)** The ratio of mean fluorescence intensity (MFI) of SAMHD1 in the nucleus relative to the cytoplasm is shown. The mean indicated in the bar chart was calculated from 16 images per condition, harboring an average of 50 cells per frame (n = 1). **(B)** Representative image sections are shown. Cellular distribution of SAMHD1 localization is highlighted.

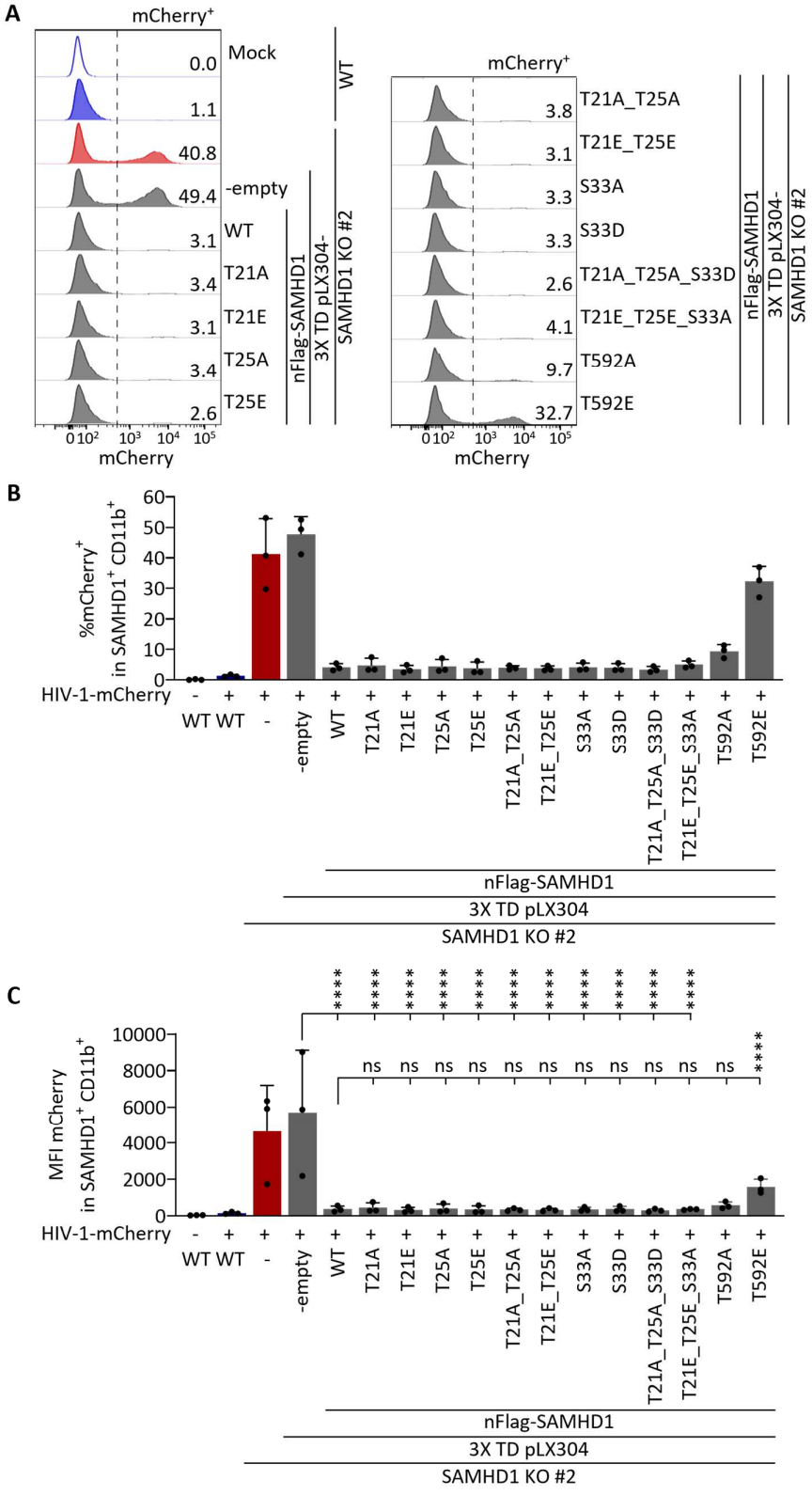
A
mCherry+
Mock
0.0
1.1
40.8
-empty
49.4
WT
3.1
T21A
3.4
T21E
3.1
T25A
3.4
T25E
2.6
WT
nFlag-SAMHD1
3X TD pLX304-
SAMHD1 KO #2
mCherry
T21A_T25A
3.8
T21E_T25E
3.1
S33A
3.3
S33D
3.3
T21A_T25A_S33D
2.6
T21E_T25E_S33A
4.1
T592A
9.7
T592E
32.7
B
%mCherry+ in SAMHD1+ CD11b+
HIV-1-mCherry
WT WT
-empty
T21A_T25A
T21E_T25E
T21A_T25A_S33D
T21E_T25E_S33A
T592A
T592E
nFlag-SAMHD1
3X TD pLX304
SAMHD1 KO #2
C
MFI mCherry in SAMHD1+ CD11b+
****
ns
HIV-1-mCherry
WT WT
-empty
T21A_T25A
T21E_T25E
T21A_T25A_S33D
T21E_T25E_S33A
T592A
T592E
nFlag-SAMHD1
3X TD pLX304
SAMHD1 KO #2

Figure 38: Differential phosphorylation of N-terminal phospho-hub has no effect on HIV-1 restriction.
Transdifferentiated BlaER1 WT or SAMHD1 KO cell clones, as well as SAMHD1 KO cells transduced with lentiviral vectors for SAMHD1 N-terminal phospho-site mutant overexpression were infected with VSV-G pseudotyped HIV-1 single cycle mCherry reporter virus pBR HIV1 M NL4.3 IRES mcherry E^- R^+ at MOI 1. **(A)** Representative histograms show the distribution of the mCherry signal in mock and HIV-1 mCherry reporter virus infected cells at 24 hpi. Percentage of $mCherry^+$ cells in living GFP^+ $CD11b^+$ $SAMHD1^+$ BlaER1 cells is indicated (representative for n = 3). Bar graphs indicate mean of experiments for **(B)** $\%mCherry^+$ cells (n = 3) or **(C)** mean fluorescent intensity (MFI) of mCherry (against -empty: all $p < 0.0001$; against -empty: WT to T21E_T25E_S33A $p > 0.999$, T592A $p = 0.8224$, T592E $p < 0.0001$, n = 3, One-way ANOVA) in the $CD11b^+$ $SAMHD1^+$ cell population. Dots represent individual biological replicates. Error bars correspond to standard deviation of biological replicates (**** $p < 0.0001$; ns, not significant).

3.5.3 Phosphorylation of SAMHD1 T579 might have an impact on its anti-viral restriction activity

Even though low in abundancy, we detected SAMHD1 T579 phosphorylation in endogenous SAMHD1, which was higher in HIV-1 permissive cycling THP-1 cells. Interestingly, pT579 and pT592 were co-regulated but seemed mutually exclusive. Therefore, we tested the effect of SAMHD1 T579 mutants, as well as combinations of T579 and T592 mutants on SAMHD1 expression and its anti-viral activity by overexpression of SAMHD1 mutants in transdifferentiated BlaER1 SAMHD1 KO cells.

Upon transduction and transdifferentiation of SAMHD1 KO BlaER1 cells, all tested nFlag-SAMHD1 mutant constructs were expressed in bulk cell preparations (Fig. 39A). Both the T579A and the T579E mutants showed reduced SAMHD1 pT592 levels in immunoblot upon overexpression in transdifferentiated BlaER1 cells, when compared to the overexpressed WT protein (Fig. 39B and C). However, pT592 phospho-status of T579A and T579E mutant did not differ significantly, indicating that the effect is independent of T579 phosphorylation. (Fig. 39C). Flow cytometry analysis reveals that all mutants tested showed a similar expression pattern on a single cell level, with a clear $SAMHD1^+$ cell population (Fig. 39D). However, while T579A and T579E mutants showed only slightly reduced frequencies of $SAMHD1^+$ cells in $CD11b^+$ cells, modification of T592 alone or in combination with T579 led to reduced frequencies of SAMHD1 expressing cells (Fig. 39E). In contrast, the MFI of SAMHD1 in $SAMHD1^+$ $CD11b^+$ cells was not affected by any of the mutants tested and comparable to overexpressed WT protein (Fig. 39F). Therefore, we conclude that T579A and T579E mutants do not affect SAMHD1

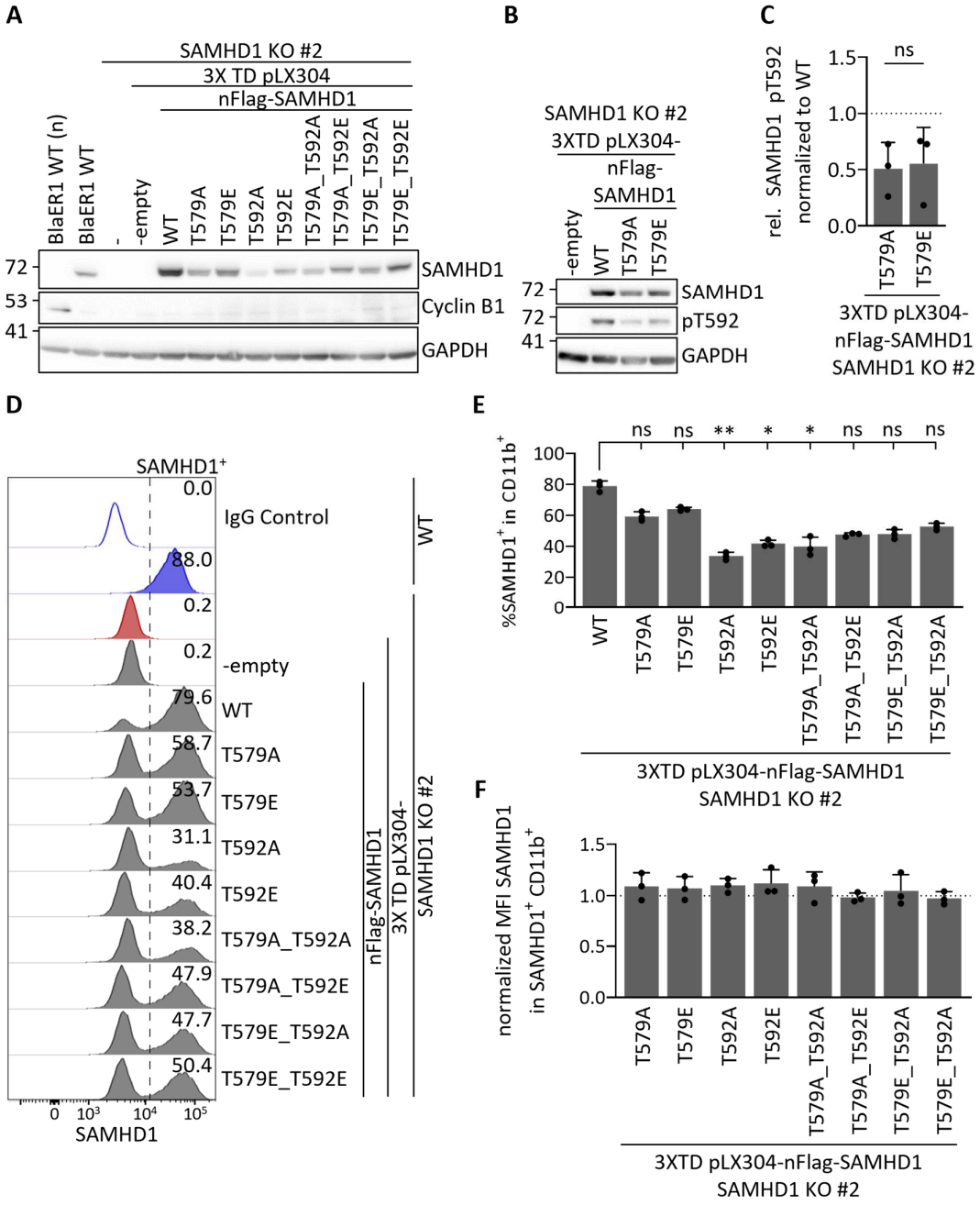

Figure 39: T579 phosphorylation does not alter SAMHD1 expression or T592 phosphorylation.

BlaER1 SAMHD1 KO clone #2 was transduced three times with lentiviral pLX304 vectors encoding WT nFlag-SAMHD1 or T579 and T592 phospho-site mutants without subsequent selection. Transduction with particles not encoding a transgene (-empty) were used as negative controls. **(A)** Immunoblot analysis of SAMHD1 and cyclin B1 expression in transduced transdifferentiated SAMHD1 KO BlaER1 cells. GAPDH was used as a loading control (representative for n = 3). **(B)** Immunoblot analysis of SAMHD1 T579 mutant phosphorylation at residue T592 (representative for n = 3). **(C)** SAMHD1 T592 phosphorylation (pT592) of T579 phospho-site mutants was normalized to total SAMHD1 expression and again to pT592 level in WT

nFlag-SAMHD1 transduced transdifferentiated SAMHD1 KO BlaER1 cells (p = 0.8492, n = 3, unpaired t-test). **(D)** Histograms show distribution of SAMHD1 expression in living GFP$^+$ CD11b$^+$ BlaER1 cells as quantified by intracellular staining of SAMHD1 and flow cytometry (representative for n = 3). The cells analyzed are infected with HIV-1-mCherry reporter as detailed below. Percentage of SAMHD1$^+$ cells in CD11b$^+$ cells is indicated. IgG isotype was used to control for unspecific staining. Bar charts show quantification of SAMHD1 expression in CD11b$^+$ transdifferentiated BlaER1 cells as percentage of SAMHD1$^+$ cells **(E)** (T579A *p > 0.9999,* T579E *p > 0.9999,* T592A *p = 0.0021,* T592E *p = 0.0270,* T579A_T592A *p = 0.0193,* T579A_T592E *p = 0.2797,* T579E_T592A *p = 0.2797,* T579E_T592E *p > 0.9999,* n = 3, Kruskal–Wallis test) and mean fluorescence intensity (MFI) of the signal corresponding to the SAMHD1 staining in SAMHD1$^+$ transdifferentiated BlaER1 cells **(F)** (n = 3). Bar graphs indicate mean of experiments. Dots represent individual biological replicates. Error bars correspond to standard deviation of biological replicates (* *p < 0.05;* ns, not significant).

expression. In combination with T592 mutants, overall expression in a bulk population might be reduced, which however should not affect downstream restriction experiments due to gating for SAMHD1$^+$ cells.

In order to assess the restriction activity of single or combinatory T579 SAMHD1 mutants, we infected transduced SAMHD1 KO BlaER1 cells after transdifferentiation and quantified HIV-1-mCherry reporter expression in the SAMHD1$^+$ CD11b$^+$ cell population (Fig. 40A). As expected, overexpression of WT nFlag-SAMHD1 and the T592A mutant led to a strong reduction in the frequency of mCherry$^+$ cells, while the T592E mutant was not able to restrict HIV-1-mCherry infection in SAMHD1 KO cells (Fig. 40B). Interestingly, SAMHD1 T579E mutation led to an increase of the percentage of mCherry$^+$ cells and a significant increase in the MFI of mCherry in SAMHD1$^+$ CD11b$^+$ BlaER1 cells in an extend similar to the T592E mutation (Fig. 40B and C). The T592A mutation showed an intermediated phenotype with a clear, but non-significant loss of restrictive activity, compared to WT. Surprisingly, any combination of both T579 and T592 phosphomimetic and -ablative mutation led to a strong loss of restriction activity, both in terms of percentage of mCherry$^+$ cells, as well as in terms of the MFI of mCherry in SAMHD1$^+$ CD11b$^+$ BlaER1 cells (Fig. 40B and C). This was especially striking since the T579A_T592A double mutant mimics the situation in transdifferentiated WT BlaER1 cells or SAMHD1 KO cells transduced with WT nFlag-SAMHD1, in which SAMHD1 is anti-virally active. Taken together our data on the mutational analysis of T579 remains inconclusive. While the partial loss of restrictive activity of the T579A mutant and the complete loss of

restriction in the combinatory mutants indicate a phospho-independent mechanism, the near complete loss of restriction by the T579E mutant, compared to the phenotype of the T579A mutant might still hint towards a regulatory role of pT579.

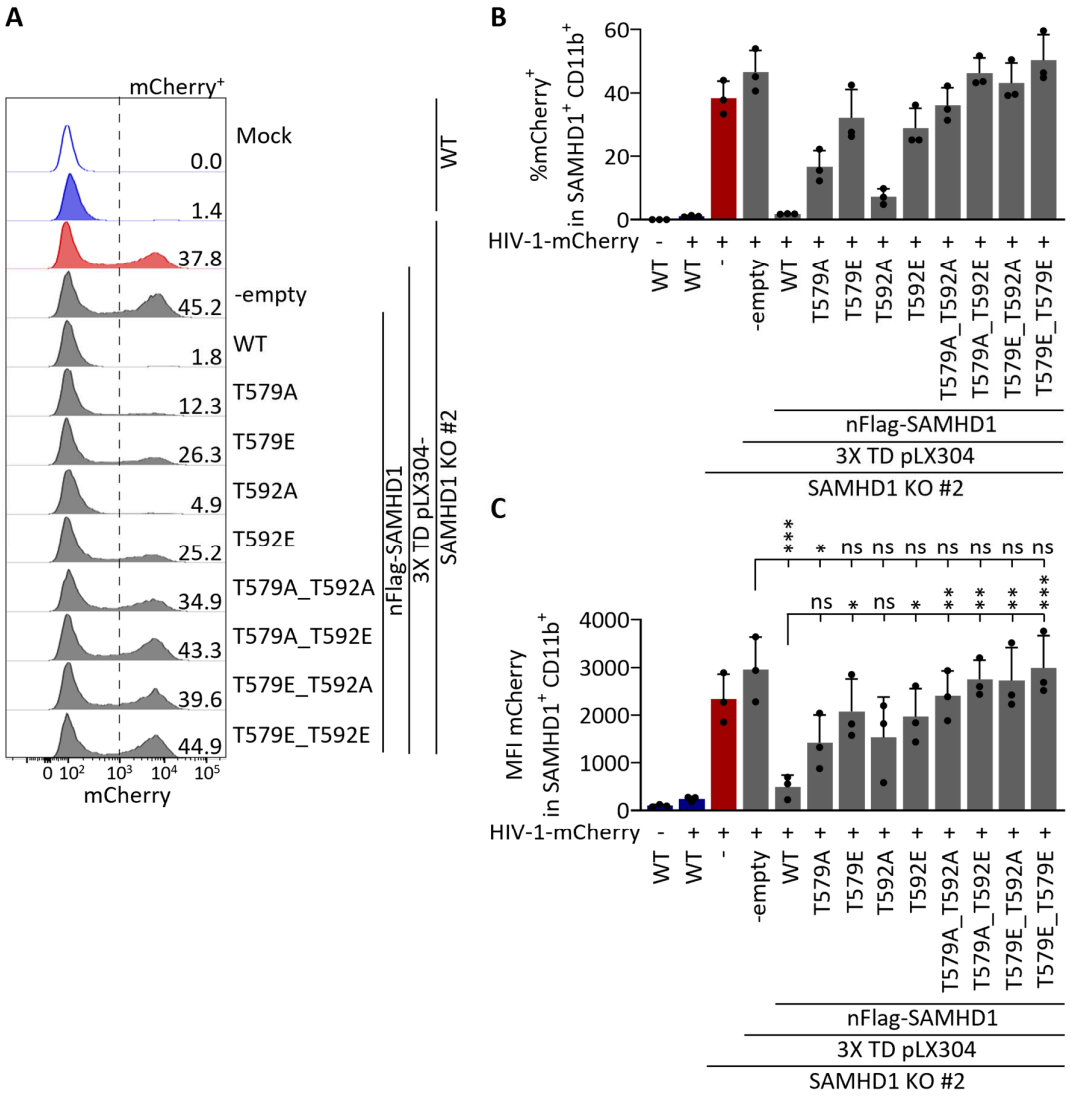

Figure 40: T579 phosphorylation affects anti-viral restriction activity.

Transdifferentiated BlaER1 WT or SAMHD1 KO cell clones, as well as SAMHD1 KO cells transduced with lentiviral vectors for SAMHD1 T579 and T592 phosphorylation-site mutant overexpression were infected with VSV-G pseudotyped HIV-1 single cycle mCherry reporter virus pBR HIV1 M NL4.3 IRES mcherry E^- R^+ at MOI 1. **(A)** Representative histograms show the distribution of the mCherry signal in mock and HIV-1 mCherry reporter virus infected cells at 24 hpi. The percentage of $mCherry^+$ cells in living GFP^+ $CD11b^+$ $SAMHD1^+$ BlaER1 cells is indicated (representative for n = 3). Bar graphs indicate mean of experiments for **(B)** percentage of $mCherry^+$ cells (n = 3) or **(C)** mean fluorescent intensity (MFI) of mCherry (against WT: T579A *p = 0.3411*, T579E *p = 0.0288,* T592A *p = 0.2333,* T592E *p = 0.0467,* T579A_T592A *p = 0.0073*,

T579A_T592E *p = 0.0016, T579E*_T592A *p = 0.0018, T579E*_T592E *p = 0.0006;* against -empty: WT *p = 0.0006*, T579A *p = 0.0385*, T579E *p = 0.4260,* T592A *p = 0.0627,* T592E *p = 0.2998,* T579A_T592A *p = 0.8466*, T579A_T592E *p = 0.9994, T579E*_T592A *p = 0.9976, T579E*_T592E *p > 0.9999,* n = 3, One-way ANOVA) in the $CD11b^+$ $SAMHD1^+$ cell population. Dots represent individual biological replicates. Error bars correspond to standard deviation of biological replicates (* *p < 0.05;* ** *p < 0.01*; *** *p < 0.001*; **** *p < 0.0001*; ns, not significant).

3.6 Analysis of the role of SAMHD1 in CRISPR/Cas9 KI and KO induced R-loop dynamics

3.6.1 SAMHD1 depletion has no effect on CRISPR/Cas9 knock-out efficiency

Genetic separation of SAMHD1's anti-viral and dNTPase activity, indicates that the dNTPase activity is not or not solely mediating anti-viral restriction. Which function of SAMHD1 imposes a block to HIV-1 infection is thus still not clear (Majer et al. 2019). Recently SAMHD1 was proposed to prevent R-loop formation in the context of genome stability (Park et al. 2021). R-loops are DNA-RNA hybrid structures, occurring among others at transcription-replication conflict sites (García-Muse and Aguilera 2019). Physiological R-loops are difficult to manipulate and to control in an experimental setup. However, CRISPR/Cas9 editing also generates DNA-RNA hybrid structures, which resemble R-loops in many aspects (García-Muse and Aguilera 2019). CRISPR/Cas9 editing can be precisely controlled in a time- and sequence-specific manner. Therefore, we decided to study the role of SAMHD1 in the context of CRISPR/Cas9 R-loop formation.

To do so, we generated HeLa single cell clones that have previously been transduced with very low titers of pLX304-EGFP particles to create clonal single copy integrant EGFP reporter cell lines. By nucleofection of CRISPR/Cas9 RNPs containing crRNA-GFP-1, we were now able to measure loss of GFP expression by flow cytometry, as a surrogate for CRISPR/Cas9 KO efficiency. Treatment of HeLa-EGFP cells with VLP-Vpx directly after nucleofection of crRNA-GFP-1 or a non-targeting control, lead to a near complete degradation of SAMHD1 at least until 48 h (Fig. 41A). Frequency of $EGFP^-$ cells in living HeLa cells was strongly increased upon crRNA-GFP-1 treatment after 7 days, while in the crRNA-NTC-1 treatment groups all cells remained $EGFP^+$ (Fig. 41B). Inversely, frequency of $EGFP^+$ cells was reduced after 9 days, correlating with the amount of RNP used for

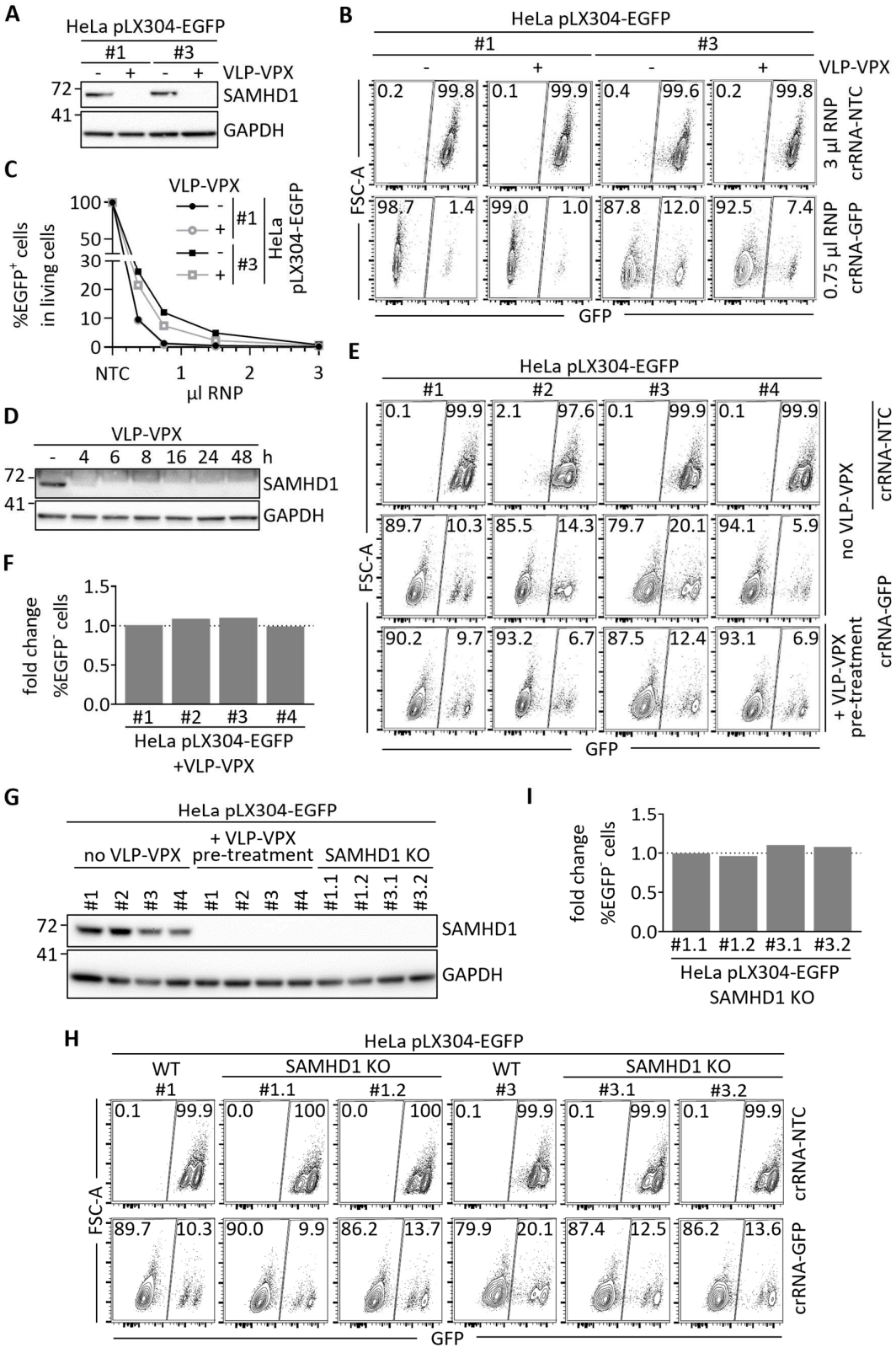
A
HeLa pLX304-EGFP
#1
#3
VLP-VPX
SAMHD1
GAPDH
B
HeLa pLX304-EGFP
3 µl RNP crRNA-NTC
0.75 µl RNP crRNA-GFP
FSC-A
GFP
C
VLP-VPX
%EGFP+ cells in living cells
µl RNP
NTC
HeLa pLX304-EGFP
D
VLP-VPX
SAMHD1
GAPDH
E
HeLa pLX304-EGFP
no VLP-VPX
+ VLP-VPX pre-treatment
crRNA-NTC
crRNA-GFP
F
fold change %EGFP- cells
HeLa pLX304-EGFP +VLP-VPX
G
HeLa pLX304-EGFP
no VLP-VPX
+ VLP-VPX pre-treatment
SAMHD1 KO
SAMHD1
GAPDH
I
fold change %EGFP- cells
HeLa pLX304-EGFP SAMHD1 KO
H
HeLa pLX304-EGFP
WT
SAMHD1 KO
crRNA-NTC
crRNA-GFP

Figure 41 : SAMHD1 depletion has no effect on CRISPR/Cas9 knock-out efficiency.

(A) Immunoblot shows SAMHD1 expression in HeLa pLX304-EGFP single cell clones treated with VLP-Vpx for 48 h. GAPDH was used as loading control. **(B, C)** Flow cytometry analysis and quantification of EGFP expression in VLP-Vpx treated or non-treated HeLa pLX304-EGFP single cell clones 9 days after nucleofection with the indicated amount of crRNA-NTC or crRNA-GFP containing CRISPR/Cas9 RNPs. **(B)** Frequencies of $EGFP^+$ and $EGFP^-$ cells in living cells are indicated. **(D)** Immunoblot analysis of SAMHD1 expression 4 to 48 h after VLP-Vpx treatment of HeLa cells. Non-treated cells served as a control. **(E, F)** EGFP expression in HeLa pLX304-EGFP single cell clones pre-treated for 8 h with VLP-Vpx. 9 days after nucleofection of 0.75 µl of crRNA-NTC or crRNA-GFP containing CRISPR/Cas9 RNPs, cells were analyzed by flow cytometry. **(E)** Frequencies of $EGFP^+$ and $EGFP^-$ cells in living cells are indicated. **(F)** Percentage of $EGFP^-$ cells in living cells was normalized to those of the respective clone not treated with VLP-Vpx. **(G)** Immunoblot analysis of SAMHD1 expression at the time point of nucleofection of VLP-Vpx pre-treatment of HeLa pLX304-EGFP single cell clones. Also, lysates obtained from CRISPR/Cas9 mediated SAMHD1 KO HeLa pLX304-EGFP single cell clones #1 and #3 are shown. Non-treated cells served as a control. GAPDH was used as loading control. **(H, I)** EGFP expression in HeLa pLX304-EGFP single cell clones and SAMHD1 KO clones derived from clones #1 and #3. 9 days after nucleofection of 0.75 µl of crRNA-NTC or crRNA-GFP containing CRISPR/Cas9 RNPs, cells were analyzed by flow cytometry. **(H)** Frequencies of $EGFP^+$ and $EGFP^-$ cells in living cells are indicated. **(I)** Percentage of $EGFP^-$ cells in living cells in SAMHD1 KO cell clones was normalized to those of the respective parent WT clone (n = 1 for all experiments).

treatment in both clones (Fig. 41C). SAMHD1 depletion by VLP-Vpx co-treatment resulted in a slight but consistent reduction in $EGFP^+$ cell frequency in HeLa-EGFP clone #3, implicating a slightly increased CRISPR/Cas9 KO efficiency upon SAMHD1 depletion. We hypothesized that the low effect might be due to a non-optimal timing and thus optimized VLP-Vpx treatment. Addition of VLP-Vpx to HeLa cells led to a fast degradation of SAMHD1 protein, with no SAMHD1 detectable after 6 h until 48 h post treatment (Fig. 41D). In order to assure low SAMHD1 levels already at the time point of crRNA-GFP-1 nucleofection, we thus pre-treated HeLa-EGFP single cell clones with VLP-Vpx for 8 h before introducing crRNA-GFP-1 or non-targeting control RNPs by nucleofection. With this experimental setup SAMHD1 was completely degraded at the time point of nucleofection (Fig. 41G). However, using our reporter assay we were only able to detect a slight increase in CRISPR/Cas9 GFP KO efficiency for clone #2 and #3, while KO efficiency in clone #1 and #4 remained unchanged (Fig. 41E and F).

In order to substantiate our results, we generated SAMHD1 KO single cell clones derived from two HeLa-EGFP single cell clones using CRISPR/Cas9. SAMHD1 KO was confirmed by allele specific Sanger sequencing and the absence of SAMHD1 expression in immunoblot (Fig. 41G). SAMHD1 KO however did not increase the percentage of $EGFP^-$ cells 9 days after nucleofection of crRNA-GFP containing RNPs, when compared to the parental WT HeLa pLX304-EGFP single cell clone (Fig, 41I and H). Therefore, we conclude that SAMHD1 depletion likely does not alter CRISPR/Cas9 KO efficiency in HeLa cells.

3.6.2 SAMHD1 depletion has no effect on CRISPR/Cas9 knock-in efficiency

HR to introduce CRISPR/Cas9 KI mutations requires the presence of an ssDNA correction template. We hypothesized that R-loops induced by CRISPR/Cas9 KI might be more complex and thus more sensitive to alterations in R-loop stability and dynamics. Hence, we analyzed the effect of SAMHD1 KO on the efficiency of CRISPR/Cas9-mediated KI. EGFP can be converted to BFP by single amino acid exchange using the crRNA-GFP containing RNPs and the ssDNA_GFPtoBFP oligo as a template for homologous recombination (Glaser et al. 2016). By measuring the efficiency of EGFP to BFP conversion in HeLa pLX304-EGFP single cell clones compared to SAMHD1 KO clones derived from these cell lines after nucleofection of crRNA-GFP containing RNPs and ssDNA_GFPtoBFP, we were able to quantify CRISPR/Cas9 KI efficiency by flow cytometry.

Quantification of the percentage of BFP^+ cells 9 days after nucleofection revealed no consistent differences between WT and the derived HeLa pLX304-EGFP SAMHD1 KO cells (Fig. 42A, B). While, both SAMHD1 KO clones derived from HeLa pLX304-EGFP clone #1 showed slightly enhanced EGFP to BFP conversion efficiency, the efficiency in SAMHD1 KO cells derived from clone #3 was similar or lower to the parental WT cell clone (Fig. 42B). Consequently, we conclude that SAMHD1 KO has no influence on CRISPR/Cas9 KI efficiencies in HeLa cells. Our findings speak against the hypothesis that SAMHD1 has a role in maintaining or resolving R-loops introduced by CRISPR/Cas9 KO or KI.

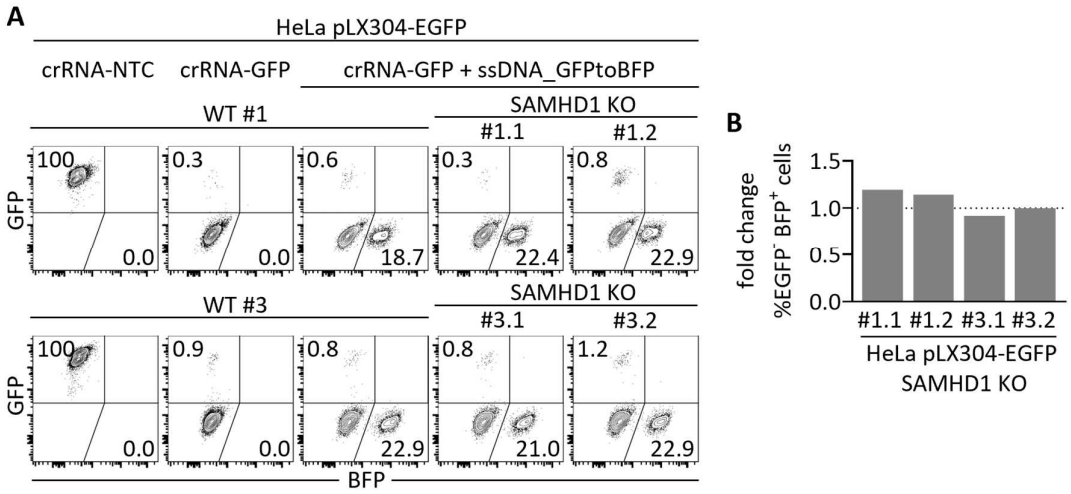

Figure 42 : SAMHD1 depletion has no effect on CRISPR/Cas9 knock-in efficiency.

(A, B) BFP expression, as a consequence of GFP to BFP conversion, was quantified in HeLa pLX304-EGFP single cell clones and SAMHD1 KO clones derived from clones #1 and #3. Cells were analyzed by flow cytometry 9 days after nucleofection of 0.75 µl of crRNA-NTC or crRNA-GFP containing CRISPR/Cas9 RNPs. As an HDR template ssDNA_GFPtoBFP oligonucleotide was provided by nucleofection together with crRNA-GFP containing RNP. **(A)** Frequencies of single positive $EGFP^+$ BFP^- and $EGFP^-$ BFP^+ cells in living cells are indicated. **(B)** Percentage of $EGFP^-$ BFP^+ cells in living cells measured in SAMHD1 KO cell clones was normalized to those of the respective parental WT clone (n = 1).

4. DISCUSSION

4.1 BlaER1 cells are a valuable tool to study SAMHD1-mediated HIV-1 restriction

SAMHD1 is a major cellular dNTPase and a potent HIV-1 restriction factor (Berger et al. 2011; Goldstone et al. 2011; Laguette et al. 2011; Hrecka et al. 2011; Baldauf et al. 2012; Descours et al. 2012; Franzolin et al. 2013). However, whether SAMHD1 dNTPase activity or dNTPase activity alone is meditating its anti-viral function and how this is regulated by T592 phosphorylation is still a matter of debate (Fig. 9) (Welbourn and Strebel 2016; Majer et al. 2019).

4.1.1 Transdifferentiation robustly generates macrophage-like BlaER1 cells

To tackle this question with a novel toolkit, we used transdifferentiated BlaER1 cells as an alternative and versatile myeloid model to study HIV-1 infection in macrophage-like cells. Transdifferentiated BlaER1 cells closely resemble human macrophages and have successfully been used to study innate immune signaling (Rapino et al. 2013; Gaidt et al. 2016). In contrast to PMA activated THP-1 or U937 cells, BlaER1 cell transdifferentiation relies on the activation of a fusion protein consisting of macrophage transcription factor C/EBPα and the estradiol receptor. It might therefore be an interesting physiological model for HIV-1 infection in macrophage-like cells (Rapino et al. 2013; Gaidt et al. 2018). For BlaER1 transdifferentiation, we applied an adapted protocol (Stefan Bauer, unpublished) which allows to generate high numbers of macrophage-like cell in the 6 well format and thus to reduce cost and workload of the original 96 well based protocol (Gaidt et al. 2018). Rigorous quality control of the transdifferentiation approaches alongside experiments showed that using this adapted protocol we achieved high and consistent rates of transdifferentiation comparable to what has been published previously for the original transdifferentiation method (Fig. 15) (Rapino et al. 2013). This also allowed to forgo on routine enrichment of macrophage-like cells by magnetic bead depletion of $CD19^+$ cells.

Transdifferentiated BlaER1 cells have been shown to closely resemble human MDMs, with regards to their transcriptomic profile (Rapino et al. 2013). In support of this, we could observe that cell surface expression of important myeloid markers such as CD14, CD163, CD206 and CD11c were highly expressed on transdifferentiated, but not on native BlaER1 cells, in line with the transcriptomic data (Fig. 16) (Rapino et al. 2013). Expression of CD14, CD163, CD206 and CD11c is in concordance with a tissue resident macrophage-like or monocyte derived cell phenotype of transdifferentiated BlaER1 cells, whereas the differential expression profile of CD14 could point towards one or several subpopulations of macrophage- or monocyte-like cells (Fig. 16) (Uhlen et al. 2019; Karlsson et al. 2021). For experiments sensitive to myeloid subset distribution, theses subpopulations should be investigated further. In addition to myeloid marker expression, transdifferentiated BlaER1 cells harbor HIV-1 (co-) receptors CD4, CXCR4 and CCR5 (Fig. 16), which makes them accessible to CCR5 and CXCR4 tropic HIV-1 WT virus infection and would allow spreading replication, or co-culture experiments (Keele et al. 2008; Wilen et al. 2012). This again highlights the versatility of the BlaER1 cell model to study HIV-1 infection in myeloid cells.

4.1.2 Transdifferentiated BlaER1 cells are less suitable to study HIV-1 sensing

Because BlaER1 cells were employed successfully to study innate immunity pathways, we also envisaged a potential use to investigate HIV-1 sensing in myeloid cells (Gaidt et al. 2016; Gaidt et al. 2017; Greulich et al. 2019). Unfortunately, BlaER1 cells were reported to be contaminated with SMRV (Oliver Keppler, Veith Hornung, Stefan Bauer, personal communication). Conclusively, we could detect SMRV contamination in all BlaER1 cell lines tested both on DNA and on RT activity level (Fig. 17A and B) (Uphoff et al. 2010; Uphoff et al. 2019). Furthermore, we measured elevated ISG baseline levels in transdifferentiated BlaER1 cells (Fig. 17C). The presence of reverse transcription products of an endogenized retrovirus, which could be sensed by cellular PRRs, rather disqualifies transdifferentiated BlaER1 cells as an optimal model for HIV-1 sensing (Yin et al. 2020). Well-designed control experiments however might overcome this caveat. Remarkably, even though SAMHD1 in principle could be restrictive towards SMRV reverse transcription (Gramberg et al. 2013; Majer et al. 2019), SAMHD1 KO did not increase the level of SMRV

DNA integration and RT activity in transdifferentiated BlaER1 cells (Fig. 17A and B), indicating that despite SMRV contamination, BlaER1 cells are a valid model to study the anti-viral restriction activity of SAMHD1.

4.1.3 SAMHD1 blocks HIV-1 infection in transdifferentiated BlaER1 cells

Transdifferentiated but not native BlaER1 cells express SAMHD1 at levels comparable to cycling THP1 cells (Fig. 18). Importantly, SAMHD1 is completely dephosphorylated at residue T592 in transdifferentiated BlaER1 cells, indicative of an active anti-viral state. Quantitatively, SAMHD1 dephosphorylation was even more pronounced in transdifferentiated BlaER1 cells at residue T592, but also at further residues such as T579, and residues of the N-terminal phospho-hub, which are dephosphorylated in macrophage-like cells (Fig. 34 and 35) (White et al. 2013b).

Using SAMHD1 degradation by providing Vpx *in trans* or CRISPR/Cas9-mediated SAMHD1 KO, we could show that SAMHD1 is a major restriction factor for HIV-1 infection in transdifferentiated BlaER1 cells (Fig. 19, 21 and 28). This observation was independent of the reporter system and the MOI used to test SAMHD1-mediated restriction of HIV-1 single cycle virus infection (Fig. 19, 21 and 28). Also, presence or absence of a functional Vpr gene did not impact the qualitative outcome of SAMHD1 restriction experiments (Fig. 21). However, the observed loss of restriction phenotype in SAMHD1 KO cells was more pronounced upon depletion of $CD19^+$ or when specifically analyzing HIV-1 restriction in $CD11b^+$ transdifferentiated BlaER1 cells (Fig. 21C). This was likely due to the absence of SAMHD1 expression and HIV-1 restriction in the remaining $CD11b^-$ native like cell population after bulk transdifferentiation, highlighting the superior performance of the flow cytometry based restriction assay (Fig. 21D to G). In conclusion, transdifferentiated BlaER1 cells are well suited to study SAMHD1 in the context of HIV-1 restriction in macrophages.

4.2 CRISPR/Cas9-mediated knock-in constitutes an elegant approach to validate the restrictive activity of SAMHD1

4.2.1 A pipeline to generate mutants of SAMHD1 by CRISPR/Cas9-mediated knock-in

To test mutants of SAMHD1 for anti-viral restriction activity in a physiological genetic and relevant cellular context, we combined transdifferentiated BlaER1 cells, as a novel myeloid model, with CRISPR/Cas9 mediated knock-in. We developed a gene editing strategy compromising CRISPR/Cas9 RNP and ssDNA oligo introduction by nucleofection, KASP screening of single cell clones and rigorous validation by sequencing and qgPCR (Fig. 24A). The frequency of HDR events at the SAMHD1 T592 locus was low in transdifferentiated BlaER1 cells and in the range of KI efficiency reported by others previously in various cell lines (Fig. 24E) (van Chu et al. 2015; Hu et al. 2018c). Efficiency of CRISPR/Cas9 KI in BlaER1 cells is likely target specific, because several fold higher KI efficiencies were obtained for the optimized GFP to BFP conversion assay (Fig. 23) (Glaser et al. 2016). A high distance of cutting to editing site at the T592 locus, due to absence of appropriate crRNA target sites likely corrupted KI efficiency, highlighting the need for gene editing tools, which are less restricted to specific PAM sequences (Paquet et al. 2016; Hu et al. 2018b). Using a cocktail of small molecule inhibitors for NHEJ we were able to further increase the efficiency of CRISPR/Cas9 KI (Fig. 23), indicating that in principle HDR can be achieved at even higher efficiency in BlaER1 cells (Skarnes et al. 2019).

Although HDR efficiency was low in our setting, we were able to introduce point mutations that correspond to phosphoablative T592A and phosphomimetic T592E mutations into the genomic *SAMHD1* locus. Our streamlined pipeline, in particular the KASP screening assay, made this possible. As an alternative to KASP screening, traditional PCR methods using mutant specific primers can be an option, if more than one single nucleotide exchange allow sufficient sequence discrimination (data not shown). For homozygous KI clone validation we employed rigorous allele specific Sanger sequencing and qgPCR to detect large genomic deletions at CRISPR editing sites (Fig. 24C and D) (Kosicki et al. 2018; Weisheit et al. 2020). The identification of one pseudo-homozygous clone, out of six tested clones, highlights the necessity of such analysis. In

summary, we developed a streamlined CRISPR/Cas9 KI pipeline, which enables the generation of homozygous mutants even at target sites with relatively low accessibility. Likely, the efficiency and versatility of gene editing by CRISPR/Cas9 KI or similar techniques will increase, as better NHEJ inhibitors or HDR enhancer are developed (Liu et al. 2018a). Also, novel approaches such as prime editing will favor the use gene editing to validate mutant phenotypes (Anzalone et al. 2019; Petri et al. 2022).

4.2.2 CRISPR/Cas9 knock-in as a superior genetic tool to study regulatory mutants of SAMHD1

Overexpression of SAMHD1 mutants in the U937 background using retroviral transduction has several technical limitations. Even though PMA-activated U937 cells are often considered to be SAMHD1-negative, they can express small amounts of endogenous SAMHD1, which can be further enhanced upon interferon treatment (Riess et al. 2017). In this context it is interesting that we observed full restrictive activity of minimal amounts of exogenously expressed SAMHD1 in transdifferentiated BlaER1 cell clones and no correlation between the levels of SAMHD1 expression and anti-viral restriction capacity (Fig. 30). Conclusively, the presence of even low amounts of endogenous WT SAMHD1 in PMA-activated U937 cells might affect the function of overexpressed mutant SAMHD1 in heterotetramers. In addition, strong exogenous, often viral, promotors drive SAMHD1 expression, leading to high protein levels and to non-physiological phosphorylation ratios, *i.e.* hyperphosphorylation (Fig. 22). This might not only be valid for the T592 site but also for other yet to be discovered PTM sites. In mutants generated by CRISPR/Cas9 KI, modified SAMHD1 is expressed from the endogenous promotor, in a physiological context and under normal regulation.

In BlaER1 cells, SAMHD1 is only expressed upon transdifferentiation (Fig. 18). As this is also the case for SAMHD1 mutants (data not shown), this supports a WT-like regulation of endogenous SAMHD1 mutants. Absence of SAMHD1 expression in native BlaER1 cells likely avoids an effect of constitutively expressed SAMHD1 mutants on cycling BlaER1 cells. In line with this, we were unable to generate homozygous SAMHD1 T592 mutants in THP-1 cells, indicating that inducible expression of endogenous SAMHD1 is a considerable advantage of the BlaER1 cell system (data not shown).

The idea to use gene editing to study the biology and relevance of PTMs in cells emerged relatively recently (Portegijs et al. 2016; Sanchez et al. 2019). However, this methodology has proven to be remarkably versatile and useful to answer questions related to protein regulation in complex settings (Sankar et al. 2022). We are convinced that it will also gain importance in the field of anti-viral restriction and innate immunity. Therefore, our pipeline for CRISPR/Cas9 KI in relevant HIV-1 target cells might prove useful in multiple contexts.

4.2.3 CRISPR/Cas9 knock-in validates the role of T592 phospho-regulation for anti-viral restriction

By generating several clones of homozygous SAMHD1 T592A and T592E mutants in BlaER1 cells, we were able to test the restrictive phenotype of endogenous SAMHD1 mutants. We observed loss of HIV-1 restriction in transdifferentiated BlaER1 cells harboring homozygous SAMHD1 T592E mutations (Fig. 25). This is in concordance with a number of publications showing that, in contrast to SAMHD1 WT or the T592A mutant, overexpression of phosphomimetic T592E or T592D mutants is not able to confer resistance to HIV-1 infection in PMA differentiated U937 cells (Tab. 18) (Laguette et al. 2011; Lahouassa et al. 2012; White et al. 2013b; Arnold et al. 2015). For the first time, we were thus able to validate the phenotypic consequence of SAMHD1 T592E phosphomimetic mutation, and hence the effect of T592 phosphorylation, for its anti-viral restriction activity in myeloid macrophage-like cells, using a genetic model not based on overexpression.

4.3 SAMHD1 dNTPase activity might not or not solely be responsible for HIV-1 restriction

4.3.1 SAMHD1 actively suppresses dNTP levels in transdifferentiated BlaER1 cells

The connection between SAMHD1 phospho-regulation and dNTPase activity still is not resolved (Fig. 9). To corroborate findings in U937 cells overexpressing SAMHD1 mutants, we therefore analyzed dNTP levels in transdifferentiated WT SAMHD1 KO and homozygous T592A and T592E mutant BlaER1 cells. In transdifferentiated WT BlaER1

cells we measured dNTP levels and concentrations, which were slightly lower or similar compared to dNTP concentrations in resting T cells (Tab. 17) (Diamond et al. 2004). After depletion of $CD19^+$ native-like cells from bulk preparations of transdifferentiated BlaER1 cells, we were able to further reduce the levels of all dNTPs, to values which were lower than those found in resting T cells (Tab. 17) (Diamond et al. 2004).

Considering HIV-1 reverse transcriptase K_m and K_d values measured *in vitro*, together with structured RNA regions in the HIV-1 RNA genome, which are thought to increase substrate requirements, this indicates that the dNTP concentrations found in transdifferentiated BlaER1 cells could in principle be low enough to restrict or delay HIV-1 reverse transcription (Klarmann et al. 1993; Derebail and DeStefano 2004; Kennedy et al. 2010).

Concomitantly, SAMHD1 KO raised cellular dNTP concentrations in transdifferentiated BlaER1 cells up to 4-fold (Fig. 26), which is reminiscent of the 5- to 8-fold increase in the dNTP pool size upon T cell activation and would be predicted to allow optimal HIV-1 reverse transcription (Diamond et al. 2004; Kennedy et al. 2010). In summary, SAMHD1 is an active dNTPase in transdifferentiated BlaER1 cells and maintains cellular dNTP levels below the threshold for efficient HIV-1 replication.

4.3.2 Endogenous SAMHD1 T592E mutation genetically uncouples anti-viral restriction and dNTPase activity

In stark contrast to SAMHD1 KO, neither endogenous SAMHD1 T592E, nor T592A mutations increased cellular dNTP concentrations in transdifferentiated BlaER1 cells (Fig. 26). This finding is in line with previous data on dNTP levels from overexpression studies on SAMHD1 T592 mutants (Welbourn et al. 2013; White et al. 2013b; Welbourn and Strebel 2016). Our results indicate that the loss of restriction observed in the endogenous T592E mutants cannot be caused by increased dNTP levels or reduced SAMHD1 dNTPase activity in transdifferentiated BlaER1 cells. In addition, SAMHD1 T592E and T592A mutations had no consistent effect on dNTP pool composition in transdifferentiated BlaER1 cells, ruling out an effect of the phosphomimetic mutation on SAMHD1 dNTPase substrate preferences and thus dNTP ratios, as proposed earlier (Fig. 27) (Jang et al. 2016). More specifically, in contrast to the findings by Jang et al.

endogenous SAMHD1 T592E mutations did not increase the cellular dCTP concentration (Fig. 26).

Taken together mutagenic analysis of the residue T592 of endogenous SAMHD1 indicates that SAMHD1 dNTPase activity or substrate preference in transdifferentiated BlaER1 cells is not regulated by T592 phosphorylation. Consequently, loss of HIV-1 restriction in SAMHD1 T592E mutants cannot be attributed to changes in SAMHD1 dNTPase activity. Thus, in line with previous reports (Welbourn and Strebel 2016), our data confirms that SAMHD1 anti-viral activity is not, or at least not exclusively, mediated by SAMHD1 dNTPase activity in macrophage-like cells.

4.3.3 The functions of SAMHD1 in DNA damage response and replication could be linked to HIV-1 restriction

SAMHD1 T592 phosphorylation may however regulate another functional entity of SAMHD1, which is necessary for full anti-viral restriction capacity (Majer et al. 2019). Multiple cellular functions of SAMHD1 have been described, which could be participating in anti-viral restriction (Fig. 5). SAMHD1 takes part in the resolution of stalled replication forks, which can occur under stress in cycling cells and, if not resolved, can lead to ssDNA intermediates and DNA double strand breaks (Coquel et al. 2018; Patel and Weiss 2018). Endo-/exonuclease MRE11 degrades part of the nascent DNA strand to generate 3' ssDNA, which in turn facilitates fork reversal and resolution. SAMHD1 seems to be involved in endonuclease MRE11 recruitment and activation (Coquel et al. 2018). Interestingly, SAMHD1 T592 phosphorylation appears to be required for SAMHD1 participation in DNA end resection and resolution of stalled replication forks (Coquel et al. 2018). Complex lentiviral reverse transcription shares several features with cellular replication and eukaryotic replication forks (Majer et al. 2019). As an example, DNA polymerization, RNase activity, ssDNA, dsDNA and RNA:DNA hybrid structures, DNA bifurcations, as well as strand invasion and template switching are found in both processes (Arhel et al. 2007; Le Grice 2012; Hughes 2015; Meng and Zhao 2017). Thus, one could speculate that SAMHD1 more directly interferes with HIV-1 restriction, by modifying the structure of the reverse transcription-nucleic acid complex or by recruiting endo-/exonucleases or further downstream effectors (Majer et

al. 2019). Interestingly, Coquel et al. found that the Y315A mutation leads to loss of SAMHD1-mediated resolution of stalled replication. Our initial data shows that the SAMHD1 Y315A mutant maintains its restrictive potential (Fig. 32). However, this contrasts with published reports and needs to be carefully validated (Tab. 18) (Arnold et al. 2015).

DNA end resection is also involved in homologous recombination, a DNA double strand repair pathway active in S- and G_2-phase (Ranjha et al. 2018). In this context, SAMHD1 was shown to recruit CtIP, another endonuclease, to sites of DNA double strand breaks, to thereby promote end resection and to enable homologous recombination (Daddacha et al. 2017). Also, SAMHD1 modulates the outcome of NHEJ and modulates the length of random dNTP insertions at the break site (Akimova et al. 2021). HIV-1 replication is linked to the DNA damage response at multiple levels. HIV-1 infection can lead to DNA damage signaling through the ATR/Chk1 axis, replication stress and G_2-arrest through the action of Vpr (Roshal 2003, Zimmermann 2006). Here, activation of SLX4-associated MUS81-EME1 endonuclease might be involved, again linking DNA damage associated endo-/exonucleases to HIV-1 replication (Laguette et al. 2014; Berger et al. 2015; Fregoso and Emerman 2016). Also, NHEJ pathway components, such as DNA-PKcs, are crucial for successful HIV-1 integration and prevent the activation of DNA damage signaling and apoptosis in response to HIV-1 infection (Daniel et al. 1999; Li et al. 2001; Skalka and Katz 2005). Thus, the role of SAMHD1 in DNA damage pathways could be linked to the restriction of HIV-1 replication. This could be at the level of reverse transcription, formation of the PIC or integration itself. However, since SAMHD1 was shown to specifically inhibit also reverse transcription, this would mean that such a mechanism either acts early or in addition to an early acting function of SAMHD1 (Goujon et al. 2007; Srivastava et al. 2008; Hrecka et al. 2011; Baldauf et al. 2012; Descours et al. 2012). Interestingly, while the modulation of NHEJ by SAMHD1 seems to be dependent on its dNTPase activity (Akimova et al. 2021), Daddacha et al. proposed that the function of SAMHD1 in HR is independent an active catalytic center. This would be in line with our preliminary results on dNTPase deficient mutants (Fig. 32). If the role of SAMHD1 in DNA damage response is regulated by pT592 is currently unknown.

How the ability of SAMHD1 to recruit DNA endo-/exonucleases relates to its anti-viral activity is not resolved (Majer et al. 2019). Still, it is imaginable that SAMHD1 T592

phosphorylation regulates different functional states of SAMHD1. Processes facilitated by SAMHD1 can possibly be mutually exclusive. When phosphorylated at residue T592, SAMHD1 could participate in the resolution of stalled replication forks or homologous recombination in cycling cells in S-Phase and G2-phase. However, then it would not be inhibiting viral replication. In contrast, upon transition into G_1 or G_0, SAMHD1 is rapidly dephosphorylated at residue T592. This mechanism could be essential in order to keep the time window, in which cells are permissive to DNA and retrovirus infection, restricted to cell cycle phases in which end resection is crucial (Schott et al. 2018).

Through which mechanism SAMHD1 is able to recruit endo-/exonucleases to sites of stalled replication and DNA double strand breaks is not resolved. SAMHD1 was shown to bind to single-stranded RNA and DNA, as well as to RNA or DNA with complex secondary structures *in vitro* (Beloglazova et al. 2013; Seamon et al. 2015). If this is contributing to the recruitment of endo-/exonucleases in cells or anti-viral activity, is still open. In this direction, a recent report presents evidence that short phosphorothioate oligonucleotides can bind to the allosteric sites of SAMHD1, promoting formation of a distinct SAMHD1 tetramer (Yu et al. 2021). Mutations that abolish phosphorothioate oligonucleotide binding also reduced HIV-1 restriction potential. How SAMHD1 nucleic acid binding activity is regulated is currently not clear. The SAMHD1 phosphomimetic T592E mutant had no influence on ssRNA and ssDNA binding *in vitro* (Seamon et al. 2015). Intriguingly, ssDNA or ssRNA binding to SAMHD1's dimer-dimer interface can inhibit the formation of catalytically active SAMHD1 tetramer and thus interferes with dNTPase activity (Seamon et al. 2016). This again could be reminiscent of SAMHD1 moonlighting between two mutually exclusive functions.

Conversely, it could be hypothesized that two functions of SAMHD1 mechanistically linked and that both are necessary for full SAMHD1 function. This could follow an additive or synergistic logic. However, our preliminary data on depletion of SAMHD1 T592E KI mutants, rather speaks against a second, T592 phospho-regulation independent function of SAMHD1 (Fig. 28, for detailed discussion see 4.4.1). Alternatively, two functional entities of SAMHD1 could follow an AND logic, in which on function licenses the other. As an example, low dNTP levels could sensitize HIV-1 reverser transcription for additional anti-viral functions, such as DNA damage response associated mechanisms due to rNTP misincorporation, mutagenic stress and enhanced

pausing of RT (Hu and Temin 1990; Kennedy et al. 2012). Also, SAMHD1's nucleic acid binding activity could modulate the localization and interactome of SAMHD1 and thereby allow context dependent anti-viral mechanisms (see section 4.4.2). A deeper investigation is needed to understand these phenomena in cells and to test whether this might be regulated by post-translational modifications.

4.4.4 SAMHD1 might have a role in R-loop resolution, but does not alter CRISPR/Cas9 editing efficiency

Recently, SAMHD1 was suggested to play a role in the prevention or resolution of R-loops. R-loops are trimeric RNA:DNA structures that form at transcription-replication conflict sites, but also at sites of DNA damage (Fig. 7) (Park et al. 2021; García-Muse and Aguilera 2019). MRE11 complex and other endo-/exonucleases are important for the resolution of R-loops (Chang et al. 2019; García-Muse and Aguilera 2019). Thus, SAMHD1 could be responsible for recruitment of factors, *i.e.* endo-/exonucleases, mediating R-loop resolution. Furthermore, other proposed cellular functions of SAMHD1 strongly overlap with biological phenomena in which R-loops are involved, such as telomere maintenance and antibody class switch recombination (Fig. 5 and 7) (Majerska et al. 2018; García-Muse and Aguilera 2019; Husain et al. 2020). Accordingly, whether the role of SAMHD1 in R-loop prevention, resolution of stalled replication forks, DNA damage response and class switch recombination are functionally connected, should be carefully addressed.

In this line, subsequent proteins involved in nucleic acid metabolism have recently been shown to affect the abundancy of R-loops. Mutants of RNAse H2 and TREX1, known to cause AGS in patients, have been demonstrated to elevate the genomic R-loop burden and thereby to release immune stimulatory RNA:DNA hybrids, which are subject to cGAS-mediated sensing and could be causative for elevated IFN signaling and neuroinflammation in AGS patients (Chatzidoukaki et al. 2021; Cristini et al. 2022; Giordano et al. 2022). A similar relationship for SAMHD1 mutants leading to AGS, is still to be demonstrated.

R-loops at transcription-replication conflicts are difficult to control and thus to study experimentally. However, R-loop-like structures also form during CRISPR/Cas9 gene

editing, which would allow tight experimental control of R-loop formation. Therefore, we studied the role of SAMHD1 in CRISPR/Cas9 gene editing by using KO or KI efficiency as a surrogate for R-loop stability and dynamics. Yet, we were unable to define a relationship between SAMHD1 depletion and altered CRISPR/Cas9 KO and KI efficiency (Fig. 41 and 42). Conclusively, SAMHD1 seems not to affect R-loop dynamics in the context of CRISPR/Cas9 gene editing.

However, even though CRISPR/Cas9 complexes bound to genomic DNA resemble physiological R-loops in several aspects, such as RNA:DNA hybrid regions and displaced ssDNA, the detailed structure and composition probably differs (García-Muse and Aguilera 2019). Also, the mechanisms leading to displacement or resolution of the tertiary nucleic acid complex, as well as the cellular factors recruited to the R-loop, will likely not be the same. Different gene editing tools, such as a growing repertoire of Cas proteins, or prime editors might adopt alternative DNA:RNA:protein conformations and therefore might be more accessible to cellular factors modulating R-loop biology (Anzalone et al. 2019; Nidhi et al. 2021). Understanding if SAMHD1 plays a role in these settings, might bring new answers to the question of whether SAMHD1 alters R-loop stability and dynamics. Elucidating the role of SAMHD1 in R-loop biology is of special importance since complex RNA:DNA hybrids are intermediates of HIV-1 reverse transcription (Flint et al. 2015). One hypothesis could be that SAMHD1 inhibits reverse transcription by directly interfering with the stability of these nucleic acid species. Again, understanding timing and localization of reverse transcription and uncoating is essential to estimate if SAMHD1 could directly access and interfere with the HIV-1 replication complex.

4.4 Towards a unified model of SAMHD1 function, T592 phospho-regulation and HIV-1 restriction

4.4.1 Two functional entities could be necessary to form the complete anti-viral restriction potential of SAMHD1

As outlined above, we were able to genetically uncouple anti-viral restriction and dNTPase function with CRISPR/Cas9 KI mutants of the phospho-regulatory T592 site. This is in support of previous data on the effect of T592 mutants in overexpression

systems on anti-viral restriction and cellular dNTP levels (Tab. 18) (Welbourn et al. 2013; White et al. 2013b; Welbourn and Strebel 2016). However, the paradigm that the dNTPase activity of SAMHD1 is the major driver of anti-viral activity still is widely accepted and shared in the field (Baldauf et al. 2012; Lahouassa et al. 2012; Kim et al. 2012; Arnold et al. 2015; Welbourn and Strebel 2016; Schott et al. 2018; Majer et al. 2019; Bowen et al. 2021). Combining CRISPR/Cas9 KI with BlaER1 cells as a novel myeloid model, we were now able to demonstrate that the separation of the loss of restriction phenotype and the maintenance of SAMHD1 dNTPase activity is not due to technical artifacts (Fig. 25 and 26) (Majer et al. 2019).

Uncoupling of SAMHD1-mediated anti-viral restriction and dNTPase activity does not exclude the possibility that the SAMHD1 dNTPase activity is participating to or required for anti-viral restriction. A yet to be defined second SAMHD1 enzymatic activity or property (see sections 4.3.3, 4.3.4 and 4.4.2 for details), might in addition be required for full anti-viral restriction capacity of SAMHD1. This second SAMHD1 functional entity could be regulated by T592 phosphorylation. In a scenario of an additive dual dependency, the two entities of SAMHD1 would independently restrict HIV-1 replication. Also, the relationship between two functional entities of SAMHD1 could be synergistic. In synergism the two functional entities are not completely independent, but one function supports or enhances the other function of SAMHD1. Both options could lead to a scenario in which the restrictive effect of several anti-viral mechanisms are necessary to block HIV-1 replication, potentially in a cell type-dependent manner. Such a hypothesis would be in line with the notion that a SAMHD1 function independent of the regulation of dNTP level is required for anti-viral restriction in cycling cells (Welbourn and Strebel 2016).

Using Vpx-mediated SAMHD1 depletion in transdifferentiated SAMHD1 T592A and T592E KI mutant BlaER1 cells, we tried to address the question of whether a second function of SAMHD1, independent of T592 phospho-regulation, *i.e.* the dNTPase activity, contributes to anti-viral restriction. Upon SAMHD1 T592E mutant depletion, we observed only a minor increase of HIV-1-mCherry reporter virus infection, to the same level observed in SAMHD1 KO cells (Fig. 28). Thus, our preliminary data rather speaks against a second functional entity of SAMHD1 contributing to HIV-1 restriction in an

additive of synergistic manner. However, this preliminary result requires further support from biological replicates.

4.4.2 Interaction partners or SAMHD1 sub-cellular localization could license HIV-1 restriction

An alternative hypothesis could be that T592 phosphorylation regulates a property of SAMHD1, which is absolutely required for dNTPase-mediated anti-viral restriction. As an example, T592 phosphorylation could modulate SAMHD1 sub-cellular localization, as well as SAMHD1 recruitment to interaction partners or multi-protein complexes. In this line, it is interesting that SAMHD1 recruitment to stalled replication forks is dependent on T592 phosphorylation (Coquel et al. 2018). We and others recently were able to identify a large number of potential SAMHD1 interaction partners (St Gelais et al. 2014; Schott et al. 2018). These analyses are based on transient or stable overexpression of tagged protein. Overexpressed SAMHD1 is hyperphosphorylated (Fig. 22). To better understand pT592-dependent SAMHD1 complex formation, it will be crucial to investigate the interactome of SAMHD1 with defined phospho-status, side by side in a comparable system. In addition, interactomes based on endogenously expressed protein might increase the fidelity and relevance of identified interaction partners and reduce the number of candidates. Similarly, the analysis of endogenous protein interactomes would reduce the burden of mislocalization, which can be a problem in overexpression (Dalvai et al. 2015; Stockhammer et al. 2021). Using proximity labeling with new biotinylation enzymes such as TurboID, in combination with endogenous tagging, will allow time resolved mapping of transient SAMHD1 interactions in different conditions (Branon et al. 2018; Cho et al. 2020; Stockhammer et al. 2021). Comparing the interactome of endogenous SAMHD1 in THP-1 cells stimulated or not with PMA could reveal differential interaction networks of phosphorylated and un-phosphorylated SAMHD1. However, PMA-activation could also heavily modulate the expression of potential SAMHD1 interaction partners. As an alternative, we believe that SAMHD1 T592A and T592E KI mutants in transdifferentiated BlaER1 cells can be an attractive tool to define the T592 phospho-dependent interactome of endogenous SAMHD1.

Even more, interactions and complex recruitment of SAMHD1 differentially phosphorylated at residue T592 could modulate SAMHD1 sub-cellular localization. SAMHD1 is predominantly localized nuclear (Brandariz-Nuñez et al. 2012). However, SAMHD1 is not evenly distributed in the nucleus (Fig. 37). Also, SAMHD1 mutants could have an impact on how SAMHD1 is localized in the nuclear compartment (Paula Rauch, unpublished). Compartmentalization of SAMHD1, so far, was only analyzed using overexpression systems. Overexpressed protein might be dysregulated in terms of localization and subject to artefacts due to enforced episomal expression (Batalis et al. 2021). Recent advances in endogenous protein tagging and high resolution fluorescence imaging could increase our understanding of SAMHD1 localization and bring new insights into phospho-dependent SAMHD1 recruitment to sub-nuclear structures (Bukhari and Müller 2019; Cho et al. 2022). It would also allow live cell imaging. Again, we believe that the endogenous T592A and T592E BlaER1 KI mutants can serve as an interesting starting point to understand the effect of pT592 on SAMHD1 nuclear distribution.

Interestingly, HIV-1 replication was recently proposed to take place in specialized nuclear compartments, so called nuclear speckles (Francis et al. 2020; Rensen et al. 2021). As proposed, HIV-1 capsid containing the RTC is transported from the nuclear pore into nuclear speckles in a CPSF6-dependent manner. HIV-1 infection is able to remodel nuclear speckles and to lead to CPSF6 re-localization (Francis et al. 2020; Rensen et al. 2021). The idea that SAMHD1 could be co-shuttled or even specifically recruited into these compartments upon HIV-1 infection is intriguing. Nuclear speckles are phase-separated membraneless compartments. Restricted diffusion in these compartments could increase a local SAMHD1-dependent gradient of dNTPs and thereby foster SAMHD1-mediated restriction of HIV-1 reverse transcription (Mitrea et al. 2018; Floris et al. 2021). Careful imaging experiments using endogenously tagged SAMHD1 in presence and absence of HIV-1 would allow to understand if SAMHD1 localization is responsive towards HIV-1 infection.

4.4.3 Re-evaluation of mutagenic data on SAMHD1 dNTPase function is needed to better understand anti-viral restriction

A large body of evidence supports the notion that the dNTPase activity is involved in anti-lentiviral restriction (Majer et al. 2019). First, there is a number of correlative data linking cellular dNTP levels, HIV-1 RT enzyme kinetics and anti-viral restriction in MDMs and $CD4^+$ T cells, as well as in cell cycle synchronized HeLa cells (Diamond et al. 2004; Kennedy et al. 2010; Lahouassa et al. 2012; Schott et al. 2018). Also, the affinity of HIV-1 RT inversely correlates with the SAMHD1 sensitivity of HIV-1 mutants (Lahouassa et al. 2012; Arnold et al. 2015). Second, the SAMHD1-mediated HIV-1 restriction capacity can be altered by manipulation of cellular dNTP levels, *i.e.* by adding exogenous dNs or blocking RNR-mediated dNTP *de novo* synthesis using HU (Baldauf et al. 2012; Lahouassa et al. 2012; Welbourn and Strebel 2016). Finally, SAMHD1 mutants of the catalytic core residues, such as H206, D207 and D311, or truncated SAMHD1 partially or completely lacking the HD domain, as well as mutants of the allosteric binding pockets did not restrict HIV-1 replication when overexpressed in PMA-activated U937 cells (Tab. 18) (Laguette et al. 2011; Lahouassa et al. 2012; White et al. 2013a; Ryoo et al. 2014; Arnold et al. 2015). However, our initial data again seems to contradict these results.

In order to study a large number of SAMHD1 mutants by overexpression, we adopted a SAMHD1 staining and flow cytometry strategy to overcome hurdles, such as non-homogenous and unstable SAMHD1 expression in bulk transduced cell populations (Fig. 29 and 30). This method is superior to the previously published assays to analyze the restriction activity of SAMHD1 mutants because it allows the specific quantification of HIV-1 reporter virus infection in cells expressing SAMHD1 (compare Fig. 29 to 31). Transduction rates or low expression of SAMHD1 mutants have only a minor impact on the outcome of the improved restriction assay (Fig. 31). As an example, this allowed us to reproduce HIV-1 restriction by SAMHD1 T592A mutant overexpression (Fig. 31). Also, SAMHD1 intracellular staining and flow cytometry enables the quantification of SAMHD1 protein expression on the single cell level.

By analyzing a small set of SAMHD1 mutants, for which previous reports showed loss of restriction towards HIV-1, we identified several interesting differences to the published phenotypes (Tab. 18, Fig. 32). When overexpressed in PMA-activated U937 cells, the catalytic core mutants D311A and Y315A were previously reported to not show activity

against HIV-1 (Tab. 18) (Ryoo et al. 2014; Arnold et al. 2015). Y315 is stabilizing the dNTP triphosphate at the γ-phosphate in the substrate pocket, while D311 makes contacts to the α-phosphate and the catalytic Fe^{3+} ion (Fig. 6) (Morris et al. 2020). Both residues are critical for dNTP catalysis, with the D311A mutant not showing any residual dNTPase activity (Fig. 32B) (Goldstone et al. 2011; Beloglazova et al. 2013; Ryoo et al. 2014; Bhattacharya et al. 2016; Bowen et al. 2021). Surprisingly however, in our assay, SAMHD1 D311A and Y315A mutants showed a considerable degree of restrictive activity towards HIV-1, which was comparable to the restrictive SAMHD1 T592A mutant (Fig. 32D).

Furthermore, D137N, a mutant of allosteric site 1, which reportedly is dNTPase deficient due to a lack of allosteric activation, showed residual restrictive activity (Fig. 32D) (Goldstone et al. 2011; Ryoo et al. 2014). Interestingly, this observation was made earlier by several groups and served as an argument in favor of the RNase activity mediating the anti-viral effect of SAMHD1 (Fig. 17) (Ryoo et al. 2014; Choi et al. 2015; Antonucci et al. 2016). Later, the idea of a SAMHD1 RNase activity was strongly questioned and shown to rather be due to impurities in preparations of SAMHD1 for *in vitro* assays (Antonucci et al. 2016; Seamon et al. 2016). Also, in our hands the reportedly RNase-negative Q548A mutant resulted in only a minor loss of restriction, which probably was due to altered expression patterns (Fig. 32C and D) (Ryoo et al. 2014; Choi et al. 2015; Antonucci et al. 2016).

Furthermore, several mutants with a reported loss of dNTPase and anti-viral restriction activity, such as the allosteric site mutant R145Q and mutants of the catalytic Fe^{3+} coordinating residues H167A and H206A, showed a severe loss of expression both in bulk and on single cell level (Fig. 32A and C) (Goldstone et al. 2011; Goncalves et al. 2012). In line with this, we previously observed mislocalization of several poorly expressed mutants, such as the R145Q, the Q548A and the H206A_D207A mutant (Paula Rauch, unpublished). If this is an artifact due to dysfunctional mutant overexpression or an intrinsic property of the specific mutants is an open question. Still, especially mutants of the metal ion coordinating residues have extensively been used as an argument supporting the hypothesis that the dNTPase activity is the central HIV-1 restrictive functional entity of SAMHD1 (Laguette et al. 2011; Lahouassa et al. 2012; White et al. 2013a; Arnold et al. 2015).

Our observation, that the loss of proper expression and potentially aggregation in nuclear compartments might cause failure of anti-viral restriction in transdifferentiated BlaER1 cells, urges for a systematic re-analysis of the catalytic SAMHD1 residues and independent validation of the restrictive phenotype of published SAMHD1 mutants in myeloid cells (Tab. 18) (Morris et al. 2020). Accordingly, in order to answer the question of whether the SAMHD1 dNTPase activity is required for anti-viral restriction, we will need to support the preliminary data in this work by further mutants and biological replicates. Data on dNTPase activity and sub-cellular localization will be essential to form new hypothesis on the relation of SAMHD1 function and anti-viral restriction. Again, CRISPR/Cas9 KI will be critical to validate selected functional mutants of SAMHD1 in an endogenous setting.

Table 18: HIV-1 restriction and dNTPase activity of published SAMHD1 mutants

Mutation	HIV-1 restriction?	dNTPase activity?	References
1-114	No		(Arnold et al. 2015)
1-328	No	No	(White et al. 2013a)
1-575	Yes		(Cribier et al. 2013)
1-583	No		(Arnold et al. 2015)
1-595	No	Yes	(Martinat et al. 2021)
1-597	No	Yes	(Martinat et al. 2021)
1-600	Yes	Yes	(Martinat et al. 2021)
15-626	Yes	Yes	(White et al. 2013a)
34-583	No		(Arnold et al. 2015)
34-626	Yes		(Arnold et al. 2015)
112-582	Yes	Yes	(White et al. 2013a)
112-626	Yes		(White et al. 2013a; White et al. 2013b)
112-626_T592D	No	Yes	(White et al. 2013b)
115-526	Yes		(Arnold et al. 2015)
115-583	Yes	No	(Arnold et al. 2015)
115-626	Yes	Yes	(Arnold et al. 2015)
Δ27-113	Yes		(Arnold et al. 2015)
Δ(27-113)-583	No		(Arnold et al. 2015)
Δ45-110	No	No	(White et al. 2013a)
S6A	Yes		(Welbourn et al. 2013)
S6E	Yes		(Welbourn et al. 2013)
S18A	Yes		(White et al. 2013b)
S18D	Yes		(White et al. 2013b)
T21A	Yes		(Welbourn et al. 2013; White et al. 2013b)
T21D	Yes		(White et al. 2013b)
T21E	Yes		(Welbourn et al. 2013)
T25A	Yes		(White et al. 2013b)
T25E	Yes		(White et al. 2013b)
S33A	Yes		(Welbourn et al. 2013; White et al. 2013b)
S33D	Yes		(White et al. 2013b)

S33E	Yes		(Welbourn et al. 2013)
S93A	No	No	(Hu et al. 2021)
D137N	Yes	No	(Goldstone et al. 2011; Ryoo et al. 2014; Arnold et al. 2015; Choi et al. 2015; Antonucci et al. 2016)
R143C	No		(Arnold et al. 2015)
R145A	No		(Arnold et al. 2015)
R145Q	No	No	(Goldstone et al. 2011; Arnold et al. 2015)
R164A	No	No	(Goldstone et al. 2011; Arnold et al. 2015)
H167A	No	No	(Beloglazova et al. 2013; Arnold et al. 2015)
H206A	No	No	(Beloglazova et al. 2013; Arnold et al. 2015)
H206A_D207A	No	No	(Goldstone et al. 2011; Laguette et al. 2011; Lahouassa et al. 2012; White et al. 2013a; Arnold et al. 2015)
H206N_D207N	No	No	(Welbourn and Strebel 2016)
D207A	No	No	(Beloglazova et al. 2013; Arnold et al. 2015)
D207N	No	No	(Ryoo et al. 2014; Choi et al. 2015)
H233A	No	No	(Arnold et al. 2015; Morris et al. 2020)
D311A	No	No	(Goldstone et al. 2011; Beloglazova et al. 2013; Ryoo et al. 2014; Bhattacharya et al. 2016; Bowen et al. 2021).
K312A	No		(Arnold et al. 2015)
Y315A	No	No	(Beloglazova et al. 2013; Arnold et al. 2015)
C341S	No	Yes	(Wang et al. 2018)
C350S	Yes	Yes	(Wang et al. 2018)
R366C	No	No	(Bowen et al. 2021)
R366H	No	No	(Bowen et al. 2021)
R372D	No		(Arnold et al. 2015)
R451A_L453A	No	No	(St Gelais et al. 2018)
F454W	Yes	Yes	(St Gelais et al. 2018)
K469R	Yes		(Martinat et al. 2021)
K469R_ K622R	Yes	Yes	(Martinat et al. 2021)
E471Q	Yes		(Martinat et al. 2021)
E471Q_D624N	Yes	Yes	(Martinat et al. 2021)
K469R_K595R_K622R	No	Yes	(Martinat et al. 2021)
E471Q_E597Q_D624N	Yes	Yes	(Martinat et al. 2021)
L488A_L489A_V491A	No		(Martinat et al. 2021)
L488A_L489A_ V491A_T592A	No		(Martinat et al. 2021)
C522S	No	Yes	(Wang et al. 2018)
Q548A	No/Yes	Yes	(Beloglazova et al. 2013; Ryoo et al. 2014; Choi et al. 2015; Antonucci et al. 2016)
R566Q	Yes	Yes (red.)	(Monit et al. 2019)
A574L	Yes	Yes (red.)	(Monit et al. 2019)
A574S	Yes (red.)	Yes (red.)	(Monit et al. 2019)
T592A	Yes	Yes	(White et al. 2013b; Welbourn et al. 2013; Arnold et al. 2015; Welbourn and Strebel 2016)
T592A_K595R	Yes		(Martinat et al. 2021)
T592A_Q597Q	No		(Martinat et al. 2021)

T592D	No	Yes	(White et al. 2013b; Ryoo et al. 2014; Arnold et al. 2015)
T592E	No	Yes	(White et al. 2013b; Welbourn et al. 2013; Arnold et al. 2015; Welbourn and Strebel 2016)
T592V	Yes	Yes	(White et al. 2013b)
P593A	Yes	Yes	(White et al. 2013b)
Q594L	Yes	Yes (red.)	(Monit et al. 2019)
Q594N	Yes	Yes	(Martinat et al. 2021)
Q594R	Yes (red.)	Yes (red.)	(Monit et al. 2019)
K595A	No	Yes	(Martinat et al. 2021)
K595R	No	Yes	(Martinat et al. 2021)
K596D	Yes (red.)	Yes (red.)	(Monit et al. 2019)
K596L	Yes	Yes (red.)	(Monit et al. 2019)
K596M	Yes (red.)	Yes (red.)	(Monit et al. 2019)
K596P	Yes	Yes (red.)	(Monit et al. 2019)
K597Q	No	Yes	(Martinat et al. 2021)
K622R	Yes		(Martinat et al. 2021)
D624N	Yes		(Martinat et al. 2021)
1-579-SUMO1	No	Yes	(Martinat et al. 2021)
1-579-SUMO2	Yes	Yes	(Martinat et al. 2021)
1-579_T592A-SUMO2	Yes	Yes	(Martinat et al. 2021)
1-579_T592E-SUMO2	No	Yes	(Martinat et al. 2021)

4.4.4 SAMHD1 regulation is more complex than previously assumed

Several recent lines of evidence suggest that SAMHD1 regulation is more complex than previously anticipated. SAMHD1 is modified by acetylation, SUMOylation, ubiquitination and O-GlcNAcylation (White et al. 2013b; Welbourn et al. 2013; Kim et al. 2019a; Ochoa et al. 2020; Lee et al. 2017; Lamoliatte et al. 2014; Hendriks et al. 2017; Lumpkin et al. 2017; Elia et al. 2015; Hu et al. 2021). Also, SAMHD1 was demonstrated to harbor redox sensitive cysteine residues, which affect both dNTPase and anti-viral activity (Tab. 18) (Mauney et al. 2017; Wang et al. 2018). SAMHD1 acetylation at residue K405 was shown to affect SAMHD1 dNTPase activity *in vitro.* However, the effect on its anti-viral restriction activity is unclear (Lee et al. 2017). O-GlcNAcylation at S93 was proposed to increase SAMHD1 stability and thus HIV-1 and HBV restriction (Hu et al. 2021).

Recently, SAMHD1 SUMOylation at residue K595 was shown to be required for HIV-1 restriction in PMA-activated U937 cells. PMA-activated U937 cells in which SAMHD1 mutants, abrogating SUMOylation at residue K595 and anti-viral restriction, were overexpressed, did not show increased dATP levels. Thus, SUMOylation deficient mutants phenocopy phosphomimetic T592 mutants of SAMHD1 (Martinat et al. 2021). SAMHD1 phosphorylation at residue T592 seems not to affect SAMHD1 SUMOylation at

K595. Both residues can be co-modified (Hendriks et al. 2017; Martinat et al. 2021). However, K595 is part of the ^{592}TPQK^{595} CDK target motif, which is essential for T592 phosphorylation (Cribier et al. 2013; White et al. 2013b; Monit et al. 2019; Martinat et al. 2021). Therefore, it will be interesting to investigate in more detail how T592 phosphorylation and K595 SUMOylation are integrated. Again, our model systems based on transdifferentiated BlaER1 cells and CRISPR/Cas9 KI will be helpful to better define the effect of these PTMs on the anti-viral restriction activity of SAMHD1.

4.4.5 SAMHD1 is differentially phosphorylated at multiple sites

In addition to residue T592, the first studies on SAMHD1 phospho-regulation using mass spectrometry of endogenous and overexpressed SAMHD1, suggested residues S6, S18, S21 T25 and S33 to be phosphorylated. However, mutants of these residues did not affect anti-viral activity (Welbourn et al. 2013; White et al. 2013b). To verify if and how theses residues are modified in a myeloid endogenous setting, such as in THP-1 and transdifferentiated BlaER1 cells, we performed targeted LC-MS/MS (Fig. 33). Indeed, we were able to confirm the modification of several residues in endogenously expressed SAMHD1 (Fig. 43).

At most potential sites, phosphorylation was reduced in myeloid cells, when compared to cycling THP-1 (Fig. 34 and 35D). Surprisingly, pinpoint analysis and quantification revealed a differentially regulated N-terminal phospho-hub in which S33 is upregulated in PMA-activated THP-1 and transdifferentiated BlaER1 cells, whereas two other residues in the n-terminus, T21 and T25, are downregulated (Fig. 35D and E). Even though the N-terminus is largely disordered (Fig. 43), such an anti-regulatory phospho-hub could modulate folding or interactions of the SAMHD1 N-terminus and thereby SAMHD1 function. However, we could not identify differences in the anti-viral restriction potential of combinatory mutants of S33, T21 and T25 (Fig. 38). In addition, combined mutation of S33, T21 and T25 did not affect SAMHD1 T592 phosphorylation, expression or localization (Fig. 36 and 37). This is in line with previous data on the restrictive potential and localization of single residue T21, T25 and S33 mutants (Tab. 18) (Welbourn et al. 2013; White et al. 2013b). Nevertheless, dNTPase activity of these mutants or another functional entity of SAMHD1 could be affected. Also, a detailed

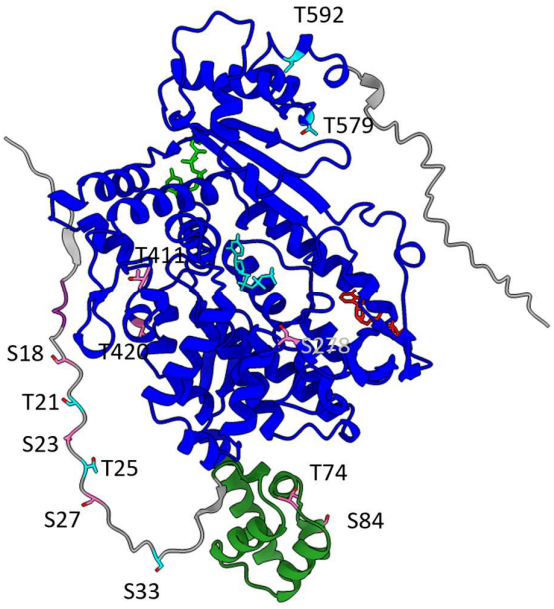

Figure 43: Position of potential SAMHD1 phosphorylation sites.

The position of potential SAMHD1 phosphorylation sites is indicated in light blue and coral for investigated and non-investigated sites respectively. SAMHD1 structure model was used as predicted by AlphaFold (AF-Q9Y3Z3-F1-model_v2) (Jumper et al. 2022).

pinpoint analysis, suggested that even more combinations of differentially regulate residues at the n-terminus are possible (Fig. 35E). A careful mutagenic analysis of these sites will be required to understand the contribution of the N-terminal phospho-hub to SAMHD1 regulation.

Apart from the potential N-terminal phospho-sites, mass spectrometric data from our group on SAMHD1 overexpressed in insect Sf9 cells, revealed several further phosphorylation site candidates such as T74, S102, and T579 (Kerstin Schott, unpublished). Indeed, T74 and T579 seemed phosphorylated. The level of pT74 was similar in all cell types. In contrast pT579 was downregulated after PMA-activation in THP-1 cells and low in transdifferentiated BlaER1 cells, reminiscent of T592 phospho-regulation (Fig. 35A and B). However, we did not detect pT579-pT592 double phosphorylated peptides (Fig. 34). Also, single site phospho-mutants did not affect the phospho-status of the other residue reciprocally, indicating that both phosphorylation events are independent (Fig. 34).

When testing combinations or single residue mutants of the T579 and T592 site, we observed a loss of HIV-1 restriction of the overexpressed T579E mutant, similar to the phenotype of T592E (Fig. 40). This could mean that T579 phosphorylation acts as a redundant switch to T592 phosphorylation. Surprisingly however, all T579 and T592

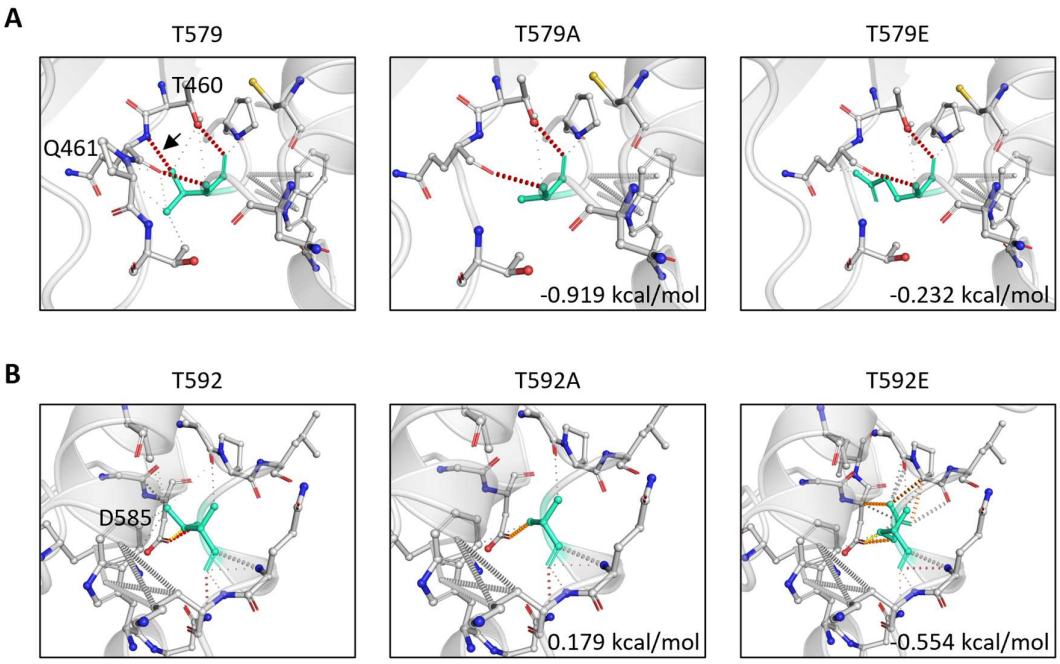

Figure 44 : Prediction of structural consequence of T579 and T592 mutations for protein stability.
Structure and interactions of the **(A)** T579 and **(B)** T592 sites and respective T to A or T to E mutants are shown as modeled by DynaMut (Rodrigues et al. 2018) based on the SAMHD1 AlphaFold model (AF-Q9Y3Z3-F1-model_v2) (Jumper et al. 2022). T579 and T592 are highlighted in light blue. Hydrogen Bonds (red), weak hydrogen bonds (orange) and ionic interactions (yellow) of the respective residue are depicted. For the mutants, predicted changes in folding free energy is shown as a measure for loss (< 0) or gain (> 0) of protein folding stability (Rodrigues et al. 2018). **(A)** The arrow indicates a hydrogen bond lost in T579A and T579E mutants.

double mutants, independent of the combination of phosphomimetic and -ablative modifications, led to a complete loss of restriction (Fig. 40). This phenotype might be more reminiscent of an artefact due to the introduction of mutants at the T579 site. The T579 residue stabilizes the folding of the structured C-terminal loops through formation of multiple hydrogen bonds (Fig. 43 and 44A). Both T579A and T579E mutants would lead to a loss of hydrogen bonds in this area and are predicted to increase the flexibility of the C-terminus (Fig. 44A) (Rodrigues et al. 2018). Also, mutants of T592 could have a destabilizing phenotype (Fig. 44B) (Rodrigues et al. 2018). Therefore, combined mutation of both residues independent of the phosphomimetic or -ablative nature of the mutations, could lead to a drastic re- or de-structuration of the C-terminus (Fig. 43). As both residues are not commonly co-modified in cycling THP-1 cells and overall

abundancy of pT579 is low (Fig. 34), this phenomenon is not likely to be relevant for anti-viral restriction in cells. However, this finding could indicate that a structured C-terminus is important for SAMHD1 regulation. Interestingly, even though the available AlphaFold structure from the Protein Structure Database indicates a disordered extreme C-terminus (Fig. 6) (Jumper et al. 2021; Varadi et al. 2022), all models extracted from *de novo* predictions of SAMHD1 structure using AlphaFold2 (Mirdita et al. 2022) or RoseTTAfold (Baek et al. 2021) showed a C-terminus, which at least partially was folded into α-helices (data not shown). A structured c-terminus, for which folding is affected by PTMs of C-terminal residues such as pT592, pT579 or K595 SUMOylation could modulate intra- or intermolecular interactions. For example, formation of an active tetramer or the interaction with other proteins, mediating, supporting or licensing for anti-viral restriction could be affected. We believe that the myeloid models and genetic tools we introduced in this work might be essential to understand how T592 phosphorylation can dominate the anti-viral function of SAMHD1 and how additional phosphorylation sites contribute to phospho-regulation.

4.5 Conclusion

The regulation of SAMHD1-mediated HIV-1 restriction is clearly governed by T592 phosphorylation. However, the connection to enzymatic functions of SAMHD1 is still unclear. Using a novel genetic toolkit and physiologic myeloid models we were able to confirm and define this discrepancy. A better and more integrated concept of SAMHD1 regulation in relevant HIV-1 target cells, will improve our understanding of how SAMHD1 inhibits HIV-1 replication and which conditions license SAMHD1 anti-viral capacity. In future, this might inspire therapeutic strategies, which could modulate anti-viral immunity or limit HIV-1 replication. Also, vaccination strategies would profit from a better understanding of SAMHD1 regulation. Again, physiologic and reliable model systems will be crucial to test and validate these approaches.

IV. SUMMARY

Despite enormous efforts to develop curative treatments or effective vaccination strategies against human immunodeficiency virus 1 (HIV-1), the virus still is a substantial global health thread and a social and economic burden. Understanding host-HIV-1 interactions will be essential to advance treatment options. Numerous pro- and anti-viral host factors are known to date, the latter are referred to as restriction factors.

Sterile α motif and HD domain-containing protein 1 (SAMHD1) is a potent restriction factor for HIV-1, active in myeloid and resting $CD4^+$ T cells, which both are important HIV-1 target cells. To complete its obligate reverse transcription step, HIV-1 requires deoxyribonucleoside triphosphate (dNTPs) as a substrate for DNA synthesis. SAMHD1 is a dNTP triphosphate triphosphohydrolase (dNTPase). Therefore, SAMHD1 was proposed to limit cellular dNTP levels, which is supported by correlative data.

The anti-viral activity of SAMHD1 is regulated by dephosphorylation of the residue T592. However, the impact of T592 phosphorylation on its dNTPase activity is still under debate. This might be in part due to limitations in the myeloid models and genetic tools, which are available to genetically study the relationship between SAMHD1 T592 phosphorylation, anti-viral restriction and enzymatic functions of SAMHD1. Also, additional cellular functions of SAMHD1, as well as additional post-translational modifications could impact anti-viral restriction.

To overcome technical limitations and the lack of knowledge, we used BlaER1 cells as a novel human macrophage transdifferentiation model combined with CRISPR/Cas9 knock-in (KI) to study SAMHD1 mutations in a physiological context. Transdifferentiated BlaER1 cells, resembling primary human macrophages, harbor active dephosphorylated SAMHD1, strongly inhibiting HIV-1 reporter virus infection. Co-delivery of Vpx or CRISPR/Cas9-mediated SAMHD1 knock-out relieves the block to HIV-1 replication.

We developed a pipeline to introduce specific mutations into the genomic *SAMHD1* locus via CRISPR/Cas9-mediated homologous recombination and were able to generate homozygous phosphomimetic SAMHD1 T592E and phosphoablative SAMHD1 T592A mutants. Homozygous T592E mutation, but not T592A, leads to loss of HIV-1 restriction, confirming the role of T592 dephosphorylation in the regulation of anti-viral activity. In stark contrast however, T592E KI cells retain wild type dNTP levels and dNTP pool

composition. Thus, the role of the T592 phospho-site for anti-viral restriction was confirmed in an endogenous physiological context. Importantly, loss of restriction in T592E mutant cells does not correlate with increased dNTP levels, indicating that the regulation of anti-viral and dNTPase activity of SAMHD1 might be uncoupled.

To further understand if SAMHD1 dNTPase activity contributes to HIV-1 restriction, we developed an advanced overexpression system to reliably screen mutants of SAMHD1 for their restrictive potential in macrophage-like BlaER1 cells. Indeed, we could identify mutants, which lack dNTPase activity, but seemed to maintain their restrictive potential. In line with this, we were unable to show an additional T592 phospho-regulation independent SAMHD1 function.

SAMHD1 was recently proposed to play a role in the resolution of R-loops, tertiary DNA:RNA structures, which occur at sites of transcription-replication conflicts. As a surrogate model for the role of SAMHD1 in R-loop biology, we tested the effect of SAMHD1 depletion on CRISPR/Cas9 induced R-loops. We did not detect alterations of CRISPR/Cas9 KO and KI efficiency in absence of SAMHD1. Nevertheless, modulation of R-loop stability might still contribute to cellular and anti-viral functions of SAMHD1.

The lack of experimental correlation between SAMHD1 dNTPase activity, HIV-1 restriction and T592 phospho-status might also be due to an incomplete understanding of the complexity of SAMHD1 regulation. To obtain a more sophisticated image of SAMHD1 phosphorylation sites, we performed a targeted mass spectrometric analysis of endogenous SAMHD1 phosphopeptides in restrictive versus non-restrictive myeloid cells. We were able to identify several differentially phosphorylated residues in addition to T592. The N-terminal phospho-hub consistent of T21, T25 and S33 seemed not to influence SAMHD1 localization, expression, T592 phosphorylation or HIV-1 replication. In contrast, T579 emerged as a potential phosphorylation site regulating HIV-1 restriction. However, mutants of T579 might affect SAMHD1 stability and further experiments will be necessary to confirm the role of pT579.

We think that BlaER1 as a novel cell model for SAMHD1-mediated HIV-1 restriction and CRISPR/Cas9-mediated KI, will be helpful to unravel the interplay between SAMHD1-mediated HIV-1 restriction, SAMHD1 post-translational regulation and cellular functions of SAMHD1. This knowledge might be essential for the future development of curative or preventive strategies against HIV-1.

V. ZUSAMMENFASSUNG

Trotz großer Anstrengungen zur Entwicklung von Therapien und Impfstrategien gegen das humane Immundefizienz Virus 1 (HIV-1) stellt das Virus nach wie vor eine erhebliche Bedrohung für die globale Gesundheit dar. Um Behandlungen zu verbessern ist ein tieferes Verständnis der Wechselwirkungen zwischen Wirt und HIV-1 entscheidend. Es sind zahlreiche pro- und antivirale Wirtsfaktoren bekannt, wobei letztere als Restriktionsfaktoren bezeichnet werden. Sterile α motif and HD domain-containing protein 1 (SAMHD1) ist ein HIV-1 Restriktionsfaktor, der in myeloiden und ruhenden $CD4^+$ T-Zellen aktiv ist. Während HIV-1 Desoxyribonukleosidtriphosphate (dNTPs) für die DNA-Synthese benötigt, begrenzt SAMHD1 mit seiner dNTP-Triphosphohydrolase (dNTPase) Aktivität den zellulären dNTP-Spiegel.

Die antivirale Aktivität von SAMHD1 wird durch Dephosphorylierung des Rests T592 reguliert. Die Auswirkungen der T592-Phosphorylierung auf die dNTPase-Aktivität sind jedoch unklar. Es stehen nur wenige myeloide Modelle und genetische Instrumente zur Verfügung, um die Beziehung zwischen der T592-Phosphorylierung von SAMHD1, der antiviralen Restriktion und den enzymatischen Funktionen von SAMHD1 zu untersuchen. Außerdem könnten zusätzliche zelluläre Funktionen von SAMHD1, sowie zusätzliche post-translationale Modifikationen die antivirale Restriktion beeinflussen. Um die technischen Einschränkungen und diese Wissenslücken zu überwinden, haben wir BlaER1-Zellen als neuartiges menschliches Makrophagen-Modell in Kombination mit CRISPR/Cas9 Knock-in (KI) verwendet, um SAMHD1-Mutationen in einem physiologischen Kontext zu untersuchen. Transdifferenzierte BlaER1-Zellen ähneln primären menschlichen Makrophagen und exprimieren aktives dephosphoryliertes SAMHD1, dass die Infektion mit HIV-1-Reporterviren blockiert. Vpx oder CRISPR/Cas9 Knock-out (KO) von SAMHD1 erlaubt wiederum die HIV-1 Replikation.

Mithilfe einer von uns entwickelten Pipeline zur CRISPR/Cas9-vermittelter homologen Rekombination, konnten wir homozygote phosphomimetische SAMHD1 T592E- und phosphoablative SAMHD1 T592A KI-Mutationen in den genomischen SAMHD1 Lokus einbringen. Die homozygote T592E Mutation, nicht aber T592A, führt zum Verlust der HIV-1-Restriktion, was die Rolle der Dephosphorylierung von T592 bei der Regulierung der antiviralen Aktivität bestätigt. In Gegensatz dazu ist der dNTP-Spiegel und die

Zusammensetzung des dNTP-Pools in den Zellen mit einer T592E KI-Mutation jedoch unbeeinflusst. Dies bestätigt die Rolle der T592-Phospho-Stelle für die antivirale Restriktion in einem endogenen physiologischen Kontext. Da kein Effekt auf die dNTP-Spiegel festgestellt wurde, deutet das darauf hin, dass die Regulierung der antiviralen Aktivität und die der dNTPase von SAMHD1 möglicherweise entkoppelt sind.

Um herauszufinden, ob die dNTPase-Aktivität von SAMHD1 zur HIV-1-Restriktion beiträgt, haben wir ein Überexpressionssystem weiterentwickelt, mit dem wir SAMHD1-Mutanten in BlaER1-Makrophagen zuverlässig auf ihr restriktives Potenzial untersuchen können. Dadurch konnten wir dNTPase-defiziente Mutanten identifizieren, die HIV-1 weiterhin inhibieren. Ebenso konnten wir keine von der T592-Phosphoregulation unabhängige SAMHD1-Funktion nachweisen.

Neue Ergebnisse deuten darauf hin, dass SAMHD1 R-Loops, tertiären DNA:RNA-Strukturen an Transkriptions-Replikationskonflikten, beeinflusst. Als Modell hierfür, haben wir die Wirkung einer SAMHD1-Depletion auf CRISPR/Cas9-induzierte R-Loops getestet. Wir konnten keine Veränderungen der Effizienz von CRISPR/Cas9 KO und KI feststellen, was aber nicht ausschließt, dass SAMHD1 endogene R-Loops moduliert.

Die fehlende experimentelle Korrelation zwischen der dNTPase-Aktivität von SAMHD1, antiviraler Restriktion und T592-Phospho-Status könnte auch auf ein mangelndes Verständnis der Komplexität der Regulation von SAMHD1 zurückzuführen sein. Um ein differenzierteres Bild der Phosphorylierungsstellen zu erhalten, haben wir eine massenspektrometrische Analyse der endogenen SAMHD1-Phosphopeptide in restriktiven und nicht restriktiven myeloiden Zellen durchgeführt. Neben T592 konnten wir eine Reihe von phosphorylierten Resten identifizieren. T21, T25 und S33 schienen keinen Einfluss auf die SAMHD1-Lokalisierung, Expression, T592-Phosphorylierung oder die Replikation von HIV-1 zu haben. Im Gegensatz dazu erwies sich T579 als eine potenzielle Phosphorylierungsstelle, die die HIV-1-Restriktion regulieren könnte. Daher sind weitere Experimente erforderlich, um die Rolle von pT579 zu bestätigen.

Wir glauben, dass die hier vorgestellten Zellmodelle und die genetische Methodik hilfreich sein werden, um das Zusammenspiel zwischen HIV-1-Restriktion, post-translationaler Regulierung und zellulären Funktionen von SAMHD1 zu entschlüsseln. Dieses Wissen könnte für die künftige Entwicklung kurativer oder präventiver Strategien gegen HIV-1 von entscheidender Bedeutung sein.

VI. REFERENCES

Ablasser, Andrea; Hur, Sun (2020): Regulation of cGAS- and RLR-mediated immunity to nucleic acids. In *Nature immunology* 21 (1), pp. 17–29. DOI: 10.1038/s41590-019-0556-1.

Accola, M. A.; Bukovsky, A. A.; Jones, M. S.; Göttlinger, H. G. (1999): A conserved dileucine-containing motif in p6(gag) governs the particle association of Vpx and Vpr of simian immunodeficiency viruses SIV(mac) and SIV(agm). In *J Virol* 73 (12), pp. 9992–9999.

Ackermann, Mania; Kuhn, Alexandra; Kunkiel, Jessica; Merkert, Sylvia; Martin, Ulrich; Moritz, Thomas; Lachmann, Nico (2017): Ex vivo Generation of Genetically Modified Macrophages from Human Induced Pluripotent Stem Cells. In *Transfusion medicine and hemotherapy : offizielles Organ der Deutschen Gesellschaft fur Transfusionsmedizin und Immunhamatologie* 44 (3), pp. 135–142. DOI: 10.1159/000477129.

Ahmad, Iqbal; Li, Sunan; Li, Rongrong; Chai, Qingqing; Zhang, Lixin; Wang, Bin et al. (2019): The retroviral accessory proteins S2, Nef, and glycoMA use similar mechanisms for antagonizing the host restriction factor SERINC5. In *Journal of Biological Chemistry* 294 (17), pp. 7013–7024. DOI: 10.1074/jbc.RA119.007662.

Ahn, Jinwoo; Hao, Caili; Yan, Junpeng; DeLucia, Maria; Mehrens, Jennifer; Wang, Chuanping et al. (2012): HIV/simian immunodeficiency virus (SIV) accessory virulence factor Vpx loads the host cell restriction factor SAMHD1 onto the E3 ubiquitin ligase complex CRL4DCAF1. In *The Journal of biological chemistry* 287 (15), pp. 12550–12558. DOI: 10.1074/jbc.M112.340711.

Akimova, Ekaterina; Gassner, Franz Josef; Schubert, Maria; Rebhandl, Stefan; Arzt, Claudia; Rauscher, Stefanie et al. (2021): SAMHD1 restrains aberrant nucleotide insertions at repair junctions generated by DNA end joining. In *Nucleic acids research* 49 (5), pp. 2598–2608. DOI: 10.1093/nar/gkab051.

Akiyama, Hisashi; Miller, Caitlin M.; Ettinger, Chelsea R.; Belkina, Anna C.; Snyder-Cappione, Jennifer E.; Gummuluru, Suryaram (2018): HIV-1 intron-containing RNA expression induces innate immune activation and T cell dysfunction. In *Nature communications* 9 (1), p. 3450. DOI: 10.1038/s41467-018-05899-7.

Albanese, Manuel; Ruhle, Adrian; Mittermaier, Jennifer; Mejías-Pérez, Ernesto; Gapp, Madeleine; Linder, Andreas et al. (2022): Rapid, efficient and activation-neutral gene editing of polyclonal primary human resting CD4+ T cells allows complex functional analyses. In *Nature methods* 19 (1), pp. 81–89. DOI: 10.1038/s41592-021-01328-8.

Amie, Sarah M.; Bambara, Robert A.; Kim, Baek (2013): GTP is the primary activator of the anti-HIV restriction factor SAMHD1. In *The Journal of biological chemistry* 288 (35), pp. 25001–25006. DOI: 10.1074/jbc.C113.493619.

Antonucci, Jenna M.; St Gelais, Corine; Silva, Suresh de; Yount, Jacob S.; Tang, Chenxiang; Ji, Xiaoyun et al. (2016): SAMHD1-mediated HIV-1 restriction in cells does not involve ribonuclease activity. In *Nature medicine* 22 (10), pp. 1072–1074. DOI: 10.1038/nm.4163.

Anzalone, Andrew V.; Randolph, Peyton B.; Davis, Jessie R.; Sousa, Alexander A.; Koblan, Luke W.; Levy, Jonathan M. et al. (2019): Search-and-replace genome editing without double-strand breaks or donor DNA. In *Nature*. DOI: 10.1038/s41586-019-1711-4.

Apolonia, Luis; Schulz, Reiner; Curk, Tomaž; Rocha, Paula; Swanson, Chad M.; Schaller, Torsten et al. (2015): Promiscuous RNA binding ensures effective encapsidation of APOBEC3 proteins by HIV-1. In *PLoS Pathogens* 11 (1), e1004609. DOI: 10.1371/journal.ppat.1004609.

Aravind, L.; Koonin, Eugene V. (1998): The HD domain defines a new superfamily of metal-dependent phosphohydrolases. In *Trends in biochemical sciences* 23 (12), pp. 469–472. DOI: 10.1016/s0968-0004(98)01293-6.

Arhel, Nathalie J.; Souquere-Besse, Sylvie; Munier, Sandie; Souque, Philippe; Guadagnini, Stéphanie; Rutherford, Sandra et al. (2007): HIV-1 DNA Flap formation promotes uncoating of the pre-integration complex at the nuclear pore. In *The EMBO journal* 26 (12), pp. 3025–3037. DOI: 10.1038/sj.emboj.7601740.

Arnold, Laurence H.; Groom, Harriet C. T.; Kunzelmann, Simone; Schwefel, David; Caswell, Sarah J.; Ordonez, Paula et al. (2015): Phospho-dependent Regulation of SAMHD1 Oligomerisation Couples Catalysis and Restriction. In *PLoS Pathogens* 11 (10), e1005194. DOI: 10.1371/journal.ppat.1005194.

Avellino, Roberto; Delwel, Ruud (2017): Expression and regulation of C/EBPα in normal myelopoiesis and in malignant transformation. In *Blood* 129 (15), pp. 2083–2091. DOI: 10.1182/blood-2016-09-687822.

Ayinde, Diana; Bruel, Timothée; Cardinaud, Sylvain; Porrot, Françoise; Prado, Julia G.; Moris, Arnaud; Schwartz, Olivier (2015): SAMHD1 Limits HIV-1 Antigen Presentation by Monocyte-Derived Dendritic Cells. In *Journal of Virology* 89 (14), pp. 6994–7006. DOI: 10.1128/JVI.00069-15.

Badia, Roger; Pujantell, Maria; Riveira-Muñoz, Eva; Puig, Teresa; Torres-Torronteras, Javier; Martí, Ramón et al. (2016): The G1/S Specific Cyclin D2 Is a Regulator of HIV-1 Restriction in Non-proliferating Cells. In *PLoS Pathogens* 12 (8), e1005829. DOI: 10.1371/journal.ppat.1005829.

Baek, Minkyung; DiMaio, Frank; Anishchenko, Ivan; Dauparas, Justas; Ovchinnikov, Sergey; Lee, Gyu Rie et al. (2021): Accurate prediction of protein structures and interactions using a three-track neural network. In *Science (New York, N.Y.)* 373 (6557), pp. 871–876. DOI: 10.1126/science.abj8754.

Baldauf, Hanna-Mari; Pan, Xiaoyu; Erikson, Elina; Schmidt, Sarah; Daddacha, Waaqo; Burggraf, Manja et al. (2012): SAMHD1 restricts HIV-1 infection in resting CD4(+) T cells. In *Nature medicine* 18 (11), pp. 1682–1687. DOI: 10.1038/nm.2964.

Barré-Sinoussi, F.; Chermann, J. C.; Rey, F.; Nugeyre, M. T.; Chamaret, S.; Gruest, J. et al. (1983): Isolation of a T-lymphotropic retrovirus from a patient at risk for acquired immune deficiency syndrome (AIDS). In *Science (New York, N.Y.)* 220 (4599), pp. 868–871. DOI: 10.1126/science.6189183.

Barrett, BradleyS; Nguyen, David H.; Xu, Joella; Guo, Kejun; Shetty, Shravida; Jones, Sean T. et al. (2022): SAMHD1 Promotes the Antiretroviral Adaptive Immune Response in

Mice Exposed to Lipopolysaccharide. In *Journal of immunology (Baltimore, Md. : 1950)* 208 (2), pp. 444–453. DOI: 10.4049/jimmunol.2001389.

Bartok, Eva; Hartmann, Gunther (2020): Immune Sensing Mechanisms that Discriminate Self from Altered Self and Foreign Nucleic Acids. In *Immunity* 53 (1), pp. 54–77. DOI: 10.1016/j.immuni.2020.06.014.

Basmaciogullari, Stéphane; Pizzato, Massimo (2014): The activity of Nef on HIV-1 infectivity. In *Front Microbiol* 5, p. 232. DOI: 10.3389/fmicb.2014.00232.

Batalis, Stephanie; Rogers, LeAnn C.; Hemphill, Wayne O.; Mauney, Christopher H.; Ornelles, David A.; Hollis, Thomas (2021): SAMHD1 Phosphorylation at T592 Regulates Cellular Localization and S-phase Progression. In *Frontiers in molecular biosciences* 8, p. 724870. DOI: 10.3389/fmolb.2021.724870.

Beck, Juergen (2007): Hepatitis B virus replication. In *WJG* 13 (1), p. 48. DOI: 10.3748/wjg.v13.i1.48.

Bedwell, Gregory J.; Engelman, Alan N. (2021): You can keep your coat on. In *eLife* 10. DOI: 10.7554/eLife.69887.

Bejarano, David Alejandro; Peng, Ke; Laketa, Vibor; Börner, Kathleen; Jost, K. Laurence; Lucic, Bojana et al. (2019): HIV-1 nuclear import in macrophages is regulated by CPSF6-capsid interactions at the nuclear pore complex. In *eLife* 8. DOI: 10.7554/eLife.41800.

Bejarano, David Alejandro; Puertas, Maria C.; Börner, Kathleen; Martinez-Picado, Javier; Müller, Barbara; Kräusslich, Hans-Georg (2018): Detailed Characterization of Early HIV-1 Replication Dynamics in Primary Human Macrophages. In *Viruses* 10 (11). DOI: 10.3390/v10110620.

Beloglazova, Natalia; Flick, Robert; Tchigvintsev, Anatoli; Brown, Greg; Popovic, Ana; Nocek, Boguslaw; Yakunin, Alexander F. (2013): Nuclease activity of the human SAMHD1 protein implicated in the Aicardi-Goutieres syndrome and HIV-1 restriction. In *The Journal of biological chemistry* 288 (12), pp. 8101–8110. DOI: 10.1074/jbc.M112.431148.

Berg, Randi K.; Melchjorsen, Jesper; Rintahaka, Johanna; Diget, Elisabeth; Søby, Stine; Horan, Kristy A. et al. (2012): Genomic HIV RNA induces innate immune responses through RIG-I-dependent sensing of secondary-structured RNA. In *PLOS ONE* 7 (1), e29291. DOI: 10.1371/journal.pone.0029291.

Berger, André; Sommer, Andreas F. R.; Zwarg, Jenny; Hamdorf, Matthias; Welzel, Karin; Esly, Nicole et al. (2011): SAMHD1-deficient CD14+ cells from individuals with Aicardi-Goutières syndrome are highly susceptible to HIV-1 infection. In *PLoS Pathogens* 7 (12), e1002425. DOI: 10.1371/journal.ppat.1002425.

Berger, Gregory; Lawrence, Madeleine; Hué, Stephane; Neil, Stuart J. D. (2015): G2/M cell cycle arrest correlates with primate lentiviral Vpr interaction with the SLX4 complex. In *Journal of Virology* 89 (1), pp. 230–240. DOI: 10.1128/JVI.02307-14.

Bermejo, Mercedes; López-Huertas, María Rosa; García-Pérez, Javier; Climent, Núria; Descours, Benjamin; Ambrosioni, Juan et al. (2016): Dasatinib inhibits HIV-1 replication through the interference of SAMHD1 phosphorylation in CD4+ T cells. In *Biochemical pharmacology* 106, pp. 30–45. DOI: 10.1016/j.bcp.2016.02.002.

Bertram, Kirstie M.; Botting, Rachel A.; Baharlou, Heeva; Rhodes, Jake W.; Rana, Hafsa; Graham, J. Dinny et al. (2019): Identification of HIV transmitting CD11c+ human epidermal dendritic cells. In *Nature communications* 10 (1), p. 2759. DOI: 10.1038/s41467-019-10697-w.

Bhattacharya, Akash; Wang, Zhonghua; White, Tommy; Buffone, Cindy; Nguyen, Laura A.; Shepard, Caitlin N. et al. (2016): Effects of T592 phosphomimetic mutations on tetramer stability and dNTPase activity of SAMHD1 can not explain the retroviral restriction defect. In *Scientific reports* 6, p. 31353. DOI: 10.1038/srep31353.

Bogerd, Hal P.; Cullen, Bryan R. (2008): Single-stranded RNA facilitates nucleocapsid: APOBEC3G complex formation. In *RNA (New York, N.Y.)* 14 (6), pp. 1228–1236. DOI: 10.1261/rna.964708.

Boneh, Avihu; Mandla, Suzan; Tenenhouse, Harriet S. (1989): Phorbol myristate acetate activates protein kinase C, stimulates the phosphorylation of endogenous proteins and inhibits phosphate transport in mouse renal tubules. In *Biochimica et Biophysica Acta (BBA) - Molecular Cell Research* 1012 (3), pp. 308–316. DOI: 10.1016/0167-4889(89)90113-4.

Bonifati, Serena; Daly, Michele B.; St Gelais, Corine; Kim, Sun Hee; Hollenbaugh, Joseph A.; Shepard, Caitlin et al. (2016): SAMHD1 controls cell cycle status, apoptosis and HIV-1 infection in monocytic THP-1 cells. In *Virology* 495, pp. 92–100. DOI: 10.1016/j.virol.2016.05.002.

Bowen, Nicole E.; Temple, Joshua; Shepard, Caitlin; Oo, Adrian; Arizaga, Fidel; Kapoor-Vazirani, Priya et al. (2021): Structural and functional characterization explains loss of dNTPase activity of the cancer-specific R366C/H mutant SAMHD1 proteins. In *Journal of Biological Chemistry* 297 (4), p. 101170. DOI: 10.1016/j.jbc.2021.101170.

Brandariz-Nuñez, Alberto; Valle-Casuso, Jose Carlos; White, Tommy E.; Laguette, Nadine; Benkirane, Monsef; Brojatsch, Jurgen; Diaz-Griffero, Felipe (2012): Role of SAMHD1 nuclear localization in restriction of HIV-1 and SIVmac. In *Retrovirology* 9, p. 49. DOI: 10.1186/1742-4690-9-49.

Branon, Tess C.; Bosch, Justin A.; Sanchez, Ariana D.; Udeshi, Namrata D.; Svinkina, Tanya; Carr, Steven A. et al. (2018): Efficient proximity labeling in living cells and organisms with TurboID. In *Nature biotechnology* 36 (9), pp. 880–887. DOI: 10.1038/nbt.4201.

Brass, Abraham L.; Dykxhoorn, Derek M.; Benita, Yair; Yan, Nan; Engelman, Alan; Xavier, Ramnik J. et al. (2008): Identification of host proteins required for HIV infection through a functional genomic screen. In *Science (New York, N.Y.)* 319 (5865), pp. 921–926. DOI: 10.1126/science.1152725.

Braun, Elisabeth; Hotter, Dominik; Koepke, Lennart; Zech, Fabian; Groß, Rüdiger; Sparrer, Konstantin M. J. et al. (2019): Guanylate-Binding Proteins 2 and 5 Exert Broad Antiviral Activity by Inhibiting Furin-Mediated Processing of Viral Envelope Proteins. In *Cell Rep* 27 (7), 2092-2104.e10. DOI: 10.1016/j.celrep.2019.04.063.

Brinkman, Eva K.; Kousholt, Arne N.; Harmsen, Tim; Leemans, Christ; Chen, Tao; Jonkers, Jos; van Steensel, Bas (2018): Easy quantification of template-directed CRISPR/Cas9 editing. In *Nucleic acids research* 46 (10), e58. DOI: 10.1093/nar/gky164.

Buckland, Robert J.; Watt, Danielle L.; Chittoor, Balasubramanyam; Nilsson, Anna Karin; Kunkel, Thomas A.; Chabes, Andrei (2014): Increased and imbalanced dNTP pools symmetrically promote both leading and lagging strand replication infidelity. In *PLoS genetics* 10 (12), e1004846. DOI: 10.1371/journal.pgen.1004846.

Buffone, Cindy; Martinez-Lopez, Alicia; Fricke, Thomas; Opp, Silvana; Severgnini, Marco; Cifola, Ingrid et al. (2018): Nup153 Unlocks the Nuclear Pore Complex for HIV-1 Nuclear Translocation in Nondividing Cells. In *J Virol* 92 (19). DOI: 10.1128/JVI.00648-18.

Bukhari, Hassan; Müller, Thorsten (2019): Endogenous Fluorescence Tagging by CRISPR. In *Trends in Cell Biology* 29 (11), pp. 912–928. DOI: 10.1016/j.tcb.2019.08.004.

Burdick, Ryan C.; Li, Chenglei; Munshi, MohamedHusen; Rawson, Jonathan M. O.; Nagashima, Kunio; Hu, Wei-Shau; Pathak, Vinay K. (2020): HIV-1 uncoats in the nucleus near sites of integration. In *Proceedings of the National Academy of Sciences of the United States of America* 117 (10), pp. 5486–5493. DOI: 10.1073/pnas.1920631117.

Businger, Ramona; Deutschmann, Janina; Gruska, Iris; Milbradt, Jens; Wiebusch, Lüder; Gramberg, Thomas; Schindler, Michael (2019): Human cytomegalovirus overcomes SAMHD1 restriction in macrophages via pUL97. In *Nature Microbiology* 4 (12), pp. 2260–2272. DOI: 10.1038/s41564-019-0557-8.

Bussmann, Lars H.; Schubert, Alexis; Vu Manh, Thien Phong; Andres, Luisa de; Desbordes, Sabrina C.; Parra, Maribel et al. (2009): A robust and highly efficient immune cell reprogramming system. In *Cell Stem Cell* 5 (5), pp. 554–566. DOI: 10.1016/j.stem.2009.10.004.

Cameron, J. M.; McDougall, I.; Marsden, H. S.; Preston, V. G.; Ryan, D. M.; Subak-Sharpe, J. H. (1988): Ribonucleotide reductase encoded by herpes simplex virus is a determinant of the pathogenicity of the virus in mice and a valid antiviral target. In *J Gen Virol* 69 (Pt 10), pp. 2607–2612. DOI: 10.1099/0022-1317-69-10-2607.

Campbell, Edward M.; Hope, Thomas J. (2015): HIV-1 capsid. The multifaceted key player in HIV-1 infection. In *Nature reviews. Microbiology* 13 (8), pp. 471–483. DOI: 10.1038/nrmicro3503.

Cano-Ortiz, Lucía; Luedde, Tom; Münk, Carsten (2022): HIV-1 restriction by SERINC5. In *Med Microbiol Immunol*, pp. 1–8. DOI: 10.1007/s00430-022-00732-x.

Castagna, M.; Takai, Y.; Kaibuchi, K.; Sano, K.; Kikkawa, U.; Nishizuka, Y. (1982): Direct activation of calcium-activated, phospholipid-dependent protein kinase by tumor-promoting phorbol esters. In *Journal of Biological Chemistry* 257 (13), pp. 7847–7851. DOI: 10.1016/S0021-9258(18)34459-4.

Chabes, A.; Thelander, L. (2000): Controlled protein degradation regulates ribonucleotide reductase activity in proliferating mammalian cells during the normal cell cycle and in response to DNA damage and replication blocks. In *Journal of Biological Chemistry* 275 (23), pp. 17747–17753. DOI: 10.1074/jbc.M000799200.

Chabes, Andrei; Stillman, Bruce (2007): Constitutively high dNTP concentration inhibits cell cycle progression and the DNA damage checkpoint in yeast Saccharomyces cerevisiae. In *Proceedings of the National Academy of Sciences* 104 (4), pp. 1183–1188. DOI: 10.1073/pnas.0610585104.

Chai, Qingqing; Li, Sunan; Collins, Morgan K.; Li, Rongrong; Ahmad, Iqbal; Johnson, Silas F. et al. (2021): HIV-1 Nef interacts with the cyclin K/CDK13 complex to antagonize SERINC5 for optimal viral infectivity. In *Cell Rep* 36 (6), p. 109514. DOI: 10.1016/j.celrep.2021.109514.

Chang, Emily Yun-Chia; Tsai, Shuhe; Aristizabal, Maria J.; Wells, James P.; Coulombe, Yan; Busatto, Franciele F. et al. (2019): MRE11-RAD50-NBS1 promotes Fanconi Anemia R-loop suppression at transcription-replication conflicts. In *Nature communications* 10 (1), p. 4265. DOI: 10.1038/s41467-019-12271-w.

Chanput, Wasaporn; Mes, Jurriaan; Vreeburg, Robert A. M.; Savelkoul, Huub F. J.; Wichers, Harry J. (2010): Transcription profiles of LPS-stimulated THP-1 monocytes and macrophages: a tool to study inflammation modulating effects of food-derived compounds. In *Food & function* 1 (3), pp. 254–261. DOI: 10.1039/c0fo00113a.

Chatzidoukaki, Ourania; Stratigi, Kalliopi; Goulielmaki, Evi; Niotis, George; Akalestou-Clocher, Alexia; Gkirtzimanaki, Katerina et al. (2021): R-loops trigger the release of cytoplasmic ssDNAs leading to chronic inflammation upon DNA damage. In *Science advances* 7 (47), eabj5769. DOI: 10.1126/sciadv.abj5769.

Chen, Bing (2019): Molecular Mechanism of HIV-1 Entry. In *Trends in microbiology* 27 (10), pp. 878–891. DOI: 10.1016/j.tim.2019.06.002.

Chen, Fuqiang; Pruett-Miller, Shondra M.; Huang, Yuping; Gjoka, Monika; Duda, Katarzyna; Taunton, Jack et al. (2011): High-frequency genome editing using ssDNA oligonucleotides with zinc-finger nucleases. In *Nature methods* 8 (9), pp. 753–755. DOI: 10.1038/nmeth.1653.

Chen, Shuliang; Bonifati, Serena; Qin, Zhihua; St Gelais, Corine; Kodigepalli, Karthik M.; Barrett, Bradley S. et al. (2018): SAMHD1 suppresses innate immune responses to viral infections and inflammatory stimuli by inhibiting the NF-κB and interferon pathways. In *Proceedings of the National Academy of Sciences of the United States of America*. DOI: 10.1073/pnas.1801213115.

Cho, Kelvin F.; Branon, Tess C.; Udeshi, Namrata D.; Myers, Samuel A.; Carr, Steven A.; Ting, Alice Y. (2020): Proximity labeling in mammalian cells with TurboID and split-TurboID. In *Nature protocols* 15 (12), pp. 3971–3999. DOI: 10.1038/s41596-020-0399-0.

Cho, Nathan H.; Cheveralls, Keith C.; Brunner, Andreas-David; Kim, Kibeom; Michaelis, André C.; Raghavan, Preethi et al. (2022): OpenCell: Endogenous tagging for the cartography of human cellular organization. In *Science (New York, N.Y.)* 375 (6585), eabi6983. DOI: 10.1126/science.abi6983.

Choi, Jongsu; Ryoo, Jeongmin; Oh, Changhoon; Hwang, Sungyeon; Ahn, Kwangseog (2015): SAMHD1 specifically restricts retroviruses through its RNase activity. In *Retrovirology* 12, p. 46. DOI: 10.1186/s12977-015-0174-4.

Chougui, Ghina; Munir-Matloob, Soundasse; Matkovic, Roy; Martin, Michaël M.; Morel, Marina; Lahouassa, Hichem et al. (2018): HIV-2/SIV viral protein X counteracts HUSH repressor complex. In *Nature Microbiology*. DOI: 10.1038/s41564-018-0179-6.

Chun, T. W.; Davey, R. T.; Engel, D.; Lane, H. C.; Fauci, A. S. (1999): Re-emergence of HIV after stopping therapy. In *Nature* 401 (6756), pp. 874–875. DOI: 10.1038/44755.

Claireaux, Mathieu; Robinot, Rémy; Kervevan, Jérôme; Patgaonkar, Mandar; Staropoli, Isabelle; Brelot, Anne et al. (2022): Low CCR5 expression protects HIV-specific CD4+ T cells of elite controllers from viral entry. In *Nature communications* 13 (1), p. 521. DOI: 10.1038/s41467-022-28130-0.

Cohen, Dorit; Adamovich, Yaarit; Reuven, Nina; Shaul, Yosef (2010): Hepatitis B virus activates deoxynucleotide synthesis in nondividing hepatocytes by targeting the R2 gene. In *Hepatology (Baltimore, Md.)* 51 (5), pp. 1538–1546. DOI: 10.1002/hep.23519.

Coiras, Mayte; Bermejo, Mercedes; Descours, Benjamin; Mateos, Elena; García-Pérez, Javier; López-Huertas, María-Rosa et al. (2016): IL-7 Induces SAMHD1 Phosphorylation in CD4+ T Lymphocytes, Improving Early Steps of HIV-1 Life Cycle. In *Cell reports* 14 (9), pp. 2100–2107. DOI: 10.1016/j.celrep.2016.02.022.

Compton, Alex A.; Bruel, Timothée; Porrot, Françoise; Mallet, Adeline; Sachse, Martin; Euvrard, Marine et al. (2014): IFITM proteins incorporated into HIV-1 virions impair viral fusion and spread. In *Cell host & microbe* 16 (6), pp. 736–747. DOI: 10.1016/j.chom.2014.11.001.

Compton, Alex A.; Hirsch, Vanessa M.; Emerman, Michael (2012): The host restriction factor APOBEC3G and retroviral Vif protein coevolve due to ongoing genetic conflict. In *Cell host & microbe* 11 (1), pp. 91–98. DOI: 10.1016/j.chom.2011.11.010.

Connor, R. I.; Chen, B. K.; Choe, S.; Landau, N. R. (1995): Vpr is required for efficient replication of human immunodeficiency virus type-1 in mononuclear phagocytes. In *Virology* 206 (2), pp. 935–944. DOI: 10.1006/viro.1995.1016.

Coquel, Flavie; Silva, Maria-Joao; Técher, Hervé; Zadorozhny, Karina; Sharma, Sushma; Nieminuszczy, Jadwiga et al. (2018): SAMHD1 acts at stalled replication forks to prevent interferon induction. In *Nature* 557 (7703), pp. 57–61. DOI: 10.1038/s41586-018-0050-1.

Cribier, Alexandra; Descours, Benjamin; Valadão, Ana Luiza Chaves; Laguette, Nadine; Benkirane, Monsef (2013): Phosphorylation of SAMHD1 by cyclin A2/CDK1 regulates its restriction activity toward HIV-1. In *Cell reports* 3 (4), pp. 1036–1043. DOI: 10.1016/j.celrep.2013.03.017.

Cristini, Agnese; Tellier, Michael; Constantinescu, Flavia; Accalai, Clelia; Albulescu, Laura Oana; Heiringhoff, Robin et al. (2022): RNase H2, mutated in Aicardi-Goutières syndrome, resolves co-transcriptional R-loops to prevent DNA breaks and inflammation. In *Nature communications* 13 (1), p. 2961. DOI: 10.1038/s41467-022-30604-0.

Crow, Yanick J.; Chase, Diana S.; Lowenstein Schmidt, Johanna; Szynkiewicz, Marcin; Forte, Gabriella M. A.; Gornall, Hannah L. et al. (2015): Characterization of human disease phenotypes associated with mutations in TREX1, RNASEH2A, RNASEH2B, RNASEH2C, SAMHD1, ADAR, and IFIH1. In *American journal of medical genetics. Part A* 167A (2), pp. 296–312. DOI: 10.1002/ajmg.a.36887.

Da Santos Silva, Eveline; Shanmugapriya, Shanmugapriya; Malikov, Viacheslav; Gu, Feng; Delaney, M. Keegan; Naghavi, Mojgan H. (2020): HIV-1 capsids mimic a microtubule regulator to coordinate early stages of infection. In *The EMBO journal* 39 (20), e104870. DOI: 10.15252/embj.2020104870.

Daddacha, Waaqo; Koyen, Allyson E.; Bastien, Amanda J.; Head, PamelaSara E.; Dhere, Vishal R.; Nabeta, Geraldine N. et al. (2017): SAMHD1 Promotes DNA End Resection to Facilitate DNA Repair by Homologous Recombination. In *Cell reports* 20 (8), pp. 1921–1935. DOI: 10.1016/j.celrep.2017.08.008.

Dalvai, Mathieu; Loehr, Jeremy; Jacquet, Karine; Huard, Caroline C.; Roques, Céline; Herst, Pauline et al. (2015): A Scalable Genome-Editing-Based Approach for Mapping Multiprotein Complexes in Human Cells. In *Cell Rep* 13 (3), pp. 621–633. DOI: 10.1016/j.celrep.2015.09.009.

Daniel, R.; Katz, R. A.; Skalka, A. M. (1999): A role for DNA-PK in retroviral DNA integration. In *Science (New York, N.Y.)* 284 (5414), pp. 644–647.

Daniel, René; Greger, James G.; Katz, Richard A.; Taganov, Konstantin D.; Wu, Xiaoyun; Kappes, John C.; Skalka, Anna Marie (2004): Evidence that stable retroviral transduction and cell survival following DNA integration depend on components of the nonhomologous end joining repair pathway. In *Journal of Virology* 78 (16), pp. 8573–8581. DOI: 10.1128/JVI.78.16.8573-8581.2004.

Deeks, Steven G.; Overbaugh, Julie; Phillips, Andrew; Buchbinder, Susan (2015): HIV infection. In *Nature reviews. Disease primers* 1, p. 15035. DOI: 10.1038/nrdp.2015.35.

Derebail, Suchitra S.; DeStefano, Jeffrey J. (2004): Mechanistic analysis of pause site-dependent and -independent recombinogenic strand transfer from structurally diverse regions of the HIV genome. In *The Journal of biological chemistry* 279 (46), pp. 47446–47454. DOI: 10.1074/jbc.M408927200.

Descours, Benjamin; Cribier, Alexandra; Chable-Bessia, Christine; Ayinde, Diana; Rice, Gillian; Crow, Yanick et al. (2012): SAMHD1 restricts HIV-1 reverse transcription in quiescent CD4(+) T-cells. In *Retrovirology* 9, p. 87. DOI: 10.1186/1742-4690-9-87.

Deutschmann, Janina; Schneider, Andrea; Gruska, Iris; Vetter, Barbara; Thomas, Dominique; Kießling, Melissa et al. (2019): A viral kinase counteracts in vivo restriction of murine cytomegalovirus by SAMHD1. In *Nature Microbiology* 4 (12), pp. 2273–2284. DOI: 10.1038/s41564-019-0529-z.

Dharan, Adarsh; Bachmann, Niklas; Talley, Sarah; Zwikelmaier, Virginia; Campbell, Edward M. (2020): Nuclear pore blockade reveals that HIV-1 completes reverse transcription and uncoating in the nucleus. In *Nature Microbiology* 5 (9), pp. 1088–1095. DOI: 10.1038/s41564-020-0735-8.

Di Nunzio, Francesca; Danckaert, Anne; Fricke, Thomas; Perez, Patricio; Fernandez, Juliette; Perret, Emmanuelle et al. (2012): Human nucleoporins promote HIV-1 docking at the nuclear pore, nuclear import and integration. In *PLOS ONE* 7 (9), e46037. DOI: 10.1371/journal.pone.0046037.

Diamond, Tracy L.; Roshal, Mikhail; Jamburuthugoda, Varuni K.; Reynolds, Holly M.; Merriam, Aaron R.; Lee, Kwi Y. et al. (2004): Macrophage tropism of HIV-1 depends on efficient cellular dNTP utilization by reverse transcriptase. In *The Journal of biological chemistry* 279 (49), pp. 51545–51553. DOI: 10.1074/jbc.M408573200.

Dicks, Matthew D. J.; Betancor, Gilberto; Jimenez-Guardeño, Jose M.; Pessel-Vivares, Lucie; Apolonia, Luis; Goujon, Caroline; Malim, Michael H. (2018): Multiple components

of the nuclear pore complex interact with the amino-terminus of MX2 to facilitate HIV-1 restriction. In *PLoS Pathogens* 14 (11), e1007408. DOI: 10.1371/journal.ppat.1007408.

Doench, John G.; Fusi, Nicolo; Sullender, Meagan; Hegde, Mudra; Vaimberg, Emma W.; Donovan, Katherine F. et al. (2016): Optimized sgRNA design to maximize activity and minimize off-target effects of CRISPR-Cas9. In *Nature biotechnology* 34 (2), pp. 184–191. DOI: 10.1038/nbt.3437.

Doench, John G.; Hartenian, Ella; Graham, Daniel B.; Tothova, Zuzana; Hegde, Mudra; Smith, Ian et al. (2014): Rational design of highly active sgRNAs for CRISPR-Cas9-mediated gene inactivation. In *Nature biotechnology* 32 (12), pp. 1262–1267. DOI: 10.1038/nbt.3026.

Dubé, Mathieu; Bego, Mariana G.; Paquay, Catherine; Cohen, Éric A. (2010): Modulation of HIV-1-host interaction: role of the Vpu accessory protein. In *Retrovirology* 7, p. 114. DOI: 10.1186/1742-4690-7-114.

Dubé, Mathieu; Paquay, Catherine; Roy, Bibhuti Bhusan; Bego, Mariana G.; Mercier, Johanne; Cohen, Eric A. (2011): HIV-1 Vpu antagonizes BST-2 by interfering mainly with the trafficking of newly synthesized BST-2 to the cell surface. In *Traffic (Copenhagen, Denmark)* 12 (12), pp. 1714–1729. DOI: 10.1111/j.1600-0854.2011.01277.x.

Duggal, Nisha K.; Emerman, Michael (2012): Evolutionary conflicts between viruses and restriction factors shape immunity. In *Nature reviews. Immunology* 12 (10), pp. 687–695. DOI: 10.1038/nri3295.

Dull, T.; Zufferey, R.; Kelly, M.; Mandel, R. J.; Nguyen, M.; Trono, D.; Naldini, L. (1998): A third-generation lentivirus vector with a conditional packaging system. In *Journal of Virology* 72 (11), pp. 8463–8471. DOI: 10.1128/JVI.72.11.8463-8471.1998.

Eickbush, Thomas H.; Jamburuthugoda, Varuni K. (2008): The diversity of retrotransposons and the properties of their reverse transcriptases. In *Virus research* 134 (1-2), pp. 221–234. DOI: 10.1016/j.virusres.2007.12.010.

Eisinger, Robert W.; Dieffenbach, Carl W.; Fauci, Anthony S. (2019): HIV Viral Load and Transmissibility of HIV Infection: Undetectable Equals Untransmittable. In *JAMA* 321 (5), pp. 451–452. DOI: 10.1001/jama.2018.21167.

Elia, Andrew E. H.; Boardman, Alexander P.; Wang, David C.; Huttlin, Edward L.; Everley, Robert A.; Dephoure, Noah et al. (2015): Quantitative Proteomic Atlas of Ubiquitination and Acetylation in the DNA Damage Response. In *Molecular cell* 59 (5), pp. 867–881. DOI: 10.1016/j.molcel.2015.05.006.

Espada, Constanza E.; St Gelais, Corine; Bonifati, Serena; Maksimova, Victoria V.; Cahill, Michael P.; Kim, Sun Hee; Wu, Li (2021): TRAF6 and TAK1 Contribute to SAMHD1-Mediated Negative Regulation of NF-κB Signaling. In *J Virol* 95 (3). DOI: 10.1128/JVI.01970-20.

Etienne, Lucie; Hahn, Beatrice H.; Sharp, Paul M.; Matsen, Frederick A.; Emerman, Michael (2013): Gene loss and adaptation to hominids underlie the ancient origin of HIV-1. In *Cell host & microbe* 14 (1), pp. 85–92. DOI: 10.1016/j.chom.2013.06.002.

Fernandez, Juliette; Machado, Anthony K.; Lyonnais, Sébastien; Chamontin, Célia; Gärtner, Kathleen; Léger, Thibaut et al. (2019): Transportin-1 binds to the HIV-1 capsid

via a nuclear localization signal and triggers uncoating. In *Nature Microbiology* 4 (11), pp. 1840–1850. DOI: 10.1038/s41564-019-0575-6.

Field, H. J.; Wildy, P. (1978): The pathogenicity of thymidine kinase-deficient mutants of herpes simplex virus in mice. In *The Journal of hygiene* 81 (2), pp. 267–277.

Finzi, D.; Blankson, J.; Siliciano, J. D.; Margolick, J. B.; Chadwick, K.; Pierson, T. et al. (1999): Latent infection of CD4+ T cells provides a mechanism for lifelong persistence of HIV-1, even in patients on effective combination therapy. In *Nature medicine* 5 (5), pp. 512–517. DOI: 10.1038/8394.

Flint, S. Jane; Racaniello, V. R.; Rall, Glenn F.; Skalka, Anna Marie; Enquist, L. W. (2015): Principles of virology. Fourth edition. Washington, D.C.: ASM Press.

Floris, Elisa; Piras, Andrea; Dall'Asta, Luca; Gamba, Andrea; Hirsch, Emilio; Campa, Carlo C. (2021): Physics of compartmentalization: How phase separation and signaling shape membrane and organelle identity. In *Computational and Structural Biotechnology Journal* 19, pp. 3225–3233. DOI: 10.1016/j.csbj.2021.05.029.

Foster, Toshana L.; Wilson, Harry; Iyer, Shilpa S.; Coss, Karen; Doores, Katie; Smith, Sarah et al. (2016): Resistance of Transmitted Founder HIV-1 to IFITM-Mediated Restriction. In *Cell host & microbe* 20 (4), pp. 429–442. DOI: 10.1016/j.chom.2016.08.006.

Francis, Ashwanth C.; Marin, Mariana; Singh, Parmit K.; Achuthan, Vasudevan; Prellberg, Mathew J.; Palermino-Rowland, Kristina et al. (2020): HIV-1 replication complexes accumulate in nuclear speckles and integrate into speckle-associated genomic domains. In *Nat Commun* 11 (1), p. 3505. DOI: 10.1038/s41467-020-17256-8.

Francis, Ashwanth C.; Melikyan, Gregory B. (2018): Single HIV-1 Imaging Reveals Progression of Infection through CA-Dependent Steps of Docking at the Nuclear Pore, Uncoating, and Nuclear Transport. In *Cell host & microbe* 23 (4), 536-548.e6. DOI: 10.1016/j.chom.2018.03.009.

Franzolin, Elisa; Pontarin, Giovanna; Rampazzo, Chiara; Miazzi, Cristina; Ferraro, Paola; Palumbo, Elisa et al. (2013): The deoxynucleotide triphosphohydrolase SAMHD1 is a major regulator of DNA precursor pools in mammalian cells. In *Proceedings of the National Academy of Sciences of the United States of America* 110 (35), pp. 14272–14277. DOI: 10.1073/pnas.1312033110.

Fregoso, Oliver I.; Ahn, Jinwoo; Wang, Chuanping; Mehrens, Jennifer; Skowronski, Jacek; Emerman, Michael (2013): Evolutionary toggling of Vpx/Vpr specificity results in divergent recognition of the restriction factor SAMHD1. In *PLoS Pathogens* 9 (7), e1003496. DOI: 10.1371/journal.ppat.1003496.

Fregoso, Oliver I.; Emerman, Michael (2016): Activation of the DNA Damage Response Is a Conserved Function of HIV-1 and HIV-2 Vpr That Is Independent of SLX4 Recruitment. In *MBio* 7 (5). DOI: 10.1128/mBio.01433-16.

Freund, Emily C.; Lock, Jaclyn Y.; Oh, Jaehak; Maculins, Timurs; Delamarre, Lelia; Bohlen, Christopher J. et al. (2020): Efficient gene knockout in primary human and murine myeloid cells by non-viral delivery of CRISPR-Cas9. In *J Exp Med* 217 (7). DOI: 10.1084/jem.20191692.

Friedman, Alan D. (2015): C/EBPα in normal and malignant myelopoiesis. In *International journal of hematology* 101 (4), pp. 330–341. DOI: 10.1007/s12185-015-1764-6.

Fuchs, Nina V.; Schieck, Maximilian; Neuenkirch, Michaela; Tondera, Christiane; Schmitz, Heike; Wendeburg, Lena et al. (2020): Generation of three induced pluripotent cell lines (iPSCs) from an Aicardi-Goutières syndrome (AGS) patient harboring a deletion in the genomic locus of the sterile alpha motif and HD domain containing protein 1 (SAMHD1). In *Stem cell research* 43, p. 101697. DOI: 10.1016/j.scr.2019.101697.

Gaidt, Moritz M.; Ebert, Thomas S.; Chauhan, Dhruv; Ramshorn, Katharina; Pinci, Francesca; Zuber, Sarah et al. (2017): The DNA Inflammasome in Human Myeloid Cells Is Initiated by a STING-Cell Death Program Upstream of NLRP3. In *Cell* 171 (5), 1110-1124.e18. DOI: 10.1016/j.cell.2017.09.039.

Gaidt, Moritz M.; Ebert, Thomas S.; Chauhan, Dhruv; Schmidt, Tobias; Schmid-Burgk, Jonathan L.; Rapino, Francesca et al. (2016): Human Monocytes Engage an Alternative Inflammasome Pathway. In *Immunity* 44 (4), pp. 833–846. DOI: 10.1016/j.immuni.2016.01.012.

Gaidt, Moritz M.; Rapino, Francesca; Graf, Thomas; Hornung, Veit (2018): Modeling Primary Human Monocytes with the Trans-Differentiation Cell Line BLaER1. In *Methods in molecular biology (Clifton, N.J.)* 1714, pp. 57–66. DOI: 10.1007/978-1-4939-7519-8_4.

Gaillard, R. K.; Barnard, J.; Lopez, V.; Hodges, P.; Bourne, E.; Johnson, L. et al. (2002): Kinetic Analysis of Wild-Type and YMDD Mutant Hepatitis B Virus Polymerases and Effects of Deoxyribonucleotide Concentrations on Polymerase Activity. In *Antimicrobial Agents and Chemotherapy* 46 (4), pp. 1005–1013. DOI: 10.1128/AAC.46.4.1005-1013.2002.

Gallo, R. C.; Salahuddin, S. Z.; Popovic, M.; Shearer, G. M.; Kaplan, M.; Haynes, B. F. et al. (1984): Frequent detection and isolation of cytopathic retroviruses (HTLV-III) from patients with AIDS and at risk for AIDS. In *Science (New York, N.Y.)* 224 (4648), pp. 500–503. DOI: 10.1126/science.6200936.

Gammon, Don B.; Gowrishankar, Branawan; Duraffour, Sophie; Andrei, Graciela; Upton, Chris; Evans, David H. (2010): Vaccinia virus-encoded ribonucleotide reductase subunits are differentially required for replication and pathogenesis. In *PLoS Pathogens* 6 (7), e1000984. DOI: 10.1371/journal.ppat.1000984.

Ganor, Yonatan; Real, Fernando; Sennepin, Alexis; Dutertre, Charles-Antoine; Prevedel, Lisa; Xu, Lin et al. (2019): HIV-1 reservoirs in urethral macrophages of patients under suppressive antiretroviral therapy. In *Nature Microbiology* 4 (4), pp. 633–644. DOI: 10.1038/s41564-018-0335-z.

Gao, Daxing; Wu, Jiaxi; Wu, You-Tong; Du, Fenghe; Aroh, Chukwuemika; Yan, Nan et al. (2013a): Cyclic GMP-AMP synthase is an innate immune sensor of HIV and other retroviruses. In *Science (New York, N.Y.)* 341 (6148), pp. 903–906. DOI: 10.1126/science.1240933.

Gao, Pu; Ascano, Manuel; Wu, Yang; Barchet, Winfried; Gaffney, Barbara L.; Zillinger, Thomas et al. (2013b): Cyclic G(2',5')pA(3',5')p is the metazoan second messenger

produced by DNA-activated cyclic GMP-AMP synthase. In *Cell* 153 (5), pp. 1094–1107. DOI: 10.1016/j.cell.2013.04.046.

Gao, W. Y.; Cara, A.; Gallo, R. C.; Lori, F. (1993): Low levels of deoxynucleotides in peripheral blood lymphocytes. A strategy to inhibit human immunodeficiency virus type 1 replication. In *Proceedings of the National Academy of Sciences* 90 (19), pp. 8925–8928.

Gao, Wenying; Li, Guangquan; Bian, Xuefeng; Rui, Yajuan; Zhai, Chenyang; Liu, Panpan et al. (2019): Defective modulation of LINE-1 retrotransposition by cancer-associated SAMHD1 mutants. In *Biochemical and biophysical research communications* 519 (2), pp. 213–219. DOI: 10.1016/j.bbrc.2019.08.155.

García-Muse, Tatiana; Aguilera, Andrés (2019): R Loops: From Physiological to Pathological Roles. In *Cell* 179 (3), pp. 604–618. DOI: 10.1016/j.cell.2019.08.055.

Giordano, Anna Maria Sole; Luciani, Marco; Gatto, Francesca; Abou Alezz, Monah; Beghè, Chiara; Della Volpe, Lucrezia et al. (2022): DNA damage contributes to neurotoxic inflammation in Aicardi-Goutières syndrome astrocytes. In *J Exp Med* 219 (4). DOI: 10.1084/jem.20211121.

Glaser, Astrid; McColl, Bradley; Vadolas, Jim (2016): GFP to BFP Conversion: A Versatile Assay for the Quantification of CRISPR/Cas9-mediated Genome Editing. In *Molecular therapy. Nucleic acids* 5 (7), e334. DOI: 10.1038/mtna.2016.48.

Global HIV & AIDS statistics — Fact sheet (2022). Available online at https://www.unaids.org/en/resources/fact-sheet, updated on 6/3/2022, checked on 6/3/2022.

Goffinet, Christine; Allespach, Ina; Homann, Stefanie; Tervo, Hanna-Mari; Habermann, Anja; Rupp, Daniel et al. (2009): HIV-1 antagonism of CD317 is species specific and involves Vpu-mediated proteasomal degradation of the restriction factor. In *Cell host & microbe* 5 (3), pp. 285–297. DOI: 10.1016/j.chom.2009.01.009.

Goldstein, D. J.; Weller, S. K. (1988): Herpes simplex virus type 1-induced ribonucleotide reductase activity is dispensable for virus growth and DNA synthesis. Isolation and characterization of an ICP6 lacZ insertion mutant. In *J Virol* 62 (1), pp. 196–205.

Goldstone, David C.; Ennis-Adeniran, Valerie; Hedden, Joseph J.; Groom, Harriet C. T.; Rice, Gillian I.; Christodoulou, Evangelos et al. (2011): HIV-1 restriction factor SAMHD1 is a deoxynucleoside triphosphate triphosphohydrolase. In *Nature* 480 (7377), pp. 379–382. DOI: 10.1038/nature10623.

Goncalves, Adriana; Karayel, Evren; Rice, Gillian I.; Bennett, Keiryn L.; Crow, Yanick J.; Superti-Furga, Giulio; Bürckstümmer, Tilmann (2012): SAMHD1 is a nucleic-acid binding protein that is mislocalized due to aicardi-goutières syndrome-associated mutations. In *Human mutation* 33 (7), pp. 1116–1122. DOI: 10.1002/humu.22087.

Gorry, Paul R.; Francella, Nicholas; Lewin, Sharon R.; Collman, Ronald G. (2014): HIV-1 envelope-receptor interactions required for macrophage infection and implications for current HIV-1 cure strategies. In *Journal of leukocyte biology* 95 (1), pp. 71–81. DOI: 10.1189/jlb.0713368.

Goujon, Caroline; Arfi, Vanessa; Pertel, Thomas; Luban, Jeremy; Lienard, Julia; Rigal, Dominique et al. (2008): Characterization of simian immunodeficiency virus SIVSM/human immunodeficiency virus type 2 Vpx function in human myeloid cells. In *J Virol* 82 (24), pp. 12335–12345. DOI: 10.1128/JVI.01181-08.

Goujon, Caroline; Moncorgé, Olivier; Bauby, Hélène; Doyle, Tomas; Ward, Christopher C.; Schaller, Torsten et al. (2013): Human MX2 is an interferon-induced post-entry inhibitor of HIV-1 infection. In *Nature* 502 (7472), pp. 559–562. DOI: 10.1038/nature12542.

Goujon, Caroline; Rivière, Lise; Jarrosson-Wuilleme, Loraine; Bernaud, Jeanine; Rigal, Dominique; Darlix, Jean-Luc; Cimarelli, Andrea (2007): SIVSM/HIV-2 Vpx proteins promote retroviral escape from a proteasome-dependent restriction pathway present in human dendritic cells. In *Retrovirology* 4, p. 2. DOI: 10.1186/1742-4690-4-2.

Gramberg, Thomas; Kahle, Tanja; Bloch, Nicolin; Wittmann, Sabine; Müllers, Erik; Daddacha, Waaqo et al. (2013): Restriction of diverse retroviruses by SAMHD1. In *Retrovirology* 10, p. 26. DOI: 10.1186/1742-4690-10-26.

Greenwood, Edward J. D.; Williamson, James C.; Sienkiewicz, Agata; Naamati, Adi; Matheson, Nicholas J.; Lehner, Paul J. (2019): Promiscuous Targeting of Cellular Proteins by Vpr Drives Systems-Level Proteomic Remodeling in HIV-1 Infection. In *Cell reports* 27 (5), 1579-1596.e7. DOI: 10.1016/j.celrep.2019.04.025.

Greulich, Wilhelm; Wagner, Mirko; Gaidt, Moritz M.; Stafford, Che; Cheng, Yiming; Linder, Andreas et al. (2019): TLR8 Is a Sensor of RNase T2 Degradation Products. In *Cell* 179 (6), 1264-1275.e13. DOI: 10.1016/j.cell.2019.11.001.

Gringhuis, Sonja I.; Hertoghs, Nina; Kaptein, Tanja M.; Zijlstra-Willems, Esther M.; Sarrami-Forooshani, Ramin; Sprokholt, Joris K. et al. (2017): HIV-1 blocks the signaling adaptor MAVS to evade antiviral host defense after sensing of abortive HIV-1 RNA by the host helicase DDX3. In *Nature immunology* 18 (2), pp. 225–235. DOI: 10.1038/ni.3647.

Gringhuis, Sonja I.; van der Vlist, Michiel; van den Berg, Linda M.; Dunnen, Jeroen den; Litjens, Manja; Geijtenbeek, Teunis B. H. (2010): HIV-1 exploits innate signaling by TLR8 and DC-SIGN for productive infection of dendritic cells. In *Nature immunology* 11 (5), pp. 419–426. DOI: 10.1038/ni.1858.

Gupta, Ravindra Kumar; Peppa, Dimitra; Hill, Alison L.; Gálvez, Cristina; Salgado, Maria; Pace, Matthew et al. (2020): Evidence for HIV-1 cure after CCR5Δ32/Δ32 allogeneic haemopoietic stem-cell transplantation 30 months post analytical treatment interruption: a case report. In *The Lancet HIV* 7 (5), e340-e347. DOI: 10.1016/S2352-3018(20)30069-2.

Hammonds, Jason; Wang, Jaang-Jiun; Yi, Hong; Spearman, Paul (2010): Immunoelectron microscopic evidence for Tetherin/BST2 as the physical bridge between HIV-1 virions and the plasma membrane. In *PLoS Pathogens* 6 (2), e1000749. DOI: 10.1371/journal.ppat.1000749.

Hansen, Erik C.; Seamon, Kyle J.; Cravens, Shannen L.; Stivers, James T. (2014): GTP activator and dNTP substrates of HIV-1 restriction factor SAMHD1 generate a long-lived

activated state. In *Proceedings of the National Academy of Sciences of the United States of America* 111 (18), E1843-51. DOI: 10.1073/pnas.1401706111.

Hargrave, Anna; Mustafa, Abu Salim; Hanif, Asma; Tunio, Javed H.; Hanif, Shumaila Nida M. (2021): Current Status of HIV-1 Vaccines. In *Vaccines* 9 (9). DOI: 10.3390/vaccines9091026.

Harris, Reuben S.; Bishop, Kate N.; Sheehy, Ann M.; Craig, Heather M.; Petersen-Mahrt, Svend K.; Watt, Ian N. et al. (2003): DNA Deamination Mediates Innate Immunity to Retroviral Infection. In *Cell* 113 (6), pp. 803–809. DOI: 10.1016/S0092-8674(03)00423-9.

Harris, Reuben S.; Dudley, Jaquelin P. (2015): APOBECs and virus restriction. In *Virology* 479-480, pp. 131–145. DOI: 10.1016/j.virol.2015.03.012.

Harris, Reuben S.; Hultquist, Judd F.; Evans, David T. (2012): The restriction factors of human immunodeficiency virus. In *The Journal of biological chemistry* 287 (49), pp. 40875–40883. DOI: 10.1074/jbc.R112.416925.

Harris, Reuben S.; Petersen-Mahrt, Svend K.; Neuberger, Michael S. (2002): RNA editing enzyme APOBEC1 and some of its homologs can act as DNA mutators. In *Molecular cell* 10 (5), pp. 1247–1253. DOI: 10.1016/s1097-2765(02)00742-6.

Härtlova, Anetta; Erttmann, Saskia F.; Raffi, Faizal am; Schmalz, Anja M.; Resch, Ulrike; Anugula, Sharath et al. (2015): DNA damage primes the type I interferon system via the cytosolic DNA sensor STING to promote anti-microbial innate immunity. In *Immunity* 42 (2), pp. 332–343. DOI: 10.1016/j.immuni.2015.01.012.

He, J.; Choe, S.; Walker, R.; Di Marzio, P.; Morgan, D. O.; Landau, N. R. (1995): Human immunodeficiency virus type 1 viral protein R (Vpr) arrests cells in the G2 phase of the cell cycle by inhibiting p34cdc2 activity. In *J Virol* 69 (11), pp. 6705–6711.

Hegazy, Youssef A.; Fernando, Chrishan M.; Tran, Elizabeth J. (2020): The balancing act of R-loop biology: The good, the bad, and the ugly. In *Journal of Biological Chemistry* 295 (4), pp. 905–913. DOI: 10.1016/S0021-9258(17)49903-0.

Hendriks, Ivo A.; Lyon, David; Young, Clifford; Jensen, Lars J.; Vertegaal, Alfred C. O.; Nielsen, Michael L. (2017): Site-specific mapping of the human SUMO proteome reveals co-modification with phosphorylation. In *Nature structural & molecular biology* 24 (3), pp. 325–336. DOI: 10.1038/nsmb.3366.

Herold, Nikolas; Rudd, Sean G.; Ljungblad, Linda; Sanjiv, Kumar; Myrberg, Ida Hed; Paulin, Cynthia B. J. et al. (2017a): Targeting SAMHD1 with the Vpx protein to improve cytarabine therapy for hematological malignancies. In *Nature medicine* 23 (2), pp. 256–263. DOI: 10.1038/nm.4265.

Herold, Nikolas; Rudd, Sean G.; Sanjiv, Kumar; Kutzner, Juliane; Bladh, Julia; Paulin, Cynthia B. J. et al. (2017b): SAMHD1 protects cancer cells from various nucleoside-based antimetabolites. In *Cell cycle (Georgetown, Tex.)* 16 (11), pp. 1029–1038. DOI: 10.1080/15384101.2017.1314407.

Herrmann, Alexandra; Wittmann, Sabine; Thomas, Dominique; Shepard, Caitlin N.; Kim, Baek; Ferreirós, Nerea; Gramberg, Thomas (2018): The SAMHD1-mediated block of LINE-1 retroelements is regulated by phosphorylation. In *Mobile DNA* 9, p. 11. DOI: 10.1186/s13100-018-0116-5.

Herzner, Anna-Maria; Hagmann, Cristina Amparo; Goldeck, Marion; Wolter, Steven; Kübler, Kirsten; Wittmann, Sabine et al. (2015): Sequence-specific activation of the DNA sensor cGAS by Y-form DNA structures as found in primary HIV-1 cDNA. In *Nature immunology* 16 (10), pp. 1025–1033. DOI: 10.1038/ni.3267.

Hiatt, Joseph; Cavero, Devin A.; McGregor, Michael J.; Zheng, Weihao; Budzik, Jonathan M.; Roth, Theodore L. et al. (2021a): Efficient generation of isogenic primary human myeloid cells using CRISPR-Cas9 ribonucleoproteins. In *Cell Rep* 35 (6), p. 109105. DOI: 10.1016/j.celrep.2021.109105.

Hiatt, Joseph; Cavero, Devin A.; McGregor, Michael J.; Zheng, Weihao; Budzik, Jonathan M.; Roth, Theodore L. et al. (2021b): Efficient generation of isogenic primary human myeloid cells using CRISPR-Cas9 ribonucleoproteins. In *Cell Rep* 35 (6), p. 109105. DOI: 10.1016/j.celrep.2021.109105.

Hiatt, Joseph; Hultquist, Judd F.; McGregor, Michael J.; Bouhaddou, Mehdi; Leenay, Ryan T.; Simons, Lacy M. et al. (2022): A functional map of HIV-host interactions in primary human T cells. In *Nature communications* 13 (1), p. 1752. DOI: 10.1038/s41467-022-29346-w.

Hinz, Andreas; Miguet, Nolwenn; Natrajan, Ganesh; Usami, Yoshiko; Yamanaka, Hikaru; Renesto, Patricia et al. (2010): Structural basis of HIV-1 tethering to membranes by the BST-2/tetherin ectodomain. In *Cell host & microbe* 7 (4), pp. 314–323. DOI: 10.1016/j.chom.2010.03.005.

Hladik, Florian; McElrath, M. Juliana (2008): Setting the stage: host invasion by HIV. In *Nature reviews. Immunology* 8 (6), pp. 447–457. DOI: 10.1038/nri2302.

Hollenbaugh, Joseph A.; Gee, Peter; Baker, Jonathon; Daly, Michele B.; Amie, Sarah M.; Tate, Jessica et al. (2013): Host factor SAMHD1 restricts DNA viruses in non-dividing myeloid cells. In *PLoS Pathogens* 9 (6), e1003481. DOI: 10.1371/journal.ppat.1003481.

Honeycutt, Jenna B.; Thayer, William O.; Baker, Caroline E.; Ribeiro, Ruy M.; Lada, Steven M.; Cao, Youfang et al. (2017): HIV persistence in tissue macrophages of humanized myeloid-only mice during antiretroviral therapy. In *Nature medicine* 23 (5), pp. 638–643. DOI: 10.1038/nm.4319.

Honeycutt, Jenna B.; Wahl, Angela; Baker, Caroline; Spagnuolo, Rae Ann; Foster, John; Zakharova, Oksana et al. (2016): Macrophages sustain HIV replication in vivo independently of T cells. In *The Journal of clinical investigation* 126 (4), pp. 1353–1366. DOI: 10.1172/JCI84456.

Hrecka, Kasia; Hao, Caili; Gierszewska, Magda; Swanson, Selene K.; Kesik-Brodacka, Malgorzata; Srivastava, Smita et al. (2011): Vpx relieves inhibition of HIV-1 infection of macrophages mediated by the SAMHD1 protein. In *Nature* 474 (7353), pp. 658–661. DOI: 10.1038/nature10195.

Hsiau, Tim; Conant, David; Rossi, Nicholas; Maures, Travis; Waite, Kelsey; Yang, Joyce et al. (2018): Inference of CRISPR Edits from Sanger Trace Data. DOI: 10.1101/251082.

Hu, Jie; Gao, Qingzhu; Yang, Yang; Xia, Jie; Zhang, Wanjun; Chen, Yao et al. (2021): Hexosamine biosynthetic pathway promotes the antiviral activity of SAMHD1 by enhancing O-GlcNAc transferase-mediated protein O-GlcNAcylation. In *Theranostics* 11 (2), pp. 805–823. DOI: 10.7150/thno.50230.

Hu, Jie; Qiao, Miao; Chen, Yanmeng; Tang, Hua; Zhang, Wenlu; Tang, Dan et al. (2018a): Cyclin E2-CDK2 mediates SAMHD1 phosphorylation to abrogate its restriction of HBV replication in hepatoma cells. In *FEBS letters* 592 (11), pp. 1893–1904. DOI: 10.1002/1873-3468.13105.

Hu, Johnny H.; Miller, Shannon M.; Geurts, Maarten H.; Tang, Weixin; Chen, Liwei; Sun, Ning et al. (2018b): Evolved Cas9 variants with broad PAM compatibility and high DNA specificity. In *Nature* 556 (7699), pp. 57–63. DOI: 10.1038/nature26155.

Hu, Siqi; Li, Jian; Xu, Fengwen; Mei, Shan; Le Duff, Yann; Yin, Lijuan et al. (2015): SAMHD1 Inhibits LINE-1 Retrotransposition by Promoting Stress Granule Formation. In *PLoS genetics* 11 (7), e1005367. DOI: 10.1371/journal.pgen.1005367.

Hu, W. S.; Temin, H. M. (1990): Retroviral recombination and reverse transcription. In *Science (New York, N.Y.)* 250 (4985), pp. 1227–1233.

Hu, Zheng; Shi, Zhaoying; Guo, Xiaogang; Jiang, Baishan; Wang, Guo; Luo, Dixian et al. (2018c): Ligase IV inhibitor SCR7 enhances gene editing directed by CRISPR-Cas9 and ssODN in human cancer cells. In *Cell & bioscience* 8, p. 12. DOI: 10.1186/s13578-018-0200-z.

Hughes, Stephen H. (2015): Reverse Transcription of Retroviruses and LTR Retrotransposons. In *Microbiology spectrum* 3 (2), MDNA3-0027-2014. DOI: 10.1128/microbiolspec.MDNA3-0027-2014.

Hulme, Amy E.; Perez, Omar; Hope, Thomas J. (2011): Complementary assays reveal a relationship between HIV-1 uncoating and reverse transcription. In *Proceedings of the National Academy of Sciences of the United States of America* 108 (24), pp. 9975–9980. DOI: 10.1073/pnas.1014522108.

Hultquist, Judd F.; Lengyel, Joy A.; Refsland, Eric W.; LaRue, Rebecca S.; Lackey, Lela; Brown, William L.; Harris, Reuben S. (2011): Human and rhesus APOBEC3D, APOBEC3F, APOBEC3G, and APOBEC3H demonstrate a conserved capacity to restrict Vif-deficient HIV-1. In *J Virol* 85 (21), pp. 11220–11234. DOI: 10.1128/JVI.05238-11.

Hultquist, Judd F.; Schumann, Kathrin; Woo, Jonathan M.; Manganaro, Lara; McGregor, Michael J.; Doudna, Jennifer et al. (2016): A Cas9 Ribonucleoprotein Platform for Functional Genetic Studies of HIV-Host Interactions in Primary Human T Cells. In *Cell reports* 17 (5), pp. 1438–1452. DOI: 10.1016/j.celrep.2016.09.080.

Husain, Afzal; Xu, Jianliang; Fujii, Hodaka; Nakata, Mikiyo; Kobayashi, Maki; Wang, Ji-Yang et al. (2020): SAMHD1-mediated dNTP degradation is required for efficient DNA repair during antibody class switch recombination. In *The EMBO journal* 39 (15), e102931. DOI: 10.15252/embj.2019102931.

Hütter, Gero; Nowak, Daniel; Mossner, Maximilian; Ganepola, Susanne; Müssig, Arne; Allers, Kristina et al. (2009): Long-term control of HIV by CCR5 Delta32/Delta32 stem-cell transplantation. In *The New England journal of medicine* 360 (7), pp. 692–698. DOI: 10.1056/NEJMoa0802905.

Hyeon, Seokhwan; Lee, Myoung Kyu; Kim, Young-Eui; Lee, Gwang Myeong; Ahn, Jin-Hyun (2020): Degradation of SAMHD1 Restriction Factor Through Cullin-Ring E3 Ligase Complexes During Human Cytomegalovirus Infection. In *Frontiers in cellular and infection microbiology* 10, p. 391. DOI: 10.3389/fcimb.2020.00391.

Ito, Jumpei; Gifford, Robert J.; Sato, Kei (2020): Retroviruses drive the rapid evolution of mammalian APOBEC3 genes. In *Proceedings of the National Academy of Sciences of the United States of America* 117 (1), pp. 610–618. DOI: 10.1073/pnas.1914183116.

Iwabu, Yukie; Fujita, Hideaki; Kinomoto, Masanobu; Kaneko, Keiko; Ishizaka, Yukihito; Tanaka, Yoshitaka et al. (2009): HIV-1 accessory protein Vpu internalizes cell-surface BST-2/tetherin through transmembrane interactions leading to lysosomes. In *The Journal of biological chemistry* 284 (50), pp. 35060–35072. DOI: 10.1074/jbc.M109.058305.

Iyer, Shilpa S.; Bibollet-Ruche, Frederic; Sherrill-Mix, Scott; Learn, Gerald H.; Plenderleith, Lindsey; Smith, Andrew G. et al. (2017): Resistance to type 1 interferons is a major determinant of HIV-1 transmission fitness. In *Proceedings of the National Academy of Sciences of the United States of America* 114 (4), E590-E599. DOI: 10.1073/pnas.1620144114.

Jack, I.; Seshadri, R.; Garson, M.; Michael, P.; Callen, D.; Zola, H.; Morley, A. (1986): RCH-ACV: A lymphoblastic leukemia cell line with chromosome translocation 1;19 and trisomy 8. In *Cancer genetics and cytogenetics* 19 (3-4), pp. 261–269. DOI: 10.1016/0165-4608(86)90055-5.

Jacobson, J. G.; Leib, D. A.; Goldstein, D. J.; Bogard, C. L.; Schaffer, P. A.; Weller, S. K.; Coen, D. M. (1989): A herpes simplex virus ribonucleotide reductase deletion mutant is defective for productive acute and reactivatable latent infections of mice and for replication in mouse cells. In *Virology* 173 (1), pp. 276–283.

Jacques, David A.; McEwan, William A.; Hilditch, Laura; Price, Amanda J.; Towers, Greg J.; James, Leo C. (2016): HIV-1 uses dynamic capsid pores to import nucleotides and fuel encapsidated DNA synthesis. In *Nature* 536 (7616), pp. 349–353. DOI: 10.1038/nature19098.

Jäger, Stefanie; Cimermancic, Peter; Gulbahce, Natali; Johnson, Jeffrey R.; McGovern, Kathryn E.; Clarke, Starlynn C. et al. (2011): Global landscape of HIV-human protein complexes. In *Nature* 481 (7381), pp. 365–370. DOI: 10.1038/nature10719.

Jakobsen, Martin R.; Bak, Rasmus O.; Andersen, Annika; Berg, Randi K.; Jensen, Søren B.; Tengchuan, Jin et al. (2013): IFI16 senses DNA forms of the lentiviral replication cycle and controls HIV-1 replication. In *Proceedings of the National Academy of Sciences of the United States of America* 110 (48), E4571-80. DOI: 10.1073/pnas.1311669110.

James, Claire D.; Prabhakar, Apurva T.; Otoa, Raymonde; Evans, Michael R.; Wang, Xu; Bristol, Molly L. et al. (2019): SAMHD1 Regulates Human Papillomavirus 16-Induced Cell Proliferation and Viral Replication during Differentiation of Keratinocytes. In *mSphere* 4 (4). DOI: 10.1128/mSphere.00448-19.

Jang, Sunbok; Zhou, Xiaohong; Ahn, Jinwoo (2016): Substrate Specificity of SAMHD1 Triphosphohydrolase Activity Is Controlled by Deoxyribonucleoside Triphosphates and Phosphorylation at Thr592. In *Biochemistry* 55 (39), pp. 5635–5646. DOI: 10.1021/acs.biochem.6b00627.

Jeong, Gi Uk; Park, Il-Hyun; Ahn, Kwangseog; Ahn, Byung-Yoon (2016): Inhibition of hepatitis B virus replication by a dNTPase-dependent function of the host restriction factor SAMHD1. In *Virology* 495, pp. 71–78. DOI: 10.1016/j.virol.2016.05.001.

Ji, Xiaoyun; Tang, Chenxiang; Zhao, Qi; Wang, Wei; Xiong, Yong (2014): Structural basis of cellular dNTP regulation by SAMHD1. In *Proceedings of the National Academy of Sciences of the United States of America* 111 (41), E4305-14. DOI: 10.1073/pnas.1412289111.

Ji, Xiaoyun; Wu, Ying; Yan, Junpeng; Mehrens, Jennifer; Yang, Haitao; DeLucia, Maria et al. (2013): Mechanism of allosteric activation of SAMHD1 by dGTP. In *Nature structural & molecular biology* 20 (11), pp. 1304–1309. DOI: 10.1038/nsmb.2692.

Jimenez-Guardeño, Jose M.; Apolonia, Luis; Betancor, Gilberto; Malim, Michael H. (2019): Immunoproteasome activation enables human TRIM5α restriction of HIV-1. In *Nat Microbiol* 4 (6), pp. 933–940. DOI: 10.1038/s41564-019-0402-0.

Jin, Changzhong; Peng, Xiaorong; Liu, Fumin; Cheng, Linfang; Xie, Tiansheng; Lu, Xiangyun et al. (2016): Interferon-induced sterile alpha motif and histidine/aspartic acid domain-containing protein 1 expression in astrocytes and microglia is mediated by microRNA-181a. In *AIDS (London, England)* 30 (13), pp. 2053–2064. DOI: 10.1097/QAD.0000000000001166.

Jost, Marco; Jacobson, Amy N.; Hussmann, Jeffrey A.; Cirolia, Giana; Fischbach, Michael A.; Weissman, Jonathan S. (2021): CRISPR-based functional genomics in human dendritic cells. In *eLife* 10. DOI: 10.7554/eLife.65856.

Jowett, J. B.; Planelles, V.; Poon, B.; Shah, N. P.; Chen, M. L.; Chen, I. S. (1995): The human immunodeficiency virus type 1 vpr gene arrests infected T cells in the G2 + M phase of the cell cycle. In *J Virol* 69 (10), pp. 6304–6313.

Jumper, John; Evans, Richard; Pritzel, Alexander; Green, Tim; Figurnov, Michael; Ronneberger, Olaf et al. (2021): Highly accurate protein structure prediction with AlphaFold. In *Nature* 596 (7873), pp. 583–589. DOI: 10.1038/s41586-021-03819-2.

Kane, Melissa; Rebensburg, Stephanie V.; Takata, Matthew A.; Zang, Trinity M.; Yamashita, Masahiro; Kvaratskhelia, Mamuka; Bieniasz, Paul D. (2018): Nuclear pore heterogeneity influences HIV-1 infection and the antiviral activity of MX2. In *eLife* 7. DOI: 10.7554/eLife.35738.

Kane, Melissa; Yadav, Shalini S.; Bitzegeio, Julia; Kutluay, Sebla B.; Zang, Trinity; Wilson, Sam J. et al. (2013): MX2 is an interferon-induced inhibitor of HIV-1 infection. In *Nature* 502 (7472), pp. 563–566. DOI: 10.1038/nature12653.

Karlsson, Max; Zhang, Cheng; Méar, Loren; Zhong, Wen; Digre, Andreas; Katona, Borbala et al. (2021): A single-cell type transcriptomics map of human tissues. In *Science advances* 7 (31). DOI: 10.1126/sciadv.abh2169.

Kaufmann, Stefan H. E.; Dorhoi, Anca; Hotchkiss, Richard S.; Bartenschlager, Ralf (2018): Host-directed therapies for bacterial and viral infections. In *Nature reviews. Drug discovery* 17 (1), pp. 35–56. DOI: 10.1038/nrd.2017.162.

Kaushik, Rajnish; Zhu, Xiaonan; Stranska, Ruzena; Wu, Yuanfei; Stevenson, Mario (2009): A cellular restriction dictates the permissivity of nondividing monocytes/macrophages to lentivirus and gammaretrovirus infection. In *Cell host & microbe* 6 (1), pp. 68–80. DOI: 10.1016/j.chom.2009.05.022.

Keele, Brandon F.; Giorgi, Elena E.; Salazar-Gonzalez, Jesus F.; Decker, Julie M.; Pham, Kimmy T.; Salazar, Maria G. et al. (2008): Identification and characterization of transmitted and early founder virus envelopes in primary HIV-1 infection. In *Proceedings of the National Academy of Sciences of the United States of America* 105 (21), pp. 7552–7557. DOI: 10.1073/pnas.0802203105.

Keele, Brandon F.; van Heuverswyn, Fran; Li, Yingying; Bailes, Elizabeth; Takehisa, Jun; Santiago, Mario L. et al. (2006): Chimpanzee reservoirs of pandemic and nonpandemic HIV-1. In *Science (New York, N.Y.)* 313 (5786), pp. 523–526. DOI: 10.1126/science.1126531.

Kennedy, Edward M.; Amie, Sarah M.; Bambara, Robert A.; Kim, Baek (2012): Frequent incorporation of ribonucleotides during HIV-1 reverse transcription and their attenuated repair in macrophages. In *Journal of Biological Chemistry* 287 (17), pp. 14280–14288. DOI: 10.1074/jbc.M112.348482.

Kennedy, Edward M.; Gavegnano, Christina; Nguyen, Laura; Slater, Rebecca; Lucas, Amanda; Fromentin, Emilie et al. (2010): Ribonucleoside triphosphates as substrate of human immunodeficiency virus type 1 reverse transcriptase in human macrophages. In *The Journal of biological chemistry* 285 (50), pp. 39380–39391. DOI: 10.1074/jbc.M110.178582.

Khan, M. A.; Aberham, C.; Kao, S.; Akari, H.; Gorelick, R.; Bour, S.; Strebel, K. (2001): Human immunodeficiency virus type 1 Vif protein is packaged into the nucleoprotein complex through an interaction with viral genomic RNA. In *Journal of Virology* 75 (16), pp. 7252–7265. DOI: 10.1128/JVI.75.16.7252-7265.2001.

Kim, Baek; Nguyen, Laura A.; Daddacha, Waaqo; Hollenbaugh, Joseph A. (2012): Tight interplay among SAMHD1 protein level, cellular dNTP levels, and HIV-1 proviral DNA synthesis kinetics in human primary monocyte-derived macrophages. In *The Journal of biological chemistry* 287 (26), pp. 21570–21574. DOI: 10.1074/jbc.C112.374843.

Kim, Eui Tae; Roche, Kathryn L.; Kulej, Katarzyna; Spruce, Lynn A.; Seeholzer, Steven H.; Coen, Donald M. et al. (2019a): SAMHD1 Modulates Early Steps during Human Cytomegalovirus Infection by Limiting NF-κB Activation. In *Cell Rep* 28 (2), 434-448.e6. DOI: 10.1016/j.celrep.2019.06.027.

Kim, Eui Tae; White, Tommy E.; Brandariz-Núñez, Alberto; Diaz-Griffero, Felipe; Weitzman, Matthew D. (2013): SAMHD1 restricts herpes simplex virus 1 in macrophages by limiting DNA replication. In *Journal of Virology* 87 (23), pp. 12949–12956. DOI: 10.1128/JVI.02291-13.

Kim, Kyusik; Dauphin, Ann; Komurlu, Sevnur; McCauley, Sean M.; Yurkovetskiy, Leonid; Carbone, Claudia et al. (2019b): Cyclophilin A protects HIV-1 from restriction by human TRIM5α. In *Nature Microbiology* 4 (12), pp. 2044–2051. DOI: 10.1038/s41564-019-0592-5.

Kim, Yong Chan; Kim, Kee Kwang; Yoon, Jeongheon; Scott, David W.; Shevach, Ethan M. (2018): SAMHD1 Posttranscriptionally Controls the Expression of Foxp3 and Helios in Human T Regulatory Cells. In *Journal of immunology (Baltimore, Md. : 1950)*. DOI: 10.4049/jimmunol.1800613.

Kirchhoff, Frank (2010): Immune evasion and counteraction of restriction factors by HIV-1 and other primate lentiviruses. In *Cell host & microbe* 8 (1), pp. 55–67. DOI: 10.1016/j.chom.2010.06.004.

Klarmann, G. J.; Schauber, C. A.; Preston, B. D. (1993): Template-directed pausing of DNA synthesis by HIV-1 reverse transcriptase during polymerization of HIV-1 sequences in vitro. In *Journal of Biological Chemistry* 268 (13), pp. 9793–9802. DOI: 10.1016/S0021-9258(18)98417-6.

Knyazhanskaya, Ekaterina; Anisenko, Andrey; Shadrina, Olga; Kalinina, Anastasia; Zatsepin, Timofei; Zalevsky, Arthur et al. (2019): NHEJ pathway is involved in post-integrational DNA repair due to Ku70 binding to HIV-1 integrase. In *Retrovirology* 16 (1), p. 30. DOI: 10.1186/s12977-019-0492-z.

Kodigepalli, Karthik M.; Bonifati, Serena; Tirumuru, Nagaraja; Wu, Li (2018): SAMHD1 modulates in vitro proliferation of acute myeloid leukemia-derived THP-1 cells through the PI3K-Akt-p27 axis. In *Cell cycle (Georgetown, Tex.)* 17 (9), pp. 1124–1137. DOI: 10.1080/15384101.2018.1480218.

Kondo, Naoyuki; Nakagawa, Noriko; Ebihara, Akio; Chen, Lirong; Liu, Zhi-Jie; Wang, Bi-Cheng et al. (2007): Structure of dNTP-inducible dNTP triphosphohydrolase: insight into broad specificity for dNTPs and triphosphohydrolase-type hydrolysis. In *Acta crystallographica. Section D, Biological crystallography* 63 (Pt 2), pp. 230–239. DOI: 10.1107/S0907444906049262.

König, Renate; Zhou, Yingyao; Elleder, Daniel; Diamond, Tracy L.; Bonamy, Ghislain M. C.; Irelan, Jeffrey T. et al. (2008): Global analysis of host-pathogen interactions that regulate early-stage HIV-1 replication. In *Cell* 135 (1), pp. 49–60. DOI: 10.1016/j.cell.2008.07.032.

Könnyű, Balázs; Sadiq, S. Kashif; Turányi, Tamás; Hírmondó, Rita; Müller, Barbara; Kräusslich, Hans-Georg et al. (2013): Gag-Pol processing during HIV-1 virion maturation: a systems biology approach. In *PLOS Computational Biology* 9 (6), e1003103. DOI: 10.1371/journal.pcbi.1003103.

Korin, Y. D.; Zack, J. A. (1999): Nonproductive human immunodeficiency virus type 1 infection in nucleoside-treated G0 lymphocytes. In *J Virol* 73 (8), pp. 6526–6532.

Kosicki, Michael; Tomberg, Kärt; Bradley, Allan (2018): Repair of double-strand breaks induced by CRISPR-Cas9 leads to large deletions and complex rearrangements. In *Nature biotechnology* 36 (8), pp. 765–771. DOI: 10.1038/nbt.4192.

Kotov, A.; Zhou, J.; Flicker, P.; Aiken, C. (1999): Association of Nef with the human immunodeficiency virus type 1 core. In *Journal of Virology* 73 (10), pp. 8824–8830. DOI: 10.1128/JVI.73.10.8824-8830.1999.

Krapp, Christian; Hotter, Dominik; Gawanbacht, Ali; McLaren, Paul J.; Kluge, Silvia F.; Stürzel, Christina M. et al. (2016): Guanylate Binding Protein (GBP) 5 Is an Interferon-Inducible Inhibitor of HIV-1 Infectivity. In *Cell host & microbe* 19 (4), pp. 504–514. DOI: 10.1016/j.chom.2016.02.019.

Kretschmer, Stefanie; Wolf, Christine; König, Nadja; Staroske, Wolfgang; Guck, Jochen; Häusler, Martin et al. (2015): SAMHD1 prevents autoimmunity by maintaining genome

stability. In *Annals of the rheumatic diseases* 74 (3), e17. DOI: 10.1136/annrheumdis-2013-204845.

Kruize, Zita; Kootstra, Neeltje A. (2019): The Role of Macrophages in HIV-1 Persistence and Pathogenesis. In *Front Microbiol* 10, p. 2828. DOI: 10.3389/fmicb.2019.02828.

Krupovic, Mart; Blomberg, Jonas; Coffin, John M.; Dasgupta, Indranil; Fan, Hung; Geering, Andrew D. et al. (2018): Ortervirales. New Virus Order Unifying Five Families of Reverse-Transcribing Viruses. In *J Virol* 92 (12). DOI: 10.1128/JVI.00515-18.

Kueck, Tonya; Cassella, Elena; Holler, Jessica; Kim, Baek; Bieniasz, Paul D. (2018): The aryl hydrocarbon receptor and interferon gamma generate antiviral states via transcriptional repression. In *eLife* 7. DOI: 10.7554/eLife.38867.

Kumar, Dinesh; Abdulovic, Amy L.; Viberg, Jörgen; Nilsson, Anna Karin; Kunkel, Thomas A.; Chabes, Andrei (2011): Mechanisms of mutagenesis in vivo due to imbalanced dNTP pools. In *Nucleic acids research* 39 (4), pp. 1360–1371. DOI: 10.1093/nar/gkq829.

Kumar, Swati; Morrison, James H.; Dingli, David; Poeschla, Eric (2018): HIV-1 Activation of Innate Immunity Depends Strongly on the Intracellular Level of TREX1 and Sensing of Incomplete Reverse Transcription Products. In *J Virol* 92 (16). DOI: 10.1128/JVI.00001-18.

Laguette, Nadine; Brégnard, Christelle; Hue, Pauline; Basbous, Jihane; Yatim, Ahmad; Larroque, Marion et al. (2014): Premature activation of the SLX4 complex by Vpr promotes G2/M arrest and escape from innate immune sensing. In *Cell* 156 (1-2), pp. 134–145. DOI: 10.1016/j.cell.2013.12.011.

Laguette, Nadine; Rahm, Nadia; Sobhian, Bijan; Chable-Bessia, Christine; Münch, Jan; Snoeck, Joke et al. (2012): Evolutionary and functional analyses of the interaction between the myeloid restriction factor SAMHD1 and the lentiviral Vpx protein. In *Cell host & microbe* 11 (2), pp. 205–217. DOI: 10.1016/j.chom.2012.01.007.

Laguette, Nadine; Sobhian, Bijan; Casartelli, Nicoletta; Ringeard, Mathieu; Chable-Bessia, Christine; Ségéral, Emmanuel et al. (2011): SAMHD1 is the dendritic- and myeloid-cell-specific HIV-1 restriction factor counteracted by Vpx. In *Nature* 474 (7353), pp. 654–657. DOI: 10.1038/nature10117.

Lahaye, Xavier; Gentili, Matteo; Silvin, Aymeric; Conrad, Cécile; Picard, Léa; Jouve, Mabel et al. (2018): NONO Detects the Nuclear HIV Capsid to Promote cGAS-Mediated Innate Immune Activation. In *Cell* 175 (2), 488-501.e22. DOI: 10.1016/j.cell.2018.08.062.

Lahaye, Xavier; Satoh, Takeshi; Gentili, Matteo; Cerboni, Silvia; Conrad, Cécile; Hurbain, Ilse et al. (2013): The capsids of HIV-1 and HIV-2 determine immune detection of the viral cDNA by the innate sensor cGAS in dendritic cells. In *Immunity* 39 (6), pp. 1132–1142. DOI: 10.1016/j.immuni.2013.11.002.

Lahouassa, Hichem; Daddacha, Waaqo; Hofmann, Henning; Ayinde, Diana; Logue, Eric C.; Dragin, Loïc et al. (2012): SAMHD1 restricts the replication of human immunodeficiency virus type 1 by depleting the intracellular pool of deoxynucleoside triphosphates. In *Nature immunology* 13 (3), pp. 223–228. DOI: 10.1038/ni.2236.

Lamoliatte, Frédéric; Caron, Danielle; Durette, Chantal; Mahrouche, Louiza; Maroui, Mohamed Ali; Caron-Lizotte, Olivier et al. (2014): Large-scale analysis of lysine

SUMOylation by SUMO remnant immunoaffinity profiling. In *Nature communications* 5, p. 5409. DOI: 10.1038/ncomms6409.

Lander, Eric S. (2016): The Heroes of CRISPR. In *Cell* 164 (1-2), pp. 18–28. DOI: 10.1016/j.cell.2015.12.041.

Langton, Michelle; Sun, Sining; Ueda, Chie; Markey, Max; Chen, Jiahua; Paddy, Isaac et al. (2020): The HD-Domain Metalloprotein Superfamily: An Apparent Common Protein Scaffold with Diverse Chemistries. In *Catalysts (Basel, Switzerland)* 10 (10). DOI: 10.3390/catal10101191.

Le Grice, Stuart F. J. (2012): Human immunodeficiency virus reverse transcriptase. 25 years of research, drug discovery, and promise. In *The Journal of biological chemistry* 287 (49), pp. 40850–40857. DOI: 10.1074/jbc.R112.389056.

Lee, Christopher Z. W.; Kozaki, Tatsuya; Ginhoux, Florent (2018a): Studying tissue macrophages in vitro: are iPSC-derived cells the answer? In *Nature reviews. Immunology* 18 (11), pp. 716–725. DOI: 10.1038/s41577-018-0054-y.

Lee, Eun Ji; Seo, Ji Hae; Park, Ji-Hyeon; Vo, Tam Thuy Lu; An, Sunho; Bae, Sung-Jin et al. (2017): SAMHD1 acetylation enhances its deoxynucleotide triphosphohydrolase activity and promotes cancer cell proliferation. In *Oncotarget* 8 (40), pp. 68517–68529. DOI: 10.18632/oncotarget.19704.

Lee, Wing-Yiu Jason; Fu, Rebecca Menhua; Liang, Chen; Sloan, Richard D. (2018b): IFITM proteins inhibit HIV-1 protein synthesis. In *Scientific reports* 8 (1), p. 14551. DOI: 10.1038/s41598-018-32785-5.

Lembo, D.; Gribaudo, G.; Hofer, A.; Riera, L.; Cornaglia, M.; Mondo, A. et al. (2000): Expression of an altered ribonucleotide reductase activity associated with the replication of murine cytomegalovirus in quiescent fibroblasts. In *Journal of Virology* 74 (24), pp. 11557–11565. DOI: 10.1128/jvi.74.24.11557-11565.2000.

Lembo, David; Donalisio, Manuela; Hofer, Anders; Cornaglia, Maura; Brune, Wolfram; Koszinowski, Ulrich et al. (2004): The ribonucleotide reductase R1 homolog of murine cytomegalovirus is not a functional enzyme subunit but is required for pathogenesis. In *Journal of Virology* 78 (8), pp. 4278–4288. DOI: 10.1128/jvi.78.8.4278-4288.2004.

Lenzi, Gina M.; Domaoal, Robert A.; Kim, Dong-Hyun; Schinazi, Raymond F.; Kim, Baek (2014): Kinetic variations between reverse transcriptases of viral protein X coding and noncoding lentiviruses. In *Retrovirology* 11, p. 111. DOI: 10.1186/s12977-014-0111-y.

Lepelley, Alice; Louis, Stéphanie; Sourisseau, Marion; Law, Helen K. W.; Pothlichet, Julien; Schilte, Clémentine et al. (2011): Innate sensing of HIV-infected cells. In *PLoS Pathogens* 7 (2), e1001284. DOI: 10.1371/journal.ppat.1001284.

Levin, Judith G.; Mitra, Mithun; Mascarenhas, Anjali; Musier-Forsyth, Karin (2010): Role of HIV-1 nucleocapsid protein in HIV-1 reverse transcription. In *RNA biology* 7 (6), pp. 754–774. DOI: 10.4161/rna.7.6.14115.

Levy, David N.; Aldrovandi, Grace M.; Kutsch, Olaf; Shaw, George M. (2004): Dynamics of HIV-1 recombination in its natural target cells. In *Proceedings of the National Academy of Sciences* 101 (12), pp. 4204–4209. DOI: 10.1073/pnas.0306764101.

Li, Kun; Markosyan, Ruben M.; Zheng, Yi-Min; Golfetto, Ottavia; Bungart, Brittani; Li, Minghua et al. (2013): IFITM proteins restrict viral membrane hemifusion. In *PLoS Pathogens* 9 (1), e1003124. DOI: 10.1371/journal.ppat.1003124.

Li, L.; Olvera, J. M.; Yoder, K. E.; Mitchell, R. S.; Butler, S. L.; Lieber, M. et al. (2001): Role of the non-homologous DNA end joining pathway in the early steps of retroviral infection. In *The EMBO journal* 20 (12), pp. 3272–3281. DOI: 10.1093/emboj/20.12.3272.

Li, Zhaolong; Huan, Chen; Wang, Hong; Liu, Yue; Liu, Xin; Su, Xing et al. (2020): TRIM21-mediated proteasomal degradation of SAMHD1 regulates its antiviral activity. In *EMBO reports* 21 (1), e47528. DOI: 10.15252/embr.201847528.

Liberatore, Rachel A.; Bieniasz, Paul D. (2011): Tetherin is a key effector of the antiretroviral activity of type I interferon in vitro and in vivo. In *Proceedings of the National Academy of Sciences of the United States of America* 108 (44), pp. 18097–18101. DOI: 10.1073/pnas.1113694108.

Lim, Efrem S.; Fregoso, Oliver I.; McCoy, Connor O.; Matsen, Frederick A.; Malik, Harmit S.; Emerman, Michael (2012): The ability of primate lentiviruses to degrade the monocyte restriction factor SAMHD1 preceded the birth of the viral accessory protein Vpx. In *Cell host & microbe* 11 (2), pp. 194–204. DOI: 10.1016/j.chom.2012.01.004.

Lim, Yoong Wearn; Sanz, Lionel A.; Xu, Xiaoqin; Hartono, Stella R.; Chédin, Frédéric (2015): Genome-wide DNA hypomethylation and RNA:DNA hybrid accumulation in Aicardi-Goutières syndrome. In *eLife* 4. DOI: 10.7554/eLife.08007.

Liu, Li; Oliveira, Nidia M. M.; Cheney, Kelly M.; Pade, Corinna; Dreja, Hanna; Bergin, Ann-Marie H. et al. (2011): A whole genome screen for HIV restriction factors. In *Retrovirology* 8, p. 94. DOI: 10.1186/1742-4690-8-94.

Liu, Mingjie; Rehman, Saad; Tang, Xidian; Gu, Kui; Fan, Qinlei; Chen, Dekun; Ma, Wentao (2018a): Methodologies for Improving HDR Efficiency. In *Frontiers in genetics* 9, p. 691. DOI: 10.3389/fgene.2018.00691.

Liu, Mingjie; Rehman, Saad; Tang, Xidian; Gu, Kui; Fan, Qinlei; Chen, Dekun; Ma, Wentao (2018b): Methodologies for Improving HDR Efficiency. In *Frontiers in genetics* 9, p. 691. DOI: 10.3389/fgene.2018.00691.

Liu, Rong; Paxton, William A.; Choe, Sunny; Ceradini, Daniel; Martin, Scott R.; Horuk, Richard et al. (1996): Homozygous Defect in HIV-1 Coreceptor Accounts for Resistance of Some Multiply-Exposed Individuals to HIV-1 Infection. In *Cell* 86 (3), pp. 367–377. DOI: 10.1016/s0092-8674(00)80110-5.

Liu, Ying; Fu, Yajing; Wang, Qian; Li, Mushan; Zhou, Zheng; Dabbagh, Deemah et al. (2019): Proteomic profiling of HIV-1 infection of human CD4+ T cells identifies PSGL-1 as an HIV restriction factor. In *Nature Microbiology* 4 (5), pp. 813–825. DOI: 10.1038/s41564-019-0372-2.

Liu, Zhenlong; Pan, Qinghua; Ding, Shilei; Qian, Jin; Xu, Fengwen; Zhou, Jinming et al. (2013): The interferon-inducible MxB protein inhibits HIV-1 infection. In *Cell host & microbe* 14 (4), pp. 398–410. DOI: 10.1016/j.chom.2013.08.015.

Löser, P.; Jennings, G. S.; Strauss, M.; Sandig, V. (1998): Reactivation of the previously silenced cytomegalovirus major immediate-early promoter in the mouse liver: involvement of NFkappaB. In *Journal of Virology* 72 (1), pp. 180–190. DOI: 10.1128/JVI.72.1.180-190.1998.

Lu, Jennifer; Pan, Qinghua; Rong, Liwei; He, Wei; Liu, Shan-Lu; Liang, Chen (2011): The IFITM proteins inhibit HIV-1 infection. In *J Virol* 85 (5), pp. 2126–2137. DOI: 10.1128/JVI.01531-10.

Luban, Jeremy (2012): Innate immune sensing of HIV-1 by dendritic cells. In *Cell host & microbe* 12 (4), pp. 408–418. DOI: 10.1016/j.chom.2012.10.002.

Lumpkin, Ryan J.; Gu, Hongbo; Zhu, Yiying; Leonard, Marilyn; Ahmad, Alla S.; Clauser, Karl R. et al. (2017): Site-specific identification and quantitation of endogenous SUMO modifications under native conditions. In *Nature communications* 8 (1), p. 1171. DOI: 10.1038/s41467-017-01271-3.

Maelfait, Jonathan; Bridgeman, Anne; Benlahrech, Adel; Cursi, Chiara; Rehwinkel, Jan (2016): Restriction by SAMHD1 Limits cGAS/STING-Dependent Innate and Adaptive Immune Responses to HIV-1. In *Cell reports* 16 (6), pp. 1492–1501. DOI: 10.1016/j.celrep.2016.07.002.

Majer, Catharina; Schüssler, Jan Moritz; König, Renate (2019): Intertwined. SAMHD1 cellular functions, restriction, and viral evasion strategies. In *Medical microbiology and immunology*. DOI: 10.1007/s00430-019-00593-x.

Majerska, Jana; Feretzaki, Marianna; Glousker, Galina; Lingner, Joachim (2018): Transformation-induced stress at telomeres is counteracted through changes in the telomeric proteome including SAMHD1. In *Life science alliance* 1 (4), e201800121. DOI: 10.26508/lsa.201800121.

Mali, Prashant; Yang, Luhan; Esvelt, Kevin M.; Aach, John; Guell, Marc; DiCarlo, James E. et al. (2013): RNA-guided human genome engineering via Cas9. In *Science (New York, N.Y.)* 339 (6121), pp. 823–826. DOI: 10.1126/science.1232033.

Malim, Michael H.; Bieniasz, Paul D. (2012): HIV Restriction Factors and Mechanisms of Evasion. In *Cold Spring Harbor perspectives in medicine* 2 (5), a006940. DOI: 10.1101/cshperspect.a006940.

Manel, Nicolas; Hogstad, Brandon; Wang, Yaming; Levy, David E.; Unutmaz, Derya; Littman, Dan R. (2010): A cryptic sensor for HIV-1 activates antiviral innate immunity in dendritic cells. In *Nature* 467 (7312), pp. 214–217. DOI: 10.1038/nature09337.

Manganaro, Lara; Hong, Patrick; Hernandez, Matthew M.; Argyle, Dionne; Mulder, Lubbertus C. F.; Potla, Uma et al. (2018): IL-15 regulates susceptibility of CD4+ T cells to HIV infection. In *Proceedings of the National Academy of Sciences of the United States of America*. DOI: 10.1073/pnas.1806695115.

Mangeat, Bastien; Turelli, Priscilla; Caron, Gersende; Friedli, Marc; Perrin, Luc; Trono, Didier (2003): Broad antiretroviral defence by human APOBEC3G through lethal editing of nascent reverse transcripts. In *Nature* 424 (6944), pp. 99–103. DOI: 10.1038/nature01709.

Margolis, David M.; Archin, Nancie M.; Cohen, Myron S.; Eron, Joseph J.; Ferrari, Guido; Garcia, J. Victor et al. (2020): Curing HIV: Seeking to Target and Clear Persistent Infection. In *Cell* 181 (1), pp. 189–206. DOI: 10.1016/j.cell.2020.03.005.

Mariani, Roberto; Chen, Darlene; Schröfelbauer, Bärbel; Navarro, Francisco; König, Renate; Bollman, Brooke et al. (2003): Species-Specific Exclusion of APOBEC3G from HIV-1 Virions by Vif. In *Cell* 114 (1), pp. 21–31. DOI: 10.1016/S0092-8674(03)00515-4.

Martinat, Charlotte; Cormier, Arthur; Tobaly-Tapiero, Joëlle; Palmic, Noé; Casartelli, Nicoletta; Mahboubi, Bijan et al. (2021): SUMOylation of SAMHD1 at Lysine 595 is required for HIV-1 restriction in non-cycling cells. In *Nature communications* 12 (1), p. 4582. DOI: 10.1038/s41467-021-24802-5.

Martin-Gayo, Enrique; Buzon, Maria Jose; Ouyang, Zhengyu; Hickman, Taylor; Cronin, Jacqueline; Pimenova, Dina et al. (2015): Potent Cell-Intrinsic Immune Responses in Dendritic Cells Facilitate HIV-1-Specific T Cell Immunity in HIV-1 Elite Controllers. In *PLoS Pathogens* 11 (6), e1004930. DOI: 10.1371/journal.ppat.1004930.

Maruyama, Takeshi; Dougan, Stephanie K.; Truttmann, Matthias C.; Bilate, Angelina M.; Ingram, Jessica R.; Ploegh, Hidde L. (2015): Increasing the efficiency of precise genome editing with CRISPR-Cas9 by inhibition of nonhomologous end joining. In *Nature biotechnology* 33 (5), pp. 538–542. DOI: 10.1038/nbt.3190.

Marziali, Federico; Cimarelli, Andrea (2021): Membrane Interference Against HIV-1 by Intrinsic Antiviral Factors: The Case of IFITMs. In *Cells* 10 (5). DOI: 10.3390/cells10051171.

Mathews, Christopher K. (2015): Deoxyribonucleotide metabolism, mutagenesis and cancer. In *Nature reviews. Cancer* 15 (9), pp. 528–539. DOI: 10.1038/nrc3981.

Matkovic, Roy; Morel, Marina; Lanciano, Sophie; Larrous, Pauline; Martin, Benjamin; Bejjani, Fabienne et al. (2022): TASOR epigenetic repressor cooperates with a CNOT1 RNA degradation pathway to repress HIV. In *Nature communications* 13 (1), p. 66. DOI: 10.1038/s41467-021-27650-5.

Mauney, Christopher H.; Rogers, LeAnn C.; Harris, Reuben S.; Daniel, Larry W.; Devarie-Baez, Nelmi O.; Wu, Hanzhi et al. (2017): The SAMHD1 dNTP Triphosphohydrolase Is Controlled by a Redox Switch. In *Antioxidants & redox signaling* 27 (16), pp. 1317–1331. DOI: 10.1089/ars.2016.6888.

McCauley, Sean Matthew; Kim, Kyusik; Nowosielska, Anetta; Dauphin, Ann; Yurkovetskiy, Leonid; Diehl, William Edward; Luban, Jeremy (2018): Intron-containing RNA from the HIV-1 provirus activates type I interferon and inflammatory cytokines. In *Nature communications* 9 (1), p. 5305. DOI: 10.1038/s41467-018-07753-2.

McCormack, Sheena; Dunn, David T.; Desai, Monica; Dolling, David I.; Gafos, Mitzy; Gilson, Richard et al. (2016): Pre-exposure prophylaxis to prevent the acquisition of HIV-1 infection (PROUD): effectiveness results from the pilot phase of a pragmatic open-label randomised trial. In *The Lancet* 387 (10013), pp. 53–60. DOI: 10.1016/S0140-6736(15)00056-2.

Meås, Hany Zekaria; Haug, Markus; Beckwith, Marianne Sandvold; Louet, Claire; Ryan, Liv; Hu, Zhenyi et al. (2020): Sensing of HIV-1 by TLR8 activates human T cells and

reverses latency. In *Nature communications* 11 (1), p. 147. DOI: 10.1038/s41467-019-13837-4.

Meng, Xiangzhou; Zhao, Xiaolan (2017): Replication fork regression and its regulation. In *FEMS yeast research* 17 (1). DOI: 10.1093/femsyr/fow110.

Mereby, Sarah A.; Maehigashi, Tatsuya; Holler, Jessica M.; Kim, Dong-Hyun; Schinazi, Raymond F.; Kim, Baek (2018): Interplay of ancestral non-primate lentiviruses with the virus-restricting SAMHD1 proteins of their hosts. In *The Journal of biological chemistry*. DOI: 10.1074/jbc.RA118.004567.

Mirdita, Milot; Schütze, Konstantin; Moriwaki, Yoshitaka; Heo, Lim; Ovchinnikov, Sergey; Steinegger, Martin (2022): ColabFold: making protein folding accessible to all. In *Nature methods*. DOI: 10.1038/s41592-022-01488-1.

Mitchell, Richard S.; Katsura, Chris; Skasko, Mark A.; Fitzpatrick, Katie; Lau, David; Ruiz, Autumn et al. (2009): Vpu antagonizes BST-2-mediated restriction of HIV-1 release via beta-TrCP and endo-lysosomal trafficking. In *PLoS Pathogens* 5 (5), e1000450. DOI: 10.1371/journal.ppat.1000450.

Mitrea, Diana M.; Chandra, Bappaditya; Ferrolino, Mylene C.; Gibbs, Eric B.; Tolbert, Michele; White, Michael R.; Kriwacki, Richard W. (2018): Methods for Physical Characterization of Phase-Separated Bodies and Membrane-less Organelles. In *Journal of molecular biology* 430 (23), pp. 4773–4805. DOI: 10.1016/j.jmb.2018.07.006.

Mlcochova, Petra; Sutherland, Katherine A.; Watters, Sarah A.; Bertoli, Cosetta; Am Bruin, Rob de; Rehwinkel, Jan et al. (2017): A G1-like state allows HIV-1 to bypass SAMHD1 restriction in macrophages. In *The EMBO journal* 36 (5), pp. 604–616. DOI: 10.15252/embj.201696025.

Monit, Christopher; Morris, Elizabeth R.; Ruis, Christopher; Szafran, Bart; Thiltgen, Grant; Tsai, Ming-Han Chloe et al. (2019): Positive selection in dNTPase SAMHD1 throughout mammalian evolution. In *Proceedings of the National Academy of Sciences of the United States of America* 116 (37), pp. 18647–18654. DOI: 10.1073/pnas.1908755116.

Monroe, Kathryn M.; Yang, Zhiyuan; Johnson, Jeffrey R.; Geng, Xin; Doitsh, Gilad; Krogan, Nevan J.; Greene, Warner C. (2014): IFI16 DNA sensor is required for death of lymphoid CD4 T cells abortively infected with HIV. In *Science (New York, N.Y.)* 343 (6169), pp. 428–432. DOI: 10.1126/science.1243640.

Morris, Elizabeth R.; Caswell, Sarah J.; Kunzelmann, Simone; Arnold, Laurence H.; Purkiss, Andrew G.; Kelly, Geoff; Taylor, Ian A. (2020): Crystal structures of SAMHD1 inhibitor complexes reveal the mechanism of water-mediated dNTP hydrolysis. In *Nature communications* 11 (1), p. 3165. DOI: 10.1038/s41467-020-16983-2.

Müller, Thorsten G.; Zila, Vojtech; Peters, Kyra; Schifferdecker, Sandra; Stanic, Mia; Lucic, Bojana et al. (2021): HIV-1 uncoating by release of viral cDNA from capsid-like structures in the nucleus of infected cells. In *eLife* 10. DOI: 10.7554/eLife.64776.

Murphy, Kenneth; Travers, Paul; Walport, Mark; Janeway, Charles (2012): Janeway's immunobiology. 8th ed. London: Garland Science; London : Taylor & Francis [distributor].

Naamati, Adi; Williamson, James C.; Greenwood, Edward Jd; Marelli, Sara; Lehner, Paul J.; Matheson, Nicholas J. (2019): Functional proteomic atlas of HIV infection in primary human CD4+ T cells. In *eLife* 8. DOI: 10.7554/eLife.41431.

Nabel, Christopher S.; Lee, Jae W.; Wang, Laura C.; Kohli, Rahul M. (2013): Nucleic acid determinants for selective deamination of DNA over RNA by activation-induced deaminase. In *Proceedings of the National Academy of Sciences of the United States of America* 110 (35), pp. 14225–14230. DOI: 10.1073/pnas.1306345110.

Naghavi, Mojgan H. (2021): HIV-1 capsid exploitation of the host microtubule cytoskeleton during early infection. In *Retrovirology* 18 (1), p. 19. DOI: 10.1186/s12977-021-00563-3.

Nambiar, Tarun S.; Baudrier, Lou; Billon, Pierre; Ciccia, Alberto (2022): CRISPR-based genome editing through the lens of DNA repair. In *Molecular cell* 82 (2), pp. 348–388. DOI: 10.1016/j.molcel.2021.12.026.

Ndung'u, Thumbi; McCune, Joseph M.; Deeks, Steven G. (2019): Why and where an HIV cure is needed and how it might be achieved. In *Nature* 576 (7787), pp. 397–405. DOI: 10.1038/s41586-019-1841-8.

Nègre, D.; Mangeot, P. E.; Duisit, G.; Blanchard, S.; Vidalain, P. O.; Leissner, P. et al. (2000): Characterization of novel safe lentiviral vectors derived from simian immunodeficiency virus (SIVmac251) that efficiently transduce mature human dendritic cells. In *Gene therapy* 7 (19), pp. 1613–1623. DOI: 10.1038/sj.gt.3301292.

Neil, Stuart J. D.; Sandrin, Virginie; Sundquist, Wesley I.; Bieniasz, Paul D. (2007): An interferon-alpha-induced tethering mechanism inhibits HIV-1 and Ebola virus particle release but is counteracted by the HIV-1 Vpu protein. In *Cell host & microbe* 2 (3), pp. 193–203. DOI: 10.1016/j.chom.2007.08.001.

Neil, Stuart J. D.; Zang, Trinity; Bieniasz, Paul D. (2008): Tetherin inhibits retrovirus release and is antagonized by HIV-1 Vpu. In *Nature* 451 (7177), pp. 425–430. DOI: 10.1038/nature06553.

Nidhi, Sweta; Anand, Uttpal; Oleksak, Patrik; Tripathi, Pooja; Lal, Jonathan A.; Thomas, George et al. (2021): Novel CRISPR-Cas Systems: An Updated Review of the Current Achievements, Applications, and Future Research Perspectives. In *International journal of molecular sciences* 22 (7). DOI: 10.3390/ijms22073327.

Nowak, Daniel; Stewart, Daphne; Koeffler, H. Phillip (2009): Differentiation therapy of leukemia: 3 decades of development. In *Blood* 113 (16), pp. 3655–3665. DOI: 10.1182/blood-2009-01-198911.

Ochoa, David; Jarnuczak, Andrew F.; Viéitez, Cristina; Gehre, Maja; Soucheray, Margaret; Mateus, André et al. (2020): The functional landscape of the human phosphoproteome. In *Nature biotechnology* 38 (3), pp. 365–373. DOI: 10.1038/s41587-019-0344-3.

OhAinle, Molly; Helms, Louisa; Vermeire, Jolien; Roesch, Ferdinand; Humes, Daryl; Basom, Ryan et al. (2018): A virus-packageable CRISPR screen identifies host factors mediating interferon inhibition of HIV. In *eLife* 7. DOI: 10.7554/eLife.39823.

OhAinle, Molly; Kim, Kyusik; Komurlu Keceli, Sevnur; Felton, Abby; Campbell, Ed; Luban, Jeremy; Emerman, Michael (2020): TRIM34 restricts HIV-1 and SIV capsids in a TRIM5α-dependent manner. In *PLoS Pathogens* 16 (4), e1008507. DOI: 10.1371/journal.ppat.1008507.

Oo, Adrian; Zandi, Keivan; Shepard, Caitlin; Bassit, Leda C.; Musall, Katie; Goh, Shu Ling et al. (2022): Elimination of Aicardi-Goutières syndrome protein SAMHD1 activates cellular innate immunity and suppresses SARS-CoV-2 replication. In *Journal of Biological Chemistry* 298 (3), p. 101635. DOI: 10.1016/j.jbc.2022.101635.

Ouyang, Jian; Yadav, Tribhuwan; Zhang, Jia-Min; Yang, Haibo; Rheinbay, Esther; Guo, Hongshan et al. (2021): RNA transcripts stimulate homologous recombination by forming DR-loops. In *Nature* 594 (7862), pp. 283–288. DOI: 10.1038/s41586-021-03538-8.

Pabst, T.; Mueller, B. U.; Zhang, P.; Radomska, H. S.; Narravula, S.; Schnittger, S. et al. (2001): Dominant-negative mutations of CEBPA, encoding CCAAT/enhancer binding protein-alpha (C/EBPalpha), in acute myeloid leukemia. In *Nature genetics* 27 (3), pp. 263–270. DOI: 10.1038/85820.

Paquet, Dominik; Kwart, Dylan; Chen, Antonia; Sproul, Andrew; Jacob, Samson; Teo, Shaun et al. (2016): Efficient introduction of specific homozygous and heterozygous mutations using CRISPR/Cas9. In *Nature* 533 (7601), pp. 125–129. DOI: 10.1038/nature17664.

Park, Kiwon; Ryoo, Jeongmin; Jeong, Heena; Kim, Minsu; Lee, Sungwon; Hwang, Sung-Yeon et al. (2021): Aicardi-Goutières syndrome-associated gene SAMHD1 preserves genome integrity by preventing R-loop formation at transcription-replication conflict regions. In *PLoS genetics* 17 (4), e1009523. DOI: 10.1371/journal.pgen.1009523.

Park, Ryan J.; Wang, Tim; Koundakjian, Dylan; Hultquist, Judd F.; Lamothe-Molina, Pedro; Monel, Blandine et al. (2017): A genome-wide CRISPR screen identifies a restricted set of HIV host dependency factors. In *Nature genetics* 49 (2), pp. 193–203. DOI: 10.1038/ng.3741.

Parrish, Nicholas F.; Gao, Feng; Li, Hui; Giorgi, Elena E.; Barbian, Hannah J.; Parrish, Erica H. et al. (2013): Phenotypic properties of transmitted founder HIV-1. In *Proceedings of the National Academy of Sciences of the United States of America* 110 (17), pp. 6626–6633. DOI: 10.1073/pnas.1304288110.

Passos, Vânia; Zillinger, Thomas; Casartelli, Nicoletta; Wachs, Amelie S.; Xu, Shuting; Malassa, Angelina et al. (2019): Characterization of Endogenous SERINC5 Protein as Anti-HIV-1 Factor. In *J Virol* 93 (24). DOI: 10.1128/JVI.01221-19.

Patel, Darshil R.; Weiss, Robert S. (2018): A tough row to hoe: when replication forks encounter DNA damage. In *Biochemical Society Transactions* 46 (6), pp. 1643–1651. DOI: 10.1042/BST20180308.

Pauls, Eduardo; Badia, Roger; Torres-Torronteras, Javier; Ruiz, Alba; Permanyer, Marc; Riveira-Muñoz, Eva et al. (2014a): Palbociclib, a selective inhibitor of cyclin-dependent kinase4/6, blocks HIV-1 reverse transcription through the control of sterile α motif and HD domain-containing protein-1 (SAMHD1) activity. In *AIDS (London, England)* 28 (15), pp. 2213–2222. DOI: 10.1097/QAD.0000000000000399.

Pauls, Eduardo; Ruiz, Alba; Badia, Roger; Permanyer, Marc; Gubern, Albert; Riveira-Muñoz, Eva et al. (2014b): Cell cycle control and HIV-1 susceptibility are linked by CDK6-dependent CDK2 phosphorylation of SAMHD1 in myeloid and lymphoid cells. In *Journal of immunology (Baltimore, Md. : 1950)* 193 (4), pp. 1988–1997. DOI: 10.4049/jimmunol.1400873.

Pear, W. S.; Nolan, G. P.; Scott, M. L.; Baltimore, D. (1993): Production of high-titer helper-free retroviruses by transient transfection. In *Proceedings of the National Academy of Sciences* 90 (18), pp. 8392–8396. DOI: 10.1073/pnas.90.18.8392.

Perez-Caballero, David; Zang, Trinity; Ebrahimi, Alaleh; McNatt, Matthew W.; Gregory, Devon A.; Johnson, Marc C.; Bieniasz, Paul D. (2009): Tetherin inhibits HIV-1 release by directly tethering virions to cells. In *Cell* 139 (3), pp. 499–511. DOI: 10.1016/j.cell.2009.08.039.

Pertel, Thomas; Hausmann, Stéphane; Morger, Damien; Züger, Sara; Guerra, Jessica; Lascano, Josefina et al. (2011): TRIM5 is an innate immune sensor for the retrovirus capsid lattice. In *Nature* 472 (7343), pp. 361–365. DOI: 10.1038/nature09976.

Petri, Karl; Zhang, Weiting; Ma, Junyan; Schmidts, Andrea; Lee, Hyunho; Horng, Joy E. et al. (2022): CRISPR prime editing with ribonucleoprotein complexes in zebrafish and primary human cells. In *Nature biotechnology* 40 (2), pp. 189–193. DOI: 10.1038/s41587-021-00901-y.

Pettersen, Eric F.; Goddard, Thomas D.; Huang, Conrad C.; Meng, Elaine C.; Couch, Gregory S.; Croll, Tristan I. et al. (2021): UCSF ChimeraX: Structure visualization for researchers, educators, and developers. In *Protein science : a publication of the Protein Society* 30 (1), pp. 70–82. DOI: 10.1002/pro.3943.

Pettit, Steve C.; Lindquist, Jeffrey N.; Kaplan, Andrew H.; Swanstrom, Ronald (2005): Processing sites in the human immunodeficiency virus type 1 (HIV-1) Gag-Pro-Pol precursor are cleaved by the viral protease at different rates. In *Retrovirology* 2, p. 66. DOI: 10.1186/1742-4690-2-66.

Platt, E. J.; Wehrly, K.; Kuhmann, S. E.; Chesebro, B.; Kabat, D. (1998): Effects of CCR5 and CD4 cell surface concentrations on infections by macrophagetropic isolates of human immunodeficiency virus type 1. In *Journal of Virology* 72 (4), pp. 2855–2864. DOI: 10.1128/JVI.72.4.2855-2864.1998.

Plesa, Gabriela; Dai, Jihong; Baytop, Cliff; Riley, James L.; June, Carl H.; O'Doherty, Una (2007): Addition of deoxynucleosides enhances human immunodeficiency virus type 1 integration and 2LTR formation in resting CD4+ T cells. In *Journal of Virology* 81 (24), pp. 13938–13942. DOI: 10.1128/JVI.01745-07.

Popovic, M.; Sarngadharan, M. G.; Read, E.; Gallo, R. C. (1984): Detection, isolation, and continuous production of cytopathic retroviruses (HTLV-III) from patients with AIDS and pre-AIDS. In *Science (New York, N.Y.)* 224 (4648), pp. 497–500. DOI: 10.1126/science.6200935.

Portegijs, Vincent; Fielmich, Lars-Eric; Galli, Matilde; Schmidt, Ruben; Muñoz, Javier; van Mourik, Tim et al. (2016): Multisite Phosphorylation of NuMA-Related LIN-5 Controls Mitotic Spindle Positioning in C. elegans. In *PLoS genetics* 12 (10), e1006291. DOI: 10.1371/journal.pgen.1006291.

Powell, Rebecca D.; Holland, Paul J.; Hollis, Thomas; Perrino, Fred W. (2011): Aicardi-Goutieres syndrome gene and HIV-1 restriction factor SAMHD1 is a dGTP-regulated deoxynucleotide triphosphohydrolase. In *The Journal of biological chemistry* 286 (51), pp. 43596–43600. DOI: 10.1074/jbc.C111.317628.

Qiao, Feng; Bowie, James U. (2005): The many faces of SAM. In *Science's STKE : signal transduction knowledge environment* 2005 (286), re7. DOI: 10.1126/stke.2862005re7.

Qin, Zhihua; Bonifati, Serena; St Gelais, Corine; Li, Tai-Wei; Kim, Sun-Hee; Antonucci, Jenna M. et al. (2020): The dNTPase activity of SAMHD1 is important for its suppression of innate immune responses in differentiated monocytic cells. In *The Journal of biological chemistry* 295 (6), pp. 1575–1586. DOI: 10.1074/jbc.RA119.010360.

Quinet, Annabel; Lemaçon, Delphine; Vindigni, Alessandro (2017): Replication Fork Reversal: Players and Guardians. In *Molecular cell* 68 (5), pp. 830–833. DOI: 10.1016/j.molcel.2017.11.022.

Rampazzo, Chiara; Miazzi, Cristina; Franzolin, Elisa; Pontarin, Giovanna; Ferraro, Paola; Frangini, Miriam et al. (2010): Regulation by degradation, a cellular defense against deoxyribonucleotide pool imbalances. In *Mutation research* 703 (1), pp. 2–10. DOI: 10.1016/j.mrgentox.2010.06.002.

Ran, F. Ann; Hsu, Patrick D.; Wright, Jason; Agarwala, Vineeta; Scott, David A.; Zhang, Feng (2013): Genome engineering using the CRISPR-Cas9 system. In *Nature protocols* 8 (11), pp. 2281–2308. DOI: 10.1038/nprot.2013.143.

Ranjha, Lepakshi; Howard, Sean M.; Cejka, Petr (2018): Main steps in DNA double-strand break repair: an introduction to homologous recombination and related processes. In *Chromosoma* 127 (2), pp. 187–214. DOI: 10.1007/s00412-017-0658-1.

Rapino, Francesca; Robles, Eloy F.; Richter-Larrea, Jose A.; Kallin, Eric M.; Martinez-Climent, Jose A.; Graf, Thomas (2013): C/EBPα induces highly efficient macrophage transdifferentiation of B lymphoma and leukemia cell lines and impairs their tumorigenicity. In *Cell reports* 3 (4), pp. 1153–1163. DOI: 10.1016/j.celrep.2013.03.003.

Rawson, Jonathan M. O.; Nikolaitchik, Olga A.; Keele, Brandon F.; Pathak, Vinay K.; Hu, Wei-Shau (2018): Recombination is required for efficient HIV-1 replication and the maintenance of viral genome integrity. In *Nucleic acids research* 46 (20), pp. 10535–10545. DOI: 10.1093/nar/gky910.

Ren, Huiling; Yin, Xin; Su, Chao; Guo, Miaomiao; Wang, Xue-Feng; Na, Lei et al. (2021): Equine lentivirus counteracts SAMHD1 restriction by Rev-mediated degradation of SAMHD1 via the BECN1-dependent lysosomal pathway. In *Autophagy* 17 (10), pp. 2800–2817. DOI: 10.1080/15548627.2020.1846301.

Renaud, Jean-Baptiste; Boix, Charlotte; Charpentier, Marine; Cian, Anne de; Cochennec, Julien; Duvernois-Berthet, Evelyne et al. (2016): Improved Genome Editing Efficiency and Flexibility Using Modified Oligonucleotides with TALEN and CRISPR-Cas9 Nucleases. In *Cell reports* 14 (9), pp. 2263–2272. DOI: 10.1016/j.celrep.2016.02.018.

Rensen, Elena; Mueller, Florian; Scoca, Viviana; Parmar, Jyotsana J.; Souque, Philippe; Zimmer, Christophe; Di Nunzio, Francesca (2021): Clustering and reverse transcription of HIV-1 genomes in nuclear niches of macrophages. In *The EMBO journal* 40 (1), e105247. DOI: 10.15252/embj.2020105247.

Rentoft, Matilda; Lindell, Kristoffer; Tran, Phong; Chabes, Anna Lena; Buckland, Robert J.; Watt, Danielle L. et al. (2016): Heterozygous colon cancer-associated mutations of SAMHD1 have functional significance. In *Proceedings of the National Academy of Sciences of the United States of America* 113 (17), pp. 4723–4728. DOI: 10.1073/pnas.1519128113.

Ricardo-Lax, Inna; Ramanan, Vyas; Michailidis, Eleftherios; Shamia, Tal; Reuven, Nina; Rice, Charles M. et al. (2015): Hepatitis B virus induces RNR-R2 expression via DNA damage response activation. In *Journal of hepatology* 63 (4), pp. 789–796. DOI: 10.1016/j.jhep.2015.05.017.

Rice, Andrew P.; Kimata, Jason T. (2015): Subversion of Cell Cycle Regulatory Mechanisms by HIV. In *Cell host & microbe* 17 (6), pp. 736–740. DOI: 10.1016/j.chom.2015.05.010.

Rice, Gillian I.; Bond, Jacquelyn; Asipu, Aruna; Brunette, Rebecca L.; Manfield, Iain W.; Carr, Ian M. et al. (2009): Mutations involved in Aicardi-Goutières syndrome implicate SAMHD1 as regulator of the innate immune response. In *Nature genetics* 41 (7), pp. 829–832. DOI: 10.1038/ng.373.

Richardson, Christopher D.; Ray, Graham J.; DeWitt, Mark A.; Curie, Gemma L.; Corn, Jacob E. (2016): Enhancing homology-directed genome editing by catalytically active and inactive CRISPR-Cas9 using asymmetric donor DNA. In *Nature biotechnology* 34 (3), pp. 339–344. DOI: 10.1038/nbt.3481.

Riess, Maximilian; Fuchs, Nina V.; Idica, Adam; Hamdorf, Matthias; Flory, Egbert; Pedersen, Irene Munk; König, Renate (2017): Interferons Induce Expression of SAMHD1 in Monocytes through Down-regulation of miR-181a and miR-30a. In *The Journal of biological chemistry* 292 (1), pp. 264–277. DOI: 10.1074/jbc.M116.752584.

Ringeard, Mathieu; Marchand, Virginie; Decroly, Etienne; Motorin, Yuri; Bennasser, Yamina (2019): FTSJ3 is an RNA 2'-O-methyltransferase recruited by HIV to avoid innate immune sensing. In *Nature* 565 (7740), pp. 500–504. DOI: 10.1038/s41586-018-0841-4.

Rodrigues, Carlos Hm; Pires, Douglas Ev; Ascher, David B. (2018): DynaMut: predicting the impact of mutations on protein conformation, flexibility and stability. In *Nucleic acids research* 46 (W1), W350-W355. DOI: 10.1093/nar/gky300.

Rodrigues, Vasco; Ruffin, Nicolas; San-Roman, Mabel; Benaroch, Philippe (2017): Myeloid Cell Interaction with HIV. A Complex Relationship. In *Frontiers in immunology* 8, p. 1698. DOI: 10.3389/fimmu.2017.01698.

Romani, Bizhan; Shaykh Baygloo, Nima; Aghasadeghi, Mohammad Reza; Allahbakhshi, Elham (2015): HIV-1 Vpr Protein Enhances Proteasomal Degradation of MCM10 DNA Replication Factor through the Cul4-DDB1VprBP E3 Ubiquitin Ligase to Induce G2/M Cell Cycle Arrest. In *The Journal of biological chemistry* 290 (28), pp. 17380–17389. DOI: 10.1074/jbc.M115.641522.

Rosa, Annachiara; Chande, Ajit; Ziglio, Serena; Sanctis, Veronica de; Bertorelli, Roberto; Goh, Shih Lin et al. (2015): HIV-1 Nef promotes infection by excluding SERINC5 from virion incorporation. In *Nature* 526 (7572), pp. 212–217. DOI: 10.1038/nature15399.

Ruiz, Alba; Pauls, Eduardo; Badia, Roger; Torres-Torronteras, Javier; Riveira-Muñoz, Eva; Clotet, Bonaventura et al. (2015): Cyclin D3-dependent control of the dNTP pool and

HIV-1 replication in human macrophages. In *Cell cycle (Georgetown, Tex.)* 14 (11), pp. 1657–1665. DOI: 10.1080/15384101.2015.1030558.

Ryoo, Jeongmin; Choi, Jongsu; Oh, Changhoon; Kim, Sungchul; Seo, Minji; Kim, Seok-Young et al. (2014): The ribonuclease activity of SAMHD1 is required for HIV-1 restriction. In *Nature medicine* 20 (8), pp. 936–941. DOI: 10.1038/nm.3626.

Sakai, Keiko; Dimas, Joseph; Lenardo, Michael J. (2006): The Vif and Vpr accessory proteins independently cause HIV-1-induced T cell cytopathicity and cell cycle arrest. In *Proceedings of the National Academy of Sciences* 103 (9), pp. 3369–3374. DOI: 10.1073/pnas.0509417103.

Samson, M.; Libert, F.; Doranz, B. J.; Rucker, J.; Liesnard, C.; Farber, C. M. et al. (1996): Resistance to HIV-1 infection in caucasian individuals bearing mutant alleles of the CCR-5 chemokine receptor gene. In *Nature* 382 (6593), pp. 722–725. DOI: 10.1038/382722a0.

Sanchez, Cecilia P.; Moliner Cubel, Sonia; Nyboer, Britta; Jankowska-Döllken, Monika; Schaeffer-Reiss, Christine; Ayoub, Daniel et al. (2019): Phosphomimetic substitution at Ser-33 of the chloroquine resistance transporter PfCRT reconstitutes drug responses in Plasmodium falciparum. In *Journal of Biological Chemistry* 294 (34), pp. 12766–12778. DOI: 10.1074/jbc.RA119.009464.

Sander, Jeffry D.; Joung, J. Keith (2014): CRISPR-Cas systems for editing, regulating and targeting genomes. In *Nature biotechnology* 32 (4), pp. 347–355. DOI: 10.1038/nbt.2842.

Sankar, Aditya; Mohammad, Faizaan; Sundaramurthy, Arun Kumar; Wang, Hua; Lerdrup, Mads; Tatar, Tulin; Helin, Kristian (2022): Histone editing elucidates the functional roles of H3K27 methylation and acetylation in mammals. In *Nature genetics*. DOI: 10.1038/s41588-022-01091-2.

Sattentau, Quentin J.; Stevenson, Mario (2016): Macrophages and HIV-1: An Unhealthy Constellation. In *Cell host & microbe* 19 (3), pp. 304–310. DOI: 10.1016/j.chom.2016.02.013.

Sauter, Daniel; Kirchhoff, Frank (2019): Key Viral Adaptations Preceding the AIDS Pandemic. In *Cell host & microbe* 25 (1), pp. 27–38. DOI: 10.1016/j.chom.2018.12.002.

Schäfer, Alexandra; Bogerd, Hal P.; Cullen, Bryan R. (2004): Specific packaging of APOBEC3G into HIV-1 virions is mediated by the nucleocapsid domain of the gag polyprotein precursor. In *Virology* 328 (2), pp. 163–168. DOI: 10.1016/j.virol.2004.08.006.

Schaller, Torsten; Pollpeter, Darja; Apolonia, Luis; Goujon, Caroline; Malim, Michael H. (2014): Nuclear import of SAMHD1 is mediated by a classical karyopherin α/β1 dependent pathway and confers sensitivity to VpxMAC induced ubiquitination and proteasomal degradation. In *Retrovirology* 11, p. 29. DOI: 10.1186/1742-4690-11-29.

Schmid-Burgk, Jonathan L.; Schmidt, Tobias; Gaidt, Moritz M.; Pelka, Karin; Latz, Eicke; Ebert, Thomas S.; Hornung, Veit (2014): OutKnocker: a web tool for rapid and simple genotyping of designer nuclease edited cell lines. In *Genome research* 24 (10), pp. 1719–1723. DOI: 10.1101/gr.176701.114.

Schmidt, Nora; Domingues, Patricia; Golebiowski, Filip; Patzina, Corinna; Tatham, Michael H.; Hay, Ronald T.; Hale, Benjamin G. (2019a): An influenza virus-triggered SUMO switch orchestrates co-opted endogenous retroviruses to stimulate host antiviral immunity. In *Proceedings of the National Academy of Sciences of the United States of America* 116 (35), pp. 17399–17408. DOI: 10.1073/pnas.1907031116.

Schmidt, Tobias T.; Sharma, Sushma; Reyes, Gloria X.; Gries, Kerstin; Gross, Maike; Zhao, Boyu et al. (2019b): A genetic screen pinpoints ribonucleotide reductase residues that sustain dNTP homeostasis and specifies a highly mutagenic type of dNTP imbalance. In *Nucleic acids research* 47 (1), pp. 237–252. DOI: 10.1093/nar/gky1154.

Schmitz, Michael H. A.; Held, Michael; Janssens, Veerle; Hutchins, James R. A.; Hudecz, Otto; Ivanova, Elitsa et al. (2010): Live-cell imaging RNAi screen identifies PP2A-B55alpha and importin-beta1 as key mitotic exit regulators in human cells. In *Nat Cell Biol* 12 (9), pp. 886–893. DOI: 10.1038/ncb2092.

Schneider, Constanze; Oellerich, Thomas; Baldauf, Hanna-Mari; Schwarz, Sarah-Marie; Thomas, Dominique; Flick, Robert et al. (2017): SAMHD1 is a biomarker for cytarabine response and a therapeutic target in acute myeloid leukemia. In *Nature medicine* 23 (2), pp. 250–255. DOI: 10.1038/nm.4255.

Schoggins, John W.; MacDuff, Donna A.; Imanaka, Naoko; Gainey, Maria D.; Shrestha, Bimmi; Eitson, Jennifer L. et al. (2014): Pan-viral specificity of IFN-induced genes reveals new roles for cGAS in innate immunity. In *Nature* 505 (7485), pp. 691–695. DOI: 10.1038/nature12862.

Schoggins, John W.; Wilson, Sam J.; Panis, Maryline; Murphy, Mary Y.; Jones, Christopher T.; Bieniasz, Paul; Rice, Charles M. (2011): A diverse range of gene products are effectors of the type I interferon antiviral response. In *Nature* 472 (7344), pp. 481–485. DOI: 10.1038/nature09907.

Schott, Kerstin; Fuchs, Nina V.; Derua, Rita; Mahboubi, Bijan; Schnellbächer, Esther; Seifried, Janna et al. (2018): Dephosphorylation of the HIV-1 restriction factor SAMHD1 is mediated by PP2A-B55α holoenzymes during mitotic exit. In *Nature communications* 9 (1), p. 2227. DOI: 10.1038/s41467-018-04671-1.

Schott, Kerstin; Majer, Catharina; Bulashevska, Alla; Childs, Liam; Schmidt, Mirko H. H.; Rajalingam, Krishnaraj et al. (2022): SAMHD1 in cancer: curse or cure? In *Journal of molecular medicine (Berlin, Germany)* 100 (3), pp. 351–372. DOI: 10.1007/s00109-021-02131-w.

Schott, Kerstin; Riess, Maximilian; König, Renate (2017): Role of Innate Genes in HIV Replication. In *Current topics in microbiology and immunology*. DOI: 10.1007/82_2017_29.

Schwartz, O.; Maréchal, V.; Le Gall, S.; Lemonnier, F.; Heard, J. M. (1996): Endocytosis of major histocompatibility complex class I molecules is induced by the HIV-1 Nef protein. In *Nature medicine* 2 (3), pp. 338–342. DOI: 10.1038/nm0396-338.

Schwefel, David; Boucherit, Virginie C.; Christodoulou, Evangelos; Walker, Philip A.; Stoye, Jonathan P.; Bishop, Kate N.; Taylor, Ian A. (2015): Molecular determinants for recognition of divergent SAMHD1 proteins by the lentiviral accessory protein Vpx. In *Cell host & microbe* 17 (4), pp. 489–499. DOI: 10.1016/j.chom.2015.03.004.

Schwefel, David; Groom, Harriet C. T.; Boucherit, Virginie C.; Christodoulou, Evangelos; Walker, Philip A.; Stoye, Jonathan P. et al. (2014): Structural basis of lentiviral subversion of a cellular protein degradation pathway. In *Nature* 505 (7482), pp. 234–238. DOI: 10.1038/nature12815.

Seamon, Kyle J.; Bumpus, Namandjé N.; Stivers, James T. (2016): Single-Stranded Nucleic Acids Bind to the Tetramer Interface of SAMHD1 and Prevent Formation of the Catalytic Homotetramer. In *Biochemistry* 55 (44), pp. 6087–6099. DOI: 10.1021/acs.biochem.6b00986.

Seamon, Kyle J.; Sun, Zhiqiang; Shlyakhtenko, Luda S.; Lyubchenko, Yuri L.; Stivers, James T. (2015): SAMHD1 is a single-stranded nucleic acid binding protein with no active site-associated nuclease activity. In *Nucleic acids research* 43 (13), pp. 6486–6499. DOI: 10.1093/nar/gkv633.

Seczynska, Marta; Bloor, Stuart; Cuesta, Sergio Martinez; Lehner, Paul J. (2022): Genome surveillance by HUSH-mediated silencing of intronless mobile elements. In *Nature* 601 (7893), pp. 440–445. DOI: 10.1038/s41586-021-04228-1.

Seki, Akiko; Rutz, Sascha (2018): Optimized RNP transfection for highly efficient CRISPR/Cas9-mediated gene knockout in primary T cells. In *The Journal of Experimental Medicine* 215 (3), pp. 985–997. DOI: 10.1084/jem.20171626.

Selyutina, Anastasia; Persaud, Mirjana; Lee, Kyeongeun; KewalRamani, Vineet; Diaz-Griffero, Felipe (2020a): Nuclear Import of the HIV-1 Core Precedes Reverse Transcription and Uncoating. In *Cell Rep* 32 (13), p. 108201. DOI: 10.1016/j.celrep.2020.108201.

Selyutina, Anastasia; Persaud, Mirjana; Simons, Lacy M.; Bulnes-Ramos, Angel; Buffone, Cindy; Martinez-Lopez, Alicia et al. (2020b): Cyclophilin A Prevents HIV-1 Restriction in Lymphocytes by Blocking Human TRIM5α Binding to the Viral Core. In *Cell Rep* 30 (11), 3766-3777.e6. DOI: 10.1016/j.celrep.2020.02.100.

Sharova, Natalia; Wu, Yuanfei; Zhu, Xiaonan; Stranska, Ruzena; Kaushik, Rajnish; Sharkey, Mark; Stevenson, Mario (2008): Primate lentiviral Vpx commandeers DDB1 to counteract a macrophage restriction. In *PLoS Pathogens* 4 (5), e1000057. DOI: 10.1371/journal.ppat.1000057.

Sharp, Paul M.; Hahn, Beatrice H. (2011): Origins of HIV and the AIDS pandemic. In *Cold Spring Harbor perspectives in medicine* 1 (1), a006841. DOI: 10.1101/cshperspect.a006841.

Sheehy, Ann M.; Gaddis, Nathan C.; Malim, Michael H. (2003): The antiretroviral enzyme APOBEC3G is degraded by the proteasome in response to HIV-1 Vif. In *Nature medicine* 9 (11), pp. 1404–1407. DOI: 10.1038/nm945.

Shi, Jing; Xiong, Ran; Zhou, Tao; Su, Peiyi; Zhang, Xihe; Qiu, Xusheng et al. (2018): HIV-1 Nef Antagonizes SERINC5 Restriction by Downregulation of SERINC5 via the Endosome/Lysosome System. In *J Virol* 92 (11). DOI: 10.1128/JVI.00196-18.

Shifera, Amde Selassie; Hardin, John A. (2009): PMA induces expression from the herpes simplex virus thymidine kinase promoter via the activation of JNK and ERK in the presence of adenoviral E1A proteins. In *Archives of biochemistry and biophysics* 490 (2), pp. 145–157. DOI: 10.1016/j.abb.2009.08.013.

Silva, Suresh de; Hoy, Heather; Hake, Timothy S.; Wong, Henry K.; Porcu, Pierluigi; Wu, Li (2013): Promoter methylation regulates SAMHD1 gene expression in human CD4+ T cells. In *The Journal of biological chemistry* 288 (13), pp. 9284–9292. DOI: 10.1074/jbc.M112.447201.

Silva, Thauane; Temerozo, Jairo R.; do Vale, Gabriele; Ferreira, André C.; Soares, Vinícius Cardoso; Dias, Suelen Silva Gomes et al. (2021): The Chemokine CCL5 Inhibits the Replication of Influenza A Virus Through SAMHD1 Modulation. In *Frontiers in cellular and infection microbiology* 11, p. 549020. DOI: 10.3389/fcimb.2021.549020.

Skalka, A. M.; Katz, R. A. (2005): Retroviral DNA integration and the DNA damage response. In *Cell death and differentiation* 12 Suppl 1, pp. 971–978. DOI: 10.1038/sj.cdd.4401573.

Skarnes, William C.; Pellegrino, Enrica; McDonough, Justin A. (2019): Improving homology-directed repair efficiency in human stem cells. In *Methods (San Diego, Calif.)* 164-165, pp. 18–28. DOI: 10.1016/j.ymeth.2019.06.016.

Sliva, Katja; Martin, Judith; Rhein, Christine von; Herrmann, Tobias; Weyrich, Anastasia; Toda, Masako; Schnierle, Barbara S. (2019): Interference with SAMHD1 Restores Late Gene Expression of Modified Vaccinia Virus Ankara in Human Dendritic Cells and Abrogates Type I Interferon Expression. In *Journal of Virology* 93 (22). DOI: 10.1128/JVI.01097-19.

Solis, Mayra; Nakhaei, Peyman; Jalalirad, Mohammad; Lacoste, Judith; Douville, Renée; Arguello, Meztli et al. (2011): RIG-I-mediated antiviral signaling is inhibited in HIV-1 infection by a protease-mediated sequestration of RIG-I. In *J Virol* 85 (3), pp. 1224–1236. DOI: 10.1128/JVI.01635-10.

Sommer, Andreas F. R.; Rivière, Lise; Qu, Bingqian; Schott, Kerstin; Riess, Maximilian; Ni, Yi et al. (2016): Restrictive influence of SAMHD1 on Hepatitis B Virus life cycle. In *Scientific reports* 6, p. 26616. DOI: 10.1038/srep26616.

Srinivasachar Badarinarayan, Smitha; Sauter, Daniel (2021): Switching Sides: How Endogenous Retroviruses Protect Us from Viral Infections. In *J Virol* 95 (12). DOI: 10.1128/JVI.02299-20.

Srivastava, Smita; Swanson, Selene K.; Manel, Nicolas; Florens, Laurence; Washburn, Michael P.; Skowronski, Jacek (2008): Lentiviral Vpx accessory factor targets VprBP/DCAF1 substrate adaptor for cullin 4 E3 ubiquitin ligase to enable macrophage infection. In *PLoS Pathogens* 4 (5), e1000059. DOI: 10.1371/journal.ppat.1000059.

St Gelais, Corine; Kim, Sun Hee; Maksimova, Victoria V.; Buzovetsky, Olga; Knecht, Kirsten M.; Shepard, Caitlin et al. (2018): A Cyclin-Binding Motif in Human SAMHD1 Is Required for Its HIV-1 Restriction, dNTPase Activity, Tetramer Formation, and Efficient Phosphorylation. In *Journal of Virology* 92 (6). DOI: 10.1128/JVI.01787-17.

St Gelais, Corine; Silva, Suresh de; Hach, Jocelyn C.; White, Tommy E.; Diaz-Griffero, Felipe; Yount, Jacob S.; Wu, Li (2014): Identification of cellular proteins interacting with the retroviral restriction factor SAMHD1. In *Journal of Virology* 88 (10), pp. 5834–5844. DOI: 10.1128/JVI.00155-14.

Staeheli, Peter; Haller, Otto (2018): Human MX2/MxB: a Potent Interferon-Induced Postentry Inhibitor of Herpesviruses and HIV-1. In *J Virol* 92 (24). DOI: 10.1128/JVI.00709-18.

Staudt, Ryan P.; Smithgall, Thomas E. (2020): Nef homodimers down-regulate SERINC5 by AP-2-mediated endocytosis to promote HIV-1 infectivity. In *The Journal of biological chemistry* 295 (46), pp. 15540–15552. DOI: 10.1074/jbc.RA120.014668.

Stavrou, Spyridon; Aguilera, Alexya N.; Blouch, Kristin; Ross, Susan R. (2018): DDX41 Recognizes RNA/DNA Retroviral Reverse Transcripts and Is Critical for In Vivo Control of Murine Leukemia Virus Infection. In *MBio* 9 (3). DOI: 10.1128/mBio.00923-18.

Stewart, Sheila A.; Dykxhoorn, Derek M.; Palliser, Deborah; Mizuno, Hana; Yu, Evan Y.; An, Dong Sung et al. (2003): Lentivirus-delivered stable gene silencing by RNAi in primary cells. In *RNA (New York, N.Y.)* 9 (4), pp. 493–501. DOI: 10.1261/rna.2192803.

Stockhammer, Alexander; Benz, Laila S.; Freund, Christian; Kuropka, Benno; Bottanelli, Francesca (2021): When less is more - Endogenous tagging with TurboID increases the sensitivity of proximity labelling-based experiments.

Stremlau, Matthew; Owens, Christopher M.; Perron, Michel J.; Kiessling, Michael; Autissier, Patrick; Sodroski, Joseph (2004): The cytoplasmic body component TRIM5alpha restricts HIV-1 infection in Old World monkeys. In *Nature* 427 (6977), pp. 848–853. DOI: 10.1038/nature02343.

Sumner, Rebecca P.; Harrison, Lauren; Touizer, Emma; Peacock, Thomas P.; Spencer, Matthew; Zuliani-Alvarez, Lorena; Towers, Greg J. (2020): Disrupting HIV-1 capsid formation causes cGAS sensing of viral DNA. In *The EMBO journal* 39 (20), e103958. DOI: 10.15252/embj.2019103958.

Sunseri, Nicole; O'Brien, Meagan; Bhardwaj, Nina; Landau, Nathaniel R. (2011): Human immunodeficiency virus type 1 modified to package Simian immunodeficiency virus Vpx efficiently infects macrophages and dendritic cells. In *Journal of Virology* 85 (13), pp. 6263–6274. DOI: 10.1128/JVI.00346-11.

Sürün, Duran; Schneider, Aksana; Mircetic, Jovan; Neumann, Katrin; Lansing, Felix; Paszkowski-Rogacz, Maciej et al. (2020): Efficient Generation and Correction of Mutations in Human iPS Cells Utilizing mRNAs of CRISPR Base Editors and Prime Editors. In *Genes* 11 (5). DOI: 10.3390/genes11050511.

Szaniawski, Matthew A.; Spivak, Adam M.; Cox, James E.; Catrow, Jonathan L.; Hanley, Timothy; Williams, Elizabeth S. C. P. et al. (2018): SAMHD1 Phosphorylation Coordinates the Anti-HIV-1 Response by Diverse Interferons and Tyrosine Kinase Inhibition. In *MBio* 9 (3). DOI: 10.1128/mBio.00819-18.

Sze, Alexandre; Olagnier, David; Lin, Rongtuan; van Grevenynghe, Julien; Hiscott, John (2013): SAMHD1 host restriction factor. A link with innate immune sensing of retrovirus infection. In *Journal of molecular biology* 425 (24), pp. 4981–4994. DOI: 10.1016/j.jmb.2013.10.022.

Tartour, Kevin; Appourchaux, Romain; Gaillard, Julien; Nguyen, Xuan-Nhi; Durand, Stéphanie; Turpin, Jocelyn et al. (2014): IFITM proteins are incorporated onto HIV-1 virion particles and negatively imprint their infectivity. In *Retrovirology* 11, p. 103. DOI: 10.1186/s12977-014-0103-y.

Taylor, Barbara S.; Hammer, Scott M. (2008): The challenge of HIV-1 subtype diversity. In *The New England journal of medicine* 359 (18), pp. 1965–1966. DOI: 10.1056/NEJMc086373.

Tchasovnikarova, Iva A.; Timms, Richard T.; Matheson, Nicholas J.; Wals, Kim; Antrobus, Robin; Göttgens, Berthold et al. (2015): GENE SILENCING. Epigenetic silencing by the HUSH complex mediates position-effect variegation in human cells. In *Science (New York, N.Y.)* 348 (6242), pp. 1481–1485. DOI: 10.1126/science.aaa7227.

Thientosapol, Eddy Sanchai; Bosnjak, Daniel; Durack, Timothy; Stevanovski, Igor; van Geldermalsen, Michelle; Holst, Jeff et al. (2018): SAMHD1 enhances immunoglobulin hypermutation by promoting transversion mutation. In *Proceedings of the National Academy of Sciences of the United States of America* 115 (19), pp. 4921–4926. DOI: 10.1073/pnas.1719771115.

Tramentozzi, Elisa; Ferraro, Paola; Hossain, Manzar; Stillman, Bruce; Bianchi, Vera; Pontarin, Giovanna (2018): The dNTP triphosphohydrolase activity of SAMHD1 persists during S-phase when the enzyme is phosphorylated at T592. In *Cell cycle (Georgetown, Tex.)* 17 (9), pp. 1102–1114. DOI: 10.1080/15384101.2018.1480216.

Tunbak, Hale; Enriquez-Gasca, Rocio; Tie, Christopher H. C.; Gould, Poppy A.; Mlcochova, Petra; Gupta, Ravindra K. et al. (2020): The HUSH complex is a gatekeeper of type I interferon through epigenetic regulation of LINE-1s. In *Nature communications* 11 (1), p. 5387. DOI: 10.1038/s41467-020-19170-5.

Tüngler, Victoria; Staroske, Wolfgang; Kind, Barbara; Dobrick, Manuela; Kretschmer, Stefanie; Schmidt, Franziska et al. (2013): Single-stranded nucleic acids promote SAMHD1 complex formation. In *Journal of molecular medicine (Berlin, Germany)* 91 (6), pp. 759–770. DOI: 10.1007/s00109-013-0995-3.

Uhlen, Mathias; Karlsson, Max J.; Zhong, Wen; Tebani, Abdellah; Pou, Christian; Mikes, Jaromir et al. (2019): A genome-wide transcriptomic analysis of protein-coding genes in human blood cells. In *Science (New York, N.Y.)* 366 (6472). DOI: 10.1126/science.aax9198.

Uhlén, Mathias; Fagerberg, Linn; Hallström, Björn M.; Lindskog, Cecilia; Oksvold, Per; Mardinoglu, Adil et al. (2015): Proteomics. Tissue-based map of the human proteome. In *Science (New York, N.Y.)* 347 (6220), p. 1260419. DOI: 10.1126/science.1260419.

Uphoff, Cord C.; Denkmann, Sabine A.; Steube, Klaus G.; Drexler, Hans G. (2010): Detection of EBV, HBV, HCV, HIV-1, HTLV-I and -II, and SMRV in human and other primate cell lines. In *Journal of biomedicine & biotechnology* 2010, p. 904767. DOI: 10.1155/2010/904767.

Uphoff, Cord C.; Pommerenke, Claudia; Denkmann, Sabine A.; Drexler, Hans G. (2019): Screening human cell lines for viral infections applying RNA-Seq data analysis. In *PLOS ONE* 14 (1), e0210404. DOI: 10.1371/journal.pone.0210404.

Usami, Yoshiko; Wu, Yuanfei; Göttlinger, Heinrich G. (2015): SERINC3 and SERINC5 restrict HIV-1 infectivity and are counteracted by Nef. In *Nature* 526 (7572), pp. 218–223. DOI: 10.1038/nature15400.

van Chu, Trung; Weber, Timm; Wefers, Benedikt; Wurst, Wolfgang; Sander, Sandrine; Rajewsky, Klaus; Kühn, Ralf (2015): Increasing the efficiency of homology-directed repair

for CRISPR-Cas9-induced precise gene editing in mammalian cells. In *Nature biotechnology* 33 (5), pp. 543–548. DOI: 10.1038/nbt.3198.

van Damme, Nanette; Goff, Daniel; Katsura, Chris; Jorgenson, Rebecca L.; Mitchell, Richard; Johnson, Marc C. et al. (2008): The interferon-induced protein BST-2 restricts HIV-1 release and is downregulated from the cell surface by the viral Vpu protein. In *Cell host & microbe* 3 (4), pp. 245–252. DOI: 10.1016/j.chom.2008.03.001.

Varadi, Mihaly; Anyango, Stephen; Deshpande, Mandar; Nair, Sreenath; Natassia, Cindy; Yordanova, Galabina et al. (2022): AlphaFold Protein Structure Database: massively expanding the structural coverage of protein-sequence space with high-accuracy models. In *Nucleic acids research* 50 (D1), D439-D444. DOI: 10.1093/nar/gkab1061.

Vaughan-Jackson, Alun; Stodolak, Szymon; Ebrahimi, Kourosh H.; Browne, Cathy; Reardon, Paul K.; Pires, Elisabete et al. (2021): Differentiation of human induced pluripotent stem cells to authentic macrophages using a defined, serum-free, open-source medium. In *Stem cell reports* 16 (7), pp. 1735–1748. DOI: 10.1016/j.stemcr.2021.05.018.

Verani, A.; Pesenti, E.; Polo, S.; Tresoldi, E.; Scarlatti, G.; Lusso, P. et al. (1998): CXCR4 is a functional coreceptor for infection of human macrophages by CXCR4-dependent primary HIV-1 isolates. In *Journal of immunology (Baltimore, Md. : 1950)* 161 (5), pp. 2084–2088. Available online at https://www.jimmunol.org/content/161/5/2084.

Vierbuchen, Tim; Bang, Corinna; Rosigkeit, Hanna; Schmitz, Ruth A.; Heine, Holger (2017): The Human-Associated Archaeon Methanosphaera stadtmanae Is Recognized through Its RNA and Induces TLR8-Dependent NLRP3 Inflammasome Activation. In *Frontiers in immunology* 8, p. 1535. DOI: 10.3389/fimmu.2017.01535.

Wanaguru, Madushi; Bishop, Kate N. (2021): HIV-1 Gag Recruits Oligomeric Vpr via Two Binding Sites in p6, but Both Mature p6 and Vpr Are Rapidly Lost upon Target Cell Entry. In *J Virol* 95 (17), e0055421. DOI: 10.1128/JVI.00554-21.

Wang, Zhonghua; Bhattacharya, Akash; White, Tommy; Buffone, Cindy; McCabe, Aine; Nguyen, Laura A. et al. (2018): Functionality of Redox-Active Cysteines Is Required for Restriction of Retroviral Replication by SAMHD1. In *Cell reports* 24 (4), pp. 815–823. DOI: 10.1016/j.celrep.2018.06.090.

Watt, Danielle L.; Buckland, Robert J.; Lujan, Scott A.; Kunkel, Thomas A.; Chabes, Andrei (2016): Genome-wide analysis of the specificity and mechanisms of replication infidelity driven by imbalanced dNTP pools. In *Nucleic acids research* 44 (4), pp. 1669–1680. DOI: 10.1093/nar/gkv1298.

Wei, Xiping; Decker, Julie M.; Liu, Hongmei; Zhang, Zee; Arani, Ramin B.; Kilby, J. Michael et al. (2002): Emergence of resistant human immunodeficiency virus type 1 in patients receiving fusion inhibitor (T-20) monotherapy. In *Antimicrobial Agents and Chemotherapy* 46 (6), pp. 1896–1905. DOI: 10.1128/AAC.46.6.1896-1905.2002.

Weinberg, G.; Ullman, B.; Martin, D. W. (1981): Mutator phenotypes in mammalian cell mutants with distinct biochemical defects and abnormal deoxyribonucleoside triphosphate pools. In *Proceedings of the National Academy of Sciences* 78 (4), pp. 2447–2451. DOI: 10.1073/pnas.78.4.2447.

Weisheit, Isabel; Kroeger, Joseph A.; Malik, Rainer; Klimmt, Julien; Crusius, Dennis; Dannert, Angelika et al. (2020): Detection of Deleterious On-Target Effects after HDR-Mediated CRISPR Editing. In *Cell reports* 31 (8), p. 107689. DOI: 10.1016/j.celrep.2020.107689.

Welbourn, Sarah; Dutta, Sucharita M.; Semmes, O. John; Strebel, Klaus (2013): Restriction of virus infection but not catalytic dNTPase activity is regulated by phosphorylation of SAMHD1. In *Journal of Virology* 87 (21), pp. 11516–11524. DOI: 10.1128/JVI.01642-13.

Welbourn, Sarah; Strebel, Klaus (2016): Low dNTP levels are necessary but may not be sufficient for lentiviral restriction by SAMHD1. In *Virology* 488, pp. 271–277. DOI: 10.1016/j.virol.2015.11.022.

Wheeler, Lee Adam; Trifonova, Radiana T.; Vrbanac, Vladimir; Barteneva, Natasha S.; Liu, Xing; Bollman, Brooke et al. (2016): TREX1 Knockdown Induces an Interferon Response to HIV that Delays Viral Infection in Humanized Mice. In *Cell Rep* 15 (8), pp. 1715–1727. DOI: 10.1016/j.celrep.2016.04.048.

White, Tommy E.; Brandariz-Nuñez, Alberto; Valle-Casuso, Jose Carlos; Amie, Sarah; Nguyen, Laura; Kim, Baek et al. (2013a): Contribution of SAM and HD domains to retroviral restriction mediated by human SAMHD1. In *Virology* 436 (1), pp. 81–90. DOI: 10.1016/j.virol.2012.10.029.

White, Tommy E.; Brandariz-Nuñez, Alberto; Valle-Casuso, Jose Carlos; Amie, Sarah; Nguyen, Laura Anh; Kim, Baek et al. (2013b): The retroviral restriction ability of SAMHD1, but not its deoxynucleotide triphosphohydrolase activity, is regulated by phosphorylation. In *Cell host & microbe* 13 (4), pp. 441–451. DOI: 10.1016/j.chom.2013.03.005.

Wilen, Craig B.; Tilton, John C.; Doms, Robert W. (2012): HIV: cell binding and entry. In *Cold Spring Harb Perspect Med* 2 (8), a006866. DOI: 10.1101/cshperspect.a006866.

Williams, Lindsey N.; Marjavaara, Lisette; Knowels, Gary M.; Schultz, Eric M.; Fox, Edward J.; Chabes, Andrei; Herr, Alan J. (2015): dNTP pool levels modulate mutator phenotypes of error-prone DNA polymerase ε variants. In *Proceedings of the National Academy of Sciences of the United States of America* 112 (19), E2457-66. DOI: 10.1073/pnas.1422948112.

Wing, Peter Ac; Davenne, Tamara; Wettengel, Jochen; Lai, Alvina G.; Zhuang, Xiaodong; Chakraborty, Anindita et al. (2019): A dual role for SAMHD1 in regulating HBV cccDNA and RT-dependent particle genesis. In *Life science alliance* 2 (2). DOI: 10.26508/lsa.201900355.

Worobey, Michael; Gemmel, Marlea; Teuwen, Dirk E.; Haselkorn, Tamara; Kunstman, Kevin; Bunce, Michael et al. (2008): Direct evidence of extensive diversity of HIV-1 in Kinshasa by 1960. In *Nature* 455 (7213), pp. 661–664. DOI: 10.1038/nature07390.

Xu, Chaoyi; Fischer, Douglas K.; Rankovic, Sanela; Li, Wen; Dick, Robert A.; Runge, Brent et al. (2020): Permeability of the HIV-1 capsid to metabolites modulates viral DNA synthesis. In *PLoS biology* 18 (12), e3001015. DOI: 10.1371/journal.pbio.3001015.

Xu, Hongzhan; Franks, Tamera; Gibson, Gregory; Huber, Kelly; Rahm, Nadia; Strambio De Castillia, Caterina et al. (2013): Evidence for biphasic uncoating during HIV-1 infection from a novel imaging assay. In *Retrovirology* 10, p. 70. DOI: 10.1186/1742-4690-10-70.

Yan, Junpeng; Hao, Caili; DeLucia, Maria; Swanson, Selene; Florens, Laurence; Washburn, Michael P. et al. (2015): CyclinA2-Cyclin-dependent Kinase Regulates SAMHD1 Protein Phosphohydrolase Domain. In *The Journal of biological chemistry* 290 (21), pp. 13279–13292. DOI: 10.1074/jbc.M115.646588.

Yan, Junpeng; Kaur, Sarabpreet; DeLucia, Maria; Hao, Caili; Mehrens, Jennifer; Wang, Chuanping et al. (2013): Tetramerization of SAMHD1 is required for biological activity and inhibition of HIV infection. In *The Journal of biological chemistry* 288 (15), pp. 10406–10417. DOI: 10.1074/jbc.M112.443796.

Yan, Nan; Regalado-Magdos, Ashton D.; Stiggelbout, Bart; Lee-Kirsch, Min Ae; Lieberman, Judy (2010): The cytosolic exonuclease TREX1 inhibits the innate immune response to human immunodeficiency virus type 1. In *Nature immunology* 11 (11), pp. 1005–1013. DOI: 10.1038/ni.1941.

Yang, Shen; Shan, Tongling; Zhou, Yanjun; Jiang, Yifeng; Tong, Wu; Liu, Fei et al. (2014): Molecular cloning and characterizations of porcine SAMHD1 and its roles in replication of highly pathogenic porcine reproductive and respiratory syndrome virus. In *Developmental and comparative immunology* 47 (2), pp. 234–246. DOI: 10.1016/j.dci.2014.07.024.

Yang, Shen; Zhan, Yuan; Zhou, Yanjun; Jiang, Yifeng; Zheng, Xuchen; Yu, Lingxue et al. (2016): Interferon regulatory factor 3 is a key regulation factor for inducing the expression of SAMHD1 in antiviral innate immunity. In *Scientific reports* 6, p. 29665. DOI: 10.1038/srep29665.

Yang, Xiaoping; Boehm, Jesse S.; Yang, Xinping; Salehi-Ashtiani, Kourosh; Hao, Tong; Shen, Yun et al. (2011): A public genome-scale lentiviral expression library of human ORFs. In *Nature methods* 8 (8), pp. 659–661. DOI: 10.1038/nmeth.1638.

Yang, Yang; Fricke, Thomas; Diaz-Griffero, Felipe (2013): Inhibition of reverse transcriptase activity increases stability of the HIV-1 core. In *J Virol* 87 (1), pp. 683–687. DOI: 10.1128/JVI.01228-12.

Yin, Xin; Langer, Simon; Zhang, Zeli; Herbert, Kristina M.; Yoh, Sunnie; König, Renate; Chanda, Sumit K. (2020): Sensor Sensibility-HIV-1 and the Innate Immune Response. In *Cells* 9 (1). DOI: 10.3390/cells9010254.

Yoh, Sunnie M.; Mamede, João I.; Lau, Derrick; Ahn, Narae; Sánchez-Aparicio, Maria T.; Temple, Joshua et al. (2022): Recognition of HIV-1 Capsid Licenses Innate Immune Response to Viral Infection.

Yoh, Sunnie M.; Schneider, Monika; Seifried, Janna; Soonthornvacharin, Stephen; Akleh, Rana E.; Olivieri, Kevin C. et al. (2015): PQBP1 Is a Proximal Sensor of the cGAS-Dependent Innate Response to HIV-1. In *Cell* 161 (6), pp. 1293–1305. DOI: 10.1016/j.cell.2015.04.050.

Yu, Alvin; Skorupka, Katarzyna A.; Pak, Alexander J.; Ganser-Pornillos, Barbie K.; Pornillos, Owen; Voth, Gregory A. (2020): TRIM5α self-assembly and

compartmentalization of the HIV-1 viral capsid. In *Nature communications* 11 (1), p. 1307. DOI: 10.1038/s41467-020-15106-1.

Yu, Corey H.; Bhattacharya, Akash; Persaud, Mirjana; Taylor, Alexander B.; Wang, Zhonghua; Bulnes-Ramos, Angel et al. (2021): Nucleic acid binding by SAMHD1 contributes to the antiretroviral activity and is enhanced by the GpsN modification. In *Nature communications* 12 (1), p. 731. DOI: 10.1038/s41467-021-21023-8.

Yu, Jingyou; Li, Minghua; Wilkins, Jordan; Ding, Shilei; Swartz, Talia H.; Esposito, Anthony M. et al. (2015): IFITM Proteins Restrict HIV-1 Infection by Antagonizing the Envelope Glycoprotein. In *Cell Rep* 13 (1), pp. 145–156. DOI: 10.1016/j.celrep.2015.08.055.

Yu, Xianghui; Yu, Yunkai; Liu, Bindong; Luo, Kun; Kong, Wei; Mao, Panyong; Yu, Xiao-Fang (2003): Induction of APOBEC3G ubiquitination and degradation by an HIV-1 Vif-Cul5-SCF complex. In *Science (New York, N.Y.)* 302 (5647), pp. 1056–1060. DOI: 10.1126/science.1089591.

Yurkovetskiy, Leonid; Guney, Mehmet Hakan; Kim, Kyusik; Goh, Shih Lin; McCauley, Sean; Dauphin, Ann et al. (2018): Primate immunodeficiency virus proteins Vpx and Vpr counteract transcriptional repression of proviruses by the HUSH complex. In *Nature Microbiology* 3 (12), pp. 1354–1361. DOI: 10.1038/s41564-018-0256-x.

Zeng, ChengWu; Wang, WenTao; Yu, XiBao; Yang, LiJian; Chen, ShaoHua; Li, YangQiu (2015): Pathways related to PMA-differentiated THP1 human monocytic leukemia cells revealed by RNA-Seq. In *Science China. Life sciences* 58 (12), pp. 1282–1287. DOI: 10.1007/s11427-015-4967-4.

Zhang, Chiyu; Silva, Suresh de; Wang, Jian-Hua; Wu, Li (2012): Co-evolution of primate SAMHD1 and lentivirus Vpx leads to the loss of the vpx gene in HIV-1 ancestor. In *PLOS ONE* 7 (5), e37477. DOI: 10.1371/journal.pone.0037477.

Zhang, Hui; Yang, Bin; Pomerantz, Roger J.; Zhang, Chune; Arunachalam, Shyamala C.; Gao, Ling (2003): The cytidine deaminase CEM15 induces hypermutation in newly synthesized HIV-1 DNA. In *Nature* 424 (6944), pp. 94–98. DOI: 10.1038/nature01707.

Zhang, Kun; Lv, Dong-Wen; Li, Renfeng (2019): Conserved Herpesvirus Protein Kinases Target SAMHD1 to Facilitate Virus Replication. In *Cell reports* 28 (2), 449-459.e5. DOI: 10.1016/j.celrep.2019.04.020.

Zhang, Pu; Iwasaki-Arai, Junko; Iwasaki, Hiromi; Fenyus, Maris L.; Dayaram, Tajhal; Owens, Bronwyn M. et al. (2004): Enhancement of hematopoietic stem cell repopulating capacity and self-renewal in the absence of the transcription factor C/EBP alpha. In *Immunity* 21 (6), pp. 853–863. DOI: 10.1016/j.immuni.2004.11.006.

Zhang, Xuewu; Bai, Xiao-Chen; Chen, Zhijian J. (2020): Structures and Mechanisms in the cGAS-STING Innate Immunity Pathway. In *Immunity* 53 (1), pp. 43–53. DOI: 10.1016/j.immuni.2020.05.013.

Zhao, Ke; Du, Juan; Han, Xue; Goodier, John L.; Li, Peng; Zhou, Xiaohong et al. (2013): Modulation of LINE-1 and Alu/SVA retrotransposition by Aicardi-Goutières syndrome-related SAMHD1. In *Cell reports* 4 (6), pp. 1108–1115. DOI: 10.1016/j.celrep.2013.08.019.

Zhong, Zhou; Ning, Jiying; Boggs, Emerson A.; Jang, Sooin; Wallace, Callen; Telmer, Cheryl et al. (2021): Cytoplasmic CPSF6 Regulates HIV-1 Capsid Trafficking and Infection in a Cyclophilin A-Dependent Manner. In *MBio* 12 (2). DOI: 10.1128/mBio.03142-20.

Zhou, Honglin; Xu, Min; Huang, Qian; Gates, Adam T.; Zhang, Xiaohua D.; Castle, John C. et al. (2008): Genome-scale RNAi screen for host factors required for HIV replication. In *Cell host & microbe* 4 (5), pp. 495–504. DOI: 10.1016/j.chom.2008.10.004.

Zila, Vojtech; Margiotta, Erica; Turoňová, Beata; Müller, Thorsten G.; Zimmerli, Christian E.; Mattei, Simone et al. (2021): Cone-shaped HIV-1 capsids are transported through intact nuclear pores. In *Cell* 184 (4), 1032-1046.e18. DOI: 10.1016/j.cell.2021.01.025.

Zuliani Alvarez, Lorena; Govasli, Morten L.; Rasaiyaah, Jane; Monit, Chris; Perry, Stephen O.; Sumner, Rebecca P. et al. (2022): Macrophage activation of cGAS and TRIM5 distinguish pandemic and non-pandemic HIV.

VII. APPENDIX

a. Register of academic teachers

My academic teachers at the Eberhardt-Karls Universität Tübingen:

Aicher, Autenrieth I., Auterieth S., Baatz, Barth, Bauer, Baumann, Berneburg, Beschoner, Bisdas, Bonzheim, Braeuning, Brauch, Brunner, Clausen, Dauch, Dennehy, Dillmann, Dittmann, Dufke, Duszenko, Dürr, Ehni, Eichner, Fallier-Becker, Fend, Fink, Flohr, Flötenmeyer, Forchhammer, Frick, Garaschuk, Gauglitz, Gasser, Gerold, Gouttefangeas, Gronbach, Grond, Gröbner, Guenther, Hartl, Hector, Heidenreich, Heinle, Hirschmüller, Hoffmeister, Huber, Iftner, Iglauer, Jahn, Jung, Klein, Kling, Klingel, Knipper, Kohlbacher, Kormann, Kossat-Boehlert, KönigsrainerKreidenweiss, Kühl, Lammerding-Köppel, Lammers, Lang, Liese, Liske, Lorand, Macek, Malek, Meier, Münzel, Neher, Nguyen, Nordheim, Nürnberg, Paquet-Durand, Peschel, Pfannenberg, Pichler, Planz, Proikas-Cezanne, Pusch, Rammensee, Rieber, Riess, Ruscheweyh, Schibel, Schick, Schilbach, Schindler, Schabel, Scharpf, Schick, Schittenhelm, Schittek, Schmidt, Schöffl, Schütz, Schwarz, Singer, Soboslay, Stadler, Stehle, Stevanović, Stierhof, Stoll, Stubenrauch, Suckale, Sultan, Syha, Tabatabai, Tomiuk, Tümmers, Velevan, Volkmer, Wagner, Walz, Weber, Weidenmaier, Weimer, Werz, Wiesing, Wiesinger, Wizemann, Wolz, Zentgraf

My academic teachers at the Université d'Aix-Marseille:

Aussel, Barbier, Bertrand, Bordet, Breuzard, Brugna-Ciata, Carré, Cornish-Bowden, Forquet, Galland, Garzino, Gilli, Hienerwadel, Jamin, Kreuzer, Pagalo, Porcher, Saks, Schlegel, Schmidt, Strugis

b. Acknowledgements

Science is teamwork and thus I want to use the occasion to express my deep gratitude to all of which have contributed directly or indirectly to this work. It would not have been possible without you. In addition to our team effort when it comes to science, you made me progress personally and mature on this challenge. This time would have not been the same without you.

Namely, I want to thank…

… Dr. Renate König for the possibility to do this work in her laboratory, for her outstanding support and continuous guidance all along the last years, as well as for her trust into my ideas and the freedom to pursue my projects. You were a great mentor to me.

… Prof. Dr. Stefan Bauer for his supervision during the PhD, for his advice and feedback in the thesis committee meetings, for the highly productive BlaER1 transdifferentiation protocol and finally for his time and patience with my thesis.

… the thesis committee of the Paul-Ehrlich-Institute for interesting and important discussion as well as for the appreciated feedback during our meetings. More specifically Prof. Dr. Klaus Cichutek for his experience and expertise on retroviruses, Prof. Dr. Eberhardt Hildt for his virologic viewpoint, Dr. Gerrit Praefcke for his proficiency and help with questions related to post-translational modifications and Dr. Egbert Flory for his fantastic ideas and unique angle, as well as valuable discussions in innumerable breaks.

… to all collaboration partners on this project. Explicitly Baek Kim and Adrian Oo for the dNTP measurements, Judd Hultquist for CRISPR/Cas9 RNP protocols, as well as Rita Derua and Veerle Janssens for the mass spectrometry measurements and helpful sessions discussing data and troubleshooting.

… to the members past or present of the NG3 group. Alla, Liam, Lukas, Anna, Lucas, Emily, Nina, Yiwei, Christian, Janna, Morssal, Felix, Lise, Kerstin, Nina, Manja, Christiane, Heike, Saskia, Maïwenn, Max, Catharina, Johanna, Corinna, Jonas und Carl who supported me and made the time at the Paul-Ehrlich-Institute unique. All of you made precious contributions to my work, for which I cannot express enough gratitude. Especially, I want to highlight Dr. Kerstin Schott-Hartenstein for the concepts and ideas, I had the chance to discuss with her and her important expertise on SAMHD1 and the techniques we used, Dr. Nina Hein-Fuchs for her help and experience with CRISPR tools, Saskia Mönch for her skills in producing perfect virus stocks, Paula Rauch and Morssal Zahadi for their valuable contribution to my projects and their trust in my supervision, Catharina Majer for the debates on the enigmas of SAMHD1 function and together with Johanna Wildemann for a great time and a lot of fun in the PhD office.

… to scientists and staff at the Paul-Ehrlich-Institute for small and big contributions to my work, as well as to my peers with whom I shared precious moments and which made science even more fun: Nico, Christin, Flo, Max, Matthias, Lisa, Arne, Naphang, Kevin, Kerren, Laura, to name only some of you. Also, Dr. Lacramioara Botezatu, Marcel Rommel and Sven Flindt are important to mention here since their technical expertise made direct contributions to this work.

… to important mentors supporting my scientific path, such as Prof. Dr. Alexander Weber, Dr. Stella Autenrieth, Dr. Kristin Bieber, Prof. Dr. Michael Schindler, Dr. Ramona Businger, Jean-Pierre Gorvel, Stéphane Méresse and Pierre Golstein.

… to my parents, brother and family for their support, ready ear and love.

… to my friends who chaperoned my life as a student in Tübingen, Marseille and Darmstadt.

… and last, but certainly not least to Christin for everything.